Cell biology of anammox *Planctomycetes* and methanotrophic *Verrucomicrobia*

The cell envelope of anammox *Planctomycetes*

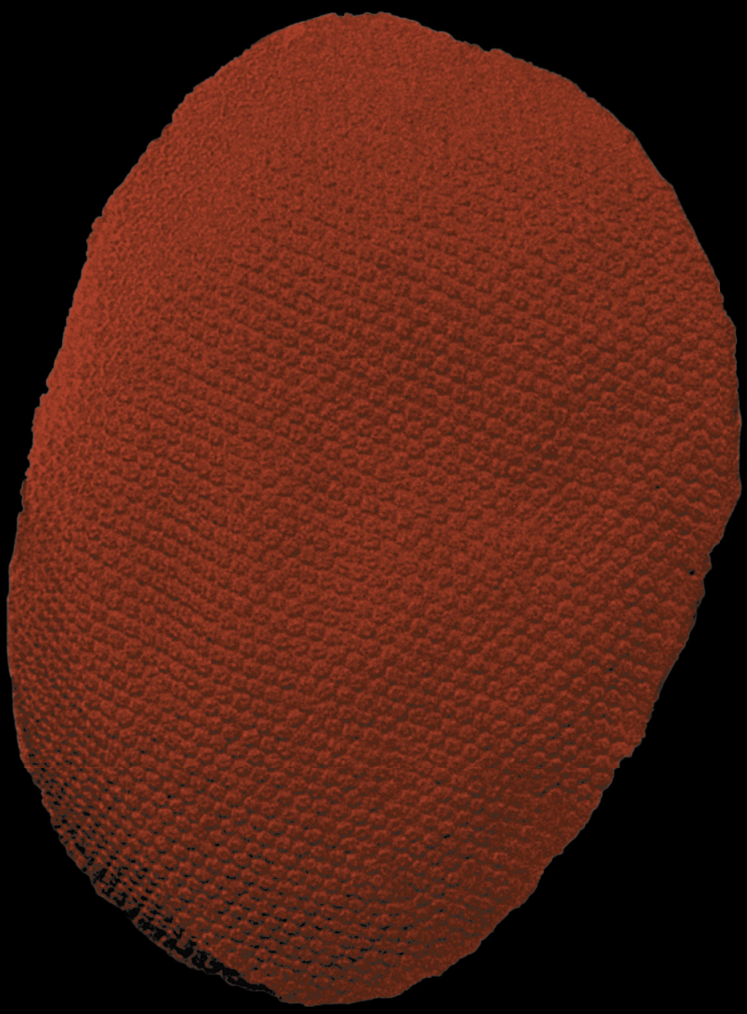

Muriel van Teeseling

Cell biology of anammox *Planctomycetes* and methanotrophic *Verrucomicrobia*

Part i

The cell envelope of anammox *Planctomycetes*

Muriel van Teeseling

Muriel van Teeseling (2015)
Cell biology of anammox *Planctomycetes* and methanotrophic *Verrucomicrobia*.
PhD thesis, Radboud University Nijmegen.

This PhD project was financially supported by ERC AG 232937.
Printing of this thesis was financially supported by SIAM gravitation grant 024002002 and by the Netherlands Society of Medical Microbiology (NVMM) and the Royal Netherlands Society for Microbiology (KNVM).

Cover: Freeze-fractured *Methylacidimicrobium fagopyrum* cell by Muriel van Teeseling.
Print: Gildeprint Drukkerijen, Enschede, the Netherlands.
ISBN: 978-94-6233-163-1.

Cell biology of anammox *Planctomycetes* and methanotrophic *Verrucomicrobia*

Proefschrift
ter verkrijging van de graad van doctor
aan de Radboud Universiteit Nijmegen
op gezag van de rector magnificus,
volgens besluit van het college van decanen
in het openbaar te verdedigen op
woensdag 13 januari 2016 om 14.30 uur precies

door
Muriël Caroline Frieda van Teeseling
geboren op 25 december 1986
te Naarden

Promotor
Prof. dr. ir. M.S.M. Jetten

Copromotor
dr. L. van Niftrik

Manuscriptcommissie
Prof. dr. C. Mariani
Prof. dr. W. Bitter (Vrije Universiteit Amsterdam)
Prof. dr. S-V. Albers (Albert-Ludwigs-Universität Freiburg, Duitsland)

Contents

2 (i)

Summary

Anammox bacteria perform anaerobic ammonium oxidation and play an important role in the biological nitrogen cycle. They are applied to efficiently remove ammonium and nitrite from wastewater via a biochemically highly interesting mechanism involving hydrazine as intermediate and dinitrogen gas as end product. Anammox bacteria are also of particular interest to cell biologists. They belong to the *Planctomycetes*, a phylum characterized by a unique cell organization. Most *Planctomycetes* have two compartments, of which the innermost was interpreted as an intracytoplasmic compartment. Anammox bacteria have a third compartment that acts as a prokaryotic organelle in which the anammox reaction takes place. The anammox cell thus consists of the following compartments (from the outside inwards): the paryphoplasm, the riboplasm and the anammoxosome. An interesting aspect of all *Planctomycetes* is the cell envelope, which was proposed to lack peptidoglycan and an outer membrane. This is striking since almost all bacteria contain peptidoglycan in their cell envelope. Furthermore all bacteria classified as Gram-negative additionally contain an outer membrane surrounding the peptidoglycan layer. Especially for anammox bacteria, many questions about the cell envelope remain, such as: Which components does the cell envelope contain? What are the characteristics of the outermost membrane (previously defined as a cytoplasmic membrane)? The research presented in this part of the thesis therefore aims to elucidate which components constitute the cell envelope of the model anammox species *Kuenenia stuttgartiensis.* With the new results we were able to answer the question if, as was postulated, this organism truly forms an exception to the Gram-negative cell plan.

Chapter 1 provides an introduction into bacterial cell (envelope) organization, (anammox) *Planctomycetes* and their cell biology. The results of **chapter 2** show that a new layer was discovered as the outermost structure of the *K. stuttgartiensis* cell. This so-called surface layer (S-layer) consists of proteins and forms a symmetrical pattern. The S-layer was characterized via freeze-etching followed by transmission electron microscopy (TEM). Enrichment of this S-layer led to the identification of the glycoprotein that builds this structure: Kustd1514. Two main glycan components were retrieved from Kustd1514 and their composition was elucidated via mass spectrometry coupled to liquid chromatography in combination with monosaccharide analysis. Immunogold localization using an antibody generated against Kustd1514 verified that this protein indeed forms the observed S-layer.

To investigate if the outermost membrane has characteristics of an outer membrane, most notably lipopolysaccharide (LPS) as specific lipids and outer membrane proteins (OMPs) as specific proteins, **chapter 3** and **chapter 4** describe in-depth investigations of this membrane. The purification and characterization of a specific OMP, Kustd1878, are described in **chapter 3**. The structure of Kustd1878 was investigated via bioinformatics, suggesting the protein has an OMP-specific ß-barrel structure. Pore-forming function, a typical characteristic of OMPs, was verified by membrane bilayer assays. Immunogold localization using an antibody generated against the purified protein furthermore suggested the presence of this protein in the outermost membrane of *K. stuttgartiensis* that can best be described as an outer membrane.

Chapter 4 aims at elucidating if LPS, the main component of the outer leaflet of outer membranes, is present in *K. stuttgartiensis* and the two non-anammox *Planctomycetes Planctopirus limnophila* and *Rhodopirellula baltica*. Genes necessary for the synthesis of lipid A, the part of the LPS that is anchored in the membrane, were identified in the genome of all three species and in the transcriptome of *K. stuttgartiensis*. Gel electrophoresis indicated the presence of LPS in all three species and polymyxin B, an antibiotic that disrupts the outer membrane upon binding to LPS, caused disruption of the membranes of *R. baltica* and to a lesser extent of *K. stuttgartiensis* and *P. limnophila*. However, the LPS components KDO and lipid A were not detected in *K. stuttgartiensis* via mass spectrometry methods. Therefore, the presence of LPS in the three *Planctomycetes* species seems plausible, but additional experiments are needed for further verification.

In **chapter 5** the proposed absence of peptidoglycan in anammox bacteria was revisited. Cryo-TEM of vitreous sections identified a layer in between the cytoplasmic and outermost membrane in *K. stuttgartiensis*. When using a peptidoglycan isolation protocol, characteristic sacculi were observed. These sacculi disintegrated upon treatment with lysozyme, an agent that cleaves the sugar backbone of peptidoglycan. In addition, the presence of peptidoglycan was demonstrated in growing cultures by fluorescent probes that are built in during peptidoglycan synthesis. The presence of peptidoglycan in *K. stuttgartiensis* was ultimately proven when muropeptide analysis showed the composition of the sacculi to be typical for Gram-negative peptidoglycan.

Based on the results of the previous chapters, **chapter 6** reaches the conclusion that (anammox) *Planctomycetes* can best be interpreted as Gram-negative bacteria. This chapter furthermore gives an overview of the cell envelope of anammox bacteria, and describes key questions and associated hypotheses and experiments in order to come to a thorough understanding of the cell biology of (anammox) *Planctomycetes*.

Samenvatting

Anammoxbacteriën voeren anaërobe ammonium-oxidatie uit en spelen een belangrijke rol in de biologische stikstofcyclus. Ze worden toegepast om op efficiënte wijze ammonium en nitriet uit afvalwater te verwijderen via een biochemisch zeer interessant mechanisme met hydrazine als tussenproduct en stikstofgas als eindproduct. Anammoxbacteriën zijn daarnaast bijzonder interessant voor celbiologen. Ze behoren tot de *Planctomyceten*, een phylum dat door een unieke celorganisatie gekarakteriseerd wordt. De meeste *Planctomyceten* hebben twee compartimenten waarvan de binnenste werd beschouwd als een intracytoplasmatisch compartiment. Anammoxbacteriën hebben daarnaast een derde compartiment dat functioneert als prokaryoot organel waarin de anammoxreactie plaatsvindt. Anammoxbacteriën bestaan dus uit de volgende compartimenten (van buiten naar binnen): het paryphoplasma, het riboplasma en het anammoxosoom. Een interessant aspect van alle *Planctomyceten* is de celenvelop, waarvan men aannam dat hierin zowel peptidoglycaan als een buitenmembraan ontbrak. Dit is opvallend aangezien bijna alle bacteriën peptidoglycaan bevatten in hun celenvelop. Daarnaast hebben alle bacteriën die als Gram-negatief worden geklassificeerd een peptidoglycaan omringende buitenmembraan. In het bijzonder voor anammoxbacteriën zijn er nog veel open vragen over de celenvelop, zoals: Uit welke componenten bestaat de celenvelop? Wat zijn de karakteristieken van de buitenste membraan (dat voorheen als cytoplasmatisch membraan gedefinieerd was)? Het onderzoek beschreven in dit deel van het proefschrift beoogt daarom op te helderen welke componenten aanwezig zijn in de celenvelop van het anammoxmodelorganisme *Kuenenia stuttgartiensis.* Met de behaalde resultaten konden we de vraag beantwoorden of dit organisme inderdaad, zoals gedacht werd, een uitzondering vormt op het Gram-negatieve celplan.

Hoofdstuk 1 geeft een introductie in de organisatie van de bacteriële cel(envelop), *Planctomyceten* inclusief anammoxbacteriën en hun celbiologie. De resultaten uit **hoofdstuk 2** laten zien dat er een nieuwe laag ontdekt werd als buitenste structuur van de *K. stuttgartiensis* cel. Deze zogeheten S-laag bestaat uit eiwitten en vormt een symmetrisch patroon. De S-laag werd gekarakteriseerd via vriesetsen gevolgd door transmissie elektronenmicroscopie (TEM). Verrijking van deze S-laag leidde tot de identificatie van het glyco-eiwit waaruit deze structuur is opgebouwd: Kustd1514. De compositie van twee belangrijke glycanen afkomstig van Kustd1514 werd opgehelderd met behulp van massaspectrometrie gekoppeld aan vloeistofchromatografie in combinatie met monosaccharidenanalyse. Immunogoudlokalisatie met een antilichaam gegenereerd tegen Kustd1514 bevestigde dat dit eiwit inderdaad de geobserveerde structuur vormt.

Om te onderzoeken of het buitenste membraan karakteristieken vertoont van een buitenmembraan, in het bijzonder lipopolysacchariden (LPS) als specifieke lipiden en buitenmembraaneiwitten (BME) als specifieke eiwitten, gaan **hoofdstuk 3** en **hoofdstuk 4** dieper in op dit membraan. De opzuivering en karakterisatie van een specifiek BME, Kustd1878, worden beschreven in **hoofdstuk 3**. De structuur van Kustd1878 werd bestudeerd met behulp van bioinformatica, waaruit bleek dat dit eiwit een BME-karakteristieke ß-ton structuur heeft. Membraanbilaagexperimenten bevestigden dat dit

eiwit net als andere BMEs poriën in een membraan kan vormen. Immunogoudlokalisatie met een antilichaam gegenereerd tegen het opgezuiverde eiwit suggereert dat dit eiwit zich in het buitenste membraan bevindt en dat dit membraan het beste als buitenmembraan kan worden beschouwd.

Hoofdstuk 4 beoogt de vraag te beantwoorden of LPS, de hoofdcomponent van de buitenste laag van de buitenmembraan, aanwezig is in *K. stuttgartiensis* en de twee niet-anammox *Planctomyceten Planctopirus limnophila* en *Rhodopirellula baltica*. Genen benodigd voor de synthese van lipide A, het deel van LPS wat in het membraan is verankerd, werden geïdentificeerd in het genoom van alle drie de organismen en in het transcriptoom van *K. stuttgartiensis*. Gelelektroforese toonde de aanwezigheid van LPS aan in de drie soorten en polymyxin B, een antibioticum wat LPS bindt en vervolgens de buitenmembraan verstoort, leidde tot verstoring van de membranen van *R. baltica* en in mindere mate van die van *K. stuttgartiensis* en *P. limnophila*. Daarentegen werden de LPS componenten KDO en lipide A niet gedetecteerd in *K. stuttgartiensis* met massaspectrometrische methoden. Samenvattend lijkt het waarschijnlijk dat LPS aanwezig is in de drie *Planctomyceten*, hoewel aanvullende experimenten noodzakelijk zijn ter bevestiging.

In **hoofdstuk 5** wordt de gesuggereerde afwezigheid van peptidoglycaan opnieuw bekeken. Cryo-TEM op secties van bevroren cellen liet een laag zien tussen het cytoplasmatische en buitenmembraan in *K. stuttgartiensis*. Na een peptidoglycaan isolatie konden karakteristieke sacculi worden gedetecteerd. Deze sacculi vielen uiteen na behandeling met lysozym, een enzym dat de suikerverbindingen in peptidoglycaan openbreekt. Daarnaast werd peptidoglycaan aangetoond in groeiende culturen via specifieke fluorescente verbindingen die kunnen worden ingebouwd tijdens de synthese van peptidoglycaan. De ontdekking via muropeptidenanalyse dat de sacculi bestonden uit typische bouwstenen van Gram-negatief peptidoglycaan was het ultieme bewijs van de aanwezigheid van peptidoglycaan in *K. stuttgartiensis*.

Op basis van de resultaten van de voorgaande hoofdstukken, komt **hoofdstuk 6** tot de conclusie dat (anammox) *Planctomyceten* het best beschouwd kunnen worden als Gram-negatieve bacteriën. Bovendien geeft dit hoofdstuk een overzicht van de celenvelop van anammoxbacteriën en beschrijft het de belangrijke vragen en bijbehorende hypothesen en experimenten om te komen tot een goed begrip van de celbiologie van (anammox) *Planctomyceten*.

8 (i)

Chapter 1

General introduction

Life cannot exist without chemical reactions and chemical reactions cannot take place without local gradients and concentrations of macromolecules that surpass a certain threshold. To achieve these concentrations of macromolecules and create the possibility of gradients that can be used to conserve energy, life takes place in confined structures called cells. All known living beings consist of cells and two types of cells can be distinguished based on their architecture. The eukaryotic cell is characterized by the presence of a membrane-bound nucleus and in general has a more complex internal organization with (multiple) organelles, whereas the prokaryotic cell (either archaeal or bacterial) lacks a nucleus and (as was thought for a long time) organelles and thus has a more simple organization. Each cell, being prokaryotic or eukaryotic, is surrounded by at least one membrane, of which the omnipresent cytoplasmic or plasma membrane is most crucial in cell confinement. In some cells, additional structures such as cell walls are present on the outside of the cytoplasmic membrane. The cell wall can best be defined as "all structures outside the cytoplasmic membrane whose main function is to provide cells with rigidity". The cell wall is particularly crucial for single-celled organisms, since in their case the cell is exposed to the environment and thus needs an especially stable structure as confinement. The cell confinement as a whole, thus consisting of the cytoplasmic membrane, the cell wall and additional membranes if present, is called the cell envelope. Some researchers, however, see the cytoplasmic membrane as an entity not belonging to the cell envelope.

Two types of bacterial cell envelopes: Gram-positive and Gram-negative

Two types of cell envelope organization are recognized in bacteria: Gram-positive and Gram-negative. These types were introduced based on the reaction to the so-called Gram-stain procedure (Gram, 1884), which was later discovered to reflect a different organization of the cell envelope (Popescu & Doyle, 1996; Beveridge, 2001). Whereas the cell envelope of Gram-positive bacteria (Fig. 1A) consists of a cytoplasmic membrane covered by a thick layer of peptidoglycan, Gram-negative bacteria (Fig. 1B) possess a thin layer of peptidoglycan and an additional membrane, called the outer membrane. Of course, as with almost all classification efforts in biology, several variations are present within each cell envelope type.

Gram-positive bacteria

In Gram-positive bacteria the cytoplasmic membrane is covered by a relatively thick layer of peptidoglycan, which is the attachment site of polysaccharide components termed secondary cell wall polymers (SCWPs) (Ward, 1981; Schäffer & Messner, 2005). These SCWPs can account for up to 60% of the weight of the bacterial cell wall (Schäffer & Messner, 2005). Multiple groups of chemically diverse SCWPs exist, for instance teichoic (Brown et al, 2013) and teichuronic acids (Lazarevic et al, 2005) (both negatively charged polysaccharides) and several components classified as non-classical SCWPs (Schäffer & Messner, 2005). Most SCWPs have repeating units of sugar components connected via phosphodiester linkages in the case of teichoic acids and via uronic acids in the case of teichuronic acids (Lazarevic et al, 2005). Multiple roles for SCWPs have been described, such as binding of divalent cations (Beveridge & Murray, 1980) and mediating the attachment of proteins, notably surface (S-) layer proteins (Ilk et al, 1999; Mesnage et al, 2000), to the cell wall. If present, S-layer proteins non-covalently bind SCWPs via a specific motif: the SLH (S-layer homology) domain

(Lupas et al, 1994) or the CWB2 (cell wall binding 2) (Fagan et al, 2011) motif. Both motifs can also be used by non-S-layer proteins that attach to the cell wall (Fagan & Fairweather, 2014).

In Gram-positive bacteria with S-layers, the S-layer protein has to be transported through the cytoplasmic membrane and peptidoglycan layer before it can anchor to the cell wall. This process has only been studied in two organisms, which both use the accessory Sec secretion system, including two copies of the ATPase SecA (Braunstein et al, 2001) and the membrane channel SecYEG, for S-layer secretion (Fagan & Fairweather, 2011; Nguyen-Mau et al, 2012).

Gram-negative bacteria

Gram-negative bacteria lack secondary cell wall polymers but do have an additional membrane –the outer membrane- surrounding a relatively thin peptidoglycan layer (Silhavy et al, 2010). The space that is bordered by the cytoplasmic membrane on one side and the outer membrane on the other side is called the periplasm. The outer membrane is supposed to have a higher permeability than the cytoplasmic membrane as a consequence of pores formed by outer membrane proteins (OMPs). Each OMP has a β-barrel structure that forms a channel lined by 8-24 β-strands (Fairman et al, 2011) through which specific molecules can diffuse through the outer membrane. Many OMPs insert into the membrane as trimers forming three channels (Schulz, 2002). The residues of the OMP that are facing the membrane are often hydrophobic, thereby ensuring that the protein is well anchored into the membrane. The diameter and especially the characteristics of the residues facing the channel dictate which substrates can diffuse through the OMP and with which specificity. Multiple molecules pass over the outer membrane via OMPs, for instance sugars such as sucrose (Schmid et al, 1991; Forst et al, 1998) and small molecules under 600 Da that can passively diffuse to more or less general porins such as OmpF and PhoE (Cowan et al, 1992; Dhakshnamoorthy et al, 2013). Proteins can be exported via multiple systems involving OMPs (Kostakioti et al, 2005) and OMPs that are inserted into the outer membrane by the OMP BamA (Voulhoux et al, 2003; Noinaj et al, 2013).

Not only the membrane permeability and protein composition (presence of OMPs) are specific to the outer membrane, also the lipid composition differs between the cytoplasmic membrane and the outer membrane. The cytoplasmic membrane consists of phospholipids and the asymmetric outer membrane has a phospholipid-containing inner leaflet and an outer leaflet composed of mainly lipopolysaccharides (LPS) (Kamio & Nikaido, 1976). It is estimated that LPS makes up about 75% of the surface of this outer leaflet (Gronow & Brade, 2001). The exact composition and length of LPS molecules can differ between different strains (Weckesser et al, 1973; Škultéty et al, 1998) as well as within strains dependent on the culture conditions (McDonald & Adams, 1971; Kawahara et al, 2002). Even within cells of a strain grown under the same conditions, heterogeneity of LPS molecules can occur (Darveau et al, 2004). Each LPS molecule consists of a lipid A domain, a non-repeating core oligosaccharide and a distal polysaccharide, called the O-antigen. The lipid A, which is the component that induces an immune response via Toll-like receptors 2 and 4 (Netea et al, 2002), has a variable amount of acyl-chains with a variable length that anchors it in the membrane (Erridge et al, 2002). Attached to the lipid A is the core oligosaccharide that consists of an inner (often including the unusual sugar 3-deoxy-D-manno-octulosonic acid

(Kdo)) and an outer core (Erridge et al, 2002). The O-antigen is made out of repeating units of one to eight sugar components and the composition and length of the polysaccharide varies considerably, making this the most variable part of the LPS molecule. Some organisms entirely lack the O-antigen, while others display a range of lengths, constructing a chain of up to 50 repeating units (Erridge et al, 2002). The main function of LPS is to prevent hydrophobic substances from entering the cell by serving as a barrier (Gronow & Brade, 2001). In addition, LPS is proposed to facilitate proper folding of outer membrane proteins (de Cock et al, 1999) and act as an anchor to which proteins (notably S-layer proteins (Fagan & Fairweather, 2014)) or other molecules can attach.

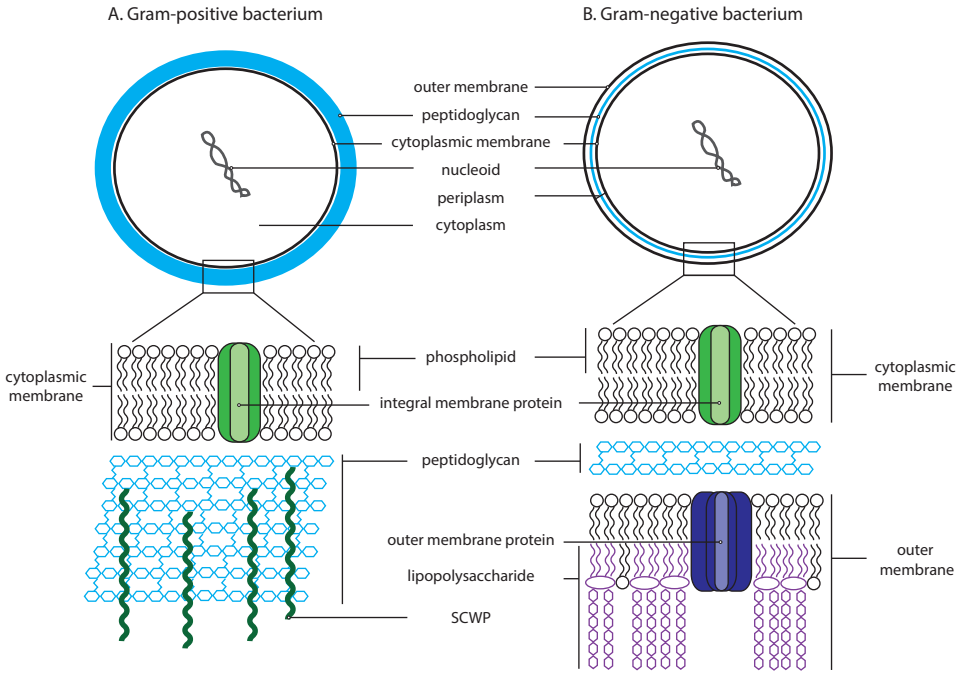

Figure 1. *Schematic representation of (A) a Gram-positive cell and a zoom-in of a Gram-positive cell envelope and (B) a Gram-negative cell and cell envelope.*

Prokaryotic cell wall structures

Both Gram-negative and Gram-positive cell envelopes contain rigid cell wall structures that aid in maintaining cell shape and integrity. Two common cell wall structures, which were already briefly mentioned in the description of the Gram-positive and Gram-negative cell envelopes, are discussed below.

Peptidoglycan

Almost all bacteria synthesize a cell wall with as a main component peptidoglycan, which is also known as murein (after the Latin word for wall, murus). Peptidoglycan is a gigantic mesh-like heteropolymer consisting of a sugar backbone of alternating β-1,4-linked *N*-acetylglucosamine (GlcNAc) and *N*-acetylmuramic acid (MurNAc) residues that are cross-linked by short D-amino acid rich peptide stems (Vollmer et al, 2008). Some of the five amino acids of the peptide stem are omnipresent, while others can vary depending on the species and growth conditions (Vollmer et al, 2008; Lam et al, 2009). The third amino acid of the peptide stem usually differs between Gram-positive and Gram-negative bacteria: in most Gram-negative bacteria a *meso*-diaminopimelic acid can be found in this position, whereas in most Gram-positive bacteria L-lysine is present (Vollmer et al, 2008). The ubiquity and importance of peptidoglycan are reflected by the fact that it is a target of many (naturally occurring) antibiotics (Lovering et al, 2012). Bacteria can alter the structure and composition of their peptidoglycan throughout their life cycle and can also adapt their peptidoglycan to changes in the environment (Cava & de Pedro, 2014). In addition, some bacteria have evolved their peptidoglycan biosynthesis pathway to become insensitive to certain peptidoglycan-targeting antibiotics (Mainardi et al., 2008). The plasticity of peptidoglycan again underlines the importance of this cell wall structure to bacteria.

Archaea do not contain a peptidoglycan cell wall, although some species (Albers & Meyer, 2011) possess a similar structure called pseudomurein. Pseudomurein is also composed of a sugar backbone, formed by β-1,3-linked GlcNAc and L-*N*-acetyltalosaminuronic acid (TalNAc) subunits, cross-linked by short peptides made up of L-amino acids (Kandler & König, 1998; Albers & Meyer, 2011). Despite the similarity in structure of pseudomurein and peptidoglycan, they appear to have evolved separately since the biosynthetic pathways involve different types of intermediates (Hartmann & König, 1990) and presumably non-homologous proteins (Steenbakkers et al, 2006). Some archaeal species synthesize other rigid polymers that function as a cell wall. Examples of these cell wall polymers are methanochondroitin in (aggregates of) *Methanosarcina*, (highly sulphated) heterosaccharides in *Halococcus* and glutaminylglycan in *Natronococcus* (Kandler & König, 1998; Albers & Meyer, 2011).

S-layers

Some bacterial cells have a proteinaceous surface- or S-layer as an additional cell wall component (Sleytr & Beveridge, 1999; Sára & Sleytr, 2000; Fagan & Fairwater, 2014). This structure is also widely present within the Archaea (Albers & Meyer, 2011). S-layers form the outermost layer of the cell envelope by enclosing the cell as a crystalline symmetrical layer consisting of self-assembled protein monomers that are often identical (Messner & Sleytr, 1992; Fagan & Fairwater, 2014). S-layer proteins are often attached to cell envelope structures underneath via non-covalent interactions (Fagan & Fairweather, 2014). In Gram-positive bacteria, the S-layer is often attached to SCWPs and in Gram-negative bacteria the S-layer proteins can attach to LPS. Since S-layers cover the entire cell, the synthesis and transport of the S-layer proteins requires an extensive energy investment thus indicating that S-layers probably have an important function for the organism. In different organisms, S-

layers have been found to have different functions such as attachment of pathogenic bacteria to host tissue (Schneitz et al, 1993; Sillanpää et al, 2000; Grogono-Thomas et al, 2000; Sakakibara et al, 2007), maintaining cell shape (Klingl et al, 2011), attachment of enzymes such as proteases (Mayr et al, 1996) or amylases (Egelseer et al, 1995) and protection against predation (Koval & Hynes, 1991). Not only the function of the S-layer, but also the sequence of the protein monomers, are found to be quite divergent and in some cases different S-layer proteins can be expressed in the same organism (Fagan & Fairwater, 2014). In many S-layers, the protein monomers are modified by glycosylation at specific amino acids, resulting in covalently bound glycans that face the extracellular environment (Messner et al, 2008). These carbohydrates can be structurally quite complicated and, particularly in the case of bacteria, can form long chains (Messner et al, 2008).

Planctomycetes

Occurrence and phylogeny

Almost all bacteria can be classified as either Gram-positive or Gram-negative, but the phylum of the *Planctomycetes* seems to be an exception to this rule, as will be discussed in detail below. The *Planctomycetes* belong to the *Planctomycetes*, *Verrucomicrobia* and *Chlamydiae* (PVC) superphylum (Wagner & Horn, 2006) and three orders can be distinguished within the phylum: Planctomycetales (Ward, 2010), Phycisphaerales (Fukunaga et al, 2009) and Brocadiales (Jetten et al, 2010). *Planctomycetes* are found in a wide range of ecosystems, including various types of soil (Borneman & Triplett, 1997; Derakshani et al, 2001; Buckley et al, 2006), marine environments (Kuypers et al, 2003; Kirkpatrick et al, 2006; Woebken et al, 2007) including marine snow (DeLong et al 1993; Fuchsman et al, 2012) and various freshwater environments (Fuerst, 1995; Strous et al, 1999; Pollet et al, 2010). Furthermore, they have been proposed to live in association with (often aquatic) eukaryotes, such as macroalgae (Fukunaga et al, 2009; Bengtsson & Øvreås, 2010; Lage & Bondoso, 2011; Bondoso et al, 2014; Yoon et al, 2014; Bondoso et al, 2015), sponges (Webster et al, 2001; Sipkema et al, 2009; Izumi et al, 2013), termite guts (Köhler et al, 2008), a protist (Lage, 2013) and a giant tiger prawn (Fuerst et al, 1991; Fuerst et al, 1997). These associations might be facilitated by appendages such as stalks and holdfasts that have been described for multiple *Planctomycetes* (Ward, 2010).

Physiology

With the exception of the anammox bacteria belonging to the order of the Brocadiales, *Planctomycetes* that have been cultivated are typically chemoheterotrophs. Many of these are able to grow on *N*-acetylglucosamine (a common ingredient in *Planctomycete*-selective media (Lage & Bondoso, 2012)) or degrade carbon-rich biopolymers (Schlesner et al, 2004; Izumi et al, 2013). It has been hypothesized that *Planctomycetes* might play an important role in the carbon cycle by degrading heteropolysaccharides and other polymers, especially in marine environments (Woebken et al, 2007; Izumi et al, 2013). The high amount of sulfatases encoded in several genomes of marine *Planctomycetes* probably makes sulfated heteropolysaccharides, which are present in large quantities in marine environments, suitable substrates for these *Planctomycetes* (Glöckner et al, 2003; Woebken et al, 2007).

Heteropolysaccharides are also proposed to be an important substrate for *Planctomycetes* found in marine snow, in which these compounds can be trapped (Woebken et al, 2007). The few known species of the Phycisphaerales can also use multiple polysaccharides, for instance agar, as substrates (Fukunaga et al, 2009; Yoon et al, 2014; Kovaleva et al, 2015).

Cell biology of Planctomycetes

Cell division

A shared characteristic of the three orders of *Planctomycetes* is that, unlike in most other bacteria (Angert, 2005), the cell division takes place without the common cell division protein FtsZ. The Planctomycetales divide by polar budding (Fuerst, 1995; Jogler et al, 2012). The molecular mechanism of division by budding in Planctomycetales (as well as in other budding bacteria) is not understood. The known species of the Brocadiales (all belonging to the anammox bacteria) divide by binary fission (van Niftrik et al, 2009). Binary fission is normally initiated by a cell division ring and such a ring was observed in multiple Brocadiales species. However, where in canonical binary fission the ring is formed by the protein FtsZ, this protein is absent from the Brocadiales. Instead another protein was identified to associate with or more probably be part of this ring in *K. stuttgartiensis* (van Niftrik et al, 2009). This protein, Kustd1438, seems to be specific to *K. stuttgartiensis* and possibly for other anammox bacteria as no homologs were detected in genomes of other *Planctomycetes* (van Niftrik et al, 2009; Jogler et al, 2012). It has not been investigated which proteins collaborate with Kustd1438 to coordinate cell division in the Brocadiales and many questions concerning their division mechanism remain open. All three species of Phycisphaerales known to date are described to divide via binary fission (Fukunaga et al, 2009; Yoon et al, 2014; Kovaleva et al, 2015). No details are known concerning the molecular mechanism of their cell division, although a protein BLAST (Altschul et al, 1990) search shows that the common cell division ring-forming protein FtsZ (Dai & Lutkenhaus, 1991) and the *Kuenenia*-specific cell division protein Kustd1438 (van Niftrik et al, 2009) are both absent from the genome of *Phycisphaera mikurensis*.

Cell plan

The *Planctomycetes* share a complicated cell plan, which is characterized by an unusual membrane organization (Fig. 2). Most *Planctomycetes* contain two membrane-bound compartments and some species have an additional, third, membrane-bound compartment. In many of the species with two compartments (for instance *Isosphaera pallida* (Lindsay et al, 2001), *Planctopirus limnophila* (Jogler et al, 2011; Scheuner et al, 2014), *Rhodopirellula rubra* (Bondoso et al, 2014) and *Roseimaritima ulvae* (Bondoso et al, 2015)) the membrane surrounding the inner compartment is highly curved, leaving a variable, often large, space in between the two membranes. A third membrane-bound compartment is present in the Brocadiaceae family (Jetten et al, 2010; Lindsay et al, 2001; van Niftrik et al, 2004) and, although this is currently under debate, the *Gemmata* genus (Fuerst & Webb, 1991; Lindsay et al, 2001; Santarella-Mellwig et al, 2013; Sagulenko et al, 2014; Acehan et al, 2014). Whether or not a third separate compartment exists in *Gemmata*, it is undebated that

extensive endomembrane systems (Acehan et al, 2014), are present that divide the cytoplasm in, also functionally (Gottshall et al, 2014), separate regions.

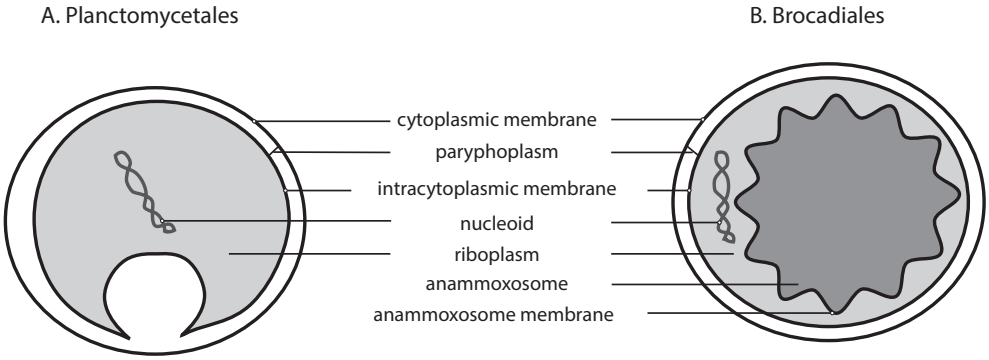

Figure 2. *Schematic overview of the cell plan of (A) Planctomycetales and (B) Brocadiales showing the different membranes and compartments. The actual size and number of invaginations varies largely within and between Planctomycetales species. No scheme of the Phycisphaerales is included, because a very limited amount of published electron micrographs exist of this order.*

Cell envelope

The planctomycetal cell envelope is a structure of which the composition is hotly debated (Lindsay et al, 2001; Fuerst & Sagulenko, 2011; Speth et al, 2012; Devos, 2014a; Devos, 2014b; Sagulenko et al, 2014). As stated before, most *Planctomycetes* have two membranes, as is the case for Gram-negative bacteria. Historically, the outermost membrane was defined as a cytoplasmic membrane (Lindsay et al, 1997; Lindsay et al, 2001). This definition was based mainly on the presence of RNA in the compartment between the two membranes and the assumption that RNA is not expected to be present in the periplasm (Lindsay et al, 1997; Lindsay et al, 2001). The cytoplasm was thus proposed to be separated into two compartments, the paryphoplasm and the pirellulosome, which are divided by the intracytoplasmic membrane (Lindsay et al, 1997; Lindsay et al, 2001). More recently, however, the outermost membrane has been proposed to be an outer membrane based on the presence of marker genes for OMP and LPS biosynthesis (Speth et al, 2012). In that scenario the paryphoplasm should be interpreted as a periplasm, the intracytoplasmic membrane as a cytoplasmic membrane and the pirellulosome as the cytoplasm. Some of the research presented in this part of the thesis aims to contribute new knowledge in order to resolve this topic.

Lack of peptidoglycan

Another remarkable feature of the planctomycetal cell envelope is the proposed lack of a peptidoglycan cell wall. Already early in *Planctomycetes* research, the peptidoglycan components *meso*-DAP (part of the peptide stem in most Gram-negative bacteria) and MurNAc (one of the two sugar components forming the glycan backbone) were not detected during an in-depth analysis of eight strains (König et al, 1984). The same peptidoglycan components appeared missing from eight additional strains and in addition it was found that

these organisms have proteinaceous cell walls rich in proline and cysteine (Liesack et al, 1986). Following these initial studies, multiple novel species were shown to also lack muramic acid and/or diaminopimelic acid as markers for peptidoglycan (Giovannoni et al, 1987; Fukunaga et al, 2009; Yoon et al, 2014). Another indication for the absence of peptidoglycan came from the finding that all *Planctomycetes* tested were insensitive to antibiotics that target peptidoglycan biosynthesis (Fuerst et al, 1991; Schlesner et al, 2004; Fukunaga et al, 2009; Kulichevskaya et al, 2009; Cayrou et al, 2010). In addition, the genome sequences of multiple *Planctomycetes* apparently lacked a varying amount of genes necessary for the biosynthesis of peptidoglycan (Glöckner et al, 2003; Strous et al, 2006; Jogler et al, 2012; Guo et al, 2014). Furthermore, peptidoglycan seemed absent from ultrathin sections studied with transmission electron microscopy (Fuerst et al, 1991; Giovannoni et al, 1987; Lindsay et al, 2001; Bondoso et al, 2011). All in all, it was concluded that *Planctomycetes* lack peptidoglycan and that they have an unusual cell envelope that does not comply to the standard Gram-negative or Gram-positive cell envelopes.

Anammox bacteria

Phylogeny, cultivation and occurrence

Within the Brocadiales order of the *Planctomycetes* phylum five genera have been described up to now: *Brocadia* (Strous et al, 1999), *Kuenenia* (Schmid et al, 2000), *Scalindua* (Kuypers et al, 2003; Schmid et al, 2003), *Anammoxoglobus* (Kartal et al, 2007) and *Jettenia* (Quan et al, 2008). The type genus is *Brocadia* (Jetten et al, 2010), but the model organism for most studies is *Kuenenia stuttgartiensis*. All five genera have a *Candidatus* status because attempts to grow these organisms in pure culture have not yet succeeded. Instead, these bacteria are grown in bioreactor set-ups in enrichment cultures (Strous et al, 1998; van der Star et al, 2008). Whereas the genus *Scalindua* is mostly present in marine environments (Schmid et al, 2007) or other environments with an enhanced salt concentration, the other genera are mostly present in freshwater systems and soils (Dale et al, 2009; Humbert et al, 2010; Sonthiphand et al, 2014). Wastewater treatment facilities form a specific habitat where many Brocadiales species occur, and where multiple species have been enriched from (Strous et al, 1999; Schmid et al, 2000; Schmid et al, 2003; Kartal et al, 2007). All representatives of the Brocadiales are so-called anammox bacteria that are named after the chemical reaction they perform: anaerobic ammonium oxidation. Since this reaction is, up to now at least, exclusive for the Brocadiales species, these organisms are often referred to as anammox bacteria.

Importance of anammox bacteria in the environment and application

As the anammox reaction combines two nitrogen-containing compounds (nitrite and ammonium) to form dinitrogen gas, it is clear that anammox bacteria play a role in the global nitrogen cycle. This role is more significant than originally thought (Francis et al, 2007), especially since anammox bacteria are present at many sites worldwide (Sonthiphand et al, 2014). Recent reports estimate that anammox bacteria are responsible for a significant percentage of the nitrogen loss from marine environments, most notably oxygen minimum zones (OMZs) (Arrigo, 2005; Francis et al, 2007; Babbin et al, 2014). When measured as a percentage of dinitrogen produced by anammox bacteria it becomes clear that they also play

a significant role in groundwater (Moore et al, 2011), lakes (Schubert et al, 2006), estuaries (Trimmer et al, 2003) and paddy soils (Zhu et al, 2011). In addition to their importance in the global nitrogen cycle, anammox bacteria are also used in wastewater treatment for removal of ammonium in an energy efficient, environmentally friendly and cost efective way (Abma et al, 2007; Kartal et al, 2010).

Biochemistry of the anammox reaction

The anaerobic oxidation of ammonium by anammox bacteria is not only significant from an environmental and applied perspective, but is also very interesting from a biochemical viewpoint. The anammox reaction uses nitrite as terminal electron acceptor and generates dinitrogen gas and this is a reaction so far found to be unique to anammox bacteria. The anammox reaction proceeds in three consecutive steps: (1) nitrite (NO_2^-) is reduced to nitric oxide (NO), (2) nitric oxide is combined with ammonium (NH_4^+) to form hydrazine (N_2H_4) and (3) hydrazine (N_2H_4) is oxidized to dinitrogen (N_2) gas (Kartal et al, 2011) (Fig. 3). The identity of the enzyme that catalyzes nitrite reduction is still under debate (Strous et al, 2006; Hira et al, 2012; Kartal et al, 2013). Although multiple candidates have been proposed, none of these is present in all investigated anammox species and it is therefore probable that different enzymes are responsible for this reaction in different anammox species (Kartal et al, 2013). Hydrazine, a highly energetic intermediate that is unique for anammox bacteria, is generated by the heterotrimeric enzyme hydrazine synthase (HZS) (Strous et al, 2006; Kartal et al, 2011; Kartal et al, 2013; Dietl et al, in press). The growth rate of anammox bacteria (the doubling time is typically in the order of 15-30 days, but can be sped up to ca. 2.8 days (Lotti et al, 2015)) is thought to be limited by the supposedly very slow HZS enzyme (Kartal et al, 2011; Kartal et al, 2013). Oxidation of hydrazine is catalyzed by hydrazine dehydrogenase (HDH) (Kartal et al, 2011). Hydrazine is a very powerful reductant and the electrons generated by its oxidation are proposed to give rise to a proton motive force (pmf) that is used to produce ATP by a membrane-bound ATP synthase (van Niftrik et al, 2010; Kartal et al, 2013). This pmf is generated over the so-called anammoxosome membrane (introduced below) using an electron transport chain, featuring a *bc_1* complex, coupled to the anammox reaction (Kartal et al, 2013) (Fig. 3). The electron transport chain is proposed to shuttle electrons to or from the quinone/quinol (Q) pool, but the proteins involved in this process, as well as the proteins that shuttle the electrons between the membrane proteins and the enzymes involved in the anammox reaction remain to be characterized (Kartal et al, 2013).

(1) $NO_2^- + 2H^+ + \mathbf{e}^-$ **->** $NO + H_2O$

(2) $NO + NH_4^+ + 2H^+ + 3\ \mathbf{e}^-$ **->** $N_2H_4 + H_2O$

(3) N_2H_4 **->** $N_2 + 4H^+ + 4\ \mathbf{e}^-$

In addition, anammox bacteria oxidize a significant amount of nitrite to nitrate (NO_3^-) and it has been proposed that this reaction generates electrons that are used as reducing equivalents in the fixation of carbon dioxide (CO_2) by the acetyl-CoA pathway (Schouten et al, 2004; Strous et al, 2006; Kartal et al, 2011; Kartal et al, 2013). The carbon fixation, however, includes several low-redox potential reactions and the redox potential of the electrons

supplied by nitrite oxidation is apparently too high (Kartal et al, 2013). It was recently shown that anammox bacteria can also grow without oxidizing nitrite, when they are grown in the presence of nitric oxide (Hu, 2014). This suggests that the electrons generated by the oxidation of nitrite are not used for carbon fixation, but alternatively for nitrite reduction to nitric oxide (Kartal et al, 2013; Hu, 2014).

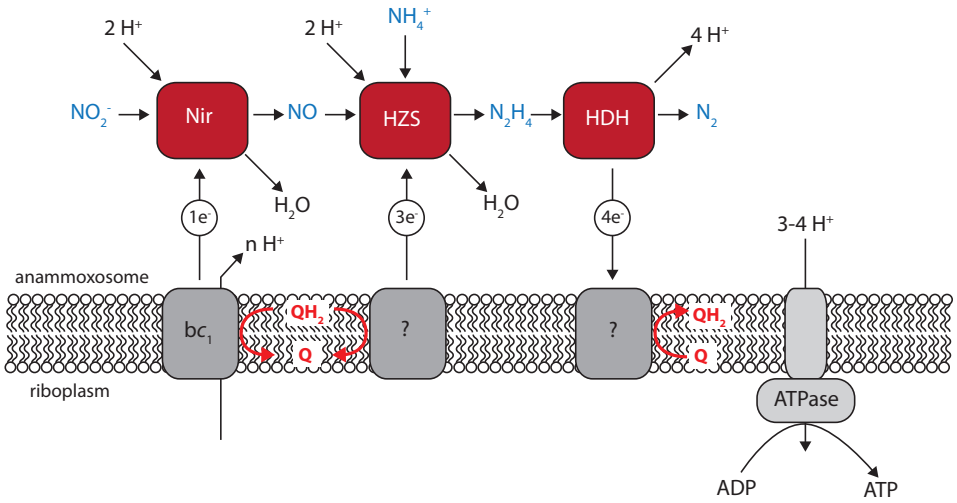

Figure 3. *Schematic overview of the anammox process coupled to an electron transport chain in the anammoxosome membrane. Dinitrogen gas (N_2) is produced from the substrates nitrite (NO_2^-) and ammonium (NH_4^+) via the intermediates nitric oxide (NO) and hydrazine (N_2H_4) using subsequently the nitrite reductase (Nir), hydrazine synthase (HZS) and hydrazine dehydrogenase (HDH) enzymes. The anammox reaction results in a proton motive force, which is used by a membrane-bound ATPase to synthesize ATP in the riboplasm. Figure adapted from Kartal et al, 2013.*

Ladderane lipids

A unique feature of anammox bacteria is the presence of so-called ladderane lipids, the first natural molecules discovered to have cyclobutane rings (Sinninghe Damsté et al, 2002). Different variants of these ladderane lipids occur in anammox cells, differing for instance in the amount of cyclobutane rings and the type of linkage between the lipid and the glycerol backbone (Sinninghe Damsté et al, 2002; Sinninghe Damsté et al, 2005). Another striking feature of the ladderane lipids is that some have ether linkages, a type of linkage that is present mainly in Archaea (Sinninghe Damsté et al, 2002). Ladderane lipids are among the most abundant lipids in the anammox membranes (Sinninghe Damsté et al, 2002). Originally it was found that the ladderane lipids were enriched specifically in one of the anammox membranes (the anammoxosome membrane, see below) (Sinninghe Damsté et al, 2002), although later on it was discovered that the ladderanes are present in all membranes in equal amounts (Neumann et al, 2014).

The proposed function of the ladderane lipids is to make the membranes more densely packed and this proposal was supported by modeling and investigation of isolated ladderane lipids that were reconstituted into membrane vesicles (Sinninghe Damsté et al, 2002; Boumann et al, 2009). This would be very useful for anammox bacteria, since the anammox process is slow and is hindered by passive diffusion of both protons and intermediates such as hydrazine (Sinninghe Damsté et al, 2002). Recent computer simulations, however, suggest that membranes containing ladderane lipids might be more permeable to hydrazine than membranes without ladderane lipids (Chaban et al, 2014). Indeed hydrazine is also detected outside anammox cells, suggesting it does diffuse out to some extent (Kartal et al, 2011). All in all, the evidence for the role of ladderane lipids in membrane permeability is conflicting and the role of ladderane lipids should be studied in further detail. Since ladderane lipids are -as far as we know- specific for anammox bacteria, they can act as biomarkers for present (Kuypers et al, 2003) and past (Rush et al, 2012) presence of anammox bacteria. Since anammox bacteria were found to synthesize ladderane lipids with a longer fatty acid chain when they were grown at a higher temperature, the ladderanes used as biomarkers can also give information about which temperature prevailed when the organisms were alive (Rattray et al, 2010).

The anammox cell

Anammoxosome

As briefly mentioned earlier in the introduction, all anammox bacteria contain three membrane-bound compartments in their cell (Fig. 2B). The inner compartment, called the anammoxosome is specific for anammox bacteria and takes up approximately 61% of the volume of the cell (Neumann et al, 2013). Electron tomography suggested the anammoxosome to be a separate compartment (van Niftrik et al, 2008b) and the isolation of intact anammoxosomes from anammox cells verified this finding (Sinninghe Damsté et al, 2002; Neumann et al, 2014). The proteins involved in the anammox process are exclusively located in the anammoxosome, as was shown by immunogold localization on cells (Lindsay et al, 2001; van Niftrik et al, 2008a; van Niftrik et al, 2010; de Almeida et al, 2015) and proteomics on isolated anammoxosomes (Neumann et al, 2014). Activity assays on isolated anammoxosomes verified that the anammox reaction is performed inside this compartment (Neumann et al, 2014). In addition to proteins involved in the anammox reaction, the anammoxosome also harbors iron-containing particles (van Niftrik et al, 2008b) and tubule-like structures. These tubule-like structures have recently been shown to consist of the NXR enzyme-complex (de Almeida et al, 2015) that is proposed to perform the oxidation of nitrite to nitrate (de Almeida et al, 2011). The highly curved anammoxosome membrane surrounds the anammoxosome and is proposed to be the location of many enzymes involved in the electron transport chain, generation of proton motive force and the subsequent synthesis of ATP (van Niftrik et al, 2010; de Almeida et al, 2015).

Riboplasm

In close proximity to the outside of the anammoxosome, located in the riboplasm (called pirellulosome in other *Planctomycetes* (Lindsay et al, 1997)), is the condensed DNA nucleoid

(Neumann et al, 2014). The riboplasm also contains ribosomes (Lindsay et al, 2001) and vesicles that store glycogen (van Niftrik et al, 2008a)). The function of the riboplasm is thus probably analogous to that of the cytoplasm of other bacteria. The riboplasm is surrounded by a membrane, which has been defined as the intracytoplasmic membrane (Lindsay et al, 2001). It is still unknown how proteins are targeted towards the other compartments of the anammox cell after being synthesized in the riboplasm. Both the Sec (secretory) pathway and TAT (twin arginine translocation) system, which are involved in transport of proteins in many bacteria, are encoded in the genome of the anammox bacterium *K. stuttgartiensis* (Strous et al, 2006). It was suggested that the TAT system might be specifically located in the anammoxosome membrane and the Sec pathway would assist in protein transport towards all compartments (Medema et al, 2010). This would imply that signal peptides that are included in the protein sequence, physicochemical characteristics of the proteins themselves or chaperones are necessary to steer the protein towards the correct compartment (Medema et al, 2010).

Paryphoplasm

The outer compartment of the anammox cell is called the paryphoplasm. Even though the paryphoplasm is relatively thin it makes up on average 21% of the total volume of the cell (Neumann et al, 2013). No ribosomes and DNA have been found inside the paryphoplasm (Lindsay et al, 2001). RNA, however, seems to be present in the paryphoplasm and it was therefore interpreted as a cytoplasmic compartment (Lindsay et al, 2001). The most apparent structure in the paryphoplasm is the non-FtsZ-based cell division ring (van Niftrik et al, 2009). The location of the cell division ring is striking since the anammoxosome also divides during cell division and no membrane links have been observed between the anammoxosome and the other anammox membranes (van Niftrik et al, 2009). It is unknown which mechanism drives the division of the anammoxosome. Another interesting point concerning the location of the anammox cell division ring is that in all other (non-anammox) species investigated up to now the cell division ring is located in the cytoplasm and never in the periplasm. This might be an indication that either the paryphoplasm should be interpreted as a cytoplasmic compartment or that the cell division in anammox bacteria is more unique than previously assumed since it takes place in a different compartment compared to other bacteria.

Outermost membrane

The membrane lining the paryphoplasm has often been called the cytoplasmic membrane, or when avoiding a functional interpretation, the outermost membrane. No details about the components of this specific membrane are known, except for the fact that immunogold labeling against an F-ATPase showed this ATPase to be present on this membrane (van Niftrik et al, 2010). Since it is generally believed that the Gram-negative outer membrane is not energized, because of its relative permeability and hence the inability to establish an electrochemical gradient over this membrane, the presence of this ATPase has often been seen as a clear indication that this membrane is in fact a cytoplasmic membrane. It would, however, be necessary to investigate the composition of this membrane further to determine if LPS and OMPs are present in this membrane, as has been suggested by genomic

analysis (Strous et al, 2006; Speth et al, 2012). This is one of the objectives of the research described in this thesis.

Cell envelope

The composition of the cell envelope of anammox bacteria has not yet been investigated. Analogous with the proposed absence of peptidoglycan in other *Planctomycetes*, it was thought that anammox bacteria also have a peptidoglycan-less cell wall. The apparent absence of peptidoglycan in ultrathin sections strengthened this viewpoint (see TEM images in: Lindsay et al, 2001; Kartal et al, 2007; Kartal et al, 2008; van Niftrik et al, 2008a). And even though initial studies suggested anammox bacteria to be resistant to peptidoglycan-targeting antibiotics (van de Graaf et al, 1995; Güven et al, 2005), a recent in-depth study used long-term continuous culturing in bioreactors showed that anammox bacteria are actually inhibited by penicillin and lysozyme (Hu et al, 2013). This suggests that a previously undetected peptidoglycan-like molecule might be present in anammox bacteria. This suggestion is strengthened by the finding that the genome of the anammox bacterium *K. stuttgartiensis* encodes for almost all genes necessary for peptidoglycan biosynthesis, except for *pbp1a* and *pbp1b*. It was generally accepted that the proteins encoded by these genes are necessary for polymerization of the peptidoglycan backbone, until it was recently shown that multiple *Chlamydiae* species that lack these genes can still form a full peptidoglycan cell wall (Pilhofer et al, 2013; Liechti et al, 2014). One of the goals of the research presented in this thesis is to elucidate if a peptidoglycan-like cell wall is present in anammox bacteria. In addition, it would be interesting to study if other cell wall components, such as S-layers, are present in anammox bacteria. Other *Planctomycetes* were found to contain a proteinaceous cell wall (Liesack et al, 1986) and it is possible that proteins have a role in the cell wall of anammox bacteria as well.

Outline and aim of the study

In this part of the thesis, the cell envelope of the anammox *Planctomycete Kuenenia stuttgartiensis* was investigated. Bacterial cell envelopes consist of multiple structures that either provide the cell with its shape and structural integrity or facilitate interaction of bacteria with their environment. Combining transmission electron microscopy (TEM) with isolation, purification and structural characterization of various macromolecules, multiple previously unnoticed structures were identified in the cell envelope. This thesis presents the different structures of the cell envelope of *Kuenenia stuttgartiensis* from the outside inwards.

In **chapter 2**, a hitherto undiscovered proteinaceous surface layer was identified and characterized. In addition to describing the appearance of this S-layer using freeze-etching and TEM, an S-layer protein enrichment procedure was developed. The protein content of this fraction was analyzed and specific antibodies were generated and used for immunogold localization. Furthermore, the composition of glycans stemming from the S-layer protein were enriched and elucidated.

Chapter 3 and **chapter 4** focus on the membrane that is located underneath the S-layer, the outermost membrane. The investigations described in **chapter 3** aimed at elucidating the presence of outer membrane proteins (OMPs) in this membrane. Therefore, the purification, characterization and immunogold localization are described of a putative OMP that is highly abundant in the anammox bacterium *K. stuttgartiensis*.

Another hallmark characteristic of the Gram-negative outer membrane is the presence of lipopolysaccharide (LPS). This was investigated in **chapter 4** by studying cells that were treated with LPS targeting antibiotics with TEM and by employing different protocols to isolate and analyze LPS from whole cells. Next to the anammox bacterium *K. stuttgartiensis*, two other *Planctomycetes* were included in part of the study.

In Gram-negative bacteria a peptidoglycan layer is usually present underneath the outer membrane. Peptidoglycan was always proposed to be absent from the cell envelope of *Planctomycetes*. **Chapter 5**, however revisits this hypothesized absence of peptidoglycan making use of cryoTEM, specific peptidoglycan labeling techniques and UPLC analysis.

Chapter 6 gives an overview and discussion of the results obtained in the previous chapters. An integrative view on the anammox cell envelope is given and implications on the anammox and planctomycetal cell plan, as well as possible directions for future research are discussed.

Chapter 2

A new addition to the cell plan of anammox bacteria: *Kuenenia stuttgartiensis* has a protein surface layer (S-layer) as outermost layer of the cell

The main part has been published as:

Muriel C.F. van Teeseling[1], Naomi M. de Almeida[1], Andreas Klingl[2,3], Daan R. Speth[1], Huub J.M. Op den Camp[1], Reinhard Rachel[2], Mike S.M. Jetten[1], Laura van Niftrik[1] (2014) A new addition to the cell plan of anammox bacteria: *Kuenenia stuttgartiensis* has a protein surface layer (S-layer) as outermost layer of the cell. *J. Bacteriol* 196: 80-89.

[1]Department of Microbiology, Institute for Water and Wetland Research, Faculty of Science, Radboud University, Nijmegen, the Netherlands.
[2]Centre for Electron Microscopy, Institute for Anatomy, University of Regensburg, Regensburg, Germany.
[3]present address: Plant Development, Biocenter of the LMU Munich, Planegg-Martinsried, Germany.

Additional information concerning the S-layer glycans is included in this chapter. The authors involved in this part of the study are:

Muriel C.F. van Teeseling[1], Daniel Maresch[2], Cornelia Rath[3], Hans J.C.T. Wessels[4], Andreas Hofinger-Horvath[5], Friedrich Altmann[2], Paul Kosma[5], Christina Schäffer[3], Paul Messner[3], Mike S.M. Jetten[1], Laura van Niftrik[1]

[1]Department of Microbiology, Institute for Water and Wetland Research, Faculty of Science, Radboud University, Nijmegen, the Netherlands.
[2] Division of Biochemistry, Department of Chemistry, Universität für Bodenkultur Wien, Vienna, Austria.
[3] NanoGlycobiology Unit, Department of NanoBiotechnology, Universität für Bodenkultur Wien, Vienna, Austria.
[4]Nijmegen Centre for Mitochondrial Disorders, Centre for Proteomics, Glycomics and Metabolomics, Laboratory of Genetic, Endocrine, and Metabolic Disease, Department of Laboratory Medicine, Radboud University Medical Centre, Nijmegen, the Netherlands.
[5]Division of Organic Chemistry, Department of Chemistry, Universität für Bodenkultur Wien, Vienna, Austria.

Abstract

Anammox bacteria perform **an**aerobic **amm**onium **ox**idation (anammox) and have a unique compartmentalized cell consisting of three membrane-bound compartments (from inside outwards): anammoxosome, riboplasm and paryphoplasm. The cell envelope of anammox bacteria has been proposed to deviate from typical bacterial cell envelopes by lacking both peptidoglycan and a typical outer membrane. However, the composition of the anammox cell envelope is presently unknown. Here, we investigated the outermost layer of the anammox cell and identified a proteinaceous surface (S-) layer (a crystalline array of protein subunits) as the outermost component of the cell envelope of the anammox bacterium *Kuenenia stuttgartiensis*. This is the first description of an S-layer in the phylum of the *Planctomycetes* and a new addition to the cell plan of anammox bacteria. This S-layer showed hexagonal symmetry with a unit cell consisting of six protein subunits. The enrichment of the S-layer from the cell led to a 160 kDa candidate protein, Kustd1514, which has no homology to any known protein. This protein is present in glycosylated form and (at least) two different *O*-linked glycans, present in multiple variants, are attached to the protein. Antibodies were generated against the glycoprotein and used for immunogold localization. The antiserum localized Kustd1514 to the S-layer and thus verified that this protein forms the *K. stuttgartiensis* S-layer.

Introduction

Anammox bacteria are able to perform **an**aerobic **amm**onium **ox**idation, thereby converting ammonium and nitrite to dinitrogen gas (van de Graaf et al, 1995; Strous et al, 1999). Anammox bacteria are applied in wastewater treatment to remove ammonium from wastewater (Kartal et al, 2010) and play an important role in the biological nitrogen cycle (Jetten et al, 2009; Lam & Kuypers, 2011). They comprise five genera (which all have a "*Candidatus*" status, since they are described from phylotypes that are not in pure culture) that belong to the phylum of *Planctomycetes* in the order of Brocadiales (Jetten et al, 2010). The species *Kuenenia stuttgartiensis* is the most extensively studied anammox bacterium and its genome (Strous et al, 2006), proteome and metabolism (Kartal et al, 2011b) have been described previously. Functional gene analysis remains difficult since no genetic system is available for anammox bacteria.

The phylum of the *Planctomycetes* is known for encompassing strikingly complex cell plans involving multiple cellular compartments and extensive membrane invaginations (Lindsay et al, 2001). Currently, the cell organization of *Planctomycetes* is under debate (Lieber et al, 2009; Yee et al, 2012; Speth et al, 2012; Santarella-Mellwig et al, 2013). Even within this phylum, the cell biology of anammox bacteria is remarkable, since the anammox cells are divided in no less than three compartments, separated by bilayer membranes (Fig. 1). The inner compartment, the anammoxosome, is a so-called "prokaryotic organelle" (van Niftrik et al, 2004; van Teeseling et al, 2013) in which the anammox reaction is assumed to take place. During the anammox reaction (Strous et al, 2006; Kartal et al, 2011b; Kartal et al, 2013), a proton motive force (*pmf)* is established over the anammoxosome membrane. Membrane-bound ATPases could utilize this *pmf* for ATP production in the riboplasm. The riboplasm (which is topologically equivalent to the 'pirellulosome' compartment in non-anammox

planctomycete species) is the compartment that surrounds the anammoxosome and it contains ribosomes and the nucleoid, thereby resembling the classical bacterial cytoplasm. The function of the outermost, apparently ribosome-free compartment, the paryphoplasm, has not yet been elucidated.

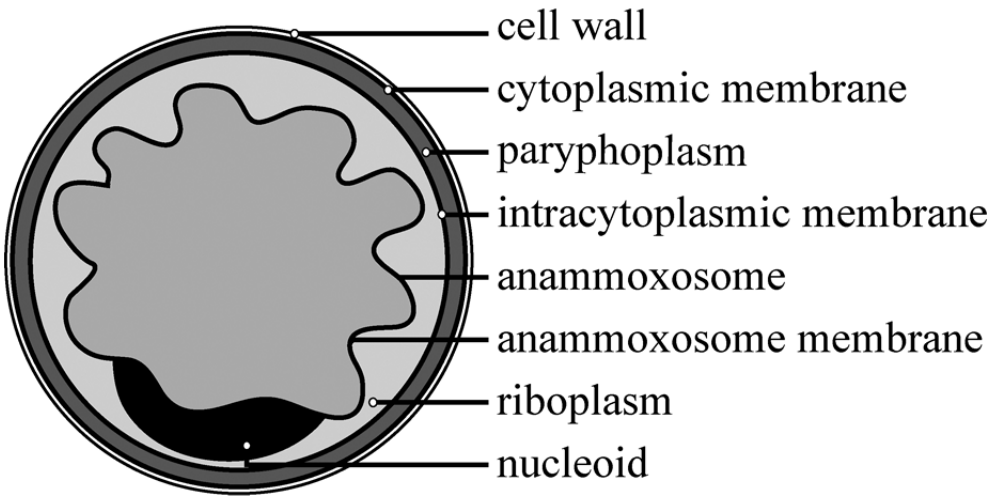

Figure 1. *Proposed cell plan of the anammox cell showing the three different compartments and their surrounding membranes. The riboplasm compartment has been defined pirellulosome in* Planctomycetes*.*

The composition of the cell envelope which encloses the paryphoplasm is unknown but has been proposed to deviate from both the typical Gram-positive and Gram-negative bacterial cell envelope type because it is proposed to lack both peptidoglycan (Jetten et al, 2003) and a typical outer membrane. The proposed lack of peptidoglycan is based on (a) the close relationship of anammox bacteria to other *Planctomycetes* where the cell wall composition has been chemically analyzed (König et al, 1984; Liesack et al, 1986) and (b) on the fact that not all genes necessary for the biosynthesis of peptidoglycan are present in the genome. Interestingly, most peptidoglycan biosynthesis genes are encoded in the genome, except those encoding the penicillin binding proteins (PBP) 1a and 1b (Strous et al, 2006; Neumann et al, 2013) that are required for polymerization of peptidoglycan precursors into polymeric peptidoglycan. Although in the transcriptome a small number of reads is found for all peptidoglycan genes, none of their respective proteins, besides the protein D-alanine-D-alanine ligase (Ddl), could be detected in the *K. stuttgartiensis* proteome (Kartal et al, 2011b). Peptidoglycan is proposed to contribute to the integrity of the cell and, in some cases, to the maintenance of cell shape (van Heijenoort, 2001). This raises the question whether the cell envelope of anammox bacteria contains another structure that helps maintaining the integrity of the cell. It is therefore of high interest to investigate the cell envelope of anammox bacteria in more detail.

Another interesting feature of the anammox cell plan is the outermost membrane, which surrounds the paryphoplasm. This membrane has been defined as a cytoplasmic membrane, which is also consistent with the immunogold localization of an ATPase to this membrane

(van Niftrik et al, 2010). However, several outer membrane proteins and key proteins in the outer membrane biosynthesis have been detected in both the genome and proteome of two anammox species (Strous et al, 2006; van Niftrik et al, 2010; Kartal et al, 2011b; Speth et al, 2012), although none of these have yet been localized to any particular cell structure. At the moment, the identity of the cytoplasmic membrane of anammox bacteria remains under debate and needs further investigation.

In Gram-negative and Gram-positive bacteria as well as Archaea, a proteinaceous S-layer can be present as the outermost component of the cell envelope (Sleytr, 1978; Beveridge, 1981; Kandler & König, 1985; Klingl et al, 2013). S-layers constitute a 2D crystalline array of (usually) identical protein subunits covering the entire cell surface. The regular pattern as formed by the S-layer can exist in oblique (p1, p2), square (p4) or hexagonal (p3, p6) symmetry, which is dictated by the arrangement and number of protein subunits (indicated by the number behind the p) that form the single morphological unit. The (self-)assembly of the proteins into the regular pattern is thought to be driven by entropical forces (Sleytr & Messner, 1983). S-layer proteins have a broad molecular mass range between 40 and 200 kDa and isoelectric points between pH 3 and 6. These proteins typically consist of 40-60% hydrophobic amino acids (Sleytr & Messner, 1983), although S-layer proteins with a predominant amount of hydrophilic amino acids have also been described (Sumper et al, 1990). Many S-layer proteins are glycosylated (i.e. glycoproteins) by either *N*- or *O*-glycosylation (Messner & Sleytr, 1991; Sumper & Wieland, 1995; Messner & Schäffer, 2000; Eichler & Adams, 2005; Eichler, 2013). In some rare cases, both glycosylation types can be found on the same protein (Kandler & König, 1985; Schäffer et al, 2001). One clear distinction between the various S-layers on different prokaryotic cells is the anchor to the underlying cell envelope component. In Gram-positive bacteria, S-layers are linked to the underlying cell wall components including peptidoglycan and so-called secondary cell wall polymers (SCWP) (Mesnage et al, 2000; Sára, 2001; Schäffer & Messner, 2005; Messner et al, 2009; Messner et al, 2010; Messner et al, 2013). In Gram-negative bacteria, S-layers are anchored in the outer membrane (Sleytr & Messner, 1983), while in Archaea, S-layers are always found anchored in the cytoplasmic membrane (Lechner & Wieland, 1989; Engelhardt & Peters, 1998; Haft et al, 2012; Halim et al, 2013).

In the present study we investigated the cell envelope of the anammox bacterium *K. stuttgartiensis*. We found a proteinaceous S-layer as the outermost component of the cell (envelope) using transmission electron microscopy on freeze-etched cells as well as in thin sections of cryofixed, freeze-substituted and Epon-embedded cells. The S-layer was found to have a hexagonal (p6) symmetry, in which each S-layer motif is formed by six identical proteins. Enrichment of the S-layer led to the identification of a candidate S-layer glycoprotein, which was used to generate specific antibodies. In addition, S-layer glycopeptides were enriched and the composition of two different glycans was elucidated via (liquid chromatography-mass spectrometry/mass spectrometry) LC-MS/MS analysis. Immunogold localization showed the antibody to bind to the outermost rim of the cell, where the S-layer is located, and thus verified that this protein forms the S-layer.

Materials & Methods

Freeze-etching. Freeze-etching was performed as described previously (Rachel et al, 2010; Wu et al, 2012) on concentrated *Kuenenia stuttgartiensis* cells, taken from the single cell membrane bioreactor and centrifuged for 4 min at 12900 x g. The freeze-etched replicas were cleaned on 70% H_2SO_4 for 2-16 h, then twice on MilliQ water for 10 min each, picked up on copper grids and investigated via TEM (as described above).

Freeze-drying. Samples obtained after S-layer enrichment were visualized by freeze-drying, in order to investigate the presence of S-layers. After the application of 5 µl of sample to a piece of freshly cleaved mica (Baltic preparation, Niesgrau, Germany), the mica was blotted briefly on filter paper (Whatman, Dassel, Germany) and plunge frozen in liquid nitrogen. The sample was then inserted in a Cressington CFE-50 freeze-etch machine at < −170°C and a pressure of below 10^{-6} bar. The sample was heated up to -80°C and held at that temperature for 60-120 min in order to sublimate the water from the samples after which the samples were shadowed with approximately 2 nm Pt-C (angle 45°) and approximately 15 nm C (angle 90°). The replicas were floated off the mica on 70% H_2SO_4 and incubated on the acid for 1 h, then twice on MilliQ water for 10 min each, picked up on copper grids and investigated using TEM (as described above).

Cryofixation, freeze-substitution, Epon-embedding and sectioning. Cryofixation, freeze-substitution, Epon-embedding, sectioning and imaging via TEM were performed as described previously (Wu et al, 2012).

Image processing. Fast Fourier Transform (FFT) power spectra of freeze-etched *K. stuttgartiensis* cells displaying S-layers were acquired using the real-time FFT option in EM-MENU (Version 4, Tietz Video & Image Processing Systems GmbH, Gauting, Germany). Correlation averaging images, showing the noise-reduced S-layer lattice, and relief reconstruction images, representing the height distribution of a small piece of S-layer lattice, were made using the SEMPER software package (Saxton, 1996) according to the previously described methods (Engelhardt, 1988) or using the Animetra Crystals software (Fuchs et al, 1995).

Library preparation, sequencing and data analysis. Sequencing of the *K. stuttgartiensis* continuous culture was performed on occasion, in order to check for changes after the initial genome sequencing (Strous et al, 2006). All kits mentioned in this paragraph were obtained from Life technologies (Life technologies, Carlsbad, CA, USA). Genomic DNA was sheared for 5 minutes using the Ion Xpress™ Plus Fragment Library Kit following the manufacturer's instructions. Further library preparation was performed using the Ion Plus Fragment Library Kit following manufacturer's instructions. Size selection of the library was performed using an E-gel 2% agarose gel, resulting in a median fragment size of 331 bp. Emulsion PCR was performed using the Onetouch 200 bp kit and sequencing was performed on an IonTorrent PGM using the Ion PGM 200 bp sequencing kit and an Ion 316 chip. The resulting 2.33 million reads with an average length of 187 bp were quality trimmed and assembled using default settings of the CLC genomics workbench (v6.04, CLCbio, Aarhus, Denmark). Contigs were assigned to *K. stuttgartiensis* based on coverage. Comparison with the reference draft

genome (NCBI PRJNA16685) was performed using the read mapper and BLASTn as implemented in the CLC genomics workbench (v6.04, CLCbio, Aarhus, Denmark).

S-layer enrichment. Cells were harvested from a *K. stuttgartiensis* single cell membrane bioreactor at an OD_{600} of 1.1 and were centrifuged for 10 min at 4000 x g to concentrate them 40-fold in their original growth medium (Kartal et al, 2011a). Cells were then stored at -80°C and thawed just before the S-layer enrichment procedure. The procedure of freezing and thawing already partially disrupts the cells. The concentrated cells were resuspended in 20 mM HEPES buffer pH 7.5 (including 15 mM $NaHCO_3$, 2 mM $CaCl_2$ and 0.8 mM $MgSO_4$), after which the protease inhibitor PMSF and DNAse II were added to final concentrations of 24 mg/l and 6.0 10^{-5} mg/ml, respectively. The cells were then further disrupted using a Potter homogenizer (50 strokes) and the disrupted cells were left at RT for 20 min (DNAse incubation time). After this incubation, the detergent Triton-X100 was added to a final concentration of 0.5% (v/v) and the disrupted cells were incubated for 30 min at RT. The enriched S-layers were then pelleted by centrifugation at 31000 x g for 20 min. The pellet was resuspended in the HEPES buffer described above and washed three times by centrifuging at 20800 x g for 15 min and resuspending in HEPES buffer each time. The final pellets were resuspended in a small amount of buffer. This sample was analyzed by SDS-PAGE as well as TEM after freeze-etching using a Philips CM 12 (FEI, Eindhoven, the Netherlands) operated at 120 kV. Dominant bands in the SDS-PAGE were cut out of the SDS gel to be analyzed by matrix-assisted laser desorption/ionization time of floght (MALDI-TOF) MS and LC-MS/MS.

SDS-PAGE. Samples obtained by S-layer enrichment were denatured by incubation of the proteins for 7 min at 100°C with 158 mM Tris-HCl buffer pH 7 containing 5% β-mercaptoethanol, 2.6% sodium dodecyl sulfate (SDS) and 16% glycerol. SDS polyacrylamide gel electrophoresis (SDS-PAGE) was performed on 8% slab gels in the running buffer described previously (Laemmli, 1970). After separation of the proteins, gels were either stained with Coomassie Brilliant Blue (G250) to visualize the proteins or with Periodic Acid Schiff's (PAS) reagent to visualize glycoproteins (Segrest & Jackson, 1972). Gels for PAS were first fixed in 40% ethanol and 5% acetic acid for 30 min, followed by an oxidation step in 0.7% periodic acid in 5% acetic acid for 120 min and a reduction step in 0.2% sodium metabisulfite in 5% acetic acid for 30 min. Staining was performed for 18 h in Schiff's reagent (Carl Roth, Karlsruhe, Germany) and rendered the possible glycoproteins a magenta colour.

MALDI-TOF MS and LC-MS/MS of protein bands. Bands cut out of the SDS-PAGE gels were prepared for MS analysis by alternately washing the gel pieces in acetonitrile and then in 50 mM ammonium bicarbonate buffer, followed by reduction in a 10 mM dithiothreitol (DTT) solution and alkylation in 50 mM 2-chloroacetamide (Nielsen et al, 2008) in 50 mM ammonium bicarbonate buffer. Trypsin digestion was performed overnight using 12.5 ng/µl trypsin in 50 mM ammonium bicarbonate buffer. The peptides were extracted from the gel pieces using a mix of 0.05% trifluoroacetic acid and 50% acetonitrile. For MALDI-TOF MS, the samples were applied to a MALDI plate and analyzed using a Bruker Biflex III MALDI-TOF MS (Farhoud et al, 2005). For LC-MS/MS, the gel pieces were analyzed as described previously (Wessels et al, 2009). Proteins were identified using the MASCOT search tool (Matrix Science,

London, United Kingdom) and a database of the *K. stuttgartiensis* predicted proteome available at Genoscope (https://www.genoscope.cns.fr/agc/microscope/export/export.php?format=Prot&S_id=260).

Enrichment and analysis of glycopeptides from enriched S-layer proteins. S-layers were enriched from cells concentrated in their original growth medium (van de Graaf et al, 1995) that were then frozen at -20˚C. These cells were thawed and resuspended in 20 mM phosphate buffer pH 7 with 750 mM 6-amino caproic acid. After breaking the cells by a French press (three passages at 138 MPa) and removing the unbroken cells by centrifugation ((4500 g, 15 min), the membrane fraction (including the S-layer protein), was collected after ultracentrifugation (184000 g, 60 min). The membrane fraction was washed three times and lyophilized until further use. The lyophilized membrane fraction was resuspended in 50 mM Tris HCl pH 7.5 and dialysed for 36 h at 25˚C and 12 h at 4˚C in a 12-14 kDa dialysis tube against 50 mM Tris HCl pH 7.5 to get rid of the extensive amounts of 6-amino caproic acid. After ultracentrifugation and washing with Tris HCl pH 7.5, the pellet was resuspended in 125 mM Tris HCl pH 6.8 including 0.5% SDS and incubated at 37˚C for 75 min in order to solubilize the membranes.

Glycopeptides were obtained from the material after S-layer enrichment by digesting with pronase E (Sigma, St. Louis, MO, USA) (0.2 mg per mg pellet) at 37˚C for 16 h. Additional pronase E was added (in total ca 0.21 mg pronase per mg pellet) and the sample was incubated at 45˚C for 24 h. After pronase treatment, the sample was spun down and the volume of the supernatant was reduced on a Rotavapor and then loaded onto a gel permeation chromatography column (P-4; Bio-Rad, Hercules, CA, USA), using 0.1 mM NaCl as an eluent. Glycopeptides were further purified by another gel permeation chromatography column (P-30, Bio-Rad) using 0.1 mM NaCl as eluent, followed by a cation exchange chromatography column (Dowex 50W-X8, H^+ form, Bio-rad) using MilliQ water as an eluent (Schäffer et al, 2000).

At this stage the composition of the glycopeptides was evaluated via monosaccharide analysis performed after hydrolysis of the sample with 25% TFA at 110˚C for 4 h. Released monosaccharides were analyzed on a ICS3000 Ion Chromatograph (Dionex, Sunnyvale, CA, USA) equipped with a PA1 column (Dionex). The monosaccharides were eluted using the following program: 18 min 16 mM NaOH, in 2 min from 16 to 50 mM NaOH, 10 min at 50 mM NaOH, in 2 min from 50 mM to 200 mM NaOH and 3 min at 200 mM NaOH. In a parallel run with the same conditions, a mixture of monosaccharides was run to act as standards. The following monosaccharides were included in this run: digitoxose, fucose, 2-deoxygalactose, rhamnose, galactosamine, mannosamine, glucosamine, galactose, glucose, mannose, fructose and ribose.

As a final step of the purification, the glycopeptides were applied to a reversed phase HPLC (Ultimate 3000, Dionex) using a nucleosil 120-3C_{18} column. Elution was performed by a gradient from 0-15% acetonitrile (in 100-85% MilliQ water) in 45 min, afterwards the acetonitrile concentration was increased to 100% in 5 min, stayed at 100% for 2 min and was then gradually decreased to 0% in 6 min. After each column, elution of glycopeptides was followed by detection of carbohydrates that coloured pink after incubating a TLC plate on

which 3 µl per fraction was spotted, in a thymol solution (0.5% thymol, 95% (v/v) ethanol, 5% (v/v) sulphuric acid) for 30 sec, air drying it and incubating it at 110˚C for 10 min.

NMR spectra were recorded of the enriched glycopeptides after reversed phase HPLC using a Bruker Avance III 600 instrument (600.22 MHz for ^{1}H, 150.93 MHz for ^{13}C) at 300 K using standard Bruker NMR software. ^{1}H NMR spectra were referenced to δ 0.00 (D_2O, external calibration to 2,2-dimethyl-2-silapentane-5-sulfonic acid) ppm. ^{13}C NMR spectra were referenced to δ 67.40 (D_2O, external calibration to 1,4-dioxane) ppm. COSY experiments were recorded using the program cosygpqf, respectively, with 2048 x 256 data points and 16 and 8 scans, respectively per t1-increment. The multiplicity edited heteronuclear single quantum coherence spectrum (HSQC) was measured using the program hsqcedetgp with 1024 x 128 data points and 1024 scans per t1-increment.

Release of enriched *N*-linked glycans from S-layer proteins. S-layers were enriched as described above. To release *N*-linked glycans, the enriched S-layer protein sample was incubated with peptide-*N*-glycosidase F (PNGaseF) (0.25 µl per µl S-layer enrichment) at 37˚C for 10 h. As a negative control enriched S-layer protein was incubated without PNGaseF for 10 h at 37˚C. After the incubation, the samples were analyzed via SDS-PAGE as described above.

Release and analysis of *O*-linked glycans from S-layer protein. *O*-linked glycans were released from the S-layer protein after gel electrophoresis via β-elimination (Strecker, 1995; Schäffer et al, 2002). This was performed on SDS-PAGE gel bands with S-layer protein at an apparent molecular mass of 250 kDa. Gel bands were washed in 0.5 M sodium hydroxide by vortexing and subsequent centrifugation (short pulse). After removing the supernatant, the gel pieces were incubated overnight at 50°C in 1 M sodium borohydride in 0.5 M sodium hydroxide. The samples were loaded on a hypercarb hypersep column (25 mg bed weight; Thermo Scientific, Rockwood, TN, USA) that was cleaned with 60% acetonitrile (once) and MilliQ (twice). For cleaning, the columns were loaded and centrifuged at 155 g for 30 sec. After loading the sample on the column, the column was washed with MilliQ (in both steps centrifugation was performed at 68 g, 30 sec). The glycans were eluted by washing with 60% acetonitrile (155 g, 30 sec) and dried in the speed vac.

The glycan mixture was analyzed using an Ultimate 3000 liquid chromatography system (Dionex) directly linked to an amaZon seed ETD iontrap (Bruker, Billerica, MA, USA) equipped with the standard ESI source in the positive ion, DDA mode (= switching to MSMS mode for eluting peaks), ICC 100000, 200 msec, enhanced resolution. MS-scans were recorded (range: 400-1650 Da) and the 10 highest peaks were selected for fragmentation. Instrument calibration was performed using ESIcalibration mixture (Agilent, Santa Clara, CA, USA). For separation of the glycans a Hypercarb column (0.32 × 150 mm) (Thermo Scientific) was used. A gradient from 99% solvent A (65 mM ammonium formiate buffer) and 1% solvent B (100% ACCN) to 21% B in 45 min was applied, followed by a 15 min gradient from 21% B to 50% B, at a flow rate of 6 µl/min.

Antibody generation. The antiserum containing the antibodies against the putative S-layer protein Kustd1514 were generated against protein bands cut out of an SDS-PAGE gel. For this

purpose, a sample obtained after S-layer enrichment was loaded on an 8% SDS-PAGE gel that was stained and destained with solutions that included EtOH instead of MetOH. The band corresponding to a protein of approximately 250 kDa (Kustd1514) was cut out and sent in to Davids Biotechnology (Regensburg, Germany) for immunization of rabbits. To verify the contents of this protein band, one band from the same gel was analyzed by LC-MS/MS.

Immunoblotting. Blots were made from 8% SDS-PAGE gels containing cell-free extract of *K. stuttgartiensis* cells. These were prepared by harvesting *K. stuttgartiensis* by centrifugation, after which the cell pellet was resuspended in one volume of 20 mM potassium phosphate buffer (pH 7.0). The cells were passed through a French press at 138 MPa in three passages and centrifuged at 4°C for 15 min at 2200 x g. The resulting supernatant was the cell-free extract containing *K. stuttgartiensis* proteins. This cell-free extract was boiled for 7 min in sample buffer (as described above) and an amount of 20 µg protein per lane was loaded onto 8% SDS-PAGE gels. After separation, the proteins were transferred from the gel to a Protran nitrocellulose transfer membrane with pore size 0.45 µm (Whatman, Dassel, Germany) with the semi-dry transfer cell blotting system (Bio-Rad, Veenendaal, the Netherlands). Two different blotting buffers were used, both consisting of 48 mM Tris and 39 mM glycine. The buffer in which the gel was incubated had an additional 0.05% SDS, the one that was used for the membrane contained 20% methanol. The blotting was performed at 50 mA for 60 min at room temperature and afterwards, dried blots were stored at 4°C.

Immunoblotting was performed on blots that were incubated in deionized water (dH_2O) for 30 min and afterwards for 30 min in protein-free (TBS) blocking buffer (Thermo Scientific, Rockford, USA). The blots were then incubated 60 min in antiserum diluted 1000-fold in blocking buffer. Two negative controls were performed; instead of antiserum, one was incubated in blocking buffer and the other was incubated in pre-immune serum diluted 1000-fold in blocking buffer. The blots were then washed three times 10 min in TBS containing 0.05% Tween and incubated for 60 min in monoclonal mouse anti-rabbit IgG alkaline posphatase conjugate (Sigma, Zwijndrecht, The Netherlands) diluted 150000-fold in blocking buffer. The blots were then washed two times 10 min in TBS containing 0.05% Tween and two times 10 min in 10 mM TBS containing 8% NaCl and 0.2% KCl and finally incubated in BCIP/NBT liquid substrate system (Sigma, Zwijndrecht, The Netherlands) for 9 min and rinsed 10 min in dH_2O. All lanes were imaged with the same settings.

Immunogold localization. Samples for immunogold localization were prepared using the rehydration method (van Donselaar et al, 2007) as described previously (van Niftrik et al, 2010). In short, high-pressure frozen cells were freeze-substituted in acetone containing 0.5% glutaraldehyde, 0.1% uranyl acetate and 1% H_2O, rehydrated in a graded acetone series on ice, embedded in gelatin, cut into small cubes, infiltrated with sucrose and frozen in liquid nitrogen. Ultrathin cryosections (65 nm) were cut using a UC7/FC7 cryo-ultramicrotome (Leica Microsystems, Vienna, Austria) and picked up with a drop of 1% methylcellulose and 1.15 M sucrose in PHEM buffer (60 mM PIPES, 25 mM HEPES, 10 mM EGTA, 2 mM MgCl2, pH 6.9) and transferred to carbon-formvar-coated grids.

Grids containing ultrathin cryosections of *K. stuttgartiensis* cells were washed for 30 min at 37°C on PHEM and for 10 min at room temperature in drops of PHEM containing 20 mM glycine. Blocking was achieved by incubation on drops of PHEM containing 1% BSA for 15 min, after which the grids were incubated for 60 min with antiserum diluted 100-fold in PHEM containing 1% BSA. Negative controls were incubated in PHEM containing 1% BSA without antiserum for 60 min. In an additional control, grids were incubated with pre-immune serum instead of antiserum. After this incubation, the grids were washed for 11 min on drops of PHEM with 1% BSA and incubated for 20 min with the secondary antibody, protein A coupled to 10 nm gold (PAG-10, CMC UMC Utrecht), diluted 70-fold in PHEM with 1% BSA. The grids were then washed 5 min on drops of PHEM with 1% BSA and 10 min on drops of PHEM. The cryosections on the grids were fixed by incubating for 5 min on drops of 1% glutaraldehyde in PHEM and were consequently washed for 10 min on drops of MilliQ water. Post-staining was performed by incubating 5 min in 2% uranyl acetate in 0.15 M oxalic acid set to pH 7.0 with 30% ammonium hydroxide, after which the grids were quickly washed on two drops of water. The grids were then immediately washed on two drops of 1.8% methylcellulose containing 0.4% aqueous uranyl acetate on ice. The sections were embedded by incubating 5 min on ice on a drop of methylcellulose containing uranyl acetate. After air drying the sections, the grids containing labeled cryosections were investigated at 100 kV in a JEOL (Tokyo, Japan) JEM-1010 TEM. Images were recorded using the SIS Mega View III camera (Olympus, Münster, Germany).

Results

An S-layer with hexagonal symmetry is present on *K. stuttgartiensis* cells. *K. stuttgartiensis* single cells were freeze-etched and visualized via transmission electron microscopy (TEM) to investigate the outermost layer of the cell. The freeze-etched *K. stuttgartiensis* cells clearly showed S-layers with a hexagonal symmetry (Fig. 2A,C) on top of the cytoplasmic membrane (Fig. 2D). The Fast Fourier Transform (FFT) power spectra confirmed the regular structure of the S-layer (Fig. 2B) and the hexagonal symmetry. Analysis of the FFT power spectra showed a center-to-center spacing between the S-layer unit cells of about 20 nm, which fits in the range of 2.5-35 nm that is typical for S-layers (Sleytr & Messner, 1983). With the use of correlation averaging, the S-layer fine structure and lattice can be visualized with a higher signal-to-noise ratio (Engelhardt, 1988). Through these analyses (Fig. 3A) it became apparent that each S-layer unit cell consisted of six protein densities surrounding a central pore. This was further visualized by a relief reconstruction (Guckenberger, 1985) resulting in a three-dimensional model of the surface of the S-layer (Fig. 3B). The relief reconstruction showed that the protein densities appear cylindrical. Both the correlation averaging and the relief reconstruction are consistent with hexagonal p6 symmetry, although p3 symmetry cannot be excluded at the present level of resolution.

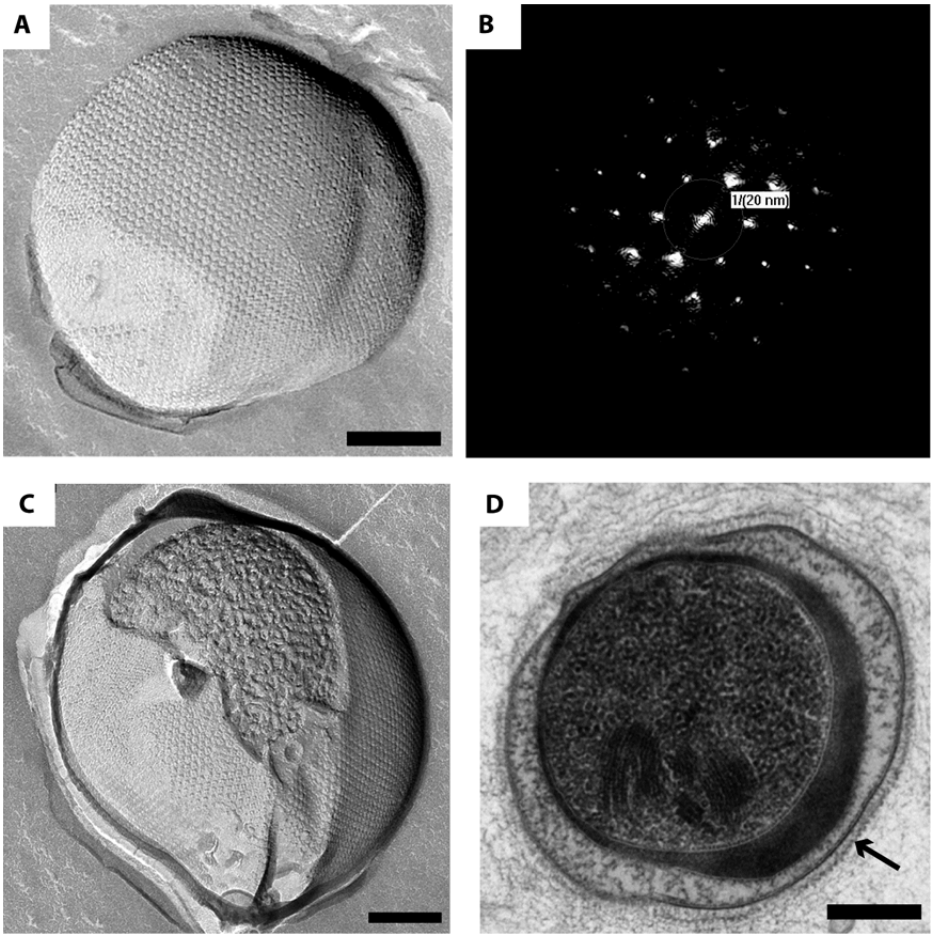

Figure 2. K. stuttgartiensis *cells display S-layers as observed by TEM after multiple types of sample preparation. A.* K. stuttgartiensis *cells are covered by a hexagonal S-layer as observed after freeze-etching. B. The FFT power spectrum of a part of the S-layer seen in panel A reflects the regular pattern of the S-layer. The p6 symmetry and center-to-center spacing of 20 nm for the S-layer of* K. stuttgartiensis *are reflected by the FFT power spectrum. C. A freeze-fracture through the S-layer gives an inside into the* K. stuttgartiensis *cell underneath. D. The S-layer (indicated by the arrow) forms a zigzag layer on top of the outermost membrane in* K. stuttgartiensis *cells that were cryofixed, freeze-substituted in acetone containing 2% osmium tetroxide, 0.2% uranyl acetate and 1% water, Epon-embedded and thin sectioned. Scale bars: 200 nm.*

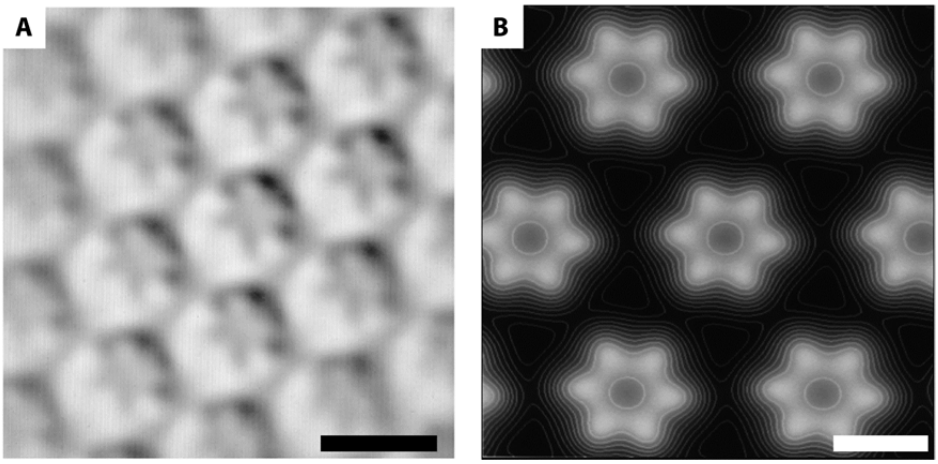

Figure 3. *The S-layer of* K. stuttgartiensis *visualized by image processing. A. Correlation averaging shows that the S-layer of* K. stuttgartiensis *has hexagonal symmetry with a unit cell consisting of six protein densities surrounding a central pore. Scale bar: 20 nm. B. Relief reconstruction gives an impression of the surface of the S-layer in three dimensions. White represents high and black represents low areas. Scale bar: 10 nm.*

Identification of Kustd1514 as the protein that forms the S-layer. To investigate which protein forms the observed S-layer of *K. stuttgartiensis*, the S-layer was enriched from whole cells. After treating the cells with a Potter homogenizer and the detergent Triton-X100, (patches of) S-layers were present as visualized by TEM of freeze-dried samples (Fig. 4). In addition to the S-layers, membrane patches were also present as seen with negative staining (data not shown). The protein composition of the sample obtained by S-layer enrichment was analyzed by SDS-PAGE and subsequent MALDI-TOF MS and LC-MS/MS analysis. When comparing the crude extract (Fig. 5A) to the S-layer enrichment (Fig. 5B), only two major proteins and two less abundant proteins were detected (next to some minor bands) in the S-layer enrichment (Fig. 5B). MALDI-TOF MS and LC-MS/MS analysis and subsequent searches (Mascot, Matrix science) resulted in significant matches. The protein at about apparent 250 kDa was identified as Kustd1514 (Kustd stands for: contig d from *Kuenenia stuttgartiensis)* and the protein at about 55 kDa as the putative outer membrane protein (OMP) Kustd1878 which has a predicted β-barrel structure, which is characteristic for OMPs (Speth et al, 2012; also see chapter 3 of this thesis). The protein bands at approximately 160 and 210 kDa were both found to contain significant amounts of Kustd1514 as well.

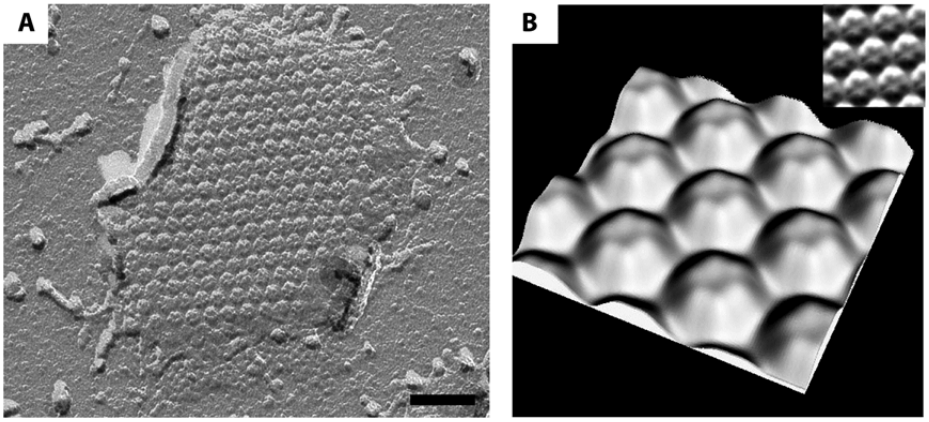

Figure 4. *S-layer patches were present after S-layer enrichment of* K. stuttgartiensis*. A. S-layer patch with typical hexagonal symmetry observed by freeze-drying. B. A three-dimensional model of the isolated S-layer shows the same relief as observed for the S-layers present on* K. stuttgartiensis *cells. Inset: correlation averaging used to come to the three-dimensional representation. Scale bar: 70 nm.*

Sequencing of the *K. stuttgartiensis* enrichment culture (that was continuously run in bioreactor systems over the period described) used for all experiments described here has been performed at two time points, namely in 2002 (accession number: NCBI Bioproject 16685) (Strous et al, 2006) and in 2012 (NCBI Bioproject PRJEB4259, which is the sequence obtained as described in the Materials and Methods and is thus first published with this publication). There are indications that during cultivation, the Kustd1514 protein sequence has undergone a sequence change at the amino acid level in part of the *K. stuttgartiensis* population since the initial metagenome analysis. Compared to the original sequence (Strous et al, 2006), the 43 amino acids at the N-terminus and 759 amino acids at the C-terminus of the new sequence are identical. For the remaining 672 amino acids between N- and C-terminus and for the 116 amino acids that are at the end of the C-terminus identities of respectively 43% and 77% have been determined. Currently, proteins with both Kustd1514 sequences (74% protein sequence identity for the total sequence as determined by the PIR pairwise alignment tool: http://pir.georgetown.edu/pirwww/search/pairwise.shtml) are present in the *K. stuttgartiensis* membrane bioreactor and detected in all three Kustd1514 protein bands from the S-layer enrichment as determined by LC-MS/MS analysis. Both proteins are similar concerning their characteristics (as listed below) and therefore the protein encoded by the original sequence (Strous et al, 2006) was used for further (bioinformatics) analysis.

Kustd1514 is glycosylated. The detection of Kustd1514 at different apparent molecular masses in the SDS-PAGE gel suggested that this protein might be present in multiple post-translationally modified states. This is supported by the predicted molecular mass for Kustd1514 (using the ExPASy compute pI/Mw tool: http://web.expasy.org/compute_pi/). Kustd1514 is predicted to consist of 1591 aa (Uniprot) for the total protein and the predicted molecular mass is 160 kDa for the protein after processing of the predicted 35 aa long signal peptide (predicted by SignalP 4.1 (Petersen et al, 2011)). This predicted molecular mass of

160 kDa matches the lowest of the three Kustd1514-containing bands observed in the SDS-PAGE gel. Glycosylation is the most common post-translational modification for S-layer proteins (Ristl et al, 2010). Therefore, a glycan detecting Periodic Acid Schiff's (PAS) stain (Segrest & Jackson, 1972) was performed on an SDS-PAGE gel containing enriched S-layers, which confirmed glycosylation of Kustd1514 (Fig. 5C).

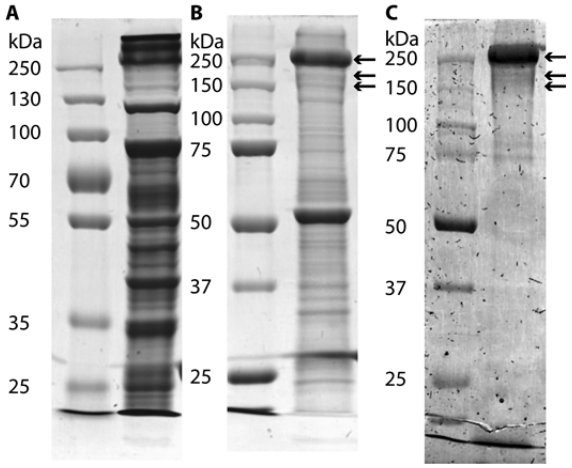

Figure 5. *Analysis of crude extract and enriched S-layers of* K. stuttgartiensis *with SDS-PAGE. A. SDS-PAGE gel stained with Coomassie G shows all proteins present in the* K. stuttgartiensis *crude extract. B. SDS-PAGE gel stained with Coomassie G shows the proteins present after S-layer enrichment. C. SDS-PAGE gel stained with Periodic Acid Schiff's reagent shows glycoproteins present after S-layer enrichment. Arrows indicate protein bands in which Kustd1514 was detected via LC-MS/MS analysis.*

Glycopeptides from enriched S-layer proteins. As the glycosensitive PAS stain after S-layer protein enrichment (Fig. 5C) showed that the S-layer band (at an apparent mass of about 250 kDa) was by far the most abundant glycoprotein, this sample was used as starting material for enrichment of S-layer glycopeptides. For this purpose the protein content of this sample was degraded by pronase E and glycans with small peptides attached were enriched via size exclusion and ion exchange column chromatography. The monosaccharide analysis showed these enriched glycopeptides contained glucose, mannose, galactosamine (GalN) and galactose in the ratio 5.4: 3: 1.6: 1 and revealed small amounts of fucose and glucosamine (GlcN). Furthermore, also some smaller peaks were observed but specific sugars could not be assigned to these peaks. NMR analysis of the glycopeptide sample further purified by an additional (reversed phase) chromatography step showed that the glycopeptide sample was quite heterogeneous. However, the presence of 6-deoxy-protons (which could belong to fucose) and acetyl signals probably originating from *O*- or *N*-acetylated hexoses (e.g. *N*-acetylgalactosamine (GalNAc) or *N*-acetylglucosamine (GlcNAc)) could be observed.

S-layer glycoproteins are probably not *N*-linked. To test if the S-layer glycans were *N*-linked to the protein, the enriched S-layer glycoprotein was treated with PNGaseF, an enzyme that specifically cleaves N-linked glycans from the protein. SDS-PAGE demonstrated that

incubation with PNGaseF did not cleave the glycoprotein, since the pattern on an SDS gel was quite identical to that for a sample that was not incubated with PNGaseF (Fig. 6).

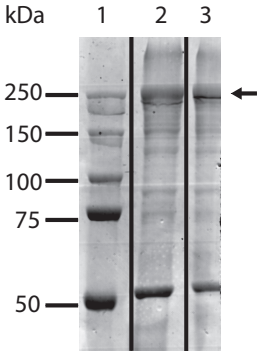

Figure 6. *SDS-PAGE analysis of* K. stuttgartiensis *S-layer protein enrichment incubated 10 h at 37°C with (lane 2) and without (lane 3) PNGaseF showed that no* N*-linked glycans were cleaved off the S-layer glycoprotein (indicated with the arrow).*

LC-MS/MS analysis shows *O*-linked S-layer glycans. *O*-linked glycans were chemically cleaved via ß-elimination from the S-layer glycoprotein (at apparent mass of 250 kDa, cut out of an SDS gel). The glycans released with this protocol were analyzed via LC-MS/MS. This analysis showed two main glycans, both present in multiple variants (Fig. 7). The most abundant glycan was found in two variants of which one (Fig. 7; peak cluster 2) contained an additional *N*-acetlyhexosamine (HexNAc) compared to the other, most abundant, variant (Fig. 7; peak cluster 1). The second glycan was present in three variants and the difference between the variants was the presence of one or two additional HexNAc residues (Fig. 7; peak cluster 3-5). It was concluded that each of these variants was present in multiple methylated states, since multiple peaks with a difference of 14 Da were observed (Fig. 7). In addition, several chains of multiple hexoses were observed. It is not clear if these stem from the protein or if these are an artifact of the sample preparation.

The glycan assigned as 2 had a total mass of 1027.6 Da and was either composed of two HexNAcs, one hexose (Hex) and three deoxyhexoses (dHexs) or of two HexNAcs, two Hexs, one dHex and one dideoxyhexose (ddHex). The fragmentation of this peak showed the presence of one dHex, one Hex and from the pattern it can be concluded that this glycan is attached to the protein with a HexNAc to which a Hex is coupled (Fig. 8). From the fragments of the peak at 1041.6 Da, which is the same structure as the peak at 1027.6 Da with a methyl group in addition, it became clear that the Hex is the residue that is methylated (spectrum not shown).

The structure resulting in the peak assigned with 3 had a mass of 573.5 Da and probably contains two HexNAcs and one dHex. MS^2 fragmentation spectra were not of high enough quality to confirm this composition. The variants of this glycan have been observed to contain up to four methyl groups.

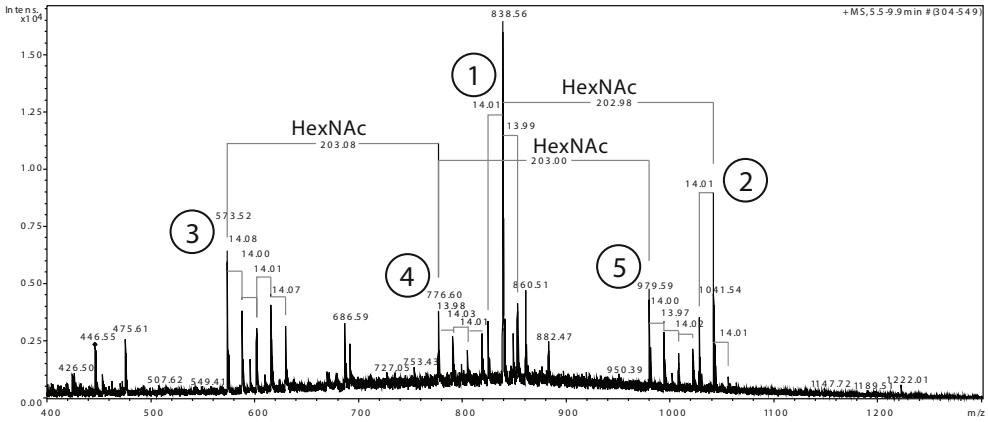

Figure 7. *MS spectrum of glycans obtained after ß-elimination of* K. stuttgartiensis *Kustd1514 gel pieces eluted after 5.5-9.9 min from the LC showed five main peaks: peak 1 and 2 are related (peak 2 contains an additional HexNAc) and peak 3, 4 and 5 are also related (again an additional HexNac between peak 3 and 4, and between peak 4 and 5). For each peak multiple methylation states were observed; each additional methyl group that is coupled adds a mass of 14 Da.*

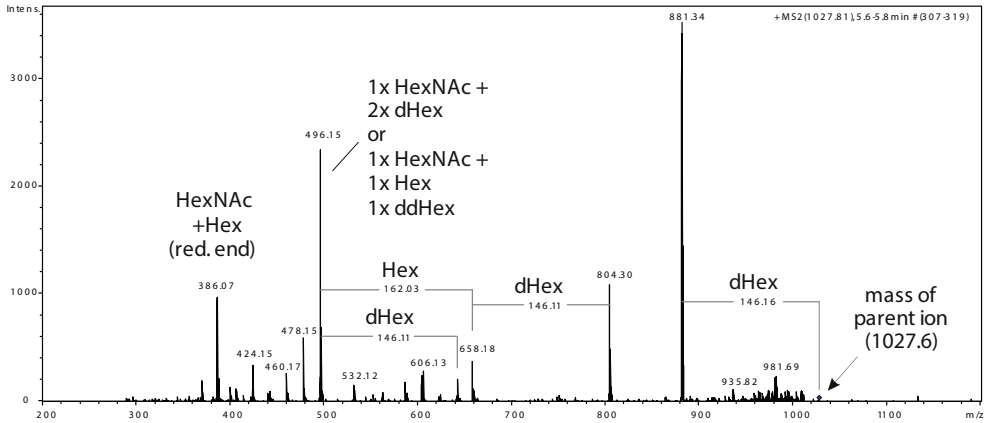

Figure 8. *MS^2 spectrum showing fragments of the unmethylated glycan shown in peak 2 of Fig. 7 that was obtained after ß-elimination of* K. stuttgartiensis *Kustd1514 gel pieces. A fragment consisting of a HexNAc and an Hex with the reducing end (m/z 386.1), meaning that this fragment was attached to the protein, was observed. In addition, a fragment of the entire molecule without a dHex (m/z 881.3) was observed. Another fragment containing either a HexNAc and two dHex residues, or a HexNac, a Hex and a ddHex was found (m/z 496.2); this fragment was also observed with an additional Hex and/or an additional dHex.*

Secondary structure of Kustd1514. The Kustd1514 protein shows no primary sequence similarity to other known (S-layer) proteins, as indicated by the lack of significant hits using BLAST (McGinnis & Madden, 2004) and PSI-BLAST (Altschul et al, 1997) searches: all hits with an e-value of < 10^{-10} are from *K. stuttgartiensis* and have a maximum query coverage of 25%. The amino acid composition of Kustd1514 is in many aspects different from the typical S-layer protein: 49.5% of the amino acids is hydrophilic (due to the abundance in serine (12.4%) and threonine (14.5%)) and only 29.7% is hydrophobic (typical value for S-layer proteins would be 40-60%). The predicted pI of Kustd1514 of 4.39 (using the ExPASy compute pI/Mw tool) fits with the typical values for S-layer proteins (pI between 3 and 6) (Sleytr & Sára, 1997). When comparing the predicted secondary structure of Kustd1514 to other proteins via HHpred (Söding, 2005; Hildebrand et al, 2009), the only hits that are found target the last 300 amino acids of the protein. When looking at the full length secondary structure prediction of Kustd1514 using PSIPRED (Buchan et al, 2010), it is noteworthy that only 2.1% of the structure is predicted to consist of α-helices, which is clearly lower than the average 20% that is reported for S-layer proteins (Sleytr, 1997). The percentage of predicted β-sheets is 44.8%, which is close to the average S-layer value of 40%. No transmembrane regions were predicted using TMHMM (Krogh et al, 2001; Sonnhammer et al, 1998). It thus becomes apparent that the S-layer protein of *K. stuttgartiensis* shows some of the global characteristics of a typical S-layer protein, but is not similar to any known protein in primary or secondary structure.

Immunogold localization verifies Kustd1514 as S-layer forming protein. The glycoprotein band at around 250 kDa obtained from the S-layer enrichment was used to immunize a rabbit in order to generate antibodies against the putative S-layer glycoprotein Kustd1514. The affinity and specificity of the antibody for the glycoprotein Kustd1514 were confirmed by immunoblotting on a blot containing *K. stuttgartiensis* cell-free extract. As expected, a specific band at approximately 250 kDa was observed after immunoblotting with the Kustd1514 antiserum (Fig. 9). This band was absent when incubations were performed with pre-immune serum or with secondary antibody only. Immunogold localization was performed using the Kustd1514 antiserum on *K. stuttgartiensis* cryosections of cells prepared via the rehydration method (van Donselaar et al, 2007). This immunogold labeling localized the Kustd1514 protein to the electron dense S-layer that forms the outermost rim of cells of *K. stuttgartiensis* (Fig. 10).

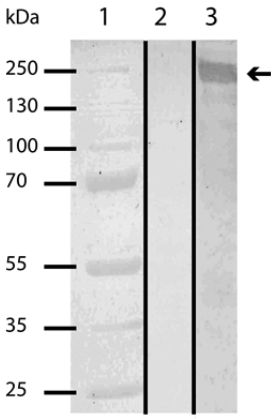

Figure 9. *Immunoblot analysis of the antiserum directed against the* K. stuttgartiensis *S-layer glycoprotein Kustd1514 tested against* K. stuttgartiensis cell-free extract*. Lane 1: Marker; lane 2: incubation with pre-immune serum; lane 3: incubation with anti-Kustd1514. Arrow: expected target size (about 250 kDa).*

Discussion

Here we have identified a glycoprotein S-layer as outermost layer of the anammox bacterium *K. stuttgartiensis*, which forms a new addition to the cell plan of anammox bacteria. The S-layer has six protein subunits per unit cell, which means that the symmetry is hexagonal (p6). The S-layer was enriched from the *K. stuttgartiensis* cells leading to the identification of a putative S-layer protein. This protein was found to be glycosylated and two *O*-linked glycans have been identified. Antibodies against this Kustd1514 protein were raised and used to localize the Kustd1514 glycoprotein to the S-layer via immunogold localization. This verified that Kustd1514 indeed forms the S-layer in *K. stuttgartiensis*.

After the S-layer enrichment, membrane patches were observed together with the S-layer. In the LC-MS/MS analysis one particular protein, the putative OMP Kustd1878 (Speth et al, 2012), was shown to be highly abundant in the S-layer enrichment. This suggests that the *K. stuttgartiensis* S-layer is relatively strongly anchored in the outermost membrane of the anammox cell. In this respect, it would be an interesting future experiment to see if the S-layer can self-assemble from isolated Kustd1514 monomers (as in (Pum et al, 1989)) without a membrane(-like) lattice underneath. The presence of Kustd1878 in the S-layer enrichment also suggests that Kustd1878 is located in the outermost membrane of *K. stuttgartiensis* but the location and function of this putative OMP need further investigation. Another interesting question to investigate is whether the S-layer proteins interact directly with Kustd1878 or instead with other proteins or molecules associated with the outermost membrane.

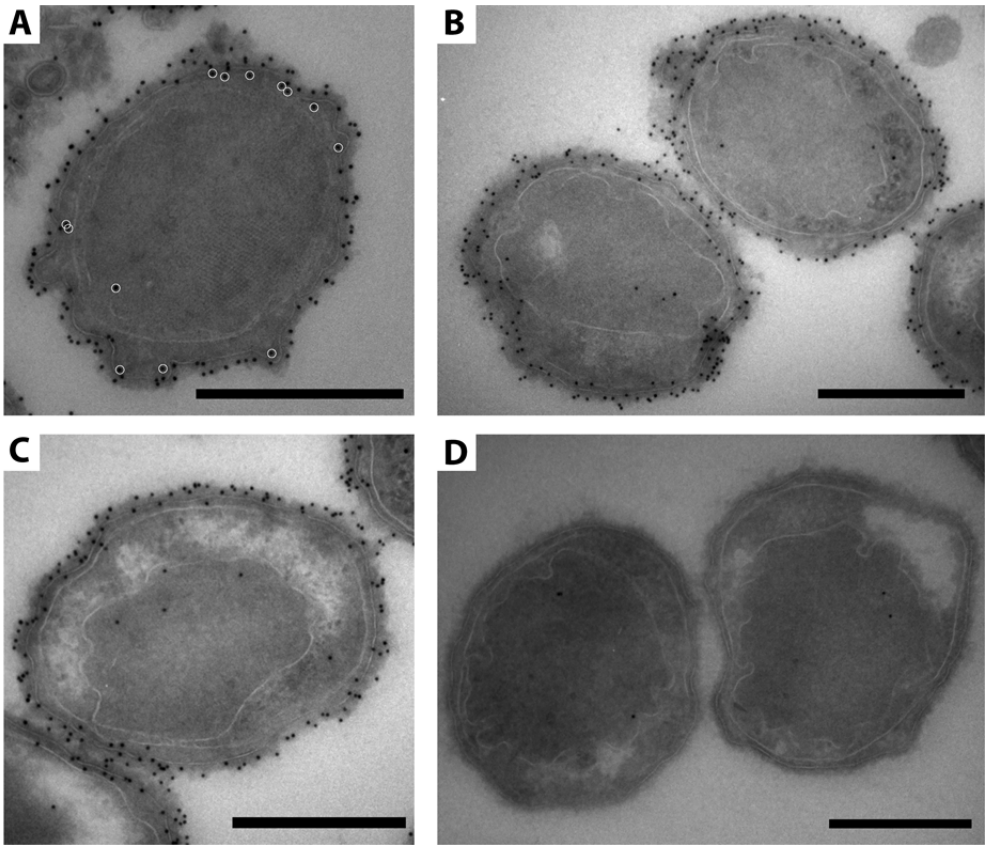

Figure 10. *A–C. Immunogold localization of the antiserum directed at Kustd1514 localizes the protein to the S-layer surrounding the cells in* K. stuttgartiensis *rehydrated cryosections. A. For clarification, white circles indicate gold labels that are localized inside of the outermost membrane (so not directly on the S-layer). Considering the length of the antibody-proteinA-gold complex (25 nm), these gold labels most likely also correspond to S-layer labeling (except for the one in the anammoxosome). D. Negative control incubated with pre-immune serum instead of antiserum. Scale bars: 500 nm.*

The intense signal in the PAS staining indicated that the Kustd1514 protein is highly glycosylated, which is a common feature for several S-layer proteins (Messner et al, 2008). In bacteria *O*-glycosylation seems most abundant, although some *N*-glycosylated (S-layer) proteins are also described (Schäffer et al, 2001; Klingl et al, 2011). The Kustd1514 protein contains both potential *O*- and *N*-glycosylation sites as found by a manual search of the protein sequence for strict "consensus" sequences and using the prediction server GlycoPP (Chauhan et al, 2012). Consensus sequences used were D/E-Y-NY-S/T (where Y can be all amino acids except P) for *N*-glycosylation (Kowarik et al, 2006) and D-S/T-A/I/L/V/M/T for *O*-glycosylation (Fletcher et al, 2009) of proteins from the phylum *Bacteroidetes*. For other prokaryotic O-glycosylation systems, so far no specific consensus sequences have been identified (Messner & Schäffer, 2003; Eichler & Adams, 2005). The fact that the migration of the glycoprotein was not affected by PNGaseF and glycans were detected after ß-elimination showed that the protein is *O*-glycosylated. It can, however, not be excluded that additional

N-glycosylation is present since it has been shown that PNGaseF is unable to cleave some bacterial *N*-glycoproteins in case of an unusual linking sugar (Scott et al, 2011). A possible experiment to elucidate if additional, *N*-glycans, are present would be to do a tryptic digest on a SDS-gel band of Kustd1514. This sample would include all glycopeptides irrespective of the linkage type. Such an experiment could also show at which sites of the protein the glycans are attached. Since the glycan caused an apparent mass shift from 160 to 250 kDa on an SDS gel it is expected that multiple, potentially charged, glycans are attached, especially since LC-MS/MS showed the glycans to be relatively small (mass of approximately 1 kDa).

LC-MS/MS analysis suggested the probable composition of the two main (*O*-linked) glycans attached to the S-layer protein. Since the mass of different sugars within the same class (e.g. the hexoses glucose and galactose) is the same, MS cannot distinguish between these. When combining the results from the monosaccharide analysis with the LC-MS/MS data, it seems most probable that the HexNAcs in peak 1 and 2 are GalNAc and the Hex residues might be glucose, mannose or galactose. It seems most probable that the GalN and GlcN that were observed in the monosaccharide analysis stem from GalNAc and GlcNac from which the *N*-acetyl groups were cleaved during the pretreatment with TFA. The only dHex that was observed in the monosaccharide analysis was fucose. It would be, however, very important to repeat a monosaccharide analysis on the exact same sample as was used for LC-MS/MS. Furthermore, some of the peaks observed in the monosaccharide analysis could not be assigned to specific sugars based on a comparison with the sugars that were used as standards in a separate run. Therefore it would be important to include a wider range of sugars (including more ddHex sugars) in follow-up monosaccharide analysis.

Analysis of fragmentation after LC-MS can often be used for deduction of the structure of molecules. In the case of peak 2, the fucose seems to break off from multiple fragments independently of other residues (Fig. 8). This could mean that fucose is present as the terminal group (of one of the branches) and can therefore break off independent of other residues. However, it has been previously observed that fucose can be transferred to other fragments upon fragmentation (Wuhrer et al, 2006) and therefore it is not possible to draw the conclusion that fucose is located at the end of the glycan. More information about the structure of the glycan might be obtained by further fragmentation of the fragments, by MS analysis of glycans treated with specific glycosidases (Mulloy et al, 2009) or via NMR. In the latter case the heterogeneity of the sample might pose problems and it might therefore be necessary to separate the different *O*-glycans via for instance HPLC (Gohlke & Blanchard, 2008) or lectin affinity chromatography (Qiu & Regnier, 2005). These samples containing, hopefully, single glycans would also be very suitable for monosaccharide analysis that could thereby determine the components present in each glycan.

To get a better understanding about the S-layer in relation to the underlying cell wall components of *K. stuttgartiensis*, it would be of interest to identify to which structure the S-layer attaches and via which mechanism. The genome organization around *kustd1514* gives no clues about possible glycosylation, secretion and attachment mechanisms. In the case of Gram-negative bacteria, much research is still required to find out common processes involved in attachment of the S-layer to the cell surface. In *Caulobacter crescentus* and

Campylobacter fetus the S-layer specifically attaches to lipopolysaccharides (LPS) (the O-antigens are crucial in the case of *C. crescentus*) via an N-terminal stretch (Awram & Smit, 2001; Dworkin et al, 1995). A bit more is known about attachment mechanisms of S-layers in Gram-positive bacteria, where the S-layer attaches to secondary cell wall polymers or the peptidoglycan itself (Engelhardt, 2007a). Many Gram-positive S-layer proteins contain a so-called S-layer homology (SLH) motif at their N-terminus that is involved in anchoring the S-layer to the secondary cell wall polymers (Sára & Sleytr, 2000; Schäffer & Messner, 2005; Messner et al, 2009; Messner et al, 2013). In Gram-positive S-layer proteins without SLH domains, an N-terminal motif (having for instance a net positive charge) or in some cases C-terminal motif seems to play a role in attachment (Dworkin et al, 1995; Engelhardt, 2007a; Messner et al, 2010; Sun et al, 2013). When a BLAST search with Kustd1514 was performed against the S-layer SLH consensus motif as proposed by Engelhardt and Peters (Engelhardt & Peters, 1998), no significant hits were found. Since peptidoglycan is proposed to be absent from *K. stuttgartiensis* (Neumann et al, 2013), the attachment mechanism of the S-layer might more resemble the attachment mechanisms for Gram-negative organisms. However, the identity (in terms of structure and function) of the outermost membrane of anammox bacteria as either an outer membrane typical of Gram-negative bacteria or a cytoplasmic membrane remains under investigation. If the outermost membrane of the cell is indeed a typical cytoplasmic membrane and the S-layer would anchor into this membrane, then this would be a unique case for Bacteria (Sleytr & Messner, 1989). Anchoring of the S-layer into the cytoplasmic membrane has thus far only been described for Archaea (Sumper & Wieland, 1995). It is thus clear that much more research is needed, focusing on possible N- or C-terminal modifications of the Kustd1514, or for instance lipid modifications which might be involved in membrane anchoring. In addition, it would be important to further investigate the composition of the entire cell envelope of anammox bacteria.

To our knowledge, the S-layer of *K. stuttgartiensis* is the first S-layer described in a cultured Planctomycete. However, this finding fits to previous reports (König et al, 1984; Liesack et al, 1986), showing that several *Planctomycetes* have cell walls that consist predominantly of protein. If the proteinaceous cell walls in the described *Planctomycetes* (König et al, 1984; Liesack et al, 1986) might be S-layers, they are probably quite different from the *K. stuttgartiensis* S-layer. While cell walls of the described *Planctomycetes* were enriched by incubation in 10% SDS at 100°C, no S-layers have been observed by EM investigations (Liesack et al, 1986, Stackebrandt et al, 1986). In addition, boiling *K. stuttgartiensis* cells in 10% SDS yields a sample without cell walls or S-layers (van Teeseling, unpublished results). Furthermore, the reported proteinaceous cell walls were enriched in proline and cysteine (Liesack et al, 1986) and the *K. stuttgartiensis* S-layer did not contain high amounts of these amino acids, but was enriched in serine and threonine instead. It would therefore be very interesting to investigate by rigorous electron microscopy studies if S-layers are present in other *Planctomycetes* as well.

As is often seen for S-layer proteins, that of course have to cover the complete cell surface, Kustd1514 is very abundant. In the proteome of membrane preparations from *K. stuttgartiensis*, Kustd1514 is the third most abundant protein (de Almeida et al, in preparation). A significant effort of the *K. stuttgartiensis* cells is thus invested in synthesizing

S-layer proteins and it is therefore obvious to raise the question which function the S-layer has for this anammox bacterium. Multiple functions for S-layers in prokaryotes have been proposed (Sára & Sleytr, 2000), including protection against predation (Tarao et al, 2009; Chanyi et al, 2013), adhesion of cell-associated exoenzymes (Egelseer et al, 1995), osmoprotection (Engelhardt, 2007b) and maintaining cell shape and integrity (Sleytr & Messner, 1989; Pum et al, 1991; Engelhardt, 2007a; Klingl et al, 2011). The latter function seems especially interesting in the case of anammox bacteria, since they are proposed to lack peptidoglycan and might therefore be in need of a structure that maintains cell shape and integrity. In the case of Archaea, which also lack peptidoglycan (Albers & Meyer, 2011; Klingl et al, 2013), S-layers are indeed often assumed to have a function in maintaining cellular integrity, which is also substantiated by the fact that S-layer-deficient mutants in Archaea have not been found (Engelhardt, 2007a). Loss of S-layers in lab strains is a common feature in Bacteria, which probably occurs when the cells do not need their S-layers under culturing conditions in which case the S-layer deficient mutants might outgrow S-layer containing cells (Sleytr & Messner, 1983; Baldermann et al, 1998; Klingl et al, 2011). If the S-layer indeed plays a role in maintaining the integrity of the cell, this could also explain why the S-layers have not been lost in our *K. stuttgartiensis* culture even though it has been continuously cultivated in the lab for over 10 years (taking an average generation time of two weeks this would mean over 260 generations).

Future research will have to show if, as hypothesized, cellular integrity really is the (only) function of the S-layer for *K. stuttgartiensis*. Since no genetic system is available for *K. stuttgartiensis*, it is unfortunately not possible to make a knockout mutant of the S-layer to assess the function of the S-layer. A first test of this hypothesis, however would be to assess if S-layers are present on other anammox bacteria as well. It has been proposed that all anammox bacteria lack peptidoglycan and therefore, following the aforementioned hypothesis, all anammox bacteria would need an S-layer or other type of (proteinaceous) cell wall component. Further experiments thus have to show whether the S-layer that is described here is indeed the component of the cell envelope that gives these highly interesting compartmentalized cells their structural integrity.

Acknowledgments

We thank Rob Mesman and Elly van Donselaar for their assistance with and advice on the electron microscopy techniques. Hans Wessels is acknowledged for his LC-MS/MS analysis of the protein bands. Jennifer Flechsler and Thomas Heimerl are acknowledged for their help in preparing the protein sample for the immunization procedure and Karl Hermann Fuchs for Fig. 4B. We thank Sonja Zayni and Andrea Scheberl for help with the monosaccharide analysis and chromatographic purification of S-layer glycopeptides, respectively. Monique van Scherpenzeel is acknowledged for the kind gift of PNGase F.

Muriel C.F. van Teeseling and Mike S.M. Jetten are supported by the European Research Council (ERC232937), Naomi M. de Almeida and Laura van Niftrik are supported by the Netherlands Organisation for Scientific Research (respectively: ALW grant 818.02.105 and VENI grant 863.09.009), Daan R. Speth is supported by BE-Basic fp0702, Andreas Klingl is supported by the LOEWE program of the state of Hessen, Germany (LOEWE Research Centre

for Synthetic Microbiology) and Reinhard Rachel by the German Research Foundation (DFG, grant HU 703/2-2), Paul Messner and Christina Schäffer are supported by the Austrian Science Fund FWF (project P24305-B20 to PM and projects P21954-B20 and P24317-B22 to CS).

Chapter 3

The abundant protein Kustd1878 of the anammox Planctomycete *Kuenenia stuttgartiensis* is a pore-forming outer membrane protein

Muriel C.F. van Teeseling[1], Naomi M. de Almeida[1], Rob J. Mesman[1], Mike S.M. Jetten[1], Roland Benz[2], Laura van Niftrik[1]

[1]Department of Microbiology, Institute for Water and Wetland Research, Faculty of Science, Radboud University, Nijmegen, the Netherlands.
[2]Department of Life Sciences and Chemistry, Jacobs University, Bremen, Germany.

Abstract

The *Planctomycetes* are a bacterial phylum known for their complex intracellular compartmentalization. Whereas most *Planctomycetes* have two compartments, the anaerobic ammonium oxidizing (anammox) bacteria even have a third compartment in their cell. Many aspects of the planctomycetal cell plan, especially regarding the cell envelope, need to be explored in more detail. The outermost membrane has originally been defined as a cytoplasmic membrane, but recent insights suggest it might be more similar to a Gram-negative outer membrane. A specific characteristic that differentiates outer membranes from cytoplasmic membranes is the presence of specific lipids and outer membrane proteins (OMPs). The latter have a ß-barrel shape that facilitates passage of molecules through the outer membrane. This study focuses on a highly abundant putative OMP (Kustd1878) from the anammox bacterium *Kuenenia stuttgartiensis* and describes the purification, location and potential function of this protein. Bioinformatic analysis of the protein structure, as well as membrane bilayer assays made the pore-forming structure and function of this protein plausible. In addition, immunogold localization suggested the Kustd1878 protein to be present in the outermost membrane. Together with the recently described presence of peptidoglycan, this work firmly adds to the emerging cell plan of anammox bacteria as Gram-negative bacteria.

Introduction

Based on differences in the structure of the cell envelope, two types of bacterial cell plans have been defined. The cell plan of Gram-positive bacteria consists of one compartment surrounded by the cytoplasmic membrane covered by a thick layer of peptidoglycan (Vollmer et al, 2008). The cells of Gram-negative bacteria consist of an additional compartment outside the cytoplasmic membrane. This so-called periplasm is the location of a thin layer of peptidoglycan (Vollmer et al, 2008) and is surrounded by the outer membrane. Whereas the cytoplasmic membrane consists of mainly phospholipids, the outer membrane has an inner leaflet composed of phospholipids and an outer leaflet including specific outer membrane lipopolysaccharides (LPS). The outer membrane also harbours a specific type of channel-forming proteins, called outer membrane proteins (OMPs). The presence of these OMPs facilitates passage of several types of molecules over the membrane (Nikaido, 2003) and thereby makes the outer membrane more permeable than the cytoplasmic membrane. These OMPs are characterized by their ß-barrel conformation in which antiparallel amphipathic ß-sheets surround a membrane spanning pore. Many OMPs occur in the outer membrane as trimers consisting of a total of three ß-barrels (Nikaido, 2003). The maximum diameter of the pore is in the order of 5 nm (Buchanan et al, 1999) and is dictated by the amount of membrane spanning ß-strands, which usually lies between 8 and 24 (Fairman et al, 2011). The specificity of OMPs is defined by their diameter and the functional groups of the amino acids that face the inside of the pore (Nikaido, 2003). In addition, OMPs often include loops that are located either in the extracellular or the periplasmic space (Wimley, 2003). These loops can be involved in stabilization of the ß-barrel (trimer) (Cowan et al, 1992), in substrate binding (Zachariae et al, 2006) or they can decrease the effective diameter of the pore and thereby increase the selectivity (Cowan et al, 1992; Ulmke et al,

1999; van den Berg et al, 2015). OMPs, together with the specific LPS molecules, form distinct markers for the bacterial outer membrane.

The cell envelope of species belonging to the *Planctomycetes* phylum was described to have a different structure than the two types of cell envelopes introduced above. This is best appreciated when taking into account their unique cell plan, consistsing of (a minimum of) two compartments bound by membranes of which the inner is often unusually curved. The cell plan was described to consist of (from the outside inwards) a cytoplasmic membrane, the paryphoplasm compartment, an intracytoplasmic membrane and the pirellulosome compartment (Lindsay et al, 1997; Lindsay et al, 2001). The DNA is present in the pirellulosome compartment and RNA has been detected in the paryphoplasm, leading to the conclusion that this is a cytoplasmic compartment (Lindsay et al, 1997; Lindsay et al, 2001). Therefore the membrane surrounding the paryphoplasm was interpreted as a cytoplasmic membrane and since no additional membrane was observed, it was postulated that no outer membrane was present in these bacteria (Lindsay et al, 2001; Fuerst & Sagulenko, 2011). In addition, peptidoglycan had never been detected (König et al, 1984; Liesack et al, 1986), thereby giving rise to the view that *Planctomycetes* were deviant from the normal Gram types and had a unique cell plan.

Within the *Planctomycetes*, the anammox bacteria form a phylogenetically distinct group (Jogler et al, 2012). The anammox bacteria consist of multiple genera (Jetten et al, 2010) that all conserve their energy by anaerobic ammonium oxidation (anammox)(Kartal et al, 2011b; Kartal et al, 2013) and have an intricate cell plan which comprises a third membrane-bound compartment (Lindsay et al, 2001). The anammox process takes place inside this third compartment, the anammoxosome, located within the pirellulosome (van Niftrik et al, 2004; van Niftrik et al, 2008b; Neumann et al, 2014). In the anammox process, the substrates nitrite and ammonium are converted to dinitrogen gas via the intermediates nitric oxide and hydrazine (Kartal et al, 2011b). Anammox bacteria thereby play a significant role in the biological nitrogen cycle by the production of approximately 50% of the dinitrogen gas present in the atmosphere (Francis et al, 2007). In addition, anammox bacteria are applied worldwide in sustainable wastewater treatment for the removal of ammonium (Kartal et al, 2010).

The view that *Planctomycetes*, including anammox bacteria, lack an outer membrane has recently been challenged. A bioinformatic analysis identified marker genes for insertion of both OMPs and LPS into the outer membrane in the genomes of multiple *Planctomycetes*, including anammox bacteria (Speth et al, 2012). The same study also identified multiple predicted OMPs in the anammox bacteria *Kuenenia stuttgartiensis* and *Scalindua profunda* and established that many of them were abundantly detected in the transcriptome and proteome of these bacteria. These findings suggest that these bacteria do have an outer membrane and the most plausible candidate to harbour the OMPs and LPS would be the membrane that had so far been interpreted as a cytoplasmic membrane. This has led us to use (until this suggestion has been verified experimentally) an unbiased terminology based on the location of this membrane: the outermost membrane. The recent detection of peptidoglycan underneath this outermost membrane in multiple *Planctomycetes* (van

Teeseling et al, 2015 (chapter 5); Jeske et al, 2015) provides the first experimental evidence towards the viewpoint that the outermost membrane might better be interpreted as an outer membrane. For a proper redefinition of the membranes, however, it is important to investigate the composition of the outermost membrane, in order to discover if functional outer membrane specific OMPs are present. Therefore, we have selected the putative OMP with the highest expression in *K. stuttgartiensis* from the previous bioinformatic study (Speth et al, 2012) and decided to study this protein, Kustd1878, in further detail.

Materials and Methods

Bioinformatic characterization of Kustd1878. To find homologs, the amino acid sequence of Kustd1878 was subjected to a protein-protein BLAST search (Altschul et al, 1990). For secondary structure prediction of Kustd1878, PSIPRED v3.3 was used via the server (Jones, 1999; Buchan et al, 2013). The prediction by PRED-TMMB was obtained using the 'posterior probability' method using the standard settings (Bagos et al, 2004). Kustd1878 was also investigated using the OMPdb (Tsirigos et al, 2011) via the BLAST search function. A structure prediction of Kustd1878 was run via HHpred (Söding et al, 2005) using the pdb70-9jul2015 and the HHblits (Remmert et al, 2012) method with three iterations and local alignment. In addition, PHYRE^2 (Kelley et al, 2015) was used for a protein prediction of Kustd1878, using the normal modeling mode. Images of the model were prepared using the UCSF Chimera package (Pettersen et al, 2004). The signal peptide of Kustd1878 was predicted by SignalP v4.1 using the standard settings for Gram-negative bacteria (Petersen et al, 2011). The molecular mass of Kustd1878 (without predicted signal peptide) was predicted by using the ExPASy compute pI/Mw tool (Gasteiger et al, 2005).

Purification of Kustd1878. Planktonic *K. stuttgartiensis* cells were harvested from a membrane bioreactor containing an enrichment culture that consisted of approximately 95% *K. stuttgartiensis* (Kartal et al, 2011a). Cells were concentrated (4500 g, 15 min) and the pellet was resuspended in sample buffer containing 20 mM potassium phosphate (KP_i) pH 7, 0.75 M 6-aminocaproic acid, 10 % (w/v) glycerol. The cells were broken by a French press (three passages at 138 MPa). Unbroken cells were removed by centrifugation (4500 g, 15 min) and the membranes were separated from the cytosolic fraction via ultracentrifugation (184000 g, 60 min). The membrane fraction (pellet) was washed three times in the ultracentrifuge and membrane proteins were dissolved via an rotating incubation with a 6:1 (w/w) ratio laurylmaltoside:protein for 60 minutes at 4°C. The undissolved membranes were pelleted and the supernatant that contained most membrane proteins was used for further purification. The putative OMP Kustd1878 was purified from the membrane proteins via fast protein liquid chromatography (FPLC) on an ÄKTA purifier system (GE Healthcare, Sweden) running all columns at 2 ml/min. Protein elution was followed by the absorbance at 280 nm and 2 ml fractions were collected. For desalting, concentrating and washing, spinfilters with a cut-off of 30 kDa (Vivaspin 20 or 500, Sartorius Stedim Biotech, Göttingen, Germany) were used. All buffers included 0.05% (w/v) laurylmaltoside in order to keep the protein as close as possible to its native conformation. The membrane fraction was applied to a 35 ml hydroxyapatite column (buffer A: 0.2 M KP_i pH 7, buffer B: 1 M KP_i pH 7, linear gradient 0-50% B in 10 min, 50-100% B in 30 min). Kustd1878 started eluting around 0.55 M KP_i. After

washing the fractions containing Kustd1878 in DEAE buffer A (20 mM Tris HCl, pH 8) the sample was applied to a 36 ml DEAE column (buffer B: 20 mM Tris HCl, pH 8 including 1 M NaCl, gradient: 0-100% B in 30 min) and Kustd1878 started eluting around 0.3 M NaCl. The sample was washed in QSepharose buffer A (10 mM Tris HCl pH 8) and applied to a 36 ml QSepharose column (buffer B: 10 mM Tris HCl pH 8 including 1 M NaCl, gradient: 0-100% B in 30 min), from which Kustd1878 elution started around 0.15 M NaCl. After each purification step, the presence and degree of purity of Kustd1878 was checked by SDS-PAGE, by running representative fractions on 10% SDS gels (described below). Representative protein bands were digested using trypsin and analyzed via MALDI-TOF MS as described before (van Teeseling et al, 2014 (chapter 2)). The protein concentration of the purified Kustd1878 samples was measured using the 2-D Quant kit (GE Healthcare, Little Chalfont, United Kingdom) using the manufacturer's instructions.

Protein gel electrophoresis. Protein samples for SDS gel electrophoresis were denatured by incubation of the proteins in sample buffer (158 mM Tris-HCl buffer, pH 7 containing 5% β-mercaptoethanol, 2.6% SDS, and 16% glycerol) for 10 min at 100°C. SDS-PAGE was performed on 8% or 10% slab gels in running buffer as described previously (Laemmli, 1970) using 7 µl of the PageRuler Plus Prestained Protein Ladder (Life technologies, Carlsbad, CA, USA) in one lane to estimate apparent molecular masses for the proteins. For native gels, the samples were mixed with native sample buffer (same ingredients as above, except the SDS) on 10% slab gels without SDS, using running buffer without SDS. As a marker for the native gels, 7 µl of the NativeMark unstained protein standard (Life technologies, Carlsbad, CA, USA) was used in one lane. Gels were stained with Coomassie brilliant blue (G250) after separation of the proteins.

Antibody generation. Antiserum containing antibodies against the putative OMP Kustd1878 was generated against protein that was purified as described above. Antibodies were generated by Eurogentec (Seraing, Belgium) by immunization of a guinea pig in a 3 months programme.

Immunoblot. The affinity and specificity of the generated antiserum for Kustd1878 was tested using immunoblots containing both purified Kustd1878 and crude extracts of *K. stuttgartiensis*. The purified Kustd1878 was prepared as described above. The crude sera were prepared as describe previously (van Teeseling et al, 2014 (chapter 2)). In short, *K. stuttgartiensis* cells were harvested from a membrane bioreactor, concentrated (2200 g, 15 min) and disrupted by three passages through a French Press. The unbroken cells were pelleted (2200 g, 15 min) and the remaining supernatant was the crude extract. Both the purified Kustd1878 and the crude extracts were boiled in SDS sample buffer and run on 8% SDS gels as described above. The proteins were transferred onto a nitrocellulose membrane as described previously (van Teeseling et al, 2014 (chapter 2)), with the exception that the blotting was performed at 50 mV for 45 min.

Immunoblotting was performed on blots that were incubated in MilliQ water for 30 min. All steps were performed at room temperature. Blocking was performed by incubating the blots for 60 min in blocking buffer consisting of 2% skim milk powder (Frema Reform, Lüneburg, Germany) diluted in Tris-buffered saline (TBS). The blots were incubated with antiserum

generated against Kustd1878 (SAB) and pre-immune serum (control) diluted 1000-fold in blocking buffer for 60 min and subsequently washed three times 10 min each in TBS containing 0.05% Tween 20. The 60 min incubation with secondary antibody (anti-guinea pig alkaline phosphatase (Sigma, Zwijndrecht, The Netherlands); diluted 30000-fold) was followed by washing twice (10 min each) with TBS containing 0.05% Tween 20 and twice 10 min with TBS. The blots were incubated with a 5-bromo-4-chloro-3-indolylphosphate (BCIP)/nitroblue tetrazolium (NBT) liquid substrate system (Sigma, Zwijndrecht, the Netherlands) for 2¼-2½ min and rinsed for 10 min in MQ water. All lanes were imaged with the same settings.

Immunogold localization. For immunogold localization, cells (4 ml) were harvested from a membrane bioreactor and concentrated by centrifugation (800 g, 4 min, 30°C). The pellet was resuspended in 15 µl supernatant and 1.2 µl of the cell suspension was loaded in a gold-plated platelet (2 mm inner diameter, 100 µm depth) (Leica Microsystems, Vienna, Austria). Subsequently, the sample was high-pressure frozen in a HPM-100 (Leica Microsystems). Freeze-substitution was performed in an AFS2 (Leica Microsystems) in Seccosolv anhydrous acetone (Merck Millipore, Darmstadt, Germany) with 0.2% Uranyl Acetate (UAc) (Merck, Darmstadt, Germany). The substitution started at -90°C for 48 h, followed by a 2°C/h slope to -70°C, where the sample remained for 12 h. Afterwards, the temperature was raised with 2°C /h to -50°C, where the sample remained for 12 h. Next, the sample was washed with anhydrous acetone (2 changes) to remove UAc at -50°C and infiltrated with Lowicryl HM20 (Electron Microscopy Sciences, Hatfield PA, USA) in anhydrous acetone at -50°C. Infiltration was started with 12.5% HM20 for 2 h, than 2 h in 25% HM20, 2 h in 50% HM20, 2 h in 75% HM20 and 1 x 2 h in 100% HM20, 12 h in 100% HM20 and 1x 3 h in 100% HM20. After the final change of 100% HM20, the lowicryl was polymerized by UV irradiation at -50°C for 96 h and 2°C/h to 0°C, 10 h at 0°C. Ultrathin sections (ca. 50 nm) were cut using an UCT microtome (Leica Microsystems, Vienna, Austria) and applied to 100 mesh copper grids (Stork-Vesco, Eerbeek, Netherlands) containing a carbon-coated formvar film.

Immunogold labeling was performed on grids containing ultrathin sections of *K. stuttgartiensis* cells. The grids were first washed for 2 min each on 5 subsequent drops of 0.1 M PHEM buffer (60 mM piperazine-N,N'-bis(2-ethanesulfonic acid) (PIPES), 25 mM HEPES, 10 mM EGTA, 2 mM $MgCl_2$ (pH 6.9)) and subsequently blocked by incubating 15 min on 0.1 M PHEM containing 2% skim milk powder (Frema Reform, Lüneburg, Germany). Primary antibody incubation was performed for 60 min on 333-fold diluted antiserum (SAB) or pre-immune serum (control) in 0.1 M PHEM containing 2% skim milk powder. Washing was performed for 2 min each on 5 subsequent drops of 0.1 M PHEM containing 0.2% skim milk powder. The grids were subsequently incubated 45 min on protein A coupled to 10 nm gold (PAG-10; CMC UMC Utrecht), diluted 60-fold in 0.1 M PHEM containing 2% skim milk powder. Washing was performed 45 sec each on 5 drops of 0.1 M PHEM containing 2% skim milk powder and afterwards for 2 min each on 5 drops of 0.1 M PHEM. Fixation took place by incubation on 1% glutaraldehyde in 0.1 M PHEM for 5 min, after which grids were washed on 10 drops of MilliQ water (1 min incubation per drop). The grids were stained by a 20 min incubation on 2% uranyl acetate in MQ, after which the grids were washed on 5 drops of MilliQ water (1 min incubation per drop) and air-dried. The grids containing the ultrathin

sections were investigated in a JEOL JEM-1010 (Tokyo, Japan) transmission electron microscope (TEM) at 60kV. Images were recorded via an Olympus SIS Mega View III camera (Münster, Germany).

Lipid bilayer assays. Black lipid bilayer experiments have been performed using the methods described previously (Benz et al, 1978). The set-up for the black lipid bilayer experiments consisted of a Teflon chamber with two compartments with a volume of 5 ml both. The two compartments were separated by a thin wall with a circular hole with an area of about 0.4 mm^2. The hole was covered with a membrane made of 1% 1,2-diphytanoyl-sn-glycerol-3-phosphocholine (Avanti Polar Lipids Inc, Alabaster, AL, USA) in *n*-decane. Kustd1878 was diluted 1:10 in 1% Genapol (Roth, Karlsruhe, Germany) and was added to the front compartment of the membrane cell after the membrane had turned black at a concentration of 0.2-0.5 µg/ml. The membrane current was followed using a pair of Ag/AgCl electrodes with salt bridges connected (in series) to a voltage source and a home-built highly sensitive current amplifier (connected in series). This amplified signal was recorded on a strip chart recorder. Single-channel measurements were performed using the following solutions: 1 M KCl, 1 M LiCl, 1 M KCH_3COO^-, 1 M NH_4Cl and 0.1 M KCl. All solutions were buffered with 10 mM HEPES and the pH was set to pH 7.0. For each salt, 20 independent insertions were analyzed.

Results

Bioinformatic characterization of Kustd1878. The *K. stuttgartiensis* protein Kustd1878 consisted of 556 amino acids of which the first 28 were predicted to belong to a signal peptide. The proximal amino acid at the C-terminus was a phenylalanine. This is highly common for OMPs, in which this phenylaline is crucial for recognition by OmpA, the protein that inserts OMPs into the outer membrane (Struyvé et al, 1991). A BLASTp search gave no significant hits for Kustd1878 to characterized proteins, but showed that this protein is also highly preserved in the anammox species *Jettenia caeni* KSU-1 (Hira et al, 2012), *Brocadia sinica* JPN1 (Oshiki et al, 2015), *Brocadia fulgida* (Ferousi et al, 2013) and *Scalindua brodae* (Speth et al, 2015). Using the PSIPRED server, Kustd1878 was predicted to consist for 35% of ß-sheets and 5% of α-helices, when considering the protein without the predicted signal peptide (Fig. 1). It became evident from the structure prediction that there might be a long flexible polypeptide at the N-terminus since the first ß-sheet only starts at amino acid 116. The prediction by PRED-TMBB confirmed that Kustd1878 forms a ß-barrel OMP and suggested 20 transmembrane domains. Also the OMPdb listed Kustd1878 as a ß-barrel protein belonging to the Alginate export protein porin (AlgE) family with AlgE from *Pseudomonas aeruginosa* (Tan et al, 2014) as the most homologous crystal structure. The high homology of Kustd1878 (amino acids 118-556) to *P. aeruginosa* AlgE was verified by HHpred, pBLAST conserved domain detection and PHYRE[2]. The latter made a model of the Kustd1878 as an OMP (Fig. 2), based on AlgE as the most homologous structure present in the protein data bank (wwPDB, Berman et al, 2003). The model made by PHYRE[2] comprised 68% of the sequence of Kustd1878 and no structure could be predicted for the first 118 amino acids of Kustd1878. The model showed Kustd1878 as an OMP with 18 ß-sheets and multiple loops at the turns of these ß-sheets. The model showed the channel as constricted

by several of these loops, as well as by a part of a ß-sheet located inside the lumen of the channel (Fig. 2). Furthermore, the absence of the first 118 amino acids in the model suggested that an N-terminal flexible region might be present that was found to be specific for Kustd1878 and the homologous proteins in anammox bacteria, with the exception of the protein in *S. brodae* which lacks such a region.

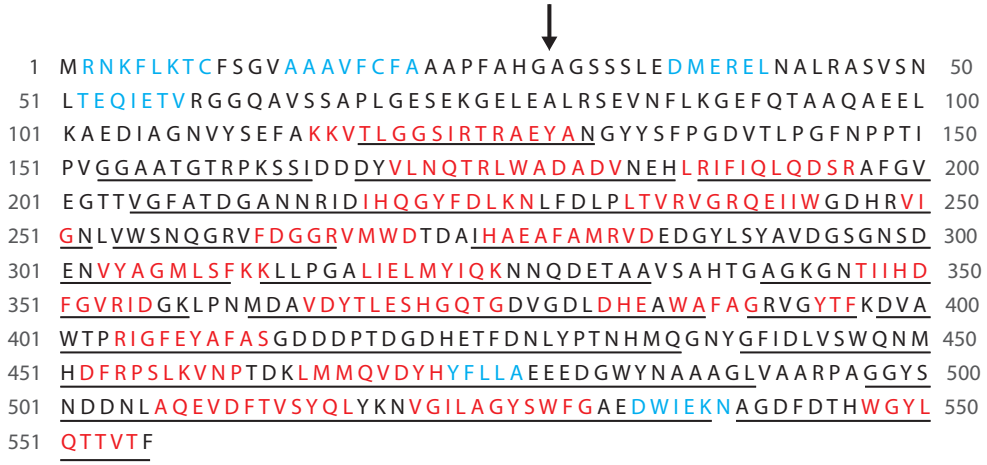

Figure 1. *The secondary structure of the* K. stuttgartiensis *putative OMP Kustd1878. The predicted signal peptide cleavage site is indicated with an arrow, residues predicted (by PSIPRED) to be in an α-helix are indicated in blue and those predicted to be in a ß-sheet in red. The predicted secondary structure of Kustd1878 is typical for an OMP protein, with multiple ß-sheets and, in this case, an exceptionally long N-terminal polypeptide which is not part of the barrel itself. The residues that are underlined are present in the model showed in Fig. 2.*

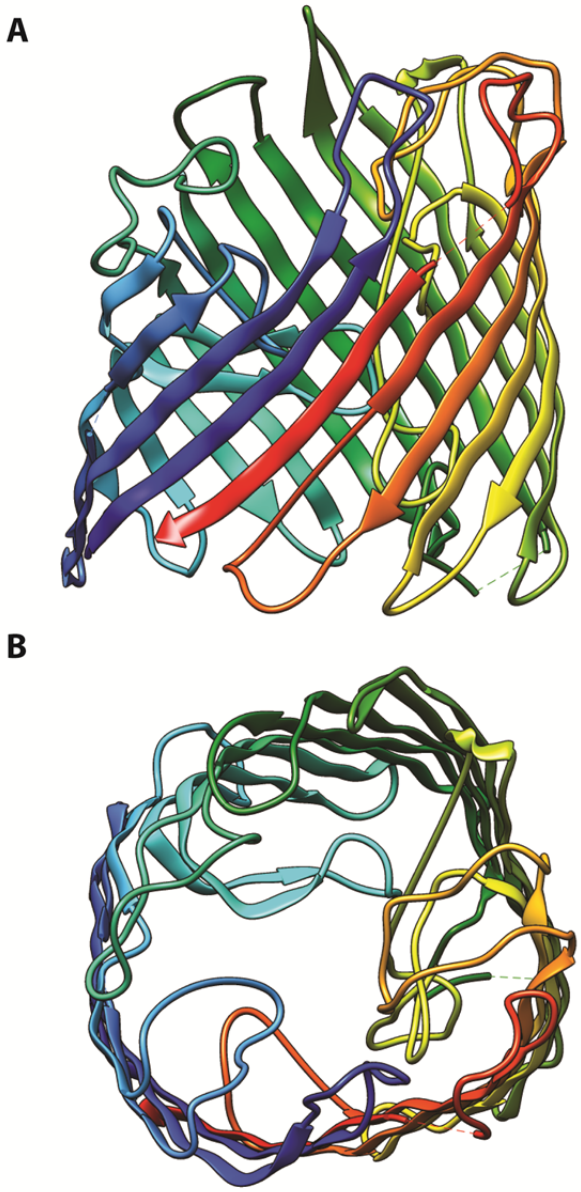

Figure 2. *Model generated by PHYRE of a major part (68%) of* K. stuttgartiensis *Kustd1878 based on the crystal structure of* P. aeruginosa *AlgE predicts that Kustd1878 is a ß-barrel OMP. The first 118 amino acids of the Kustd1878 N-terminus are not present in the predicted structure. The N-terminus is indicated in blue and the C-terminus in red. If the orientation of Kustd1878 is the same as of AlgE, the bottom in A is the periplasmic side and B shows a look into the protein from the extracellular space.*

Purification of Kustd1878. The Kustd1878 protein was purified by FPLC and analysis with SDS-PAGE identified a main band at about 55 kDa, one band around 40 kDa and minor bands around 65, 50 and 30 kDa (Fig. 3). The molecular mass of Kustd1878 (without the predicted signal peptide) was predicted to be 58 kDa and MALDI-TOF MS verified that the band at about 55 kDa consisted of Kustd1878. Also the bands at 50, 40 and 30 kDa were identified as (partial) Kustd1878. No peptides were detected for the minor band at 65 kDa. Native-PAGE showed that the protein was present in an oligomeric state after purification (Fig. 3).

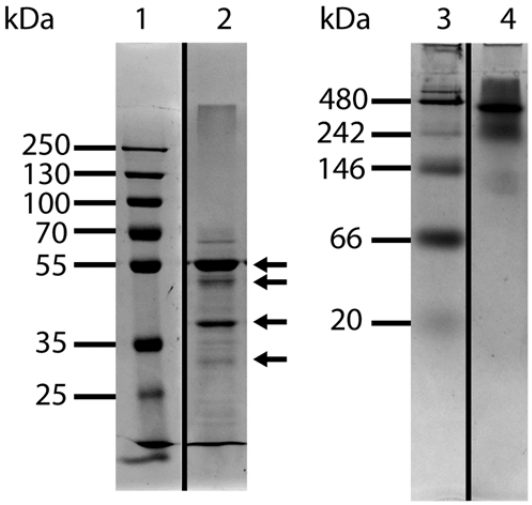

Figure 3. *SDS (1-2) and native (3-4) gel electrophoresis showed that the* K. stuttgartiensis *putative OMP Kustd1878 was highly pure and present in an oligomeric state after purification. Arrows indicate bands consisting of Kustd1878 as verified by MALDI-TOF MS analysis.*

Location of Kustd1878. The subcellular location of Kustd1878 in *K. stuttgartiensis* was investigated via immunogold localization using antibodies that were generated against the purified protein. The affinity of the antiserum against Kustd1878 was verified by an immunoblot using purified Kustd1878 showing that the antibody indeed binds Kustd1878, as seen by the signal at the expected molecular mass around 55 kDa (Fig. 4, lane 1 and 2). The specificity of the antibody was tested via an immunoblot with *K. stuttgartiensis* crude cell extract. In that case not only the expected signal around 55 kDa was apparent, but signal was also present at other molecular masses (Fig. 4, lane 3 and 4). One clear band was present above 250 kDa and a smear occurred between 250 kDa and 55 kDa. In both the crude extract and purified Kustd1878 blots, a signal was also present at the running front (around 15 kDa) (Fig. 4). The pre-immune serum showed no reaction in the immunoblot of the crude extract (Fig. 4, lane 5).

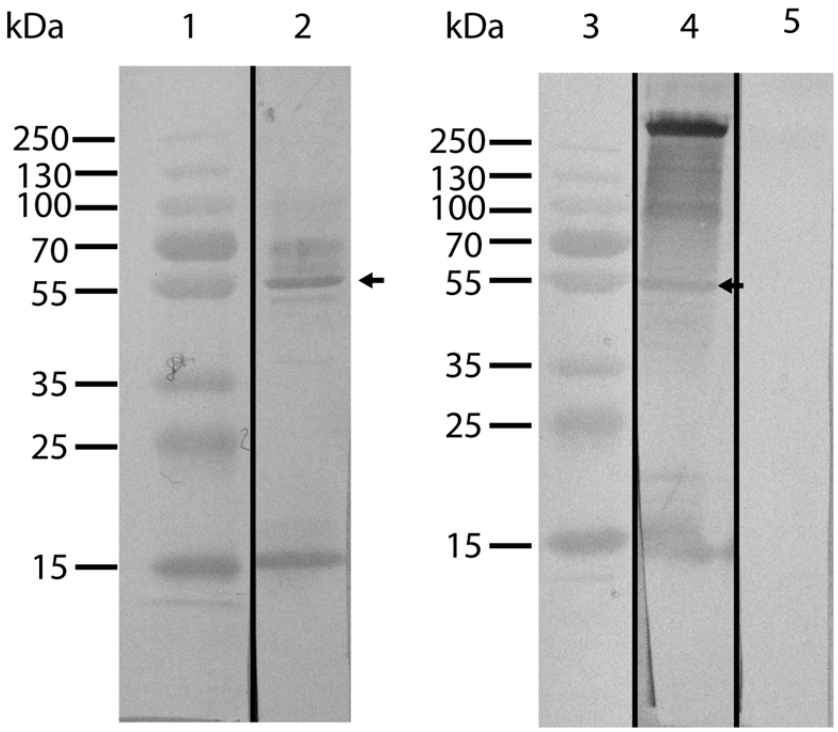

Figure 4. *Immunoblot analysis using purified Kustd1878 (2) and* K. stuttgartiensis *crude extract (4) showed that the antiserum reacts with a protein at the expected mass of Kustd1878 (indicated by arrows), but also to other protein bands in the crude extract. The pre-immune serum (5) does not react to proteins in the* K. stuttgartiensis *crude extract.*

Immunogold localization was performed on sections with high-pressure frozen, cryofixed *K. stuttgartiensis* cells embedded in lowicryl. The antibody clearly targeted the outer membrane of the *K. stuttgartiensis* cells, especially when taking into account that labels within 25 nm of the outer membrane can still be bound to an epitope in the outer membrane, since the length of an antibody-protein-A-gold complex is approximately 25 nm (Fig. 5, A-C). The amount of labeling in the negative control incubated with pre-immune serum was very low (Fig. 5, D).

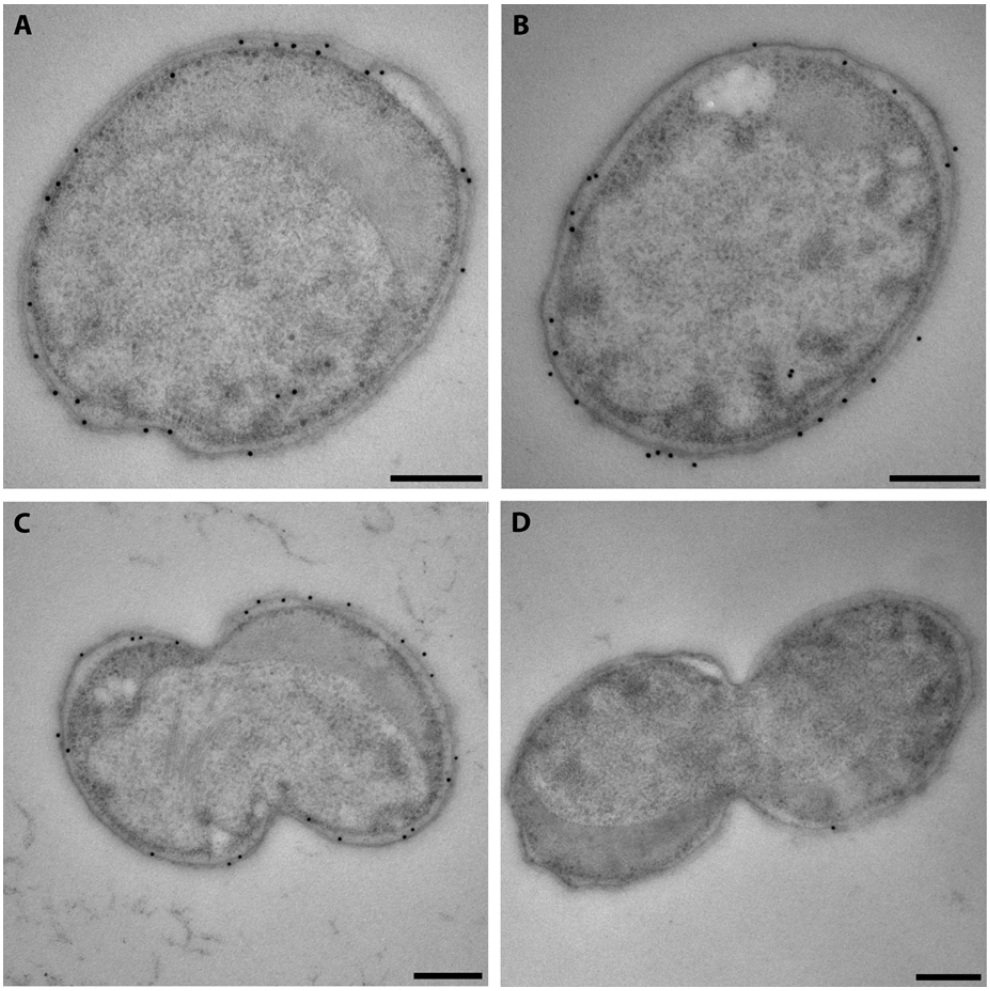

Figure 5. *Immunogold localization of the antiserum against Kustd1878 (A-C) localizes the putative OMP to the outermost membrane of* K. stuttgartiensis *cells embedded in lowicryl. Negative control incubated with pre-immune serum instead of antiserum (D) shows only a very limited amount of background labeling. Scale bars 200 nm.*

Pore formation by Kustd1878. Lipid bilayer experiments were performed to study if Kustd1878 is able to form membrane pores. In these experiments, purified Kustd1878 was applied to a Teflon cell with two compartments with an electrode in each and an artificial membrane in between the compartments. Possible pores that reconstituted into the membranes were identified by measuring the current between the two compartments in the membrane cell. The current measured indicated ion movement through these pores. With this set-up, insertion of channels into the membrane was observed only in the presence of purified Kustd1878. Since the single channels showed a rather noisy current signal (Fig. 6), it was difficult to identify the exact attribution of each additional channel to the total signal in the presence of multiple channels (Fig. 6, A&C). Nonetheless it was possible to obtain the average single-channel conductance by only taking events into account where up to two

channels at the same time were inserted in the membrane. The single-channel conductance in different salt solutions is shown in Table 1 and gives a measure for the way ions move through the channels. In 1 M potassium chloride (KCl) the average single-channel conductance was 173 pS, but the signal fluctuated between an average conductance of 66 pS and 304 pS. The single-channel conductance values were, especially taking into account the high noise level, not highly dependent on the tested salt solutions. As expected, the conductance decreased in the presence of less mobile ions (Li^+, compared to K^+ and CH_3COO^-, compared to Cl^-) (Table 1).

Table 1. *Single-channel conductance for purified* K. stuttgartiensis *Kustd1878 in different salt solutions. All single-channel conductance values were calculated from 20 independent events.*

		Single-channel conductance G (pS)		
Salt	**Concentration (M)**	**Minimum**	**Average**	**Maximum**
KCl	1	66	173	304
KCl	0,1	44	83	131
LiCl	1	34	120	255
NH_4Cl	1	81	184	308
KCH_3COO	1	53	130	248

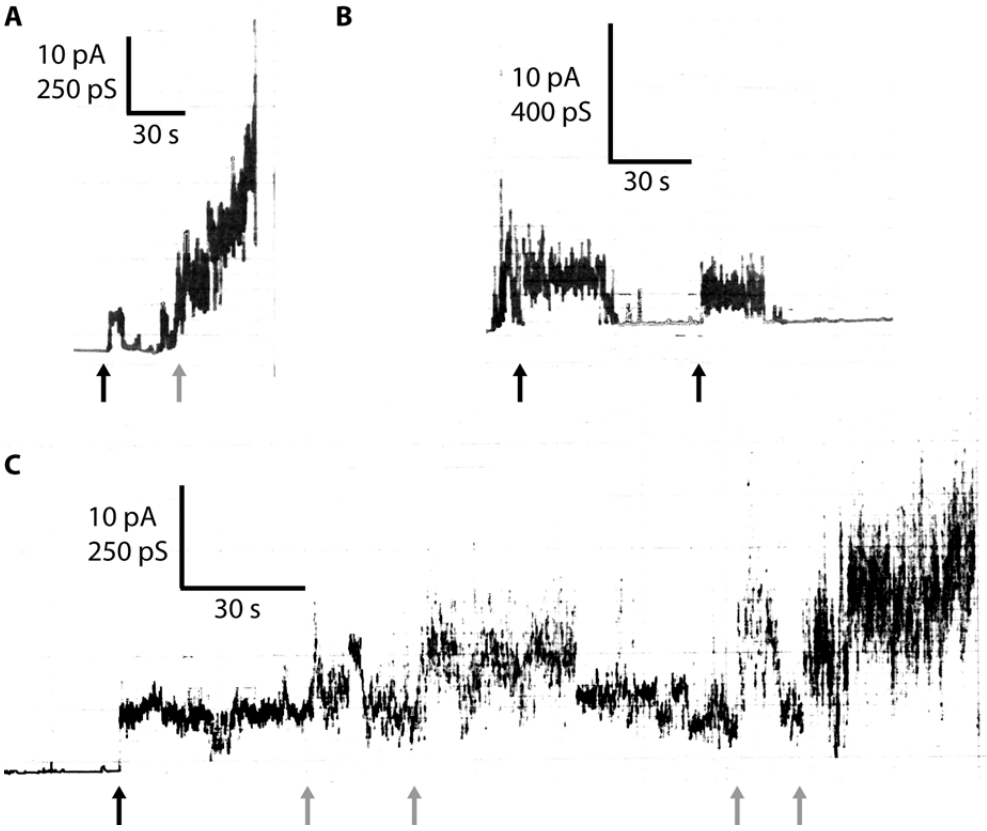

Figure 6. *Three single channel recordings in the presence of purified* K. stuttgartiensis *Kustd1878 showed an increase in current upon insertion of protein into the membrane. Single channels (black arrows) displayed a noisy behavior and upon insertion of additional proteins (grey arrows) the contribution of each protein to the total signal became difficult to determine because of this noise. Channels showed opening and closing events (e.g. B).*

Discussion

Here we describe the purification, localization and characterization of the outer membrane protein Kustd1878 from the anammox bacterium *Kuenenia stuttgartiensis*. Structure prediction and comparison with the 3D-structure of known OMPs indicated that Kustd1878 has an OMP-typical ß-barrel structure with 18 ß-sheets and multiple, probably external, loops. The protein was purified and used for lipid bilayer assays, which showed that the protein indeed formed channels in a membrane. Immunogold localization using an antibody generated against the purified protein suggested its localization at the outermost membrane. Taken together these results clearly demonstrated that Kustd1878 is an OMP and thereby showed that the outermost membrane of anammox bacteria has characteristics typical of the outer membrane of Gram-negative bacteria.

Bioinformatics analysis showed that Kustd1878 has a ß-barrel conformation and indicated its similarity with the OMP AlgE from *P. aeruginosa*. AlgE forms a channel through which the

exopolysaccharide alginate is excreted (Tan et al, 2014). Alginate acts as a protection mechanism against the immune system of the human host (Leid et al, 2005). A ring-like portal with predominantly positively charged groups decreases the diameter of the pore and is proposed to contribute to the substrate specificity of AlgE (Tan et al, 2014). In Kustd1878, even though a constriction is predicted, the sequence differs considerably at the residues that form this ring in AlgE (Tan et al, 2014). Out of nine identified crucial residues (K47, R74, N164, R152, D162, R362, R353, R459, D485), only one is present at the same position in *K. stuttgartiensis* (R74 aligns with R175 in Kustd1878). From the other eight specific residues, one is missing in *K. stuttgartiensis* altogether (R459), four are replaced by similar amino acids (K47, R152, R353, D485, align with respectively R124, E241, H423 and Q551) and three are replaced by a different amino acid (D162, N164 and R362 align with respectively G251, V253 and T432 in Kustd1878). This suggests that Kustd1878 will probably have a different specificity than AlgE and it will be a topic for further research to identify molecules that pass through the channel made by Kustd1878. If, however, Kustd1878 is (like AlgE) involved in exporting rather than importing substrates, a plausible candidate would be the previously described S-layer protein Kustd1514 (van Teeseling et al, 2014 (chapter 2)). This is probably the most abundant protein outside the outermost membrane and has an extensive polysaccharide coupled to it, possibly making it slightly similar to the substrate of AlgE. Indeed it was shown before that S-layer proteins can traverse the outer membrane via OMPs involved in secretion systems (Fagan & Fairweather, 2014). Alternatively, kustd1878 might form pores through which important substrates can enter the cells.

In addition to the ß-barrel part of the structure that is similar to AlgE, Kustd1878 also includes 88 N-terminal amino acids in the predicted mature protein that have no homology to AlgE. It would be interesting to elucidate the function of these amino acids. In many bacteria this could be performed by creating a deletion mutant without these amino acids and investigating how this mutant behaves. Unfortunately this is not yet an option in the case of *K. stuttgartiensis* since creating targeted mutants is impeded by the lack of a genetic system. Of course the complete protein and the truncated protein might be heterologously expressed in another organism. This would allow for some characterization of both proteins, for instance via lipid bilayer assays. This could for instance show if this part of the protein is responsible for (part of) the noise that was observed in the lipid bilayer assays. However, it might be better to first elucidate which molecules move through the Kustd1878 channels, before investigating the function of a specific part of the protein. More information about both the ß-barrel and the N-terminal part would be obtained when a crystal structure of Kustd1878 would be present. This would allow a more thorough comparison between AlgE and Kustd1878 and might give hints about the specificity of the channel. Co-crystallization of Kustd1878 with putative substrates might show potential interactions of parts of the protein with such a substance.

Crystallization of the protein could also show a multimeric state for Kustd1878 (as in (Kefala et al, 2010)). Indeed it is common for OMPs to be inserted in the membrane in an oligomeric configuration (Meng et al, 2009). Some oligomeric OMPs form a single ß-barrel channel together, but in most oligomers, the amount of channels equals the number of proteins present, since each protein forms an entire ß-barrel by itself. The structure predictions

showed that Kustd1878 forms one channel per monomer. Native gel electrophoresis showed the purified Kustd1878 to exist in multiple oligomeric states with apparent masses ranging from around 220 kDa to well above 480 kDa, with a clear band at around 460 kDa (Fig. 3). Since the monomer has an apparent molecular mass of 58 kDa, this could mean that the protein is present in complexes consisting of four to maybe ten proteins, with the octamer (predicted mass: 464 kDa) as the most prominent variant. This would be an interesting finding, since trimers represent by far the most abundant oligomeric state in which oligomeric OMPs occur (Meng et al, 2009). However, it is possible that lipids and detergent associated with the protein influence the migration of the protein through the gel. Indeed such an effect has been observed for blue native gel electrophoresis on membrane proteins, causing an altered migration behavior that could be mistaken for an additional mass of around 60 kDa (Crichton et al, 2013). Therefore it is difficult to conclude the exact oligomeric configuration that Kustd1878 naturally occurs in and future research will be necessary to resolve this question.

As suggested by the predicted ß-barrel configuration, lipid bilayer experiments showed that Kustd1878 is able to form channels in a membrane, albeit rather noisy. It has been shown before that noise in lipid bilayer experiments can be caused by flexible parts of OMPs that might affect the flow of ions (Killmann et al, 1996; Braun et al, 2002). In the case of the ß-barrel protein FhuA of *Escherichia coli* the removal of such flexible structures led to a remarkable decrease in the amount of noise (Braun et al, 2002). Another possible explanation for the high noise levels in single channel measurements is that a stabilizing element might be missing which leads to an increased channel breathing (Srikumar et al, 1997).

In future experiments multiple channels could be inserted in the membrane in lipid bilayer experiments. In such a set-up, the specificity of the pore for cations vs. anions could be determined. The single channel measurements suggested that the channel formed by Kustd1878 might be cation selective. This can be concluded from the observation that replacing the K^+ ion by the less mobile Li^+ ion led to a slightly lower conductance than replacing the Cl^- ion by the less mobile CH_3COO^- ion. The influence of cations of different mobility on the conductance was thus slightly larger than that of anions. Another possible application of multichannel measurements is to add putative substrates, such as the previously identified S-layer protein, and observe if partial blocking of the channel by such substrates occurs. Other putative substrates for Kustd1878 might be identified by protein-protein interaction studies (in case a protein passes through the pore and interacts strongly enough to be detected after crosslinking experiments) or by observing *K. stuttgartiensis* cells incubated with antibodies that target and possibly block the channels formed by Kustd1878.

If Kustd1878 is indeed a true OMP, it is necessary that it is inserted in the outer membrane. In the case of *K. stuttgartiensis* it is hypothesized that the so-called outermost membrane would be the most logical location for OMPs. Immunogold localization indeed suggested Kustd1878 to be located in the outermost membrane. The fact that most labels were present on the periplasmic side of the membrane suggested that the antibody might target parts of the protein that are located in the periplasmic space, possibly the N-terminal loop which is

indeed predicted to be located in the periplasm. From the immunogold localization it seems that the antibody only targeted epitopes in the outermost membrane. The immunoblot, however, suggested a suboptimal specificity of the antibody. Further experiments are needed to elucidate to which proteins on the blot the antibody reacts. In addition, other techniques should be used for validating the specificity of the antibody, such as immunoprecipitation.

All in all, it has become clear that Kustd1878 has the characteristics of an OMP. The most intriguing question that remains for further research, especially when realizing this protein is the most abundant OMP in *K. stuttgartiensis* (Kustd1878), is which molecules are transported through this OMP. Experiments such as proposed in the discussion are expected to elucidate this question and thereby lead to a more thorough understanding of the cell envelope of the intriguing anammox bacteria.

Acknowledgments

We would like to thank Ivan Barcena-Uribarri and Eva Waltenberger for instructions and discussions concerning the lipid bilayer experiments. Joachim Reimann is acknowledged for discussions. Marjan Smeulders is acknowledged for testing pre-immune sera prior to antibody generation. The General Instruments Department of the Radboud University is acknowledged for maintenance of the electron microscope. Molecular graphics and analyses were performed with the UCSF Chimera package. Chimera is developed by the Resource for Biocomputing, Visualization, and Informatics at the University of California, San Francisco (supported by NIGMS P41-GM103311).

MCFvT and MSMJ are supported by the European Research Council (ERC232937 awarded to MSMJ) and MSMJ is further supported by a Spinoza premia and SIAM Gravitation (024 002002).

Chapter 4

Lipopolysaccharides in *Planctomycetes*: present or absent?

Muriel C.F. van Teeseling[1], Cornelia Rath[2], Ellen C. Hopmans[3], Rob J. Mesman[1], Katarzyna A. Duda[4], Jaap S. Sinninghe Damsté[3], Paul Messner[2], Christina Schäffer[2], Mike S.M. Jetten[1], Laura van Niftrik[1]

[1]Department of Microbiology, Institute for Water and Wetland Research, Faculty of Science, Radboud University, Nijmegen, the Netherlands.
[2]NanoGlycobiology Unit, Department of NanoBiotechnology, Universität für Bodenkultur, Vienna, Austria.
[3]Department of Marine Organic Biogeochemistry, NIOZ Royal Netherlands Institute for Sea Research, Den Burg, Netherlands.
[4]Division of Structural Biochemistry, Research Centre Borstel, Leibniz-Center for Medicine and Biosciences, Borstel, Germany.

Abstract

The bacteria of the *Planctomycetes* phylum have a unique compartmentalized cell structure. A few years ago, the presence of marker genes for the insertion of the Gram-negative outer membrane specific lipopolysaccharide (LPS) and outer membrane proteins (OMPs) were detected in the genomes of many *Planctomycetes*, contradicting the previous viewpoint that they lack an outer membrane. This study aims at elucidating if LPS, consisting of lipid A, a core and, possibly, an O antigen, is indeed present in three *Planctomycetes*: *Planctopirus limnophila*, *Rhodopirellula baltica* and the anammox Planctomycete *Kuenenia stuttgartiensis*. Genome analysis indicated that all three species have the potential to form lipid A and gel electrophoresis of enriched LPS suggested the presence of LPS in all three investigated species. Treatment with the LPS-binding cationic antimicrobial peptide polymyxin B showed membrane disruption in *R. baltica,* to a lesser extent in *K. stuttgartiensis* and *P. limnophila*. In a more in-depth investigation into *K. stuttgartiensis* using high performance liquid chromatography electrospray ionization/mass spectrometry (HPLC-ESI/MS), however, no lipid A related peaks were detected after lipid A extraction. In addition, gas chromatography coupled to mass spectrometry did not detect the highly conserved Kdo core component in *K. stuttgartiensis*. From the combined results, the presence of LPS in the three analyzed *Planctomycetes* seems plausible, but more research is clearly necessary. We therefore propose experiments in order to clarify whether or not LPS is present in *Planctomycetes*.

Introduction

The phylum of the *Planctomycetes* is characterized by a complex compartmentalized cell plan of its members (Lindsay et al, 1997; Lindsay et al, 2001; Fuerst & Sagulenko, 2011). The cell plan of these organisms was defined to consist of (from outside to inside) a cytoplasmic membrane, a compartment called the paryphoplasm and an intracytoplasmic membrane enclosing the pirellulosome. In many species, such as *Planctopirus limnophila* (Scheuner et al, 2014) (before named *Planctomyces limnophilus* (Jogler et al, 2011)) or several *Pirellula* species (Lindsay et al, 1997), the distance between the intracytoplasmic and cytoplasmic membrane is unusually variable. Some *Planctomycetes* contain an additional compartment inside their pirellulosome. The anammox bacteria, which perform anaerobic ammonium oxidation and play an important role in the biological nitrogen cycle (Kartal et al, 2011b), have an additional compartment: the anammoxosome. This prokaryotic organelle is proposed to be the location of the anammox reaction whereby the bacteria conserve the energy needed for their growth (Lindsay et al, 2001; van Niftrik et al 2004; Neumann et al, 2014; de Almeida et al, 2015). Another interesting feature of anammox bacteria is the presence of a multitude of unique ladderane lipids (Sinninghe Damsté et al, 2002; Sinninghe Damsté et al, 2005).

New findings have intensified the discussion on the identity of the planctomycetal cytoplasmic membrane (Lindsay et al, 1997; Lindsay et al, 2001; Fuerst & Sagulenko, 2011; Speth et al, 2012; Devos, 2014a; Devos, 2014b). Historically, this membrane has been defined as a cytoplasmic membrane, mostly because the paryphoplasm was interpreted as a cytoplasmic compartment due to the detection of RNA inside (Lindsay et al, 1997; Lindsay et al, 2001). In 2012, however, genes necessary for the insertion of the typical Gram-negative

outer membrane components lipopolysaccharide (LPS) and outer membrane proteins (OMPs) were identified in the genomes of all analyzed *Planctomycetes* (Speth et al, 2012). A previous bioinformatics analysis had already detected three additional genes involved in LPS biosynthesis in the genomes of five *Planctomycetes*, including *P. limnophila* and *Rhodopirellula baltica* (Sutcliffe, 2010). In a more in-depth study, focused on the genome of *R. baltica*, multiple genes necessary for the biosynthesis of LPS were found (Glöckner et al, 2003). In addition, the genome of the anammox bacterium *Kuenenia stuttgartiensis* was found to also contain genes that are associated with a Gram-negative cell plan (Strous et al, 2006). These studies, especially the one by Speth et al, have led to the hypothesis that this 'cytoplasmic membrane' in fact harbours the outer membrane components LPS and OMPs, and might therefore be better interpreted as an outer membrane (Speth et al, 2012; Devos, 2014a; Devos, 2014b). This hypothesis awaits further verification by experimental data such as the direct detection of OMPs (see chapter 3) or LPS in *Planctomycetes*.

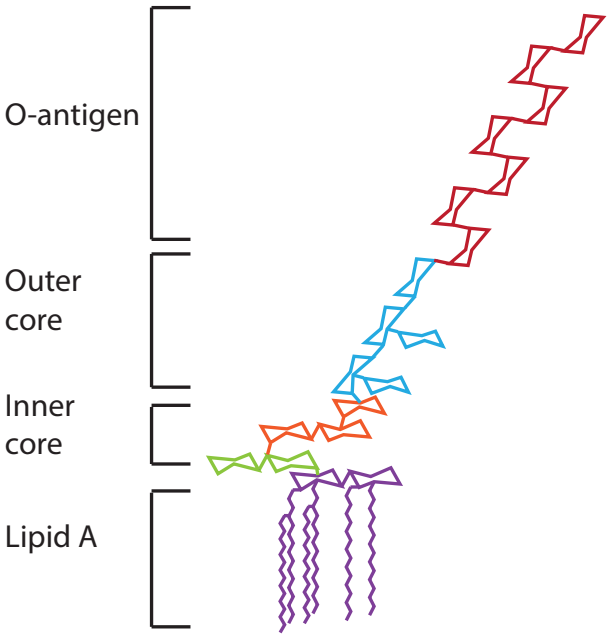

Figure 1. *Schematic overview of an LPS molecule consisting of a lipid A fraction, an inner core (Kdo in green, L,D-Hep in orange), outer core and O-antigen. The O-antigen can be much longer than the chain depicted in the scheme.*

As opposed to the symmetric cytoplasmic membrane, the outer membrane of Gram-negative bacteria is an asymmetric lipid bilayer which consists of an inner leaflet of phospholipids and an outer leaflet with LPS as a main component (Gronow & Brade, 2001; Silhavy et al, 2010). LPS has never been observed in cytoplasmic membranes and, together with the characteristic ß-barrel structured OMPs, acts as a specific marker for the Gram-negative outer membrane (Silhavy et al, 2010). The structure of LPS (Fig. 1) is quite different to that of phospholipids. Phospholipids have a relatively small head group coupled to a glycerol-3-

phosphate to which two fatty acids are attached (Cronan, 2003). LPS, however, consists of the membrane-embedded lipid A part, in most cases linked via a core oligosaccharide to a short or long polysaccharide called the O-antigen (Raetz & Whitfield, 2002). The presence of LPS in the outer leaflet of the outer membrane makes this membrane difficult to permeate for hydrophobic substances, explaining the fact that Gram-negative bacteria are often more resistant to antibiotics than Gram-positive bacteria (which only have a cytoplasmic membrane surrounded by peptidoglycan).

The lipid A molecule is the hydrophobic anchor of LPS and typically consists of a glucosamine disaccharide, to which a variable amount of four to seven acyl-chains of variable length is coupled (Trent et al, 2006). In almost all cases, these acyl-chains are LPS-specific, 12-20 C-atoms long chains with a 3'-hydroxyl group, which have therefore been used as LPS markers (Saddler & Wardlaw, 1980; Parker et al, 1982). The core region has a length of roughly 8-12 sugar units and comprises an inner and an outer core (Caroff & Karibian, 2003). The inner core often contains one or multiple 3-deoxy-manno-octulosonic acid (Kdo) residues coupled to the glucosamine that carries four acyl-chains (Raetz & Whitfield, 2002; Caroff & Karibian, 2003). In some cases, one of these Kdo residues can be replaced by the similar D-*glycero*-D-*talo*-oct-2-ulosonic acid (Ko) residue (Holst, 2007). A common constituent of the inner core is a chain of L-glycero-D-manno-heptopyranose (L,D-Hep) residues, which is coupled to the first Kdo, and often undergoes modifications (Caroff & Karibian, 2003). The outer core is more variable, but often consists of an oligosaccharide. The O-antigen is highly variable and species-specific and contains a varying number of repetitive sugar-containing subunits (Greenfield & Whitfield, 2012). In addition to the full, so-called smooth (S-) type of LPS, a rough (R-) type of LPS exists which lacks the O-antigen and sometimes pieces of the core (Caroff & Karibian, 2003).

The lipid A moiety is the most conserved part of LPS, and with the rare exception of a lipid A-deficient mutant of *Neisseria meningitides* (Steeghs et al, 1998; Steeghs et al, 2001) and a specialized group of Gram-negative bacteria containing sphingolipids instead of LPS (Kawahara et al, 1991; Kawasaki et al, 1994), all Gram-negatives are proposed to contain this structure. The biosynthesis pathway of lipid A is well conserved within Gram-negatives and variation within the lipid A structure occurs by modification afterwards (Raetz & Whitfield, 2002; Trent et al, 2006; Raetz et al, 2009; Needham & Trent, 2013). The biosynthesis of lipid A begins with the attachment of an acyl-chain to the 3-OH group of UDP-*N*-acetylglucosamine (UDP-GlcNAc) via the cytosolic enzyme LpxA (Crowell et al, 1986; Anderson & Raetz, 1987). LpxC removes the acetyl group of the glucosamine (Young et al, 1995), creating an amine group to which LpxD couples an additional acyl-chain (Kelly et al, 1993). The enzyme LpxH, which is not present in all Gram-negatives, exchanges the UDP on the 1'-position of a part of the glucosamines by a phosphate (Babinski et al, 2002). LpxB creates a disaccharide with a total of four acyl-chains by linking a diacylglucosamine with a phosphate to a diacylglucosamine which still has an UDP moiety instead (Crowell et al, 1986). The lipid A precursor inserts into the cytoplasmic membrane at this point (Trent et al, 2006). Subsequently a phosphate is coupled to the 4-hydroxyl group of the unphosphorylated glucosamine by the enzyme LpxK (Ray & Raetz, 1987; Garrett et al, 1997). LpxL and LpxM (Brozek & Raetz, 1990; Clementz et al, 1997; Vorachek-Warren et al, 2002) both couple an

additional acyl-chain to a 3-hydroxyl group of the acyl-chains that are connected to the glucosamine moiety containing the 4'-phosphate group. Some organisms encode for only one of these two enzymes in their genome (Raetz & Whitfield, 2002). *Escherichia coli* mutants synthesizing a lipid A with only four acyl-chains (because of the lack of both LpxL and LpxM) can still grow under certain conditions, although the stability of the cells is compromised (Vorachek-Warren et al, 2002). It is important to note that the fifth and sixth acyl-chains can only be coupled to the LPS precursor after the first synthesis step of the inner core, the addition of one or more Kdo sugars, has been performed by the enzyme WaaA (Clementz & Raetz, 1991; Trent et al, 2006).

Subsequently, a plethora of enzymes can modify the lipid A-Kdo, and for instance remove or add acyl-chains or modify or remove groups such as phosphate coupled to the glucosamines (Trent et al, 2006). The less conserved waa region, containing approximately 15 genes, is responsible for the biosynthesis of the core oligosaccharide (Heinrichs et al, 1998). After the core is attached to the lipid A, the LPS precursor is flipped by MsbA so it resides in the periplasmic face of the cytoplasmic membrane (Polissi & Georgopoulos, 1996; Zhou et al, 1998). In organisms with smooth LPS, the polysaccharide is synthesized on a C_{55}-undecaprenol phosphate via one of three known routes (Greenfield & Whitfield, 2012) and is coupled to the outer sugar moiety of the core region by WaaL (Raetz & Whitfield, 2002). Afterwards, the mature LPS is transported to the outer leaflet of the outer membrane by the proteins LptA-G (Silhavy et al, 2010).

The omnipresence of LPS in Gram-negative bacteria and its surface exposed location make it a perfect target for the immune system of a multitude of hosts to detect an infection by Gram-negative bacteria. Lipid A, as the most conserved part of LPS, is indeed recognized by the mammalian immune system via multiple pathways including binding of positively charged cationic antimicrobial peptides (CAMPs) or activation of the Toll-like receptor 4 (TLR4) after binding of the lipid A part by the LPS-binding protein (LBP) (Needham & Trent, 2013). CAMPs are not only produced by mammals, but can even be synthesized by Gram-positive bacteria in attempt to win the competition with Gram-negative bacteria in the same niche (Martin et al, 2003). The TLR4 pathway produces inflammatory cytokines which can, in case of high amounts of lipid A, lead to sepsis and potentially to death (Opal, 2007). Multiple pathogenic Gram-negative bacteria modify their lipid A structure in order to evade the immune system (Needham & Trent, 2013).

Here we investigated the ability of the *Planctomycetes K. stuttgartiensis*, *P. limnophila* and *R. baltica* to synthesize LPS. The genes involved in lipid A biosynthesis were studied and LPS was enriched and visualized via gel electrophoresis and analyzed for the presence of Kdo. The reaction of the cells upon incubation with the CAMP polymyxin B was observed via electron microscopy. In addition, experiments to obtain a more in-depth characterization of *K. stuttgartiensis* LPS were performed: the presence Kdo was studied by GC-MS on untreated biomass and a lipid A isolation procedure followed by HPLC-ESI/MS was performed.

Materials & Methods

Growth conditions. Planktonic *K. stuttgartiensis* cells were grown in an enrichment culture (~95% *K. stuttgartiensis*) in a membrane bioreactor operated as described before (Kartal et al, 2011a). *Escherichia coli* K12 cells for LPS extraction were grown in LB broth. *E. coli* and *Bacillus megaterium* used for polymyxin tests were grown on M3 agar plates (0.8% nutrient broth (Oxoid, Wesel, Germany) and 2% agar (VWR Chemicals, Radnor, PA, USA)). *Tannerella forsythia* was grown as described before (Posch et al, 2013). *Planctopirus limnophila* and *Rhodopirrelula baltica* were ordered from the DSMZ (Braunschweig, Germany) and grown in, respectively, PYGV and M13a liquid media (Schlesner, 1994).

Bioinformatic identifciation of genes necessary for lipid A biosynthesis. The following amino acid sequences were retrieved from Uniprot and used for BLASTp searches (McGinnis & Madden, 2004) against *K. stuttgartiensis* (taxid: 174633), *R. baltica* (taxid: 265606) and *P. limnophila* (taxid: 521674): LpxA (UniProtKB-O84536 (LPXA_CHLTR)), LpxC (UniProtKB-O84538 (LPXC_CHLTR)), LpxD (UniProtKB-P0CD76 (LPXD_CHLTR), LpxB (UniProtKB-O84416 (LPXB_CHLTR)), LpxK (UniProtKB-O84407 (LPXK_CHLTR)), WaaA (UniProtKB-P0CE14 (KDTA_CHLTR)) and LpxL, annotated under its previous name HtrB (UniProtKB-O84013 (O84013_CHLTR)) from *Chlamydia trachomatis* (strain D/UW-3/Cx), LpxL (UniProtKB-P0ACV0(LPXL_ECOLI)), LpxM (UniProtKB-P24205(LPXM_ECOLI)) and ArnT (UniProtKB-P76473 (ARNT_ECOLI)) from *E. coli* K12 and KdkA (UniprotKB-Q7MPR5 (KDKA_VIBVY)) from *Vibrio vulnificus*. An e-value cut-off of 10^{-20} was used for the *C. trachomatis* searches and an e-value cut-off of 10^{-6} was used for searches against the less related *E. coli* and *V. vulnificus*.

C. trachomatis was used in the BLAST search since this organism is known to possess LPS and is closer related to the *Planctomycetes* than for instance *E. coli*. However, the LpxL from *C. trachomatis* has a deviant substrate specificity and LpxK is absent from this organism altogether. Therefore, a BLASTp search for these proteins from *E. coli* was performed in addition. The expression and translation of the identified genes in *K. stuttgartiensis* were investigated by comparison to a previously published transcriptome (Hu et al, 2013) and proteome (Kartal et al, 2011b). The Lipid A structure displayed in figure 2 was based on a structure downloaded from the Lipidomics Gateway (Sud et al, 2006).

LPS enrichment. LPS was extracted as described before (Hitchock & Brown, 1983). In short, *K. stuttgartiensis* cells at an OD_{600} of 1.4 were harvested from a single cell membrane bioreactor and pelleted by centrifugation for 5 min at 20830 g. The cells were resuspended in 1 M Tris HCl pH 6.8 including 2% SDS, 4% β-mercaptoethanol, 10% glycerol and 0.002% Orange G, and were boiled for 10 min in this buffer. After cooling the treated cells on ice, proteinase K was added to a concentration of 0.45 mg/ml and the samples were incubated for 16 h at 55˚C while shaking at 300 rpm. These samples were used for gel electrophoresis and colorimetric detection of KDO.

Gel electrophoresis. The extracted LPS was analyzed by separation on a 15% Tris/Tricin gel run in 0.1 M Tris, 0.1 M Tricin and 0.1% SDS and stained with a LPS specific silver stain as described before (Tsai & Frasch, 1982). To analyze if proteins were still present after the LPS

extraction procedure, the samples were also analyzed with the use of normal SDS-PAGE (Laemmli, 1970) using 15% slab gels and staining with Coomassie G250.

Colorimetric detection of Kdo. The samples after LPS enrichment using the Hitchcock & Brown-protocol were tested for the presence of Kdo. Kdo was detected by the thiobarbituric acid assay as described before (Warren, 1959) using volumes of 10-30 µl of a 1 nM stock of Kdo (Sigma Aldrich, St. Louis, MO, USA) as standard. As samples, three different amounts of lysis buffer containing LPS were measured and the same amounts of lysis buffer without LPS were included as a control.

Polymyxin B incubation. Colonies (in the case of *E. coli* and *B. megaterium*) or pelleted cells grown in liquid culture (for *K. stuttgartiensis*, *R. baltica* and *P. limnophila*) were resuspended in 20 mM HEPES buffer including 1 g/l sodium bicarbonate pH 7.5. Polymyxin B was added up to a final concentration of 5 mg/ml and the cells were incubated for 30 min at 30°C. As a negative control, HEPES buffer was added instead of the polymyxin solution. After the incubation the cells were washed twice and applied to hydrophilized carbon coated grids on which they were incubated for 20 min, then washed 1 min on 0.5% uranyl acetate in MilliQ water and washed three times in MilliQ water. The binding of polymyxin B to LPS was observed as blebbing of the outer membrane (Wiegel & Quandt, 1982) and was visualized with a JEOL (Tokyo, Japan) JEM1010 TEM.

LPS extraction. Extraction of R-type LPS for HPLC-ESI/MS analysis was performed on *K. stuttgartiensis* and *E. coli* K12 biomass using the phenol-chloroform-petroleum ether (PCP) solution, as described before (Galanos et al, 1969). *K. stuttgartiensis* biomass was harvested from a membrane bioreactor and pelleted by centrifugation (15 min, 4500 g) and the pellets were frozen at -20°C and subsequently lyophilized. This lyophilized biomass was washed in ethanol (concentration 51.6 mg/ml) by stirring for 2 h after which it was pelleted (2 min, 4000 g). Thereafter, the biomass was washed twice with acetone and twice with diethylether. Dried biomass (103.2 mg/ml) was extracted while stirring for 1 h in a mixture of phenol: chloroform: petroleum ether (boiling point 40-60°C) (2:5:8, v:v:v) to which additional solid phenol was added until the solution became clear.The supernatant, containing LPS, was collected and the extraction was repeated twice on the remaining biomass. The petroleum ether and chloroform were removed from the pooled supernatants by rotary evaporation. To the remaining sample, three times the volume of acetone was added and left 16 h at 4°C to induce LPS precipitation. The precipitated LPS was pelleted (30 min, 4000 g), resuspended in water by incubation in an ultrasonic bath for 1 h followed by ultracentrifugation (5 h, 170000g). The resulting pellet was resuspended in water, frozen at -20°C and lyophilized. Subsequently, in order to obtain lipid A, an aliquot of the LPS was resuspended in 1% acetic acid in water by sonication for 10 min and refluxed while stirring at 100°C for 4 or 8 h. Lipid A was pelleted by ultracentrifugation (1 h, 100000g), resuspended in water, frozen at -20°C and lyophilized. The dried Lipid A was resuspended (concentration 0.95 mg/ml) in dichloromethane:methanol (9:1, v:v) filtered through a 0.45 µm regenerated cellulose (RC) filter (Alltech Associates Inc., Deerfield, IL, USA) prior to analysis by HPLC-ESI/MS. As a control, the same method was performed on *E. coli* K12 biomass.

HPLC-ESI/MS. Lipid A, isolated from *K. stuttgartiensis* and *E. coli* K12 as well as a monophosphorylated lipid A standard (MPLA, Avanti polar lipids, Alabaster, AL, USA), was analyzed as described previously (Sturt et al, 2004) with some modifications (Sinninghe Damsté et al, 2011). An Agilent 1200 series LC (Agilent, San Jose, CA), equipped with thermostatted auto-injector and column oven, coupled to a Thermo LTQ XL linear ion trap with Ion Max source with electrospray ionization (ESI) probe (Thermo Scientific, Waltham, MA, USA) was used. Separation was achieved on a Lichrosphere diol column (250 x 2.1 µm, 5 µm particles; Alltech Associates Inc., Deerfield, IL, USA) maintained at 30°C. The following elution program was used with a flow rate of 0.2 ml/min: 100% A for 1 min, followed by a linear gradient to 66% A: 34% B in 17 min, maintained for 12 min, followed by a linear gradient to 35% A: 65% B in 15 min, where A = hexane:2-propanol:formic acid:14.8 M NH_{3aq} (79:20:0.12:0.04, v:v:v:v) and B = 2-propanol:water:formic acid: 14.8 M NH_{3aq} (88:10:0.12:0.04, v:v:v:v). Total run time was 60 min with a re-equilibration period of 20 min in between runs. The lipid extract was analyzed by an MS routine where a positive ion scan (*m/z* 400-2000) was followed by a data dependent MS^2 experiment where the base peak of the mass spectrum was fragmented (normalized collision energy (NCE) 25, isolation width 5.0, activation Q 0.175). This was followed by a data dependent MS^3 experiment where the base peak of the MS^2 spectrum was fragmented under identical fragmentation conditions. This process was repeated on the 2nd to 4th most abundant ions of the initial mass spectrum. In addition, samples were reanalyzed as described above but with an extended run time up to 120 min to observe compounds that would possibly elute later and/or with an extended mass range up to *m/z* 3000, and in negative ionmode to potentially observe larger lipid A type molecules.

Methanolysis. *K. stuttgartiensis* biomass was harvested from a membrane bioreactor and pelleted by centrifugation (15 min, 4500 g) and the pellets were frozen at -20°C and subsequently lyophilized. The dried biomass was resuspended in 0.5 M menthanolic hydrochloric acid (HCl) to a final concentration of 1 mg/ml and weak methanolysis was performed by hydrolyzing the sample for 45 min at 85°C. The acid was evaporated under N_2 gas and the sample was washed three times with methanol. The sample was then peracetylated two times with pyridine in acetic anhydride (1:1) for 10 min and then for 20 min at 85°C before being dried under N_2 gas again.

An aliquot of the sample after weak methanolysis was subjected to strong methanolysis by hydrolyzing it in 2 M methanolic HCl (concentration 0.25 mg/ml) by incubation for 16 h at 85°C. The sample was then treated (washed, peracetylated) as described above. Aliquots of both the weak and strong methanolyzed sample were dissolved in chloroform and injected on a GC column (GC 7890 A (Agilent Technologies, Santa Clara, CA, USA) fused with a HP-5MS capillary column (30m x 0.25mm, film thickness 0.25 µm). The temperature was set to 150°C for 3 min, then increased to 250°C at 3°C/min and finally to 320°C at 25°C/min. LPS from *Salmonella minnesota* R345 was treated in the same way and used as a control. A blank was performed in exactly the same way omitting the addition of sample.

Results

Identification of genes involved in lipid A biosynthesis. BLASTp searches against selected genes involved in the lipid A biosynthesis of *C. trachomatis* were performed to identify if the genes necessary for LPS biosynthesis were present. In all three analyzed *Planctomycetes* species all genes necessary for the synthesis of a lipid A precursor consisting of a glucosamine disaccharide with five acyl-chains (Fig. 2) were present. In addition, the waaA genes for the attachment of one or more Kdo moieties to the disaccharide were identified (Table 1). No hits for the *C. trachomatis* LpxL were found in the *Planctomycetes*, but all three organisms had a protein that was homologous to the *E. coli* LpxL. Furthermore, LpxM, responsible for coupling the sixth acyl-chain to lipid A in *E. coli* was absent from *C. trachomatis* and therefore the *E. coli* LpxM was used in the BLAST search. No hits were found for the *E. coli* LpxM.

Table 1. *Presence of genes involved in lipid A biosynthesis in* K. stuttgartiensis*,* R. baltica *and* P. limnophila. *Identifier, e-value and percentage of identity are only given for the best hit. Proteins from* C. trachomatis *were used as a template, with the exception of the two last proteins for which* E. coli *K12 (Ec) was used.*

Gene		*K. stuttgartiensis*	*R. baltica*	*P. limnophila*
LpxA	Gene name/ identifier	Kusta0037	WP_007328498	Plim_0918
	e-value	$3e^{-52}$	$2e^{-41}$	$7e^{-34}$
	Identity	37%	33%	29%
LpxC	Gene name/ identifier	Kusta0035	WP_007328499	Plim_0919
	e-value	$4e^{-39}$	$1e^{-28}$	$7e^{-33}$
	Identity	33%	30%	31%
LpxD	Gene name/ identifier	Kuste4516	Q7UEV1.2	Plim_2360
	e-value	$1e^{-69}$	$2e^{-56}$	$1e^{-59}$
	Identity	38%	34%	36%
LpxB	Gene name/ identifier	Kuste4276	WP_007328098	Plim_0943
	e-value	$4e^{-34}$	$4e^{-24}$	$2e^{-23}$
	Identity	27%	25%	24%
LpxK	Gene name/ identifier	Kuste4016	WP_007337624	Plim_0158
	e-value	$4e^{-32}$	$4e^{-27}$	$1e^{-28}$
	Identity	28%	29%	30%
WaaA	Gene name/ identifier	Kustb0171	WP_007330822	Plim_2366
	e-value	$2e^{-37}$	$9e^{-39}$	$3e^{-41}$
	Identity	25%	25%	26%
LpxL	Gene name/ identifier	No hit	No hit	No hit
LpxL (*Ec*)	Gene name/ identifier	Kuste3366	WP_007329114	Plim_1862
	e-value	$1e^{-11}$	$6e^{-9}$	$2e^{-15}$
	Identity	26%	23%	30%
LpxM (*Ec*)	Gene name/ identifier	No hit	No hit	No hit

Compared to the predicted *Planctomycetes* lipid A (Fig. 2), the lipid A from *E. coli* might contain one additional phosphate coupled to each glucosamine residue, one additional acyl-chain, 3-hydroxyl groups on two of the acyl-chains that might be absent if the planctomycetal lipid A resembles the lipid A of *C. trachomatis*, and probably has a different length for some of the acyl-chains (Fig. 2 in grey). All lipid A biosynthesis genes detected in the planctomycetal genomes were also detected in the transcriptome of *K. stuttgartiensis* (Table 2) (Hu et al, 2013), but not in the proteome (Kartal et al, 2011b).

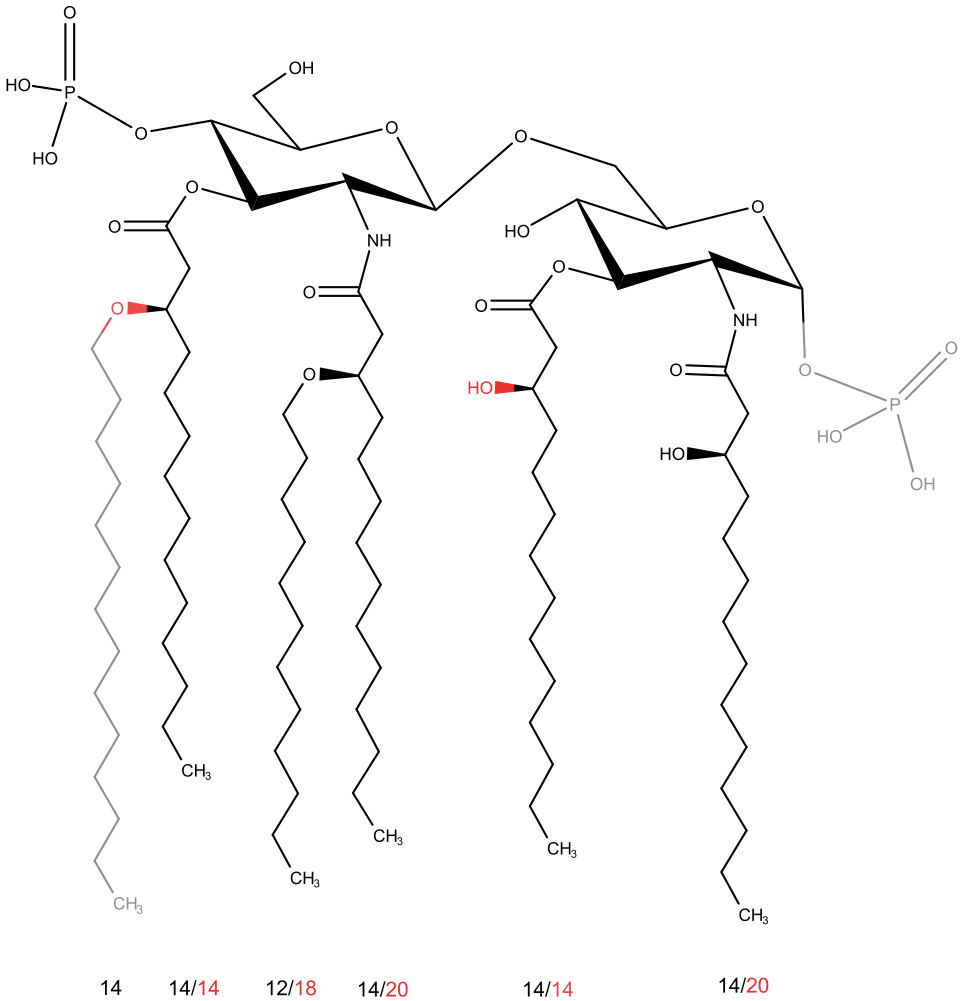

Figure 2. *An overview of the structure (in black) of the lipid A precursor for which the biosynthetic genes are present in the genomes of* K. stuttgartiensis*,* R. baltica *and* P. limnophila*. Additional moieties attached to the standard* E. coli *lipid A are indicated in grey. Moieties in red are absent in* C. trachomatis*. Lengths of the acyl chains in* E. coli *and* C. trachomatis *are given in black and red respectively.*

Characterization of enriched LPS. An LPS enrichment protocol was performed on *K. stuttgartiensis*, *R. baltica* and *P. limnophila* by treating the cells with lysis buffer followed by the degradation of proteins. After this enrichment, LPS can be visualized on Tris-Tricin acrylamide gels using an LPS-specific silver stain. The gels showed the presence of multiple bands (Fig. 3). In the case of *T. forsythia*, which is known to possess R-type LPS, a clear band was seen at a low apparent molecular mass (arrow in Fig. 3A, lane 1) after LPS specific silver staining. No significant bands were seen at higher apparent molecular masses, as is characteristic for R-type LPS. A similar pattern was observed for the enriched LPS samples from *K. stuttgartiensis* (Fig. 3A lane 2) and *R. baltica* (Fig. 3A lane 4), although some signals were present at higher apparent molecular masses. In the case of *P. limnophila*, multiple bands were observed in a ladder-like orientation, as is typical for S-type LPS. The absence of bands after Coomassie staining of a gel with enriched LPS from *T. forsythia* and *K. stuttgartiensis* (Fig. 3B) suggested that no protein background was present after the treatment and protein thus could not cause the signals observed on the silver stained gel. The enriched LPS samples were analyzed for the presence of Kdo, part of the inner core directly coupled to lipid A in many species. The colorimetric assay did not detect Kdo in *R. baltica* and *P. limnophila* enriched LPS. In the *K. stuttgartiensis* samples, Kdo was found at a concentration of approximately 30 x 10^{-12} g Kdo per gram wet weight of cells.

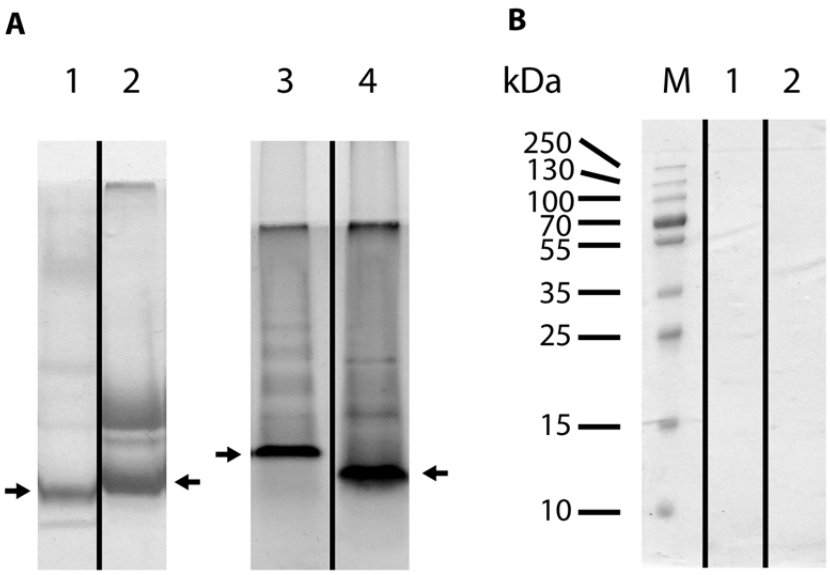

Figure 3. *(A) Gel electrophoresis followed by an LPS-specific silver stain on enriched LPS showed that* K. stuttgartiensis *(lane 2),* P. limnophila *(lane 3) and* R. baltica *(lane 4) have a band at a similar height as the positive control (indicated by arrows); LPS enriched from* T. forsythia *(lane 1). Several other (faint) bands at higher apparent molecular masses are present in all four species. (B) Gel electrophoresis followed by the protein stain Coomassie on the enriched LPS from* T. forsythia *(lane 1) and* K. stuttgartiensis *(lane 2) indicated that no protein was present after the LPS enrichment protocol.*

Microscopical analysis of cells treated with LPS-binding agent. The putative presence of LPS was investigated in intact *K. stuttgartiensis*, *R. baltica* and *P. limnophila* cells by observing negative stained cells incubated with the CAMP polymyxin B, which causes membrane blebbing upon binding to lipid A (Wiegel & Quandt, 1982). *E. coli* and *B. megaterium* were also visualized after incubation with polymyxin B, as respectively positive and negative control. As expected, the Gram-positive *B. megaterium* was unaffected by the polymyxin treatment (Fig. 4, I-J). The appearance of the membrane of *E. coli* was clearly disrupted in the cells incubated with polymyxin B compared to the negative control and treated cells seemed to accumulate more stain inside the cells (Fig. 4, G-H). For *R. baltica*, the membrane showed a strong disruption after treatment (Fig. 4, E-F). *K. stuttgartiensis* cells showed membrane blebs and a stronger staining inside the cells after incubation with polymyxin B (Fig. 4, A-B). The membrane and staining pattern of *P. limnophila* cells seemed only slightly affected by polymyxin B treatment (Fig. 4, C-D).

Figure 4 (right page). *Negatively stained cells treated with 5 mg/ml polymyxin B for 30 min.* Planctomycetes *showed very mild (*P. limnophila*; D, compared to C (negative control)), moderate (*K. stuttgartiensis*; B compared to A (negative control)) or strong (*R. baltica*; F compared to E (negative control)) membrane blebbing in reaction to polymyxin B treatment. The Gram-negative* E. coli *showed clear membrane blebbing (H compared to G (negative control)) and the Gram-positive* B. megaterium *was unaffected by polymyxin B (J compared to I (negative control). Arrows indicate (putative) membrane blebs. Scale bars 200 nm.*

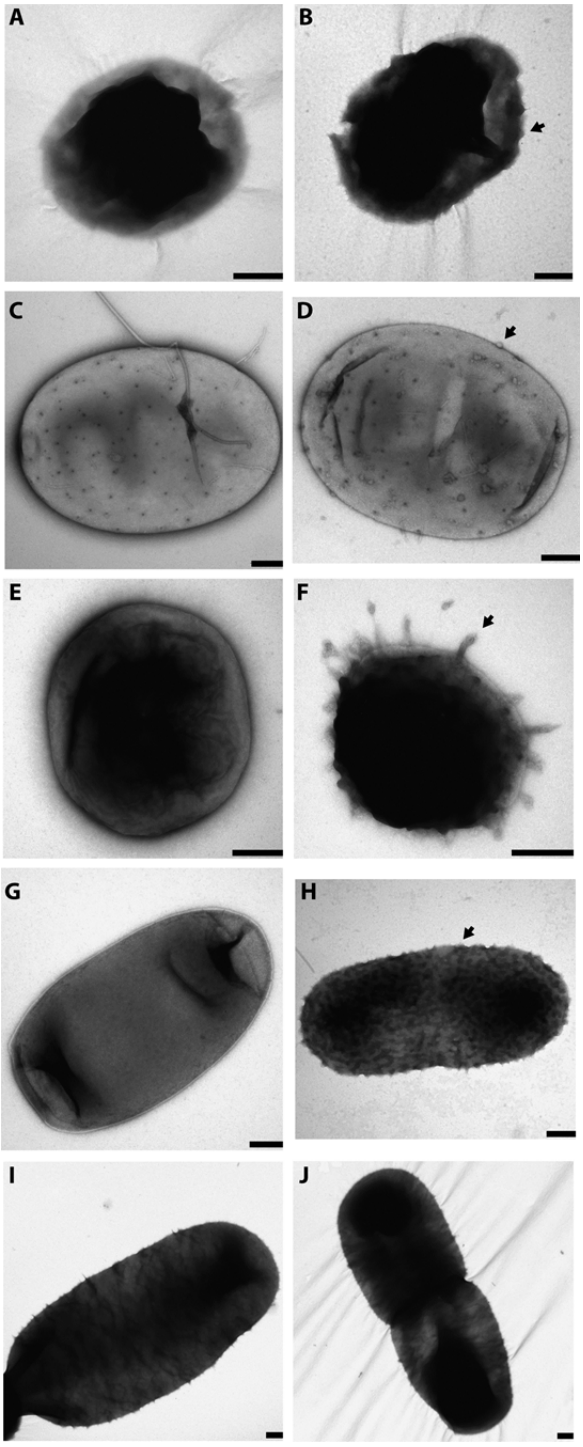
A
B
C
D
E
F
G
H
I
J

HPLC-ESI/MS analysis of isolated Lipid A. LPS was extracted from lyophilized biomass of *K. stuttgartiensis* and *E. coli* K12 using a mixture of phenol, chloroform and petroleum ether. LPS was precipitated from the extracts with acetone, which led to clearly visible white precipitates for both *K. stuttgartiensis* and *E.coli* K12 with yields of approximately 1% (g LPS per g dry weight of cells). This putative LPS was hydrolyzed in order to obtain the lipid A fraction and the yield for this step was about 40% for both species. This putative lipid A was analyzed using HPLC-ESI/MS to identify the presence and structure of the lipid A. A monophosphorylated lipid A standard generated one main peak at a retention time of 26 min, as well as several smaller peaks (Fig. 5A). The main peak represented the monophosphorylated lipid A, as verified by the presence of molecular ions in the mass spectrum (MS^1) and several diagnostic fragments and losses after MS^2 (data not shown). The chromatogram of the isolated lipid A from *E. coli* showed several peaks (labeled with I, Fig. 5B) that after fragmentation revealed the same diagnostic fragments and losses as observed in the MLPA standard. The most dominant peak eluted at 26 min and was identified as biphosphorylated lipid A (Fig. 5B). The other eluting lipid A related compounds were most likely lipid A with varying numbers of sugar moieties and/or fatty acids attached. The *K. stuttgartiensis* isolated lipid A fraction showed three main peak clusters, eluting around 25, 31 and 35 min (Fig. 5C). In this case the MS spectra of the entire molecules and their fragments revealed the presence of several anammox-specific phospholipids (Boumann et al, 2006) and a bacteriohopanepolyol (Rush et al, 2014) instead of lipid A. Additional runs with extended run time, mass range or polarity switching to negative ion mode also did not reveal the presence of lipid A containing structures in the *K. stuttgartiensis* extract (data not shown).

Figure 5 (right page). *HPLC-ESI/MS chromatogram (basepeak) of lipid A extracts showing the amount of MS signal per time point of elution. The eluted lipids are annotated based on MS and MS^2 spectra (not shown). (A) Monophosphorylated lipid A standard. (B) Extracted LPS from* E. coli K12. *(C) Extracted LPS from* K. stuttgartiensis. *MS-spectra were measured at a mass range of 400-2000 Da. Annotations of the peaks: 1: lipid A, 2: phosphoethanolamine (PE), 3: cardiolipins, 4: overlapping cluster of ladderane ether/ester lipids with PE or phosphatidylglycerol (PG) headgroups, 5: PG-ether/ester & PG-diether ladderanes, 6: BMT cyclitolether, 7: PC-monoether.*

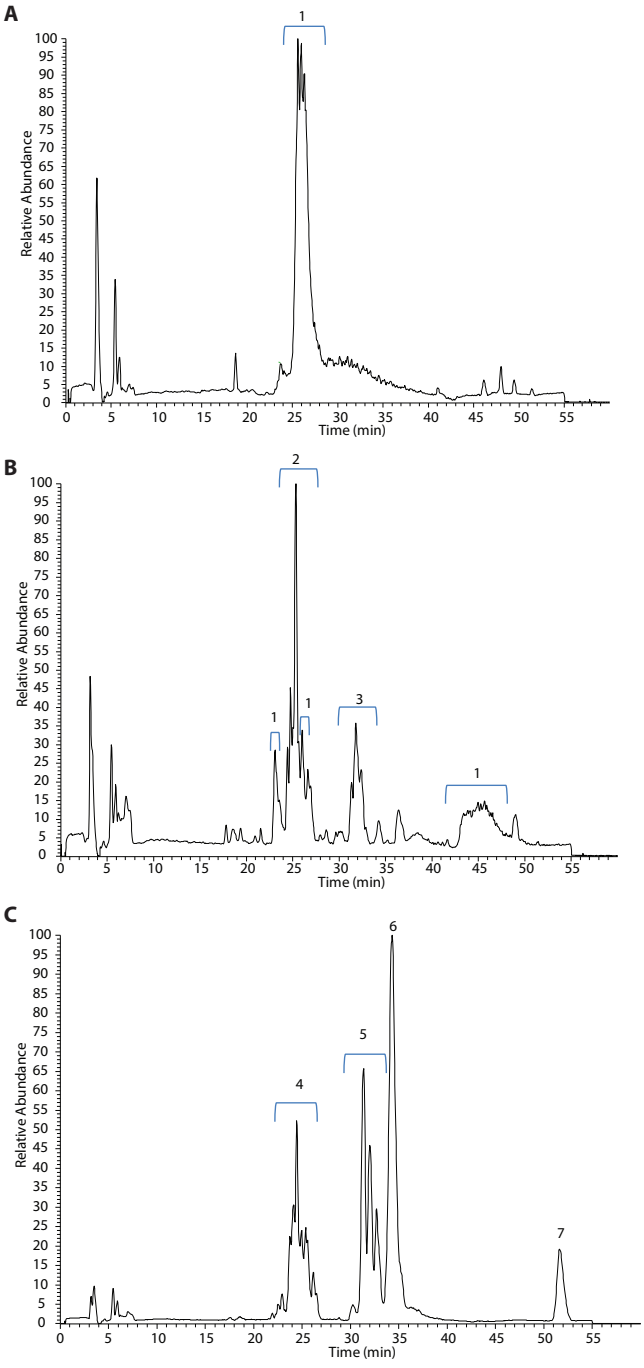
A
1
Relative Abundance
Time (min)
B
2
1
1
3
1
Relative Abundance
Time (min)
C
6
5
4
7
Relative Abundance
Time (min)

GC-MS analysis. *K. stuttgartiensis* biomass was analyzed for Kdo using GC-MS after methanolysis. Biomass from *S. minnesota* R345 was used as a positive control. A blank GC chromatogram, in the absence of sample, was used as negative control (data not shown) and showed no peaks before a retention time of 36 min, and the same peaks after 36 min as seen in all samples (Fig. 6). Although peaks were present after methanolysis of the *K. stuttgartiensis* biomass, these could be identified as hexoses and possibly heptoses (Fig. 6, B & D). No peaks were seen at the retention time (around 21 min) typical for Kdo.

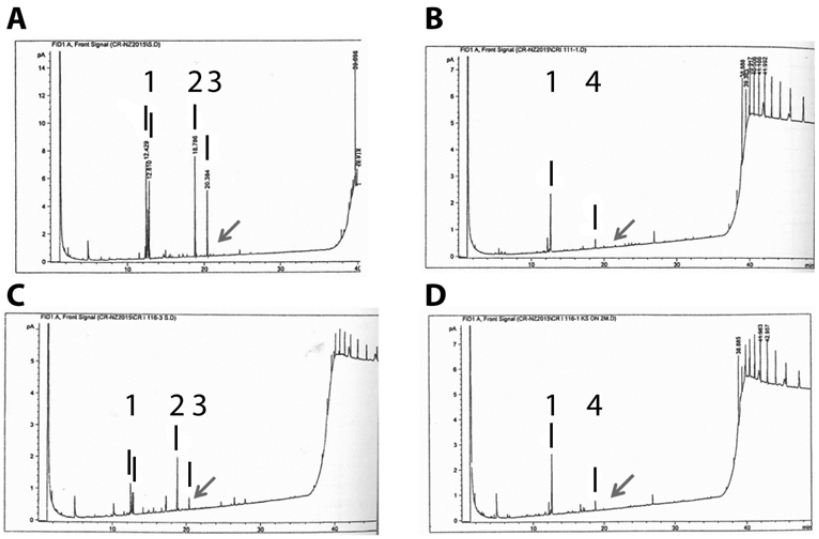

Figure 6. *GC chromatograms of* S. minnesota *R345 (A, C) and* K. stuttgartiensis (B, D) *biomass after weak (A-B) and strong (C-D) methanolysis indicated the presence of Kdo in* S. minnesota *(used as a positive control), but not in* K. stuttgartiensis *(position of Kdo in the spectra is indicated by a grey arrow). Annotation of the peaks is as follows 1: Hexose, 2: L,D-Hep, 3: Kdo, 4: possible heptose.*

Discussion

This study aimed at elucidating whether LPS is present or absent in *Planctomycetes* by studying *K. stuttgartiensis*, *P. limnophila* and *R. baltica*. Of the multiple analyses that were performed, several suggested the presence of LPS, although other, more in-depth, investigations did not detect components of LPS in *K. stuttgartiensis*. To elucidate this matter, the different methods will be discussed below also taking into account how these methods could lead to false positive or false negative results.

The genetic analysis focused on the biosynthesis of lipid A and the addition of Kdo moieties, since this is the most conserved pathway in Gram-negative LPS biosynthesis. This analysis showed that all three *Planctomycetes* contain genes that would allow them to synthesize a lipid A with five acyl-chains, one phosphate and Kdo. LpxH, responsible for coupling one of the two phosphates to lipid A, was not detected in the genomes of the *Planctomycetes*, but it is hypothesized that yet unidentified isoforms might exist that phosphorylate lipid A of organisms that lack LpxH (Raetz & Whitfield, 2002). The structure of lipid A of *C. trachomatis*,

used for most BLAST searches because of its limited phylogenetic distance to the *Plancyomycetes*, differs at some points to the *E. coli* lipid A structure (Fig. 2). In *C. trachomatis*, for instance, the length of some acyl-chains is longer than in *E. coli* and some acyl-chains lack 3-hydroxyl groups. For instance LpxL, responsible for adding the fifth acyl-chain to lipid A, of *E. coli* couples acyl-chains with a length of 12 carbon atoms instead of the 18 seen in *C. trachomatis* (Rund et al, 1999; Sweet et al, 2001). Since the LpxL from the *Planctomycetes* resembles the LpxL from *E. coli* rather than from *C. trachomatis* (although most other genes are homologous to those of *C. trachomatis*) it needs to be determined to which extent the structure of a lipid A synthesized by the *Planctomycetes* gene products resembles that of *C. trachomatis*. Previous findings of long 3-hydroxyl acyl-chains (C_{16}, C_{18} and C_{20}) in *Planctomycetes* suggest that some similarity might be present to *C. trachomatis* lipid A (Kerger et al, 1988). It has to be remarked, however, that the 3-hydroxyl acyl-chains could alternatively stem from ornithine lipids, which have been found in *Planctomycetes* (Moore et al, 2013). To resolve the structure of the putative planctomycetal lipid A, genes from each of the *Planctomycetes* could be expressed in, for instance, *E. coli* (knockouts) and the lipid A structure could be determined. All genes involved in lipid A biosynthesis were found in the previously published *K. stuttgartiensis* transcriptome (Table 2) (Hu et al, 2013). This fits with the prior detection of LptD, the OMP involved in inserting the mature LPS in the outer leaflet of the outer membrane (Speth et al, 2012). The absence of the lipid A biosynthesis proteins in the previously published proteome might be explained by a too low resolution (Kartal et al, 2011b). This suggestion is verified by a recent (membrane) proteome that has detected LpxA, LpxD, LpxB, LpxK, LpxL and WaaA (de Almeida et al, in prep). An interesting possible experiment for further research is to use specific inhibitors to inhibit LPS biosynthesis in several *Planctomycetes* and see if the cells are still viable or if such treatment is lethal. The latter would suggest the presence and importance of LPS for these species. Lipid A biosynthesis can efficiently be inhibited at the stage of LpxC via multiple classes of specific inhibitors and it would be worthwhile to test some of these (Tomaras et al, 2014).

Table 2. *Expression of genes involved in lipid A biosynthesis and modification detected in a* K. stuttgartiensis *transcriptome. Expression values taken from Hu et al 2013.*

Gene	**ORF**	**Reads**	**RPKM**[1]
Lipid A biosynthesis			
LpxA	Kusta0037	17	128.16
LpxC	Kusta0035	44	312.27
LpxD	Kuste4516	8	60.66
LpxB	Kuste4276	3	14.03
LpxK	Kuste4016	20	116.94
LpxL	Kuste3366	3	21.44
WaaA	Kustb0171	16	112.66
Lipid A modification			
KdkA	Kuste2721	5	34.42
ArnT	Kuste2285	1	3.83

[1]RPKM, Reads Per Kilobase of exon model per Million mapped reads

Gel electrophoresis of LPS enrichments of the three *Planctomycetes* suggested that LPS was present in these organisms (Fig. 3A). The Hitchcock & Brown protocol used to enrich the LPS is a quite crude protocol: the sample loaded on the gel contains the entire cell content. The proteinase K treatment should degrade the proteins to small peptides (as was verified by the Coomassie stained gel (Fig. 3B)), but nucleic acids, which have not been degraded or eliminated from the sample in this protocol, are common contaminants of LPS (Rezania et al, 2011). To decrease the chance that nucleic acids show a signal on the gel that could be mistaken for LPS, the sample can be treated with DNAse and RNAse. Another possibility for a false positive result would be that the LPS sample of *K. stuttgartiensis* visualized on the gel was caused by the small amount of cells from other species which are also present in the enrichment culture. This could, however, not have caused a signal for *P. limnophila* and *R. baltica*, since pure cultures were used for these species. To further investigate if the signal seen on the gel (Fig. 3) stems from LPS, the band(s) (of a non-silver stained lane) could be excised from the gel and the potential presence of both the lipid A part (potentially after acid hydrolysis) and the oligosaccharide fraction could be analyzed via MS analysis (Gulin et al, 2003). Alternatively, a blot could be made from an unstained gel. In this method, the putative LPS on the gel is hydrolyzed and the lipid A fraction that resides on this blot can be recognized with specific monoclonal antibodies that recognize the mono- (MAb S1) or biphosphorylated (Mab A6) disaccharide regardless of the length of the acyl-chains (Pantophlet et al, 1997). If these antibodies would be able to bind to the planctomycetal lipid A, it might be an elegant idea to perform a pulldown experiment on hydrolyzed membrane fractions or hydrolyzed enriched LPS (Hitchcock & Brown protocol). If this would succeed in capturing lipid A, this would be a good way to circumvent chemical extraction procedures to prepare sample for structural analysis. Another possible experiment that could be performed using these antibodies, together with an antibody recognizing lipid A with two Kdo residues (Mab A20), is immunogold labeling of cells embedded in sections or of freeze-etched cells (as performed on human cells before (Richter et al, 2013)).

The sample obtained via the Hitchcock & Brown protocol was analyzed for the presence of Kdo. The colorimetric assay did not detect Kdo in *P. limnophila* and *R. baltica*. The amount of Kdo detected in *K. stuttgartiensis* is 30 x 10^{-12} g Kdo per g wet weight of cells and this is extremely little in comparison to other organisms, where the Kdo content is in the order of 10^{-5}-10^{-3} g per g wet weight of cells (Luchi & Morrison, 2000). Since the thiobarbituric assay is not absolutely specific and can also detect other sialic acids (Warren, 1959), it is an option that the signal of *K. stuttgartiensis* is caused by another component than by Kdo. Another option would be that the measured signal was caused by Kdo from other organisms present in the *K. stuttgartiensis* enrichment culture. Still these results were unexpected since WaaA, the protein that couples Kdo to lipid A was identified in the genomes of all three organisms (Table 1) and was found in the *K. stuttgartiensis* transcriptome (Table 2). It is a possibility that Kdo was modified after its initial attachment to LPS and hence (almost entirely) escaped detection of the thiobarbituric assay. Indeed this assay was shown to be unable to detect phosphorylated Kdo (Han & Chai, 1991). A BLASTp search against the Kdo kinase of *V. vulnificus* indicated the presence of such a protein encoded in the genome of *K. stuttgartiensis* (Kuste2721, e-value $1e^{-16}$, identity 30%) and the transcriptome verified

expression of this gene (Table 2). No such enzymes were identified in the genomes of *P. limnophila* and *R. baltica*, although it could still be possible that alternative modifications of Kdo occur in these organisms.

In another experiment, the three *Planctomycetes* were incubated with the CAMP polymyxin B. This peptide binds best to a biphosphorylated lipid A molecule, although binding also occurred to lipid A with an attached inner core of three Kdo residues (Kellogg et al, 2001). Binding was almost absent when only one phosphate group was bound to lipid A. Upon binding to a membrane containing LPS, polymyxin B causes formation of membrane blebs (Wiegel & Quandt, 1982). Interestingly it was reported that a mutant that lacks the outer core and O-antigen displays less blebs than organisms which have more extensive molecules. Bleb formation was observed in *R. baltica* (Fig. 4F), and also the membrane of *K. stuttgartiensis* seemed affected, although to a lower degree (Fig. 4B). The effect on *P. limnophila* seemed very mild (Fig. 4D). During an investigation of 35 species, of which 13 were Gram-positive, blebs were seen in all Gram-negatives (although not always to the same extent) and never in Gram-positives (Wiegel & Quandt, 1982) and therefore it seems that the results could be best interpreted as a clear indication of LPS in the three *Planctomycetes*. The difference in the extent of membrane blebbing between the three species might be explained by the possibility that the lipid A or LPS of the three species has a different conformation which affects the binding of polymyxin B. This could be for instance caused by the absence of one of the phosphates or another modification so that polymyxin B has a lower binding affinity to (a part of) the LPS. The most prominent mechanism of polymyxin B resistance is the attachment of a 4-amino-4-deoxy-L-arabinose (L-Ara4N) to the phosphate linked to the glucosamine with three or four acyl-chains by the enzyme ArnT (Olaitan et al, 2014). A BLAST search indicates the presence of ArnT in *K. stuttgartiensis* (Kuste2285, e-value $5e^{-24}$, identity 25%), *P. limnophila* (Plim_0432, e-value $8e^{-18}$, identity 24%) and *R. baltica* (WP007337933, e-value $2e^{-30}$, identity 33%). Judging from the amount of blebbing, it seems plausible that ArnT is not highly expressed in *R. baltica* and *K. stuttgartiensis*, but that the expression in *P. limnophila* is substantial. The transcriptome indicated that ArnT expression was very low in *K. stuttgartiensis* (Table 2). Future research, using for instance quantification of mRNA by reverse transcription polymerase chain reaction, could show if ArnT is expressed in *P. limnophila* and if the amount of expression differs between the three organisms. To further investigate the effect of polymyxin B on *Planctomycetes* growing cultures could be incubated in the presence of polymyxin B. If growth inhibition or lysis occurs after a prolonged incubation this gives additional evidence of the presence and importance of LPS in these species (Krupovič et al, 2007).

To gain more information about the structure of the putative lipid A of *K. stuttgartiensis*, HPLC-ESI/MS was performed on lipid A extracted via a PCP extraction. Characteristic white precipitates appeared after overnight incubation with acetone and the weight of these precipitates was in the same range as that of the *E. coli* precipitates stemming from a PCP extraction with the same amount of biomass. However, no peaks belonging to lipid A were detected in the HPLC-ESI/MS run after hydrolysis of the *K. stuttgartiensis* extract (Fig. 5C). This could mean that lipid A is not present in *K. stuttgartiensis*, even though some of the analyses discussed above suggest otherwise. It could, however, also be the case that the PCP

protocol did not succeed in extracting the LPS from the membrane. This is indeed a known phenomenon and also the reason why several different LPS extraction protocols exist (De Castro et al, 2010). Preliminary experiments visualizing the sample after PCP extraction via gel electrophoresis indeed suggested that no LPS was present after the extraction (data not shown). Further experiments could therefore focus on using multiple extraction protocols in an attempt to isolate the *K. stuttgartiensis* LPS fraction.

In addition, GC-MS was performed on *K. stuttgartiensis* methanolyzed biomass in order to detect Kdo. No Kdo was detected via this method (Fig. 6, B&D). Previously, however, it was shown that phosphorylated Kdo (as discussed above) escaped detection by GC-MS (Han & Chai, 1991). GC-MS can also be used for the detection of the lipid A specific 3-hydroxy fatty acids. In our experiments no peaks could be assigned to Δ2-fatty acid artifacts that arise from 3-hydroxy fatty acids during methanolysis followed by GC, neither in the control nor in *K. stuttgartiensis*. Since the control LPS from *S. minnesota* R345 does contain 3-hydroxy fatty acids, the lack of signals attributable to 3-hydroxy fatty acids was not taken as evidence that these structures are absent from *K. stuttgartiensis*. Indeed 3-hydroxy fatty acids have been detected in several *Planctomycetes*, including *P. limnophila*, in the past (Kerger et al, 1988; Giovannoni et al, 1987; Sittig & Schlesner, 1993). It would however be possible that *K. stuttgartiensis* is exceptional in not incorporating 3-hydroxy acyl-chains in its lipid A because the lipid composition of anammox bacteria is unique and unprecedented. Their lipids comprise a large amount of different ladderane lipids and even though lipids without ladderane moieties have been found, these are always branched (Sinninghe Damsté et al, 2002; Sinninghe Damsté et al, 2005). Therefore it might be possible that lipid A contains ladderane lipids instead of 3-hydroxy acyl-chains. If anammox bacteria were to include typical unbranched acyl-chains in their putative lipid A, they would probably synthesize these acyl-chains specifically for the lipid A biosynthesis, since lipids containing such acyl-chains are not observed in anammox bacteria (Sinninghe Damsté et al, 2005). If anammox bacteria were to have ladderane lipids in their lipid A, this might also explain why *K. stuttgartiensis* LPS behaves differently during PCP extraction. The finding that the biosynthesis genes necessary for acylation (LpxA, LpxD and LpxL) seem to be quite homologous to the variants in *C. trachomatis* or *E. coli* would argue against the incorporation of very unusual acyl-chains by *K. stuttgartiensis*. However, it might be interesting to test *in vitro* if a set of ladderane lipids (Sinninghe Damsté et al, 2005) can act as a substrate of these (heterologously expressed) enzymes and what the specificity of these enzymes is using the *in vivo* acylation assay as was described before (Brozek & Raetz, 1990).

The detection of LPS is an important task of the immune system performed by specific LPS-recognition molecules. Using these molecules as sensors is an elegant strategy. The most commonly used technique is the limulus amebocyte lysate (LAL) assay. This assay makes use of proteins of the horseshoe crab that induce clotting of the blood upon recognition of Gram-negative bacteria via their LPS (Bang, 1956). Nowadays, the LAL assay is available in different forms, some of them facilitating quantification, for instance using chromogenic reactions (Lindsay et al, 1989). A more recent test uses only the first enzyme in this cascade, factor C, and thereby overcomes the side reaction with (1,3)-β-D-glucan that occurs in other LAL assays (Ding & Ho, 2010). Another possibility is to incubate the (lysed) cells with for instance

murine bone-marrow derived macrophages or other immune cell lines and follow the expression of the LPS specific receptor TLR4 and/or targets that are downstream of TLR4, such as MyD88 or IL-8 (He et al, 2013). All these targets are upregulated if LPS is present. Another possible method would be to use for instance LPS-binding protein (LBP) or bactericidal/permeability-increasing protein (BPI) (Tobias et al, 1997) and allow binding with putative LPS by incubating with lysed planctomycetal cells. The LPS can then be degraded to lipid A via acid hydrolysis and lipid A-protein complexes can be detected via co-immunoprecipitation using lipid A antibodies (El-Samalouti et al, 1997). The latter method is rather cumbersome and introduces a bias at the step of the lipid A antibodies, if the structure of the plantomycetal lipid A were to be modified, the antibodies would fail to pull down the lipid A-protein complexes.

An alternative "LPS-sensor" comes from a different background: bacteria belonging to the genus *Bdellovibrio* are bacterivores that replicate inside Gram-negative bacterial cells. Some *Bdellovibrio* species recognize their prey based on their LPS (and others use OMPs as recognition sites) (Schelling & Conti, 1986). It might be worthwhile to make a co-culture of LPS-recognizing *Bdellovibrio* species with several *Planctomycetes* and investigate if *Bdellovibrio* can recognize and invade these *Planctomycetes*.

Summarizing, the polymyxin B experiments, the genome and *K. stuttgartiensis* transcriptome analysis and the gel electrophoresis after LPS enrichment suggested LPS to be present in *Planctomycetes*. The HPLC-ESI/MS and GC-MS analyses performed on *K. stuttgartiensis*, however did not detect LPS. Taken all considerations as discussed above in account, the presence of LPS seems plausible. Clearly, additional experiments are necessary to thoroughly explain the negative results and to show substantial additional evidence for the presence (or absence) of LPS.

Acknowledgments

Paul Kosma and Andreas Hofinger-Horvath are acknowledged for measuring an isolated LPS sample by NMR. Daan Speth is acknowledged for compiling the gene expression data and Naomi de Almeida for screening a *K. stuttgartiensis* membrane proteome compiled by her. We thank Elisha Moore for assistance during PCP extraction. The General Instruments Department of the Radboud University is acknowledged for maintenance of the electron microscope.

MCFvT and MSMJ are supported by the European Research Council (ERC232937 awarded to MSMJ) and MSMJ is further supported by a Spinoza premium and SIAM Gravitation (024 002002).

Chapter 5

Anammox *Planctomycetes* have a peptidoglycan cell wall

This chapter has been published as:

Muriel C.F. van Teeseling[1], Rob J. Mesman[1], Erkin Kuru[2], Akbar Espaillat[3], Felipe Cava[3], Yves V. Brun[4], Michael S. VanNieuwenhze[5], Boran Kartal[1,6], Laura van Niftrik[1] (2015) Anammox *Planctomycetes* have a peptidoglycan cell wall. *Nat Commun* 6: 6878.

[1]Department of Microbiology, Institute for Water and Wetland Research, Faculty of Science, Radboud University, Nijmegen, The Netherlands.
[2]Interdisciplinary Biochemistry Program, Indiana University, Bloomington, Indiana, USA.
[3]Department of Molecular Biology and Laboratory for Molecular Infection Medicine Sweden, Umeå Centre for Microbial Research, Umeå University, Umeå, Sweden.
[4]Department of Biology, Indiana University, Bloomington, Indiana, USA.
[5]Department of Chemistry, Indiana University, Bloomington, Indiana, USA.
[6]Department of Biochemistry and Microbiology, Laboratory of Microbiology, Gent University, Gent, Belgium.

Abstract

Planctomycetes are intriguing microorganisms that apparently lack peptidoglycan, a structure which controls the shape and integrity of almost all bacterial cells. Therefore, the planctomycetal cell envelope is considered exceptional and their cell plan uniquely compartmentalized. Anaerobic ammonium-oxidizing (anammox) *Planctomycetes* play a key role in the global nitrogen cycle by releasing fixed nitrogen back to the atmosphere as N_2. Here, using a complementary array of state-of-the-art techniques including continuous culturing, cryo-transmission electron microscopy, peptidoglycan-specific probes and muropeptide analysis, we show that the anammox bacterium *Kuenenia stuttgartiensis* contains peptidoglycan. Based on the thickness, composition and location of peptidoglycan in *K. stuttgartiensis*, we propose to redefine *Planctomycetes* as Gram-negative bacteria. Our results demonstrate that *Planctomycetes* are not an exception to the universal presence of peptidoglycan in bacteria.

Introduction

Maintaining cellular integrity is crucial for life and in particular challenging for small, unicellular organisms. In bacteria, the virtually universal solution to this problem is the presence of peptidoglycan, which also determines the cell shape and facilitates cell growth and division (Vollmer et al, 2008). Peptidoglycan is a mesh-like heteropolymer consisting of a lysozyme-sensitive sugar backbone of alternating *N*-acetylglucosamine (GlcNAc) and *N*-acetylmuramic acid (MurNAc) residues cross-linked by short D-amino acid rich peptide stems attached to each of the MurNAc residues (Vollmer et al, 2008). Typically, the nascent peptide stem is a pentapeptide with the sequence of one L-alanine, one D-glutamate, one diamino acid and two D-alanines.

Traditionally, bacteria are classified into two groups based on their cell envelope properties. In Gram-positive bacteria the peptidoglycan layer is relatively thick (15-30 nm), typically contains L-lysine (L-Lys) as the third amino acid and is located outside the cytoplasmic membrane, which is the outermost membrane of the cell (Vollmer et al, 2008). The Gram-negative peptidoglycan is relatively thin (1.5-15 nm), typically contains *meso*-diaminopimelic acid (*meso*-DAP) instead of L-Lys and is located between the cytoplasmic and the Gram-negative specific outer membrane (Vollmer et al, 2008).

Planctomycetes are extraordinary organisms that belong to the evolutionarily deep-branching bacterial superphylum of *Planctomycetes*, *Verrucomicrobia* and *Chlamydiae* (PVC) (Wagner & Horn, 2006). Both *Planctomycetes* (König et al, 1984; Liesack et al, 1986; Cayrou et al, 2010) and *Chlamydiae* (McCoy & Maurelli, 2006) have been proposed to be among the few exceptions lacking peptidoglycan, which is one of the most conserved structural characteristics of bacteria. However, chlamydial species are commonly sensitive to antibiotics targeting peptidoglycan and have most of the genes involved in its biosynthesis, and the presence of peptidoglycan has recently been shown in some chlamydial species (Pilhofer et al, 2013; Liechti et al, 2014). Paradoxically, although the free-living *Planctomycetes* are expected to need a peptidoglycan shell more than the intracellular and

therefore osmotically protected *Chlamydiae*, they are usually insensitive to antibiotics targeting peptidoglycan (König et al, 1984; Cayrou et al, 2010), are reported to lack a varying number of genes crucial for its biosynthesis (Jogler et al, 2012; Guo et al, 2014), and biochemical analyses failed to show the peptidoglycan components *meso*-DAP and MurNAc in isolated cell envelopes of all eight previously tested Planctomycete strains (König et al, 1984).

Most planctomycete species, like typical Gram-negative bacteria, have two compartments enclosed by membranes. In *Planctomycetes*, the innermost membrane is unusually curved (Lindsay et al, 2001). Historically, the planctomycetal outermost membrane was defined as a cytoplasmic membrane (Lindsay et al, 2001; Sagulenko et al, 2014). However, based on bioinformatic analysis (focusing on marker genes for outer membrane protein and lipopolysaccharide insertion (Speth et al, 2012)) the outermost membrane has recently been proposed to be an outer membrane typical of Gram-negative bacteria (Speth et al, 2012; Devos, 2014a; Devos, 2014b). Based on these hypotheses, *Planctomycetes* can be defined as either uniquely compartmentalized or Gram-negative bacteria. In the absence of any apparent peptidoglycan, arguments for the first hypothesis found considerable support (Fuerst, 1995; Forterre & Gribaldo, 2010; Fuerst & Sagulenko, 2012) and a shared evolutionary link between *Planctomycetes* and Eukaryotic cells was suggested (Fuerst, 1995; Devos & Reynaud, 2010; Forterre & Gribaldo, 2010; Fuerst & Sagulenko, 2012). Therefore, we argue that showing the presence of peptidoglycan in *Planctomycetes* and elucidating its characteristics would resolve the controversy concerning the Planctomycete specific cell envelope and cell plan (Lindsay et al, 2001; Speth et al, 2012; Santarella-Mellwig et al, 2013; Sagulenko et al, 2014; Devos, 2014a; Devos, 2014b) and its contentious link to the origins of Eukaryotic cells (Fuerst, 1995; Devos & Reynaud, 2010; Forterre & Gribaldo, 2010; Fuerst & Sagulenko, 2012).

Anaerobic ammonium-oxidizing (anammox) bacteria form a distinct, phylogenetically deep-branching group within the *Planctomycetes* (Jogler et al, 2012). These microorganisms convert ammonium and nitrite to dinitrogen gas via nitric oxide and hydrazine as intermediates (Kartal et al, 2011b). They occur in aquatic and terrestrial environments and play a crucial role in the biological nitrogen cycle estimated to produce approximately half of the dinitrogen gas present in the atmosphere (Francis et al, 2007). Furthermore, the anammox process is widely applied to remove ammonium from wastewater (Kartal et al, 2010).

Compared to most other *Planctomycetes*, the anammox cell contains an additional, third, membrane-enclosed compartment (Lindsay et al, 2001; van Niftrik et al, 2008b). This innermost compartment, the anammoxosome, harbors the catabolic machinery and is surrounded by the cytoplasm (also known as riboplasm), which contains the ribosomes and nucleoid (van Niftrik et al, 2008b; Neumann et al, 2014). Depending on the interpretation of the S-layer-enclosed outermost membrane (van Teeseling et al, 2014 (chapter 2)), the outermost compartment is either a unique cytoplasmic compartment called the paryphoplasm (in accordance with the historical definition) or a periplasm typical for a Gram-negative cell envelope. Unlike other *Planctomycetes* that divide by budding (Fuerst, 1995;

Jogler et al, 2012), anammox bacteria divide by binary fission without the canonical cell division ring protein FtsZ (van Niftrik et al, 2009).

Similar to other *Planctomycetes*, the cell envelope of anammox bacteria was proposed to lack peptidoglycan. Since no anammox bacteria were included in the initial peptidoglycan-targeting biochemical analyses (König et al, 1984), the absence of peptidoglycan in anammox bacteria was based on the absence of a peptidoglycan layer in the outermost anammox compartment of resin-embedded sections of either high-pressure frozen and freeze-substituted or chemically fixed anammox cells (Lindsay et al, 2001; Neumann et al, 2013). However, all genes essential for peptidoglycan biosynthesis are present in the genome of the anammox bacterium *Kuenenia stuttgartiensis*, apart from homologs of peptidoglycan-specific glycosyltransferase (GT) class 51 (CAZy database (Lombard et al, 2014)) necessary to polymerize the sugar backbone. Despite the apparent lack of these GTs, it was recently shown (Hu et al, 2013) that *K. stuttgartiensis* cells lyze with lysozyme in the presence of EDTA and their growth is inhibited by penicillin G.

Here, we redefine the anammox Planctomycete *K. stuttgartiensis* as a Gram-negative bacterium based on the discovery and characterization of a peptidoglycan layer contained within the cell envelope. To this end, we use a complementary array of state-of-the-art techniques including continuous culturing, cryo-transmission electron microscopy (cryoTEM), incorporation of peptidoglycan-specific probes imaged with structured illumination microscopy (SIM), and ultrasensitive UPLC-based muropeptide analysis.

Materials & Methods

***Kuenenia stuttgartiensis* enrichment culture.** Free-living planktonic *Kuenenia stuttgartiensis* cells were grown in an enrichment culture (approximately 95% *K. stuttgartiensis*) in a membrane bioreactor as described previously (Kartal et al, 2011a). In short, the reactor (working volume 11 l) was fed continuously with mineral medium (van de Graaf et al, 1996) containing 45 mM nitrite and ammonium (each) at a flow rate of 4.2 ml/min (approximately 6 l/d). The pH of the reactor was controlled at 7.3 with a potassium bicarbonate solution (100 g/l). The reactor was operated at 33°C and was stirred at 300 rpm. A gas mixture of Ar/CO_2 (95/5%) with a flow of 10 ml/min was supplied to the reactor to maintain anaerobic conditions. The cells were washed out the reactor continuously (1.1 l/d) to maintain the cell density of the culture (optical density at 600 nm was 1.1-1.2).

Cryo-transmission electron microscopy. *K. stuttgartiensis* cells (4 ml) were pelleted (4 min, 600 g, 33°C) and resuspended in a small amount (50 µl) of mineral medium containing 1.25 g/l sodium bicarbonate and trace minerals (van de Graaf et al, 1996) and left to recover for 15 min at 33°C. Cells were gently mixed with an equal volume of 40% dextran (70kD MW) in *K. stuttgartiensis* growth medium, loaded in copper tubes and high-pressure frozen [HPM100 (Leica Microsystems, Vienna, Austria)]. For preparing vitreous sections, copper tubes were loaded in a cryo-ultramicrotome (Leica FC7/UC7, Leica Microsystems) pre-cooled at -145 to -150°C. Tubes were trimmed to a pyramid with a 50 by 50 µm block face using a cryo-trim 20° diamond knife (Diatome, Biel, Switzerland). Frozen-hydrated sections (45 nm) for CEMOVIS were sectioned on a 30° cryo-immuno diamond knife (Diatome). Sections were attached to

carbon-coated 200 mesh copper grids (Stork-Veco, Eerbeek, Netherlands) by electrostatic force using the Crion system (Leica Microsystems). Grids were transferred to the loading station of a high-tilt cryotomography holder (914 (Gatan, Munich, Germany)) under liquid nitrogen. Sections were imaged in a JEOL (Tokyo, Japan) JEM 2100 Transmission Electron Microscope operated at 200kV in low-dose mode. Images were recorded using the Gatan F4000 bottom-mount camera.

Isolation of peptidoglycan sacculi. *K. stuttgartiensis* cells were further enriched from the other microorganisms in the enrichment culture by density centrifugation (15 min, 1000 g) on a 15-30% Histodenz gradient in 20 mM HEPES buffer pH 7.5 including 1 g/l sodium bicarbonate. A distinct red band indicating the presence of *K. stuttgartiensis* was present approximately halfway through the gradient. Here, *K. stuttgartiensis* presence and abundance was verified by FISH microscopy using the specific Amx820 (Schmid et al, 2000) and Pla46 (Neef et al, 1998) probes. Cells were boiled in 4% SDS for 60 min at 100**°**C and applied to a glow-discharged formvar-carbon-coated copper grid. After 20 min, negative staining was performed by washing the grids once in 0.5% Uranyl acetate (UAc) in MQ, staining (60 sec) on 0.5% UAc and washing on 3 drops of MilliQ. Sacculi were visualized in a JEOL 1010 TEM operating at 60kV.

To investigate if the observed sacculi consisted of peptidoglycan, sacculi (obtained from cells taken directly from the enrichment reactor) were incubated (5 h, 37**°**C) with lysozyme (from chicken egg white) (10 mg/ml; with and without 20 mM EDTA) before visualizing via negative staining as described above. As a negative control, sacculi were incubated without lysozyme.

Incorporation of peptidoglycan specific probe EDA-DA. Cells (100 ml) harvested from the membrane bioreactor were concentrated and resuspended in 5 ml 20 mM HEPES buffer pH 7.8 including 1.25 g/l sodium bicarbonate. Afterwards, cells suspensions were made anoxic by applying under-pressure and flushing with Ar/CO_2 (95%/5%) ten times. Then the cell suspensions were transferred to a 100 ml fed-batch reactor inside an anaerobic chamber with an Ar/H_2 (95%/5%) atmosphere. O_2 in the Ar in the anaerobic chamber was removed by passing Ar over a Pd catalyst (0.2 p.p.m. residual O_2). The cells were supplied with the above-mentioned HEPES buffer containing 7 mM NH_4^+ and NO_2^- each and the peptidoglycan-specific probe EDA-DA (1mM, ethynyl-D-alanyl-D-alanine) with a flow rate of 5ml/h for 12-15 h. The fed-batch reactors were stirred at 150 rpm and incubated in the dark at 30**°**C. As a control, cells were grown under the same conditions in the presence of ELA-LA (1 mM, ethynyl-L-alanine-L-alanine). Cells were harvested, washed 3 times in the above-mentioned HEPES buffer (3000 g, 10 min) and resuspended in 4 ml HEPES buffer. The resuspended cells were put in an equal volume of 4% paraformaldehyde (PFA) in the HEPES buffer and incubated for 20 min at room temperature and subsequently for 90 min at 4**°**C. The fixed cells were pelleted by centrifugation (11700 g, 5 min) and resuspended in 0.5 ml 0.1% PFA for temporary storage. Pelleted cells grown in the presence of EDA-DA and ELA-LA were permeabilized by incubating them for 5 min in 1.5 ml PBS with 0.25% Triton X-100. The cells were washed once in PBS, and the fluorophore Alexa 488-azide (20 µM) was attached via a copper(I) catalyzed click reaction (incubation 60 min in 1.5 ml at room temperature in the Click-iT Cell Reaction Buffer Kit (ThermoFischer, Waltham, USA). Afterwards cells were

washed 3 times in PBS (1.5 ml), incubated 20 min at room temperature in the presence of 5 µg/ml Pacific Blue NHS ester (ThermoFischer, Waltham, USA), washed twice in PBS and visualized via fluorescence microscopy or structured illumination microscopy (SIM) as described previously (Kuru et al, 2012). In short, images were collected with a DeltaVision (GE Healthcare, Pittsburgh, USA) OMG Imaging System equipped with a Photometrics (Tuscon, USA) Cascade II EMCCD camera (excitation: 405 nm and emission: 419-465 nm).

Analysis of muropeptides obtained from sacculi. Sacculi were prepared from the *K. stuttgartiensis* cells (0.8 l, OD_{600} 1.1) enriched by density centrifugation as described above. Peptidoglycan was isolated largely as described before (Cava et al, 2011). Briefly, cell pellets were boiled in 4% SDS for 60 min at 100°C. After boiling for an additional 4 h, sacculi were further stirred overnight 37°C and then, SDS was washed out by ultracentrifugation. Sacculi were resuspended in 200 µl of 50 mM sodium phosphate buffer pH 4.5 and digested overnight with 30 µg/ml muramidase (cellosyl, Hoechst) at 37°C. Muramidase digestion was stopped by incubation in a boiling water bath (5 min). Coagulated protein was removed by centrifugation. The supernatants were mixed with 150 µl 0.5 M sodium borate pH 9.5, and subjected to reduction of muramic acid residues into muramitol by sodium borohydride (10 mg/ml final concentration, 30 min at room temperature) treatment. Samples were adjusted to pH 3.5 with phosphoric acid. UPLC analyses of muropeptides were performed on an ACQUITY UPLC BEH C18 Column, 130A, 1.7mm, 2.1 mm 150 mm (Water, USA) and detected at Abs. 204 nm. Muropeptides were separated using a linear gradient from buffer A (phosphate buffer 50 mM pH 4.35) to buffer B (phosphate buffer 50 mM pH 4.95 methanol 15% (v/v)) in 20 min. Muropeptide purification was performed by HPLC on an Aeris peptide column (250 x 4.6 mm; 3.6 µm particle size) (Phenomenex, USA). The identity of individual muropeptides was established by MALDI-TOF (Voyager DE-STR).

Results

CryoTEM shows a previously unobserved layer in the cell envelope. To study the cell envelope of *K. stuttgartiensis*, we used a highly enriched (>95%) culture of free-living, planktonic cells. Cryo-Electron Microscopy of Vitreous Sections (CEMOVIS) (Al-Amoudi et al, 2004), reflecting the near-native hydrated state of the cells, showed a layer in the cell envelope that was previously unobserved. This electron-dense layer was located underneath the outermost membrane (Fig. 1). The thickness of the layer varied between 4.5 and 6 nm, which is in the range reported for peptidoglycan in Gram-negative bacteria (Vollmer et al, 2008). The location of this layer, in the outermost cell compartment, matched the location of peptidoglycan in Gram-negative bacteria and therefore this layer was a good candidate to represent the peptidoglycan shell in this bacterium.

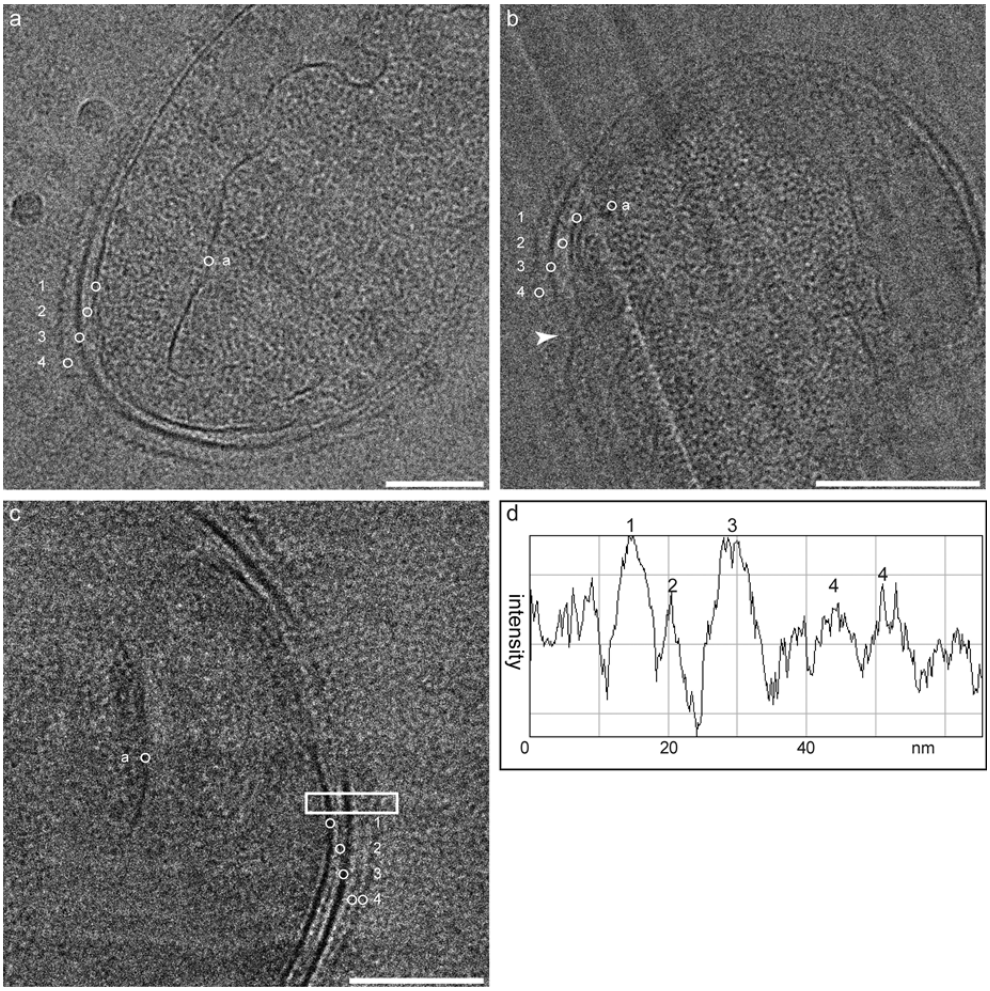

Figure 1. *CryoTEM of vitreous sections revealed a previously unobserved layer in the cell envelope of* K. stuttgartiensis. *(a-c) Single* K. stuttgartiensis *cells as observed with CEMOVIS, in which all membranes and cell envelope layers have been annotated. (b) A dividing* K. stuttgartiensis cell*, the division site is indicated with an arrowhead. (d) The intensity profile of the area in the box in (c) encompassing the cell envelope verified the extra layer to be a separate entity. a: anammoxosome membrane, 1: cytoplasmic membrane, 2: putative peptidoglycan, 3: outer membrane, 4: S-layer. Scale bars 100 nm.*

Peptidoglycan isolation yields lysozyme-sensitive sacculi. After they were harvested from an enrichment culture (>95%), *K. stuttgartiensis* cells were further enriched to 99.9% purity using density centrifugation. When this highly enriched sample was boiled in SDS and negatively stained with uranyl acetate, cell-shaped structures similar to peptidoglycan sacculi were recovered (Fig. 2A, Supplementary Fig. 1). In rare instances sacculi with a figure-eight shape, probably obtained from dividing *K. stuttgartiensis* cells, were also detected (Supplementary Fig. 2). When *K. stuttgartiensis* sacculi were incubated for 5 h with lysozyme, which cleaves peptidoglycan by hydrolyzing the β-1,4 bonds between the two sugar

components MurNAc and GlcNAc (Johnson & Phillips, 1965), the sacculi disintegrated and only fibrous material was visible (Fig. 2B). This was consistent with the previous observation of fibrous material upon enzymatically cleaving the sugar backbone of *E. coli* peptidoglycan sacculi (de Pedro et al, 1997). The disintegration of the sacculi was solely dependent on the addition of lysozyme, as sacculi incubated without lysozyme remained intact. This suggested that the sacculi were indeed composed of a peptidoglycan-like sugar backbone. Interestingly, this observation also indicated that *K. stuttgartiensis* must encode and express at least one polymerizing GT class 51 enzyme or another unknown enzyme that polymerizes the peptidoglycan sugar backbone. The apparent absence of such a gene from the *K. stuttgartiensis* genome could be due to the fact that the genome is currently only ≥98% complete (Strous et al, 2006). However, according to the CAZy database (Lombard et al, 2014) other *Planctomycetes*, as well as *Chlamydiae* (McCoy & Maurelli, 2006), also lack GT class 51 enzymes and therefore it seems more likely that the enzyme is a member of a new, perhaps *Planctomycetes*- and *Chlamydiae*-specific, uncharacterized class of GTs.

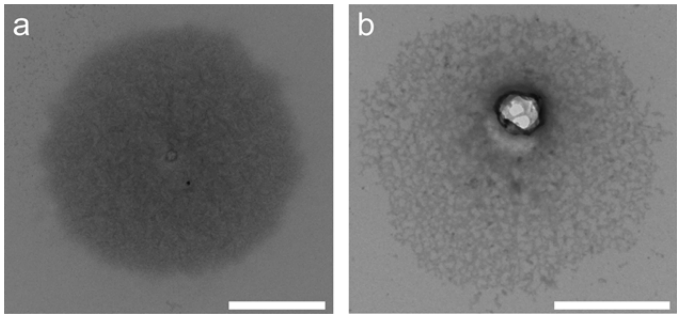

Figure 2. *Lysozyme-sensitive sacculi were obtained by boiling* K. stuttgartiensis *cells enriched by density centrifugation, in SDS. (a) TEM of* K. stuttgartiensis *sacculus using negative staining. (b) After lysozyme treatment the* K. stuttgartiensis *sacculi were absent or had a fibrous appearance, as observed by negative staining via TEM. Scale bars 1 μm.*

Peptidoglycan peptide stem was verified by specific probes. The peptidoglycan biosynthesis machinery is promiscuous (Cava et al, 2011) and therefore non-canonical D-amino acid compounds, such as fluorescent or bio-orthogonal D-amino acids or bio-orthogonal D-amino acid containing dipeptides, can be incorporated at the C-terminus of the peptide stems. This has recently been exploited to specifically stain peptidoglycan (Kuru et al, 2012; Siegrist et al, 2013; Liechti et al, 2014). When grown for a part of the cell division cycle (10–14%) in the presence of the bio-orthogonal D-amino acid dipeptide EDA-DA, *K. stuttgartiensis* cells displayed the characteristic fluorescent signal of probe incorporation after coupling with a fluorophore (Fig. 3B-C). Comparable to peptidoglycan labeling observed in other microorganisms (Kuru et al, 2012), most of the D-amino acid dipeptide incorporation occurred at the cell division site as determined by fluorescence and super resolution structured illumination microscopy (SIM), while experiments with L-amino acid dipeptide controls only resulted in background fluorescence (Fig. 3A).

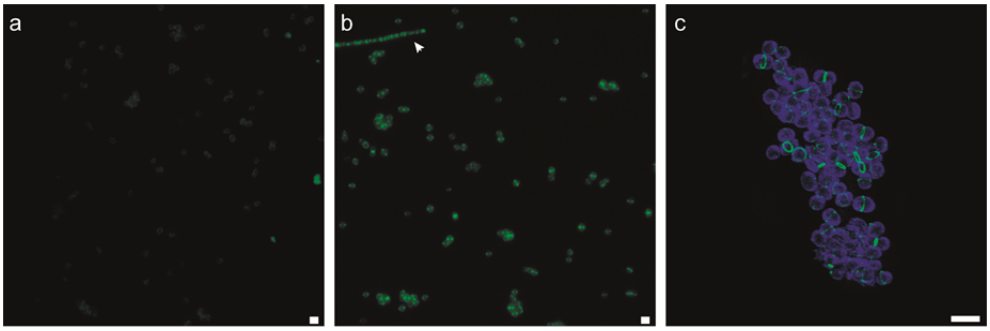

Figure 3. *Fluorescence microscopy on* K. stuttgartiensis *cells grown in the presence of peptidoglycan specific D-alanine dipeptide probes indicated the presence of peptidoglycan. (a) The negative control probe ELA-LA, which can not be incorporated, shows only a faint background. (b) Septal incorporation of EDA-DA is present, also in a rod-shaped non-anammox species present in the bioreactor (arrowhead). (c) Structured illumination microscopy (SIM) clearly shows that EDA-DA incorporates specifically at the cell division site. Probe incorporation was visualized with a complimentary fluorophore using click-chemistry (green) and cell surfaces were labeled by amine reactive Pacific Blue™ NHS ester (blue). ELA-LA: ethynyl-L-alanyl-L-alanine; EDA-DA: ethynyl-D-alanyl-D-alanine. Scale bars 2 µm.*

Muropeptide analysis confirms that sacculi contain peptidoglycan. The structure of the peptidoglycan subunits (muropeptides) was determined by ultra performance liquid chromatography (UPLC) and subsequent mass spectrometry (MS) (Fig. 4A). Muropeptides were obtained by muramidase degradation of sacculi prepared from Histodenz-purified *K. stuttgartiensis* cells (99.9%). Indeed, GlcNAc-MurNAc coupled to 2-4 amino acids (M2-M4) as well as cross-linked fragments (D43 and presumably D44) were detected in *K. stuttgartiensis* sacculi (Fig. 4B,C). The largest monomeric peptidoglycan fragment obtained (M4) was identified as GlcNac-MurNAc-L-Ala-D-Glu-*meso*-DAP-D-Ala. Strikingly, the third amino acid was identified as *meso*-DAP (Fig. 4), which is typical for Gram-negative peptidoglycan (Vollmer et al, 2008). In agreement with this observation, all genes necessary for *meso*-DAP synthesis are present in the *K. stuttgartiensis* genome (Supplementary Table 1). Furthermore, the predicted protein sequence for MurE, which couples the third amino acid to the peptidoglycan precursors, has the arginine residue (Arg416 in *E. coli*) necessary for specifically incorporating *meso*-DAP (instead of L-Lys) into the peptidoglycan precursor (Gordon et al, 2000).

Peptidoglycan from *K. stuttgartiensis* had relatively little M4 and D44 compared to *E.coli* K12. In *K. stuttgartiensis*, M3 was the most abundant monomer, which suggested that the enzyme cleaving between the third (*meso*-DAP) and fourth (D-Ala) amino acid in the peptide stem (L,D-endopeptidase) was highly active. Further investigation will be necessary to determine whether the abundance of M3 over M4 has an impact on the biology of the bacterium. The presence of D43 cross-linked muropeptides indicated the expression of D,D-transpeptidases, which was supported by the identification of homologs to Pbp2 and Pbp3 encoded in the genome of *K. stuttgartiensis* (Supplementary Table 1).

a

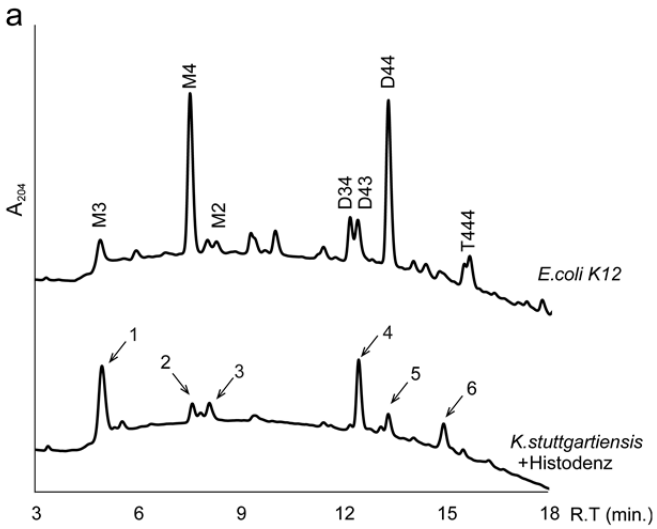

b

Peak	R.T	%	[M+H]⁺theo	[M+H]⁺det	Difference (theo-det)	Muropeptide
1	5	31.5	871.38	871.37	0.01	M3
2	7.6	5.8	942.41	942.36	0.05	M4
3	8.1	6.9	699.29	699.27	0.02	M2
4	12.5	22.3	1794.77	1794.70	0.07	D43
5	13.3	5.7	1865.81	ND	-	D44*
6	15	10.1	-	ND	-	-

c

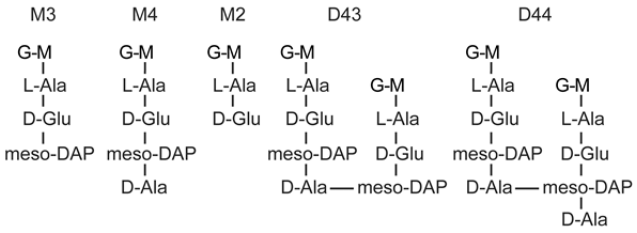

Figure 4. *Structural characterization by UPLC and mass spectrometry of the peptidoglycan present in* K. stuttgartiensis*. (a) UPLC analyses of* K. stuttgartiensis *peptidoglycan.* E. coli *K12 PG profile is included as a reference. Peaks labelled 1-6 correspond to muropeptides of* K. stuttgartiensis *Histodenz-enriched cultures. R.T: Retention time. Min: minutes. A_{204}: Absorbance 204 nm. (b) Mass analysis of the PG subunits isolated in panel A by MALDI-TOF. *: D44 was formulated based on its coincidence with E. coli D44 R.T. ND: Not determined; %: Relative abundance; theo: theoretical mass; det: determined mass. (c) Schematic representation of K. stuttgartiensis detected PG species in their reduced state. M2:* N*-acetylglucosamine-(GlcNAc)-*N*-acetylmuramic acid (MurNAc)-L-Ala-D-Glu; M3: GlcNAc-MurNac-L-Ala-D-Glu-*meso*-Diaminopimelic acid (*meso*-DAP); M4: GlcNac-MurNAc-L-Ala-D-Glu-*meso*-DAP-D-Ala; D43: dimer muropeptide of a M4 D,D-crosslinked to a M3. M: MurNAc; G: GlcNAc.*

Discussion

This study presents the first experimental evidence of peptidoglycan in an anammox Planctomycete. We show that *K. stuttgartiensis* has a relatively thin, *meso*-DAP containing peptidoglycan layer located underneath its outer membrane, which fits to the typical characteristics of Gram-negative peptidoglycan. The location of the peptidoglycan in anammox bacteria is striking since the non-FtsZ containing cell division ring (van Niftrik et al, 2009) was observed in the exact same compartment of the cell. To the best of our knowledge a cell division ring has not been previously observed in the peptidoglycan-containing compartment of any bacterium and this further substantiates that anammox bacteria divide via a unique mechanism. Based on our investigations, facilitated by new methodology that recently became available, and the results of Jeske *et al* (Jeske et al, 2015) that present similar findings in other planctomycetal lineages, we propose to redefine the *Planctomycetes* as Gram-negative microorganisms and therefore end the longstanding controversy about the planctomycetal cell plan. Taken together, these findings clearly show that *Planctomycetes* are not an exception to the universal rule of peptidoglycan cell walls in bacteria, and consequently all free-living bacteria possess peptidoglycan. These findings also lead us to conclude that an evolutionary link between *Planctomycetes* and Eukaryotes is unlikely.

Acknowledgements

Miguel A. de Pedro, Karin Aistleitner, Matthias Horn, David Kysela, Yoan Diekmann and José Pereira Leal are acknowledged for discussions. We thank Joachim Reimann and Christina Ferousi for the *Kuenenia stuttgartiensis* cells and Thomas Kieselbach for MS analysis. We thank the Indiana University Light Microscopy Imaging Center for their help with OMX super-resolution microscopy, supported by National Institutes of Health grant S10RR028697. Katharina Ettwig, Huub Op den Camp, Joachim Reimann and Daan Speth are acknowledged for critical reading of the manuscript. MvT is supported by ERC grant 232937 and RJM by the 2012 Spinoza Grant both awarded to Mike Jetten. EK and YVB are supported by NIH grant GM051986. FC and AE are supported by MIMS, KAW, Kempe Foundation and the Swedish Research Council. BK and LvN are supported by NWO VENI grant 863.11.003 and 863.09.009, respectively.

Supplements

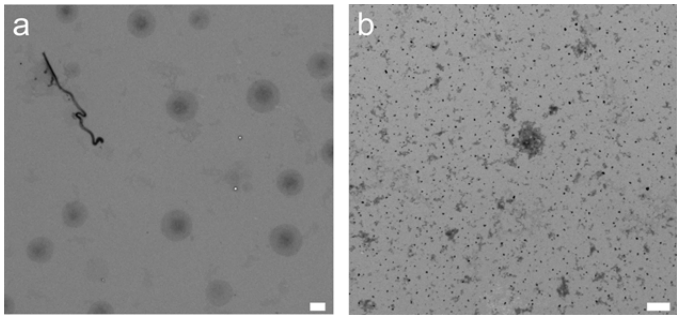

Supplementary Figure 1. *Lysozyme-sensitive sacculi were obtained by boiling* K. stuttgartiensis *cells, without enrichment by density centrifugation, in SDS. (a) An overview of a grid after negative staining shows multiple thin sacculi of* K. stuttgartiensis *(round) and a thicker sacculus from a long rod shaped cell present in the reactor alongside* K. stuttgartiensis*. (b) After lysozyme treatment the* K. stuttgartiensis *sacculi were absent or had a fibrous appearance, as observed by negative staining via TEM. Scale bars 1 µm.*

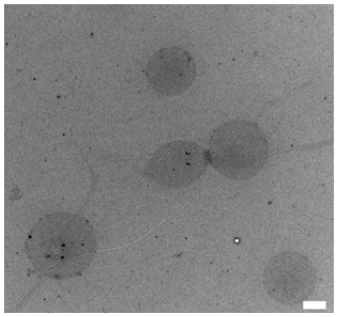

Supplementary Figure 2. *Some lysozyme-sensitive sacculi obtained by boiling* K. stuttgartiensis *cells, without enrichment by density centrifugation, in SDS appear to stem from dividing cells. A figure-eight shaped sacculus, probably obtained from a dividing* K. stuttgartiensis *cell surrounded by sacculi from non-dividing* K. stuttgartiensis *cells, as observed by negative staining via TEM. Scale bar 1 µm.*

Supplementary Table 1. *Predicted peptidoglycan biosynthesis associated proteins in* K. stuttgartiensis*. In silico identification of* K. stuttgartiensis *peptidoglycan associated proteins based on NCBI protein BLAST tool analysis using* E. coli *homologs as source, using a cutoff of* 1.10^{-5}*. Proteins highlighted in white are homologous to* E. coli *cytoplasmic synthesis proteins. Proteins in grey and light grey are homologous to* E. coli *proteins with periplasmic activities. Highlighted in grey are proteins with D,D- and L,D-transpeptidase activity and in light grey proteins with peptidoglycan hydrolysis activities. Proteins in dark grey correspond to homologous proteins involved in the biosynthetic pathways of meso-DAP.*

E. coli **peptidoglycan related proteins**	***K. stuttgartiensis*** **locus (NCBI ID)**	**Kust number**	**Query cover**	**E value**	**Identity**
MurA	emb|CAJ74073.1|	kuste3313	98%	3.00E-122	48%
MurB	emb|CAJ74091.1|	kuste3330	96%	9.00E-16	25%
MurC	emb|CAJ73131.1|	kuste2385	93%	2E-86	36%
	emb|CAJ71429.1|	kustc0684	90%	1E-57	31%
MurD	emb|CAJ74243.1|	kuste3480	87%	3.00E-45	30%
MurE	emb|CAJ73124.1|	kuste2378	94%	4.00E-88	36%
MurF	emb|CAJ73125.1|	kuste2379	99%	1.00E-69	31%
Ddl	emb|CAJ73132.1|	kuste2386	99%	4.00E-79	41%
Alr	emb|CAJ73156.1|	kuste2410	98%	8.00E-56	34%
MurI	emb|CAJ72251.1|	kustd1506	88%	2.00E-24	30%
MraY	emb|CAJ73126.1|	kuste2380	93%	5.00E-104	44%
MurG	emb|CAJ73129.1|	kuste2383	97%	7.00E-43	28%
MreB	emb|CAJ72643.1|	kustd1898	98%	4.00E-119	54%
Pbp2	emb|CAJ72640.1|	kustd1895	91%	8.00E-58	26%
Pbp3	emb|CAJ73122.1|	kuste2376	91%	3.00E-88	32%
Ynhg	emb|CAJ75008.1|	kuste4246	56%	4.00E-14	29%
Ycfs	emb|CAJ75008.1|	kuste4246	58%	1.00E-06	27%
Pbp4	emb|CAJ74399.1|	kuste3636	92%	6.00E-40	25%
MltA	emb|CAJ70755.1|	kusta0010	68%	2.00E-32	33%
Dap epi	emb|CAJ72320.1|	kustd1575	98%	2.00E-55	38%
DapA	emb|CAJ72115.1|	kustd1370	100%	7.00E-93	49%
DapB	emb|CAJ71744.1|	kustc0999	96%	1.00E-64	42%
DapE	emb|CAJ73921.1|	kuste3163	82%	1.00E-16	25%
DapF	emb|CAJ72320.1|	kustd1575	98%	2.00E-54	38%

Chapter 6

Integration & Outlook

Almost all bacterial cells either have a Gram-negative or a Gram-positive cell envelope. These cell envelopes have a different organization: the Gram-positive envelope has a thick layer of peptidoglycan surrounding its cytoplasmic membrane whereas the Gram-negative envelope has a thin layer of peptidoglycan and an outer membrane. Even though biology is not a science that likes using definitions, the cytoplasmic membrane is often defined as the boundary of cells (e.g. Silhavy et al, 2010). This implies that everything outside of the cytoplasmic membrane is often seen as officially not being part of a cell. In that view the entire cell envelope, except for the cytoplasmic membrane, would be extracellular, even though about a third of the proteome of *Escherichia coli* is associated with the cytoplasmic membrane or the structures located outside of it (Weiner & Li, 2008). I would argue that the peptidoglycan, outer membrane and potential additional components such as S-layers should be regarded as part of the cell. In my opinion, the large energy investment they demand from the cell, the tight attachment to the cytoplasmic membrane and the important functions they have for the bacteria make this view justified.

It is important to realize that the Gram-negative outer membrane is a fundamentally different entity than the cytoplasmic membrane. The cytoplasmic membrane is highly impermeable to hydrophilic molecules, but hydrophobic molecules can easily diffuse over this membrane. In contrast, the outer membrane is permeable to small water soluble molecules because of the pores created by outer membrane proteins (OMPs). The hydrophilic polysaccharide components of the lipopolysaccharide (LPS) form a rather effective barrier against hydrophobic substances. The outer membrane therefore is an effective barrier against for instance hydrophobic antibiotics that can readily diffuse through the cytoplasmic membrane (Nikaido, 1976). However, no electrochemical gradient can exist over the outer membrane because of the permeability to water soluble substances, including ions. Therefore bacteria cannot use the outer membrane for energy conservation for which they depend on the cytoplasmic membrane.

For anammox bacteria it was unclear if the outermost of their three bilayer membranes is a cytoplasmic or an outer membrane (Fig. 1). For years this membrane was seen as a cytoplasmic membrane. Even though the genome of *K. stuttgartiensis* gave some clues towards a Gram-negative organization, the explanation that these genes were probably remnants from an ancestral phase was preferred based on experimental evidence suggesting that these bacteria deviated from the Gram-negative cell plan (Strous et al, 2006; van Niftrik et al, 2010). In addition to the proposed absence of peptidoglycan, the presence of an F-type ATPase on the outermost membrane suggested that this membrane is energized (van Niftrik et al, 2010). Also the location of the cell division ring in the outermost compartment strengthened the view that this was a cytoplasmic compartment, since cell division rings are present in the cytoplasm in other bacteria (van Niftrik et al, 2009).

This controversy, fueled by the finding that some of the genes associated with (the biosynthesis of) the outer membrane are abundantly translated (Speth et al, 2012), urged a thorough investigation into the components that make up the cell envelope of anammox bacteria. This was the objective of the research described in this part of my thesis. The discovery of peptidoglycan, the characterization of an OMP located in the outermost

membrane and the indications of LPS in this membrane should, in my opinion, lead to the conclusion that this membrane is an outer membrane (Fig. 1). This interpretation implies that anammox bacteria are Gram-negative bacteria and fits with the previous results that anammox bacteria have only two compartments with a pH independent of the outside pH (van der Star et al, 2010). In Gram-negative bacteria, the permeability of the outer membrane results in a periplasmic pH that equals the extracellular pH (Wilks & Slonczewski, 2007).

This discussion chapter integrates the results of the anammox part of my thesis into an overview of the anammox cell envelope, discusses some topics that are worth studying in more detail and poses hypotheses that might explain the unexpected location of the F-type ATPase and the cell division ring.

An overview of the anammox cell envelope

When combining all results obtained in this study, an image of the cell envelope of the anammox bacterium *K. stuttgartiensis* emerges (Fig. 2). The first structure belonging to *K. stuttgartiensis* cell that is encountered when approaching the cell from the outside is an extended network of glycans that are attached to the surface layer (S-layer) proteins (chapter 2). Multiple different glycans are linked to the S-layer protein, presumably at multiple sites of each protein, via *O*-linkages. The S-layer protein itself, Kustd1514, is present in many copies that together assemble into a layer with a hexagonal symmetry. Diffusion through the S-layer seems possible via pores with an estimated diameter of around 4 nm. The distance between the S-layer and the underlying outer membrane is approximately 10-15 nm.

The next layer is the outer membrane that was shown to probably contain an OMP, Kustd1878. This OMP was shown to have the expected ß-barrel conformation and forms pores in the membrane (chapter 3). Probably several other OMPs are present in this membrane as well, since multiple OMPs were predicted in the genome and some of these were also detected in the proteome (Speth et al, 2012). Another protein that has been identified in this membrane is an F-ATPase (van Niftrik et al, 2010). This is a rather unexpected component of an outer membrane, since the ions that build the electrochemical gradient needed to drive the ATPase can proposedly easily diffuse over the membrane through OMPs. Again, the hypothesized permeability is strengthened by the previous finding that two instead of three anammox compartments have a pH independent of the environment (van der Star et al, 2010). The lipid composition of this membrane is a topic that needs further exploration. First investigations have shown indications for the presence of LPS, but further experiments are needed to verify or falsify this (chapter 4). As is the case for all anammox membranes, unique ladderane lipids are present in the outer membrane (Neumann et al, 2014).

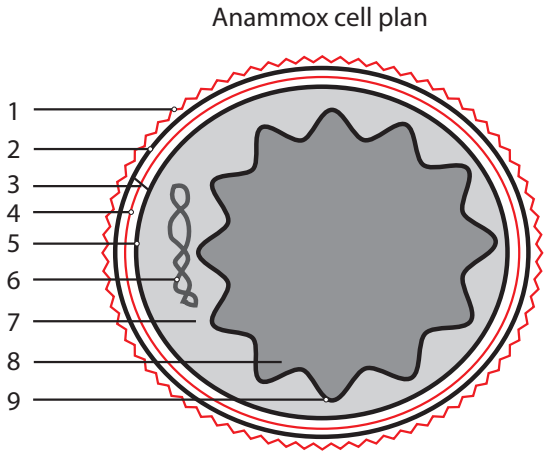

Original interpretation	Unbiased interpretation	New interpretation
1. not yet discovered	1. S-layer	1. S-layer
2. cytoplasmic membrane	2. outermost membrane	2. outer membrane
3. paryphoplasm	3. paryphoplasm	3. periplasm
4. not yet discovered	4. not yet discovered	4. peptidoglycan
5. intracytoplasmic membrane	5. middle membrane	5. cytoplasmic membrane
6. nucleoid	6. nucleoid	6. nucleoid
7. riboplasm	7. riboplasm	7. cytoplasm
8. anammoxosome	8. anammoxosome	8. anammoxosome
9. anammoxosome membrane	9. innermost membrane	9. anammoxosome membrane

Figure 1. *A schematic anammox cell plan showing the original, unbiased and new interpretation. Structures identified in this thesis are displayed in red.*

Two notable components are present inside the periplasm that is located underneath the outer membrane. A layer of peptidoglycan with a thickness of 4.5-6 nm is present halfway in between the outer and cytoplasmic membrane (chapter 5). This peptidoglycan layer has a composition that is typical for Gram-negative peptidoglycan, consisting of a backbone of polymeric *N*-acetylglucosamine and *N*-acetylmuramic acid cross-linked via peptides made of L-alanine, D-glutamate, *meso*-diaminopimelic acid and D-alanine. Another structural element with great importance for the bacteria is present in the periplasm as well: the cell division ring. The putative cell division ring-forming protein, Kustd1438, is up to now the only known protein associated with the cell division ring (van Niftrik et al, 2009). Kustd1438 has an ATP/GTPase domain and associated synergy loops, suggesting it might use ATP or GTP to polymerize into the observed division ring. The presence of the cell division ring in the periplasm is rather unexpected, since the division ring is present in the cytoplasm in all other Gram-negative bacteria studied thus far. In addition, either the formation or the breakdown of the polymerized cell division ring requires energy, probably in the form of GTP or ATP, which are proposedly not present in the periplasm.

This overview of the cell envelope is based on studies in the model anammox bacterium *K. stuttgartiensis*. Although less information is present about other anammox species, a comparison with the *K. stuttgartiensis* cell envelope is still possible at some points. In some *Scalindua sp.* the first structures encountered when approaching the cells from the outside are pili-like appendages (van Niftrik, 2008a) and, in some circumstances possibly flagella (Russ, 2015). Neither of these structures have ever been observed in *K. stuttgartiensis*, but since the genome encodes (almost) all genes necessary for the synthesis of flagella and some pili genes, it is very well possible that these cell appendages are expressed under certain conditions (Neumann et al, 2013). It seems that an S-layer is present in at least *Brocadia sinica*, since it encodes a gene (BROSI_A1236) (Oshiki et al, 2015) that is highly similar to Kustd1514 (e-value: 0, protein identity 44%) and S-layers were observed in this species (Gambelli et al, unpublished data). Whether the S-layer of this species is also glycosylated is presently unknown.

No localization of proteins has been performed in anammox bacteria other than *K. stuttgartiensis* and therefore no proteins have been unequivocally shown to be present in the outer membrane of other anammox species. Several OMPs have been detected in the proteome of *Scalindua profunda* and they would be expected to be present in the outer membrane of this species (Speth et al, 2012). Since *Jettenia caeni* (Hira et al, 2012), *B. sinica* (Oshiki et al, 2015), *Brocadia fulgida* (Ferousi et al, 2013) and *Scalindua brodae* (Speth et al, 2015) were found to contain a homolog of Kustd1878 (chapter 3), the most abundant OMP in *K. stuttgartiensis*, it is expected that these organisms have at least one OMP in their membrane (chapter 3). Whether ATPases are also present on the outer membrane in other anammox bacteria remains a topic of further research. In addition, no investigations into the presence of LPS have been performed in other anammox bacteria. However, the general lipid composition of species of *Scalindua*, *Brocadia* and *Anammoxoglobus*, prepared with a method that would probably not extract lipid A, was found to be quite similar to that of *K. stuttgartiensis* (Rattray et al, 2008).

In *B. fulgida*, the cell division ring is also described to be located in the periplasm (van Niftrik et al, 2009) and images of *Scalindua sp.* suggest the same for these species (van Niftrik et al, 2008a). A BLAST search against Kustd1438 only showed two shorter proteins from *B. fulgida* that might work together in taking over the function of Kustd1438, but no hits were found for homologs of Kustd1438 in other anammox bacteria. Further research could show which proteins are involved in cell division in (the other) anammox bacteria. It seems plausible that peptidoglycan is also present in the other anammox bacteria, since all genes necessary for its biosynthesis are identified in the genomes of *B. fulgida*, *B. sinica*, *J. caeni* and *S. brodae* and peptidoglycan has been found in multiple *Planctomycetes* in the meantime (van Teeseling et al, 2015 (chapter 5); Jeske et al, 2015).

Open questions concerning the anammox cell envelope

After the research presented in this part of the thesis, a clear overview of the anammox cell envelope has emerged (Fig. 2). Nonetheless, there are still quite some topics that deserve further elucidation in order to truly understand the cell envelope of these organisms. Some points related to the results presented in this thesis are mentioned below.

S-layer

The exact structure of the multiple glycans, as well as the pathway via which they are synthesized, transported and coupled to the protein, remains to be elucidated. Also for the S-layer protein itself, it is unknown how it is transported through and anchored into the underlying membrane. In the Gram-negative bacteria studied to date, S-layer proteins are excreted through the periplasm and outer membrane via either type I or II secretion systems (Fagan & Fairweather, 2014). Both secretion systems comprise a protein complex in the cytoplasmic membrane, a periplasm spanning tube and an outer membrane protein (complex) (Holland et al, 2005; Costa et al, 2015). A BLAST search against the *K. stuttgartiensis* genome using the canonical proteins forming the periplasmic tube, HlyD (type I) and GspC (type II) suggests that HlyD is present, but GspC is absent. The cytoplasmic component of the type I secretion system is an ABC transporter and the outer membrane protein belongs to the outer membrane factor (OMF) family (of which TolC is the most notable example). Multiple copies belonging to both protein classes are encoded in the *K. stuttgartiensis* genome and these are transcribed and translated (Strous et al, 2006; Kartal et al, 2011b; Speth et al, 2012). It is therefore possible that Kustd1514 is secreted via a type I secretion system. Other possible mechanisms of secretion can, however, not be excluded, especially since Kustd1514 has a predicted Sec signal peptide (via PRED-TAT; Bagos et al, 2010) although the type I secretion system is most often Sec-independent (Holland et al, 2005). Taking into account that many copies of the S-layer protein need to be secreted, OMPs that are abundant in the membrane are possible candidates to serve as the outer membrane part of the transport system. Therefore, Kustd1878, the OMP characterized in chapter 3, is an interesting candidate.

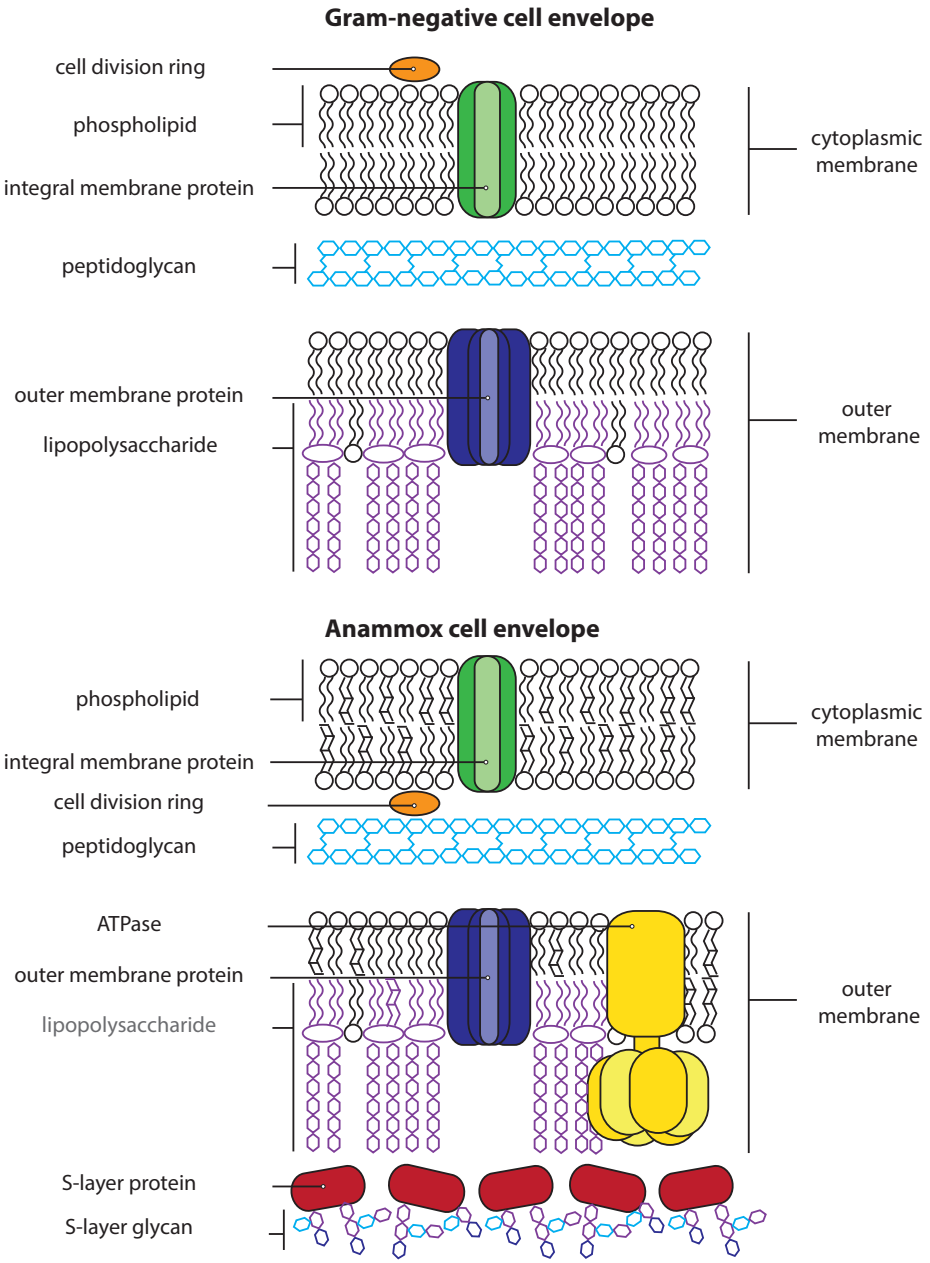

Figure 2. *A schematic cell envelope of a standard Gram-negative bacterium (without S-layer) compared to the cell envelope of the anammox bacterium* K. stuttgartiensis*. The presence of structures which name appears in grey has not yet been fully proven. The orientation and completeness of the ATPase remains to be elucidated.*

The S-layer proteins of Gram-negative bacteria are proposed to non-covalently attach to the LPS (Fagan & Fairweather, 2014). Since the presence of LPS in *K. stuttgartiensis* is not yet unambiguously proven, the structure that anchors the S-layer to the outer membrane remains to be identified. Maybe the 100 amino acids near the C-terminus of Kustd1514 play a role in LPS binding, since PHYRE^2 models these as an invasion/intimin cell-adhesion fragment previously reported to be involved in carbohydrate binding (Kelly et al, 1999). Alternatively this domain might be involved in attachment to carbohydrates of other cells or to carbohydrate components of the extrapolymeric substance (EPS), in which case the S-layer would function in attachment to other cells or aggregates. Indeed, anammox cells show a remarkable tendency to grow in aggregates and EPS, of which carbohydrates are the main component, is abundantly present in these aggregates (Ali et al, 2013). The glycosylated S-layer protein was enriched from an anammox culture living as single cells for many years already and it therefore seems unlikely that the (only) function of the S-layer would be to aid in aggregation.

As discussed in chapter 2, other possible functions of the S-layer would be protection against predation, osmoprotection, attachment of enzymes or maintaining cell shape and integrity. The most plausible function of the S-layer as proposed in chapter 2 was giving cells their structural integrity in the absence of peptidoglycan. This function has become outdated with the discovery of peptidoglycan (in chapter 5), although it is still a possibility that the S-layer aids in structural integrity. More research is necessary to elucidate the function of the S-layer in anammox bacteria. Also the function of the S-layer glycosylation is unknown and it needs to be established if it has one or several of the previously mentioned roles such as aiding in protein folding or maintenance of the structure of the S-layer, protecting against proteolysis or interaction with other cells (Calo et al, 2010).

Outer membrane

The research presented in this thesis has shown the presence of an OMP in the outermost membrane and suggests LPS might be present in this membrane as well. This has been crucial to show that this membrane can best be interpreted as an outer membrane instead of a cytoplasmic membrane. To fully understand this membrane, however, much more research will have to be performed. Towards this end, a thorough inventory of the components of the outer membrane would be very valuable. In many Gram-negative bacteria, separation of the two membranes proceeds via density centrifugation of a membrane fraction (Weiner & Li, 2008). Although the procedure might be more complicated in anammox bacteria because they have three membranes, it would be worthwhile to attempt density centrifugation, also because density centrifugation has been successfully employed to separate anammox bacterial compartments (Neumann et al, 2014). It would be highly interesting to investigate the outer membrane proteome, either focusing on proteins or on protein complexes, for instance using LC-MS/MS after (native, 2D or 1D) gel electrophoresis as performed before for *K. stuttgartiensis* membrane complexes (de Almeida et al, in prep). Possibly the glycoproteome or glycome of the outer membrane could also be investigated, for instance via lectin microarrays (Ribeiro & Mahal, 2013) or LC-MS/MS. However, additional techniques, such as NMR, have to complement both techniques in order to identify the glycan structures.

This hinders a high-throughput analysis on small sample quantities (Hitchen & Dell, 2006). Since a lipid analysis has already been performed on fractionated anammox cells (Neumann et al, 2014), it would probably be best to investigate the lipid composition of these membranes only after a suitable protocol for extraction of anammox LPS has been devised.

ATPase

As already mentioned above, the detection of an F-type ATPase in the outer membrane is a puzzling result. Additional research is clearly needed to understand the role of this protein complex, which in its full conformation consists of a soluble F_1-domain, forming the so-called head, and a membrane-associated F_O-domain. For this discussion it will be assumed that the ATPase is indeed present on the outer membrane, as was shown by previous immunogold localization, and that this ATPase is of the F-type, since the antibody was generated against a (partial) typical F-ATPase (van Niftrik et al, 2010). The first question that would need to be answered is "what is the composition of the (partial) F-ATPase located in the outer membrane?". The antibody that identified the ATPase in the outer membrane was generated against the ß-subunit (van Niftrik et al, 2010), which is located in the F_1-domain. The presence of any other proteins belonging to the F-ATPase in this membrane would need further verification, either via immunogold localization or by analyzing the proteome of isolated outer membranes as discussed before. Another interesting question is "at which side of the outer membrane is the (partial) F_1-domain located?". Answering this question could be an important step in understanding the function of this protein complex. Unfortunately, the length of the antibody complex combined with the small distance between the cytoplasmic and outer membranes and the observed labeling on the cytoplasmic membrane (van Niftrik et al, 2010) make using the previous labeling results to answer this question difficult. A promising technique to answer this question is freeze-fracture labeling, since this can differentiate between the outer and inner leaflet of membranes. Another option would be to use labeling on whole, unpermeabilized, cells visualized by cryoSEM. In such an experiment only epitopes that are present on the outside of the membrane can be labeled since the antibodies cannot penetrate intact cells.

Concerning the function of this (partial) F-ATPase, four scenarios can be foreseen (Fig. 3). The first scenario would require a full F-ATPase with its head located inside the periplasm. The full F-ATPase would be located on the outside of the outer membrane in the second scenario. In the third scenario an F_1-ATPase would be required, located inside the periplasm. In the fourth scenario a full or partial F_1-ATPase would be located on the extracellular leaflet of the outer membrane.

In the first scenario, the F-ATPase would produce ATP in the periplasm using a proton motive force over the outer membrane (de Almeida et al, in prep). If ATP were to be synthesized in the periplasm, this could be used by Kustd1438 to polymerize into the observed cell division ring. However, this scenario is rather problematic because of the OMP-caused permeability of the outer membranes to protons or ions (Nikaido, 2003). This would make the generation of a proton motive force impossible and therefore make it impossible for the ATPase to synthesize ATP. It seems improbable that the anammox membrane, in which multiple OMPs seem present, could hold a proton motive force. Measuring ATP concentrations in

fractionated *K. stuttgartiensis* cells and culture supernatant (as in (Mempin et al, 2013)) could provide interesting clues if this hypothesis is nonetheless true by showing if the ATP content in the periplasm is significantly higher than in the supernatant.

The second scenario would involve the ATPase to use a proton motive force to generate ATP extracellularly. This has the same problem as the first scenario, the unlikeliness of being able to maintain an electrochemical gradient over this membrane, and in addition it seems rather improbable that cells would choose to synthesize their costly ATP molecules outside of the cells. Unlikely as it might seem, a recent report has shown that multiple bacteria release ATP to the culture supernatant and that they hydrolyze this ATP without taking any components up into their cells (Mempin et al, 2013). This extracellular ATP was speculated to either act as signaling molecule or stimulate bacterial communities. This hypothesis could be tested by making use of the antibody against the ß-subunit. If the ATPase head is located on the outside of the membrane the antibody could bind the ß-subunit and thereby inhibit the hydrolysis of ATP by the ATPase, as was shown with a eukaryotic ectopic F-ATPase (Wen-Li et al, 2012). Comparing extracellular ATP concentration before and after inhibition of the F_1-ATP-domain might elucidate if the F-ATPase present on the anammox outer membrane is involved in generation of extracellular ATP.

Since only the F_1-domain of the ATPase is necessary to hydrolyze ATP and it seems implausible that a electrochemical gradient exists over the outer membrane, it could well be that only a full or maybe even a partial F_1-ATPase domain is present in the anammox outer membrane. If this F_1-ATPase would be present in the periplasm, it could hydrolyze ATP if this were to be present in the periplasm. What function this ATP hydrolysis would have remains uncertain. It seems rather difficult to experimentally verify this hypothesis and especially to elucidate to which process this ATP hydrolysis would be coupled. Maybe *in vivo* crosslinking studies followed by co-immunoprecipitation using the existing antibody could provide clues.

Recent findings demonstrated that entire F_1-ATPase domains and individual subunits undergo so-called moonlighting, i.e. they can have several functions, and can be located at the plasma membrane of multiple mammalian cells instead of only on the mitochondrial membrane (Vantourout et al, 2010). The (partial) F_1-ATPases are shown to be oriented towards the outside of the cells where they act as receptors for proteins, peptides or ATP analogs. It seems ATP is hydrolyzed in some pathways. With these results in mind the fourth possible role of the anammox outer membrane protein would be to act as a receptor. Most so far identified ligands (for instance apolipoprotein A1 and enterostatin (Vantourout et al, 2010)) do not seem to be relevant for environmental bacteria, such as anammox bacteria. However, the bacterial phosphoantigen-related ATP analog AppppI that can bind to F_1-ATPase might be a substance that anammox bacteria could encounter. Which importance such a potential moonlighting (partial) F_1-ATPase, present in significant amounts at the outer membrane (van Niftrik et al, 2010), could play in the life of anammox bacteria remains a mystery. Inhibiting the F_1-ATPase with the existing antibody might show if the cells are affected if this putative receptor were to be blocked. Maybe transcriptomics performed in parallel could show which pathways could be involved downstream of this receptor. Also *in*

vivo cross-linking studies could give clues about which protein or peptide is associated with the putative receptor.

When comparing all four scenarios for the ATPase on the outer membrane the fourth scenario, in which a full or partial ATPase acts as an extracellular receptor seems the most compelling scenario.

Periplasm

As in the case of the outer membrane it would be highly interesting to make an inventory of the contents of the periplasm. A periplasmic proteome of several Gram-negative bacteria (e.g. Imperi et al, 2009; Wilmes et al, 2011; Han et al, 2014) was analyzed after releasing the periplasmic proteins by osmotic shock, for instance using low temperatures, sucrose or $MgCl_2$ with lysozyme. It would be very important to verify (for instance via fluorescence microscopy using DAPI staining) if such methods indeed leave the rest of the anammox cell intact.

In addition, it is very interesting to discover how these proteins are targeted from the cytoplasm towards the periplasm. In Gram-negative bacteria the Sec and Tat protein translocation systems are responsible for delivering respectively unfolded and folded proteins to the periplasm (Sargent et al, 2006; Driessen & Nouwen, 2008). The only protein that is up to now proven to be located in the periplasm is Kustd1438 and indeed its sequence has a predicted Sec leader sequence (using PRED-TAT; Bagos et al, 2010). The protein transport in anammox bacteria is, however, more complex than in other Gram-negative bacteria because of the presence of the anammoxosome. Recently it was shown that many proteins that are located in the anammoxosome also have Sec leader sequences (de Almeida et al, 2015). This indicates that the protein translocation of anammox bacteria includes additional cues that steer the proteins towards either the anammoxosome or the periplasm, maybe via chaperones (Medema et al, 2010), and further research into these mechanisms would be needed.

Cell division (ring)

The most intriguing structure for further research concerning the periplasm is undoubtedly the cell division ring. Anammox cell division is a rather unique process in multiple ways: 1) the ring-forming protein (probably Kustd1438, at least in *K. stuttgartiensis*) is different than in most other bacteria (FtsZ), 2) the cell division ring is present in the periplasm whereas all other bacteria have the cell division ring in the cytoplasm and 3) anammox cell division needs to divide three compartments instead of two (as in Gram-negative bacteria) or one (Gram-positive bacteria). The anammox cell division thus clearly deserves further research. A good starting point would be to elucidate which components are part of or undergo association with the cell division ring. Since an antibody against Kustd1438 exists (van Niftrik et al, 2009) co-immunoprecipitation could be performed. Preceding this experiment, *in vivo* cross-linking could be performed to also capture proteins that loosely associate with the cell division ring.

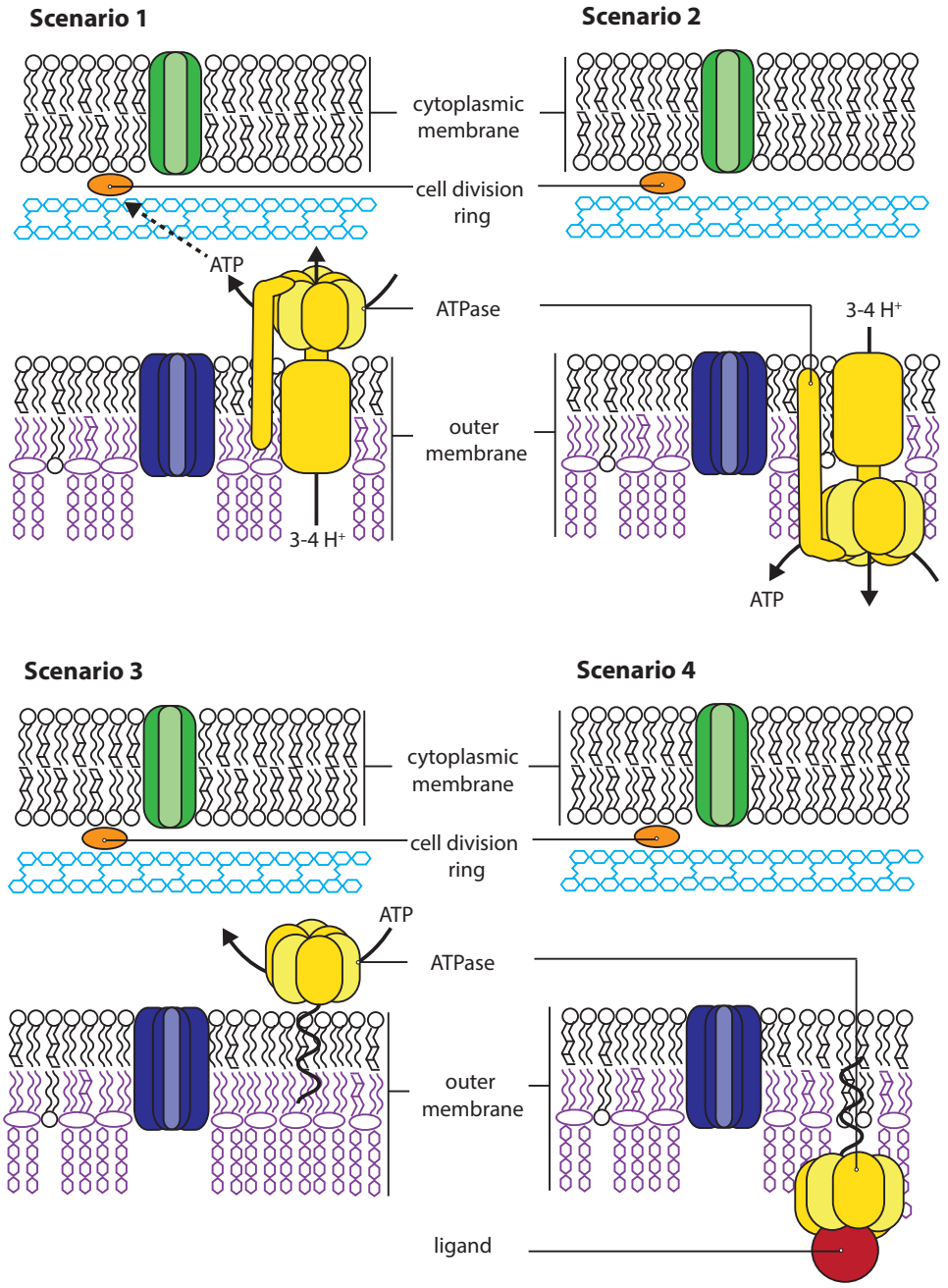

Figure 3. *Four possible scenarios for localization and function of the F-ATPase present on the outer membrane of* K. stuttgartiensis.

To investigate if Kustd1438 is the only protein necessary for the formation of the ring, purified (for instance using the antibody) or heterologously expressed Kustd1438 could be subjected to *in vitro* polymerization assays in the presence and absence of ATP or GTP. Alternatively, Kustd1438 could be added to liposomes formed in the presence of GTP and investigated if constriction of these liposomes takes place (as was the case for FtsZ in liposomes (Osawa et al, 2008)).

In addition, it would be interesting to find out if the other cell division genes that are encoded in the genome of *K. stuttgartiensis* (FtsE, FtsX and the FtsA-independent divisomal complex (FtsK, FtsQ, FtsB, FtsL, FtsW and FtsI) (van Niftrik et al, 2009)) are present in the cells and at which location. Generating antibodies against some of these proteins and using these for immunogold localization might answer this question. Since many of these proteins (FtsE, FtsX, FtsI and FtsW (Rico et al, 2013)) are proposedly involved in peptidoglycan hydrolysis and septal peptidoglycan synthesis their possible function was puzzling, until the discovery of peptidoglycan in anammox bacteria (described in chapter 5). Figure 4 shows a model proposing a possible location of these proteins in *K. stuttgartiensis* and shows the *E. coli* cell division as a reference. It would be helpful if anammox cells could use the genes encoding these proteins (i.e. FtsE, FtsX, FtsI and FtsW) to regulate peptidoglycan hydrolysis and synthesis during cell division instead of coming up with an entirely new system. Therefore, FtsE probably needs to be located in the periplasm, since it has to interact with the cell division ring before activating FtsX. FtsX would therefore need to have its FtsE binding site on the periplasmic instead of the cytoplasmic part of the protein. Since the homology of both *K. stuttgartiensis* proteins to the *E. coli* proteins are rather low and the binding site of FtsE on FtsX in *E. coli* has not yet been resolved, it is at this moment not possible to further verify this hypothesis via bioinformatics.

Knowing that the cell division ring is located in the periplasm also makes the lack of FtsA and ZipA in *K. stuttgartiensis* less problematic, since they link the FtsZ-based ring to the cytoplasmic membrane (Fig. 4). For anammox cells, there is no real necessity to link the ring to the cytoplasmic membrane: whereas in the canonical bacterial cell division the ring needs to drag the cytoplasmic membrane inwards, in the anammox case the ring could push the cytoplasmic membrane inward without links being present. Maybe this pushing motion could even lead to the division of the anammoxosome. In *E. coli*, the outer membrane is constricted together with the cytoplasmic membrane since both are linked via the Tol-Pal protein complex (Gerding et al, 2007). In *K. stuttgartiensis*, the Pal protein seems present (Kuste3333) as are most of the accessory Tol proteins, but TolA, the protein that is linked to Pal, seems absent. It seems probable that another protein is present in anammox bacteria that takes over this function since linking the two membranes together seems crucial for a proper cell division.

FtsN was recently shown to associate with FtsA (Weiss, 2015) and this might be the reason it is apparently absent from the *K. stuttgartiensis* genome. FtsN was shown to activate FtsQBL, which in turn activates peptidoglycan synthesis, possibly via FtsW and FtsI (Weiss, 2015). If activation of FtsQBL would indeed stimulate FtsW and FtsI, anammox bacteria would need an FtsN-independent way that integrates a signal from the cell division ring and associates with

FtsQBL. Such a protein might come up in *in vivo* cross-linking experiments, if it is bound tightly enough to Kustd1438.

Another interesting aspect concerning the anammox cell division ring is the way it is energized. GTP hydrolysis is required for polymerization of FtsZ (Mukherjee & Lutkenhaus, 1998; Lu et al, 1998) and in addition GTP hydrolysis seems to lead to a conformational change of FtsZ filaments that facilitates constriction (Lu et al, 2000). As Kustd1438 is predicted to contain an ATP/GTP binding site and was hypothesized to be the ring-forming protein (van Niftrik et al, 2009), it seems plausible that ATP or GTP is necessary for the dynamics of the ring formation. An interesting question is how this ATP or GTP enters the periplasm. As discussed above, it is a possibility that the ATPase on the outer membrane synthesizes ATP in the periplasm, although the expected permeability of the outer membrane is problematic. A very interesting finding poses another, more plausible scenario: an antibody generated against the ß-subunit of the ATPase-2 (Kuste4592-4600) of *K. stuttgartiensis* showed a very specific localization to the cell division site (van Niftrik, 2008). Although this antibody did not give a specific signal on an immunoblot and the specificity for the ATPase therefore needs to be verified in another way, the immunogold localization suggests this ATPase to be located on the cytoplasmic membrane just beneath the cell division ring. It was hypothesized that the ATPase-2 uses sodium ions instead of protons (Dibrova et al, 2010). This ATPase could provide ATP very locally in the periplasm and thereby make sure that as little as possible ATP leaks away into the rest of the periplasm and maybe towards the outside of the cell. This hypothesis would fit the low expression values for this ATPase gene cluster (van Niftrik et al, 2010) and the fact that it was detected in the proteome at lower amounts than the ATPase-1 (Kuste3787-3796) (de Almeida et al, in prep).

The most intriguing question is which advantage, if any, it has for anammox bacteria to locate the cell division ring outside of the cytoplasmic membrane. Clearly more research is needed to answer this question, also concerning the mechanism that couples the cell division to the division of the anammoxosome. Maybe this anammoxosome division, which sets apart anammox bacteria from all other Gram-negatives, provides the key towards understanding the unexpected location of the cell division ring.

Figure 4 (right page). *Scheme comparing cell division in* E. coli *with a proposed model for* K. stuttgartiensis *cell division. In* E. coli *the cell division ring composed of FtsZ is attached to the membrane via FtsA and ZipA. FtsE binds FtsZ and stimulates FtsX so that EnvC is recruited and in turn recruits AmiB. AmiB is an amidase that cleaves peptidoglycan in order to make new, septal, peptidoglycan insertion via FtsI (which is coupled to the membrane protein FtsW) possible. The Tol-Pal complex links the outer membrane to the cytoplasmic membrane thereby ensuring that the outer membrane is also constricted during cell division. Since the precise function of the essential FtsQBL complex (present in* E. coli *and* K. stuttgartiensis*) is not yet elucidated, this complex is not included in the scheme. Proteins surrounded by a red line have a deviant location from the* E. coli *model. No homologs against proteins in grey have been found in the* K. stuttgartiensis *genome, the model would however require such proteins to function.*

***Escherichia coli* cell division**

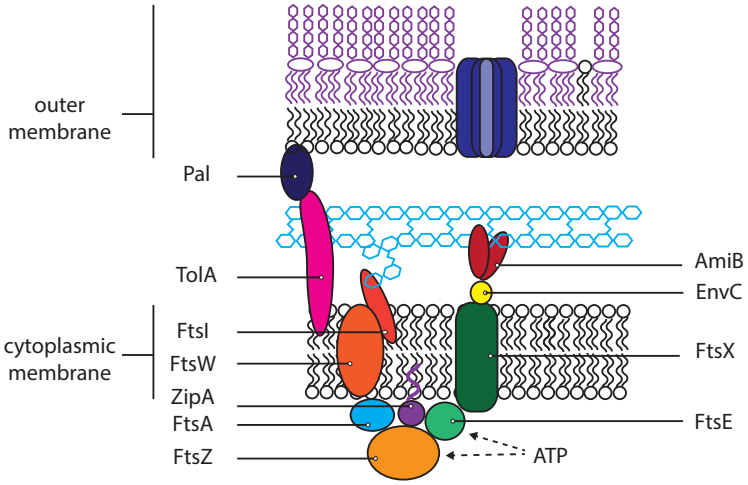

***Kuenenia stuttgartiensis* cell division**

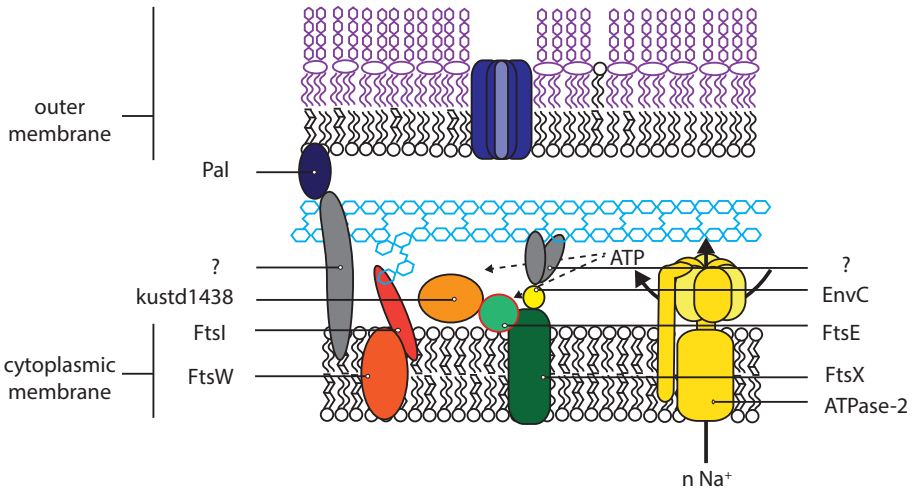

Implications for other *Planctomycetes*

The finding that anammox bacteria have a Gram-negative cell plan leads to the question if other *Planctomycetes* should also be interpreted as Gram-negative bacteria. Indeed this seems to be the case, since multiple non-anammox *Planctomycetes* species were shown to contain peptidoglycan in between two membranes (Jeske et al, 2015) and the results in chapter 4, together with previous detection of 3-hydroxy fatty acids in several *Planctomycetes* (Kerger et al, 1988; Giovannoni et al, 1987; Sittig & Schlesner, 1993) suggest LPS to be present in these organisms. In addition, analysis of the genomes of several *Planctomycetes* showed that these encode multiple predicted OMPs, including LptD and BamA, crucial for insertion of LPS and OMPs respectively (Speth et al, 2012).

These *Planctomycetes* are, however, rather unusual Gram-negative bacteria, since their cytoplasmic membrane is often unusually curved and thereby leaves sites where the periplasm is enlarged and the cytoplasmic membrane is probably not linked to the outer membrane. This cytoplasmic membrane plasticity has been suggested as a feature unique for *Planctomycetes* (Speth et al, 2012). At the time this theory was developed, peptidoglycan was not yet detected in these organisms and it was therefore hypothesized that the cytoplasmic membrane might be completely uncoupled from the outer membrane. The presence of peptidoglycan shows this view was probably too simplistic: peptidoglycan synthesis and polymerization of its backbone are coupled to the cytoplasmic membrane and the mature peptidoglycan is associated with the outer membrane. This close association of the peptidoglycan to the outer membrane was indeed observed in cryo-electron tomography on *Planctopirus limnophila* (Jeske et al, 2015) but the structures, probably (lipo)proteins, that are responsible for this anchoring mechanism remain unknown in the *Planctomycetes*.

The detection of complete peptidoglycan sacculi (Jeske et al, 2015) suggests that this layer is present in the entire cell and not only at locations where the cytoplasmic membrane is located in close proximity to the outer membrane. It is an intriguing question how *Planctomycetes* that show extensive invaginations of the cytoplasmic membrane manage to synthesize an entire sacculus. It is conceivable that the cytoplasmic invaginations are so dynamic that the cytoplasmic membrane spends enough time close to the outer membrane to synthesize peptidoglycan that is linked to the outer membrane, before the cytoplasmic membrane bends away from the outer membrane. Indeed the sometimes very complicated invaginations in for instance *P. limnophila* (Jogler et al, 2011; Scheuner et al, 2014) and most notably *Gemmata obscuriglobus* (Lieber et al, 2009; Santarella-Mellwig et al, 2010; Acehan et al, 2014; Santarella-Mellwig et al, 2013) are probably dynamic as fluorescent microscopy of stained membranes also suggests in the case of *G. obscuriglobus* (Lee et al, 2009).

The membrane coat proteins detected in the genomes of non-anammox *Planctomycetes* have been seen in association with membrane vesicles in *G. obscuriglobus* (Santarella-Mellwig et al, 2010; Lonhienne et al, 2010; Acehan et al, 2014) and could therefore be involved in membrane invaginations of other non-anammox *Planctomycetes* as well. Protein uptake, possibly via an endocytosis-like mechanism, and degradation have been associated with the vesicles or the tubulovesicular network in the periplasm of *G. obscuriglobus* (Lonhienne et al, 2010; Acehan et al, 2014). How this fascinating system of membrane

vesicles that apparently are interconnected with each other, the outer membrane and the cytoplasmic membrane is regulated, how their formation is regulated with respect to the peptidoglycan layer, and why the vesicles are proposedly used for protein uptake are questions that require further research. In addition, the function of the enlarged periplasm and/or the enlarged cytoplasmic membrane in other *Planctomycetes* remains unknown. Furthermore, it is an interesting question if the potentially dynamic invaginations of the cytoplasmic membrane and its decreased or absent degree of connection to the outer membrane have led to an alternative way of cell division in these organisms that divide through budding.

All in all, the results presented in this thesis together with results in other *Planctomycetes* (Jeske et al, 2015) have unveiled (anammox) *Planctomycetes* as Gram-negative bacteria. The results show that (anammox) *Planctomycetes* are still special within the Gram-negative bacteria, with respect to their cell division mechanisms and, in case of many non-anammox *Planctomycetes*, the unusual curvature of their cytoplasmic membrane that seems to be less closely linked to the outer membrane than in other Gram-negatives. This leaves the floor to much more in-depth studies into the cell biology of (anammox) *Planctomycetes*, which will undoubtedly provide many interesting and unexpected discoveries that enhance the understanding of these fascinating organisms. Recent and present developments allowing the use of *P. limnophila* as both a genetically amendable model organism and a source for heterologous expression of proteins for other *Planctomycetes* (Jeske, van Teeseling, Jogler, van Niftrik, unpublished results) is expected to be of crucial importance in these studies.

References

Abma WR, Schultz CE, Mulder JW, van der Star WRL, Strous M, Tokutomi T, van Loosdrecht MCM (2007) Full-scale granular sludge Anammox process. *Water Sci Technol* 55: 27-33.

Acehan D, Santarella-Mellwig R, Devos DP (2014) A bacterial tubulovesicular network. *J Cell Sci* 127: 277-280.

Al-Amoudi A, Chang J-J, Leforestier A, McDowall A, Salamin LM, Norlén LPO, Richter K, N Sartori Blanc, Studer D, Dubochet J (2004) Cryo-electron microscopy of vitreous sections. *EMBO J* 23: 3583-3588.

Albers S-V, Meyer BH (2011) The archaeal cell envelope. *Nat. rev. Microbiol.* 9: 414-426.

Ali M, Chai L-Y, Tang C-J, Zheng P, Min X-B, Yang Z-H, Xiong L, Song Y-X (2013) The increasing interest of ANAMMOX research in China: bacteria, process development, and adaptation. *Biomed Res Int* 134914.

Altschul SF, Gish W, Miller W, Myers EW, Lipman DJ (1990) Basic local alignment search tool. *J Mol Biol* 215: 403-410.

Altschul SF, Madden TL, Schäffer AA, Zhang J, Zhang Z, Miller W, Lipman DJ (1997) Gapped BLAST and PSI-BLAST: a new generation of protein database search programs. *Nucleic Acids Res* 25: 3389-3402.

Anderson MS, Raetz CRH (1987) Biosynthesis of lipid A precursors in *Escherichia coli*. A cytoplasmic acyltransferae that converts UDP-*N*-acetylglucosamine to UDP-3-O-(R-3-hydroxymyristoyl)-*N*-acetylglucosamine. *J Biol Chem* 15: 5159-5169.

Angert ER (2005) Alternatives to binary fission in bacteria. *Nat Rev Microbiol* 3: 214-224.

Arrigo KR (2005) Marine microorganisms and global nutrient cycles. *Nature* 437: 349-355.

Awram P, Smit J (2001) Identification of lipopolysaccharide O antigen synthesis genes required for attachment of the S-layer of *Caulobacter crescentus*. *Microbiology* 147: 1451-1460.

Babbin AR, Keil RG, Devol AH, Ward BB (2014) Organic matter stoichiometry, flux, and oxygen control nitrogen loss in the ocean. *Science* 344: 406-408.

Babinski KJ, Ribeiro AA, Raetz CRH (2002) The *Escherichia coli* gene encoding the UDP-2,3-diacylglucosamine pyrophosphatase of lipid A biosynthesis. *J Biol Chem* 277: 25937-25946.

Bagos PG, Liakopoulos TD, Spyropoulos IC, Hamodrakas SJ (2004) PRED-TMBB: a web server for predicting the topology of ß-barrel outer membrane proteins. *Nucl Acids Res* 32: W400-W404.

Bagos PG, Nikolaou EP, Liakopoulos TD, Tsirigos KD (2010) Combined prediction of Tat and Sec signal peptides with Hidden Markov Models. *Bioinformatics* 26: 2811-2817.

Baldermann C, Lupas A, Lubieniecki J, Engelhardt, H (1998) The regulated outer membrane protein Omp21 from *Comamonas acidovorans* is identified as a member of a new family of eight-stranded β-sheet proteins by its sequence and properties. *J Bacteriol* 180: 3741-3749.

Bang FB (1956) A bacterial disease of *Limulus polyphemus*. *Bull Johns Hopkins Hosp* 98: 325–351.

Bengtsson MM, Øvreås L (2010) Planctomycetes dominate biofilms on surfaces of the kelp *Laminaria hyperborea*. *BMC Microbiol* 10:261.

Benz R, Janko K, Boos W, Läuger P (1978) Formation of large, ion-permeable membrane channels by the matrix protein (porin) of *Escherichia coli*. *Biochim Biophys Acta* 511: 305-319.

Berman HM, Henrick K, Nakamura H (2003) Announcing the worldwide Protein Data Bank. *Nat Struct Biol* 10: 980.

Beveridge TJ (1981) Ultrastructure, chemistry, and function of the bacterial wall. *Int Rev Cytol* 72: 229-317.

Beveridge TJ (2001) Use of gram stain in microbiology. *Biotech Histochem* 76: 111-118.

Beveridge TJ, Murray RGE (1980) Sites of metal deposition in the cell wall of *Bacillus subtilis*. *J Bacteriol* 141: 876-887.

Bondoso J, Albuquerque L, Nobre MF, Lobo-da-Cunha A, da Costa MS, Lage OM (2011) *Aquisphaera giovannonii* gen.nov., sp. nov., a planctomycete isolated from a freshwater aquarium. *Int J Syst Evol Microbiol* 61: 2844-2850.

Bondoso J, Albuquerque L, Lobo-da-Cunha A, da Costa MS, Harder J, Lage OM (2014) *Rhodopirellula lusitana* sp. nov. and *Rhodopirellula rubra* sp. nov., isolated from the surface of macroalgae. *Syst Appl Microbiol* 37: 157-164.

Bondoso J, Albuquerque L, Nobre MF, Lobo-da-Cunha A, da Costa MS, Lage OM (2015) *Roseimaritima ulvae* gen. nov., sp. nov. nd *Rubripirellula obstinate* gen. nov., sp. nov. two novel planctomycetes isolated from the epiphytic community of macroalgae. *Syst Appl Microbiol* 38: 8-15.

Borneman J, Triplett EW (1997) Molecular microbial diversity in soils from eastern Amazonia: evidence for unusual microorganisms and microbial population shifts associated with deforestation. *Appl Environ Microbiol* 63: 2647-2653.

Boumann HA, Hopmans EC, van de Leemput I, Op den Camp HJM, van de Vossenberg J, Strous M, Jetten MSM, Sinninghe Damsté JS, Schouten S (2006) Ladderane phospholipids in anammox bacteria comprise phosphocoline and phosphoethanolamine headgroups. *FEMS Microbiol Lett* 258: 297-304.

Boumann HA, Longe ML, Stroeve P, Poolman B, Hopmans EC, Stuart MCA, Sinninghe Damsté JS, Schouten S (2009) Biophysical properties of membrane lipids of anammox bacteria: I. Ladderane phospholipids form highly organized fluid membranes. *Biochim Biophys Acta* 1788: 1444-1451.

Braun M, Killmann H, Maier E, Benz R, Braun V (2002) Diffusion through channel derivatives of the *Escherichia coli* FhuA transport protein. *Eur J Biochem* 269: 4948-4959.

Braunstein M, Brown AM, Kurtz S, Jacobs Jr. WR (2001) Two nonredundant SecA homologues function in mycobacteria. *J Bacteriol* 183: 6979-6990.

Brown S, Santa Maria Jr. JP, Walker S (2013) Wall teichoic acids of Gram-positive bacteria. *Annu Rev Microbiol* 67: 313-336.

Brozek KA, Raetz CRH (1990) Biosynthesis of lipid A in *Escherichia coli*. Acyl carrier protein-dependent incorporation of laurate and myristate. *J Biol Chem* 265: 15410-15417.

Buchan DWA, Ward SM, Lobley AE, Nugent TCO, Bryson K, Jones DT (2010) Protein annotation and modeling servers at University College London. *Nucleic Acids Res* 38: W563-W568.

Buchan DWA, Minneci F, Nugent TCO, Bryson K, Jones DT (2013) Scalable web services for the PSIPRED Protein Analysis Workbench. *Nucl Acids Res* 41: W340-W348.

Buchanan SK, Smith BS, Venkatramani L, Xia D, Esser L, Palnitkar M, Chakraborty R, van der Helm D, Deisenhofer J (1999) Crystal structure of the outer membrane active transporter FepA from *Escherichia coli*. *Nat Struct Biol* 6: 56-63

Buckley DH, Huangyutitham V, Nelson TA, Rumberger A, Thies JE (2006) Diversity of *Planctomycetes*in soil in relation to soil history and environmental heterogeneity. *Appl Environ Microbiol* 72: 4522-4531.

Calo D, Kaminski L, Eichler J (2010) Protein glycosylation in Archeaea: sweet and extreme. *Glycobiology* 20: 1065-1076.

Caroff M, Karibian D (2003) Structure of bacterial lipopolysaccharides. *Carbohydr Res* 338: 2431-2447.

Cava F, de Pedro MA, Lam H, Davis BM, Waldor MK (2011) Distinct pathways for modification of the bacterial cell wall by non-canonical D-amino acids. *EMBO J* 30**:** 3442-353.

Cava F, de Pedro MA (2014) Peptidoglycan plasticity in bacteria: emerging variability of the murein sacculus and their associated biological functions. *Curr Opin Microbiol* 18: 46-53.

Cayrou C, Raoult D, Drancourt M (2010) Broad-spectrum antibiotic resistance of *PLanctomycetes* organisms determined by Etest. *J Antimicrob Chemother* 65: 2119-2122.

Chaban VV, Nielsen MB, Kopec W, Khandelia H (2014) Insights into the role of cyclic ladderane lipids in bacteria from computer simulations. *Chem Phys Lipids* 181: 76-82.

Chanyi RM, Ward C, Pechey A, Koval SF (2013) To invade or not to invade: two approaches to a prokaryotic predatory life cycle. *Can J Microbiol* 59: 273-279.

Chauhan JS, Bhat AH, Raghava GPS, Rao A (2012) GlycoPP: a webserver for prediction of N-and O-glycosites in prokaryotic protein sequences. *PLOS One* 7: e40155.

Clementz T, Raetz CRH (1991) A gene coding for 3-deoxy-manno-octulosonic-acid transferase in *Escherichia coli*. Identification, mapping, cloning, and sequencing. *J Biol Chem* 266: 9687-9696.

Clementz T, Zhou Z, Raetz CRH (1997) Function of the *Escherichia coli msbB* gene, a multicopy suppressor of *htrB* knockouts, in the acylation of lipid A. *J Biol Chem* 272: 10353-10360.

Costa TRD, Felisberto-Rodrigues C, Meir A, Prevost MS, Redzej A, Trokter M, Waksman G (2015) Secretion systems in Gram-negative bacteria: structural and mechanistic insights. *Nat Rev Microbiol* 13: 343-359.

Cowan WS, Schirmer T, Rummel G, Steiert M, Ghosh R, Pauptit RA, Jansonius JN, Rosenbusch JP (1992) Crystal structures explain functional properties of two *E.coli* porins. *Nature* 358: 727-733.

Crichton PG, Harding M, Ruprecht JJ, Lee Y, Kunji ERS (2013) Lipid, detergent, and Coomassie blue G-250 affect the migration of small membrane proteins in blue native gels: mitochondrial carriers migrate as monomers and not dimers. *J Biol Chem* 228: 22163-22173.

Cronan JE (2003) Bacterial membrane lipids: where do we stand? *Annu Rev Microbiol* 57: 203-224.

Crowell DN, Anderson MS, Raetz CHR (1986) Molecular cloning of the genes for lipid A disaccharide synthase and UDP-*N*-acetylglucosamine acyltransferase in *Escherichia coli*. *J Bacteriol* 168: 152-19.

Dai K, Lutkenhaus J (1991) *ftsZ* is an essential cell division gene in *Escherichia coli*. *J Bacteriol* 173: 3500-3506.

Dale OR, Tobias CR, Song B (2009) Biogeographical distribution of diverse anaerobic ammonium oxidizing (anammox) bacteria in Cape Fear River Estuary. *Environ Microbiol* 11: 1194-1207.

Darveau RP, Pham T-TT, Lemley K, Reife RA, Bainbridge BW, Coats SR, Howald WN, Way SS, Hajjar AM (2004) *Porphyromonas gingivalis* lipopolysaccharide contains multiple lipid A species that functionally interact with both toll-like receptors 2 and 4. *Infect Immun* 72: 5041-5051.

de Almeida NM, Maalcke WJ, Keltjens JT, Jetten MSM, Kartal B (2011) Proteins and protein complexes involved in the biochemical reactions of anaerobic ammonium-oxidizing bacteria. *Biochem Soc Trans* 39: 303-308.

de Almeida NM, Neumann S, Mesman RJ, Ferousi C, Keltjens JT, Jetten MSM, Kartal B, van Niftrik L (2015) Immunogold localization of key metabolic enzymes in the anammoxosome and on the tubule-like structures of *Kuenenia stuttgartiensis*. *J Bacteriol* 197: 2432-2441.

de Almeida NM, Wessels HJCT, de Graaf R, Ferousi C, Keltjens JT, Jetten MSM, Kartal B. Membrane-bound electron transport systems of an anammox bacterium: a complexome analysis. *In preparation*.

De Castro C, Parrilli M, Holst O, Molinaro A (2010) Microbe-associated molecular patterns in innate immunity: extraction and chemical analysis of Gram-negative bacterial lipopolysaccharides, p 89-115. *In* Fukuda M (ed), Methods in Enzymology, volume 480: Glycobiology. London, UK. ISBN: 978-0-12-380999-5.

de Cock H, Brandenburg K, Wiese A, Holst O, Seydel U (1999) Non-lamellar structure and negative charges of lipopolysaccharides required for efficient folding of outer membrane protein PhoE of *Escherichia coli*. *J Biol Chem* 274: 5114-5119.

de Pedro MA, Quintela JC, Höltje JV. Schwarz H (1997) Murein segregation in *Escherichia coli*. *J Bacteriol* 179**:** 2823-2834.

DeLong EF, Franks DG, Alldredge AL (1993) Phylogenetic diversity of aggregate-attached vs. free-living marine bacterial assemblages. *Limmnol Oceanogr* 38: 924-934.

Derakshani M, Lukow T, Liesack W (2001) Novel bacterial lineages at the (sub)division level as detected by signature nucleotide-targeted recovery of 16S rRNA genes from bulk soil and rice roots of flooded rice microcosms. *Appl Environ Microbiol* 67: 623-631.

Devos DP (2014a) Re-interpretation of the evidence for the PVC cell plan supports a Gram-negative origin. *Antonie van Leeuwenhoek* 105: 271-274.

Devos DP (2014b) PVC bacteria: variation of, but not exception to, the Gram-negative cell plan. *Trends Microbiol* 22: 14-20.

Devos DP, Reynaud EG (2010) Intermediate steps. *Science* 330**:** 1187-1188.

Dhakshnamoorthy B, Ziervogel BK, Blachowicz L, Roux B (2013) A structural study of ion permeation in OmpF porin from anomalous X-ray diffraction and molecular dynamics simulations. *J Am Chem Soc* 135: 16561-16568.

Dibrova DV, Galperin MY, Mulkidjanian AY (2010) Characterization of the N-ATPase, a distinct, laterally transferred Na^+-translocating form of the bacterial F-type membrane ATPase. *Bioinformatics* 26: 1473-1476.

Dietl A, Ferousi C, Maalcke WJ, Menzel A, de Vries S, Keltjens JT, Jetten MSM, Kartal B, Barends TRM (2015) Inner workings of the hydrazine synthase multiprotein complex. *Nature* in press.

Ding JL, Ho B (2010) Endotoxin detection—from limulus amebocyte lysate to recombinant factor C. *Subcell Biochem* 53: 187-208.

Driessen AJM, Nouwen N (2008) Protein translocation across the bacterial cytoplasmic membrane. *Annu Rev Biochem* 77: 643-667.

Dworkin J, Tummuru MK, Blaser MJ (1995) A lipopolysaccharide-binding domain of the *Campylobacter fetus* S-layer protein resides within the conserved N terminus of a family of silent and divergent homologs. *J Bacteriol* 177: 1734-1741.

Egelseer E, Schocher I, Sára M, Sleytr UB (1995) The S-layer from *Bacillus stearothermophilus* DSM 2358 as an adhesio site for a high-molecular-weight amylase. *J Bacteriol* 177: 1444-1451.

Eichler J (2013) Extreme sweetness: protein glycosylation in archaea. *Nat Rev Microbiol* 11: 151-156.

Eichler J, Adams MWW (2005) Posttranslational protein modification in Archaea. *Microbiol Mol Biol Rev* 69: 393-425.

El-Samalouti VT, Schletter J, Brade H, Brade L, Kusumoto S, Rietschel ET, Flad H-D, Ulmer AJ (1997) Detection of lipopolysaccharide(LPS)-binding membrane proteins by immune-copreciptation with LPS and anti-LPS antibodies. *Eur J Biochem* 250: 418-424.

Engelhardt H (1988) Correlation averaging and 3-D reconstruction of 2-D crystalline membranes and macromolecules, p 357-413. *In* Mayer F (ed), Methods in Microbiology vol 20. Academic Press (Elsevier), London, UK. ISBN 0-12-521520-6.

Engelhardt H (2007a) Are S-layers exoskeletons? The basic function of protein surface layer revisited. *J Struct Biol* 160: 115-124.

Engelhardt H (2007b) Mechanism of osmoprotection by archaeal S-layers: a theoretical study. *J Struct Biol* 160: 190-199.

Engelhardt H, Peters J (1998) Structural research on surface layers: a focus on stability, surface layer homology domains, and surface layer-cell wall interactions. *J Struct Biol* 124: 276-302.

Erridge C, Bennet-Guerrero E, Poxton IR (2002) Structure and function of lipopolysaccharides. *Microb Infect* 4: 837-851.

Fagan RP, Fairweather NF (2011) *Clostridium difficile* has two parallel and essential Sec secretion systems. *J Biol Chem* 286: 27483-27493.

Fagan RP, Janoir C, Collignon A, Mastrantonia P, Poxton IR, Fairweather NF (2011) A proposed nomenclature for cell wall proteins of *Clostridium difficile*. *J Med Microbiol* 60: 1225-1228.

Fagan RP, Fairweather NF (2014) Biogenesis and functions of bacterial S-layers. *Nat Rev Microbiol* 12: 211-222.

Fairman JW, Noinaj N, Buchanan SK (2011) The structural biology of β-barrel membrane proteins: a summary of recent reports. *Curr Opin Struct Biol* 21: 523-531.

Farhoud MH, Wessels HJCT, Steenbakkers PJM, Mattijssen S, Wevers RA, van Engelen BG, Jetten MSM, Smeitink JA, van den Heuvel LP, Keltjens JT (2005) Protein complexes in the Archaeon *Methanothermobacter thermautotrophicus* analyzed by blue native/SDS-PAGE and mass spectrometry. *Mol Cell Proteomic* 4: 1653-1663.

Ferousi C, Speth DR, Reimann J, Op den Camp HJM, Allen JWA, Keltjens JTM, Jetten MSM (2013) Identification of the type II cytochrome *c* maturation pathway in anammox bacteria by comparative genomics. *BMC Microbiol* 13: 265.

Forst D, Welte W, Wacker T, Diederichs K (1998) Structure of the sucrose-specific porin ScrY from *Salmonella typhimurium* and its complex with sucrose. *Nat Struct Biol* 5: 37-46.

Forterre P, Gribaldo S (2010) Bacteria with a eukaryotic touch: a glimpse of ancient evolution? *Proc Natl Acad Sci USA* 107: 12739-12740.

Francis CA, Beman JM, Kuypers MMM (2007) New processes and players in the nitrogen cycle: the microbial ecology of anaerobic and archaeal ammonia oxidation. *ISME J* 1: 19-27.

Fuchs KH, Tittmann P, Krusche K, Gross H (1995) Reconstruction and representation of surface data from two-dimensional crystalline, biological macromolecules. *Bioimaging* 3: 12-24.

Fuerst JA (1995) The planctomycetes: emerging models for microbial ecology, evolution and cell biology. *Microbiology* 141: 1493-1506.

Fuerst JA, Sambhi SK, Paynter JL, Hwakins JA, Atherton JG (1991) Isolation of a bacterium resembling *Pirellula* species from primary tissue culture of the giant tiger prawn (*Penaeus monodon*). *Appl Environ Microbiol* 57: 3127-3134.

Fuerst JA, Webb RI (1991) Membrane-bounded nucleoid in the eubacterium *Gemmata obscuriglobus*. *Proc Natl Acad Sci USA* 88: 8184-8188.

Fuerst JA, Gwilliam HG, Lindsay M, Lichanska A, Belcher C, Vickers JE, Hugenholz P (1997) Isolation and molecular identification of Planctomycete bacteria from postlarvae of the giant tiger prawn, *Penaeus monodon*. *Appl Environ Microbiol* 63: 254-262.

Fuerst JA, Sagulenko E (2011) Beyond the bacterium: planctomycetes challenge our concepts of microbial structure and function. *Nat Rev Microbiol* 9: 403-413.

Fuerst JA, Sagulenko E (2012) Keys to eukaryality: planctomycetes and ancestral evolution of cellular complexity. *Front Microbiol* 3: 167.

Fuchsman CA, Staley JT, Oakley BB, Kirkpatrick JB, Murray JW (2012) Free-living and aggregate-associated *Planctomycetes* in the Black Sea. *FEMS Microbiol Ecol* 80: 402-416.

Fukunaga Y, Kurahashi M, Sakiyama Y, Ohuchi M, Yokota A, Harayama S (2009) *Phycisphaerea mikurensis* gen. nov., sp. nov., isolated from a marine alga, and proposal of *Phycisphaeraceae* fam. nov., *Phycisphaerales* ord. nov. and *Phycispaerae* classis nov. in the phylum *Planctomycetes*. *J Gen Appl Microbiol* 55: 267- 275.

Galanos C, Lüderitz O, Westphal O (1969) A new method for the extraction of R Lipopolysaccharides. *European J Biochem* 9: 245-249.

Garrett TA, Kadrmas JL, Raetz CRH (1997) Identification of the gene encoding the *Escherichia coli* lipid A 4'-kinase. Facile phosphorylation of endotoxin analogs with recombinant LpxK. *J Biol Chem* 272: 21855-21864.

Gasteiger E, Hoogland C, Gattiker A, Duvaud S, Wilkins MR, Appel RD, Bairoch A (2005) Protein identification and analysis tools on the ExPASy server, p 571-607. *In* Walker JM (ed), The proteomics protocols handbook. Humana Press, New York, USA. ISBN: 978-1-58829-343-5.

Gerding MA, Ogata Y, Pecora ND, Niki H, de Boer PAJ (2007) The *trans*-envelope Tol-Pal complex is part of the cell division machinery and required for proper outer-membrane invagination during cell constriction in *E. coli*. *Mol Microbiol* 63: 1008-1025.

Giovannoni SJ, Godchaux III W, Schabtack E, Castenholz RW (1987) Cell wall and lipid composition of *Isosphaera pallida*, a budding eubacterium from hot springs. *J Bacteriol* 169: 2702-2707.

Glöckner FO, Kube M, Bauer M, Teeling H, Lombardot T, Ludwig W, Gade D, Beck A, Borzym K, Heitmann K, Rabus R, Schlesner H, Amann R, Reinhardt R (2003) Complete genome sequence of the marine planctomycete *Pirellula* sp. strain 1. *Proc Natl Acad Sci USA* 100: 8298-8303.

Gohlke M, Blanchard V (2008) Separation of N-glycans by HPLC. *Methods Mol Biol* 446: 239-254.

Gordon E, Flouret B, Chantalat L, van Heijenoort J, Mengin-Lecreulx D, Dideberg O (2000) Crystal structure of UDP-*N*-acetylmuramoyl-L-alanyl-D-glutamate:*meso*-Diaminopimelate ligase from *Escherichia coli*. *J Biol Chem* 276: 10999-11006.

Gottshal EY, Seebart C, Gatlin JC, Ward NL (2014) Spatially segregated trasncription and translation in cells of the endomembrane-containing bacterium *Gemmata obscuriglobus*. *Proc Nat Acad Sci USA* 111: 11067-11072.

Gram HCJ (1884) Ueber die isoliertie Faerbung der Schizomyceten in Schnitt- und Trockenpraeparaten. *Fortschr Medicin* 2: 185-189.

Greenfield LK, Whitfield C (2012) Synthesis of lipopolysaccharide O-antigens by ABC transporter-dependent pathways. *Carbohydr Res* 356: 12-24.

Grogono-Thomas R, Dworkin J, Blaser MJ, Newell DG (2000) Roles of the surface layer proteins of *Campylobacter fetus* subsp. *fetus* in ovine abortion. *Infect Immun* 68: 1687-1691.

Gronow S, Brade H (2001) Lipopolysaccharide biosynthesis: which steps do bacteria need to survive. *J Endotoxin Res* 7: 3-23.

Guckenberger R (1985) Surface reliefs derived from heavy-metal-shadowed specimens- Fourier space techniques applied to periodic objects. *Ultramicroscopy* 16: 357-370.

Gulin S, Pupo E, Schweda EKH, Hardy E (2003) Linking mass spectrometry and slab-polyacrylamide gel electrophoresis by passive elution of lipopolysaccharides from reverse-stained gels: analysis of gel-purified lipopolysaccharides from *Haemophilus influenza* strain Rd. *Anal Chem* 75: 4918-4924.

Guo M, Zhou Q, Zhou Y, Yang L, Liu T, Yang J, Chen Y, Su L, Xu J, Chen J, Liu F, Chen J, Dai W, Ni P, Fang C, Yang R (2014) Genomic evolution of 11 type strains within family Planctomycetaceae. *PLoS One* doi: 10.1371/journal.pone.0086752.

Güven D, Dapena A, Kartal B, Schmid MC, Maas B, van de Pas-Schoonen K, Sozen S, Mendez R, Op den Camp HJM, Jetten MSM, Strous M, Schmidt I (2005) Propionate oxidation by and methanol inhibition of anaerobic ammonium-oxidizing bacteria. *Appl Environ Microbiol* 71: 1066-1071.

Haft DH, Payne SH, Selengut JD (2012) Archaeosortase and exosortases are widely distributed systems linking membrane transit with posttranslation modifications. *J Bacteriol* 194: 36-48.

Halim MFA, Pfeiffer F, Zou J, Frisch A, Haft D, Wu S, Tolić N, Brewer H, Payne SH, Paša-Tolić L, Pohlschroder M (2013) *Haloferax volcanii* archaeosortase required for motility, mating, and C-terminal processing of the S-layer glycoprotein. *Mol Microbiol* 88: 1164-1175.

Han T-J, Chai T-J (1991) Occurrence of 2-keto-s-deoxy-D-manno-octonic acid in lipopolysaccharides isolated from *Vibrio parahaemolyticus*. *J Bacteriol* 173: 6303-6306.

Han M-J, Kim JY, Kim JA (2014) Comparison of the large-scale periplasmic proteomes of the *Escherichia coli* K-12 and B strains. *J Biosci Bioeng* 117: 437-442.

Hartmann E, König H (1990) Comparison of the biosynthesis of the methanobacterial pseudomurein and the eubacterial murein. *Naturwissenschaften* 77: 472-475.

He W, Qu T, Yu Q, Wang Z, Lv H, Zhang J, Zhao X, Wang P (2013) LPS induced IL-8 expression through TLR4, MyD88, NF-kappaB and MAPK pathways in human dental pulp stem cells. *Int Endod J* 46: 128-136.

Heinrichs DE, Yethon JA, Whitfield C (1998) Molecular basis for structural diversity in the core regions of the lipopolysaccharides of *Escherichia coli* and *Salmonella enterica*. *Mol Microbiol* 30: 221-232.

Hildebrand A, Remmert M, Biegert A, Söding J (2009) Fast and accurate automatic structure prediction with HHpred. *Proteins* 77: 128-132.

Hira D, Toh H, Migita CT, Okubo H, Nishiyama T, Hattori M, Furukawa K, Fujii T (2012) Anammox organism KSU-1 expresses a NirK-type copper-containing nitrite reductase instead of a NirS-type with cytochrome cd_1. *FEBS Lett* 586: 1658-1663.

Hitchcock PJ, Brown TJ (1983) Morphological heterogeneity among *Salmonella* lipopolysaccharide chemotypes in silver-stained polyacrylamide gels. *J Bacteriol* 154: 269-277.

Hitchen PG, Dell A (2006) Bacterial glycoproteomics. *Microbiology* 152: 1575-1580.

Holland IB, Schmitt L, Young J (2005) Type 1 protein secretion in bacteria, the ABC-transporter dependent pathway (review). *Mol Memb Biol* 22: 29-39.

Holst O (2007) The structures of core regions from enterobacterial lipopolysaccharides - an update. *FEMS Microbiol Lett* 271: 3-11.

Hu Z, van Alen T, Jetten MSM, Kartal B (2013) Lysozyme and penicillin inhibit the growth of anaerobic ammonium-oxidizing Planctomycetes. *Appl Environ Microbiol* 79: 7763-7769.

Hu Z (2014) New insights into the physiology and application of the anammox bacteria. *PhD thesis*, Radboud Universiteit. Chapter 4, p 55-68. ISBN: 978-94-6259-391-6.

Humbert S, Tarnawski S, Fromin N, Mallet M-P, Aragno M, Zopfi J (2010) Molecular detection of anammox bacteria in terrestrial ecosystems: distribution and diversity. *ISME J* 4: 450-454.

Ilk N, Kosma P, Puchberger M, Egelseer EM, Mayer HF, Sleytr UB, Sára M (1999) Structural and functional analyses of the secondary wall polymer of *Bacillus sphaericus* CCM 2177 that serves as an S-layer-specific anchor. *J Bacteriol* 181: 7648-7646.

Imperi F, Ciccosanti F, Perdomo AB, Tiburzi F, Mancone C, Alonzi T, Ascenzi P, Piacentini M, Visca P, Fimia GM (2009) Analysis of the periplasmic proteome of *Pseudomonas aeruginosa*, a metabolically versatile opportunistic pathogen. *Proteomics* 9: 1901-1915.

Izumi H, Sagulenko E, Webb RI, Fuerst JA (2013) Isolation and diversity of planctomycetes from the sponge *Niphates* sp., seawater, and sediment of Moreton Bay, Australia. *Antonie van Leeuwenhoek* 104: 533-546.

Jeske O, Schüler M, Schumann P, Schneider A, Boedeker C, Jogler M, Bollschweiler D, Rohde M, Mayer C, Engelhardt H, Spring S, Jogler C (2015) Planctomycetes do possess a peptidoglycan cell wall. *Nature Commun* 6: 7116.

Jetten MSM, Sliekers O, Kuypers M, Dalsgaard T, van Niftrik L, Cirpus I, van de Pas-Schoonen K, Lavik G, Thamdrup B, Le Paslier D, Op den Camp HJM, Hulth S, Nielsen LP, Abma W, Third K, Engström P, Kuenen JG, Jørgensen BB, Canfield DE, Sinninghe Damsté JS, Revsbech NP, Fuerst J, Weissenbach J, Wagner M, Schmidt I, Schmid M, Strous M (2003) Anaerobic ammonium oxidation by marine and freshwater planctomycete-like bacteria. *Appl Microbiol Biotechnol* 63: 107-114.

Jetten MSM, van Niftrik L, Strous M, Kartal B, Keltjens JT, Op den Camp HJM (2009) Biochemistry and molecular biology of anammox bacteria. *Crit Rev Biochem Mol Biol* 44: 65-84.

Jetten MSM, Op den Camp HJM, Kuenen JG, Strous M (2010) Family I. "*Candidatus* Brocadiaceae" fam.nov, p 596-602. *In* Krieg NR, Staley JT, Brown DR, Hedlund B, Paster BJ, Ward N, Ludwig W, Whitman WB (ed), Bergey's manual of systematic bacteriology, 2nd ed, vol 4. Springer, New York, USA. ISBN: 978-0-387-68572-4.

Jogler C, Glöckner FO, Kolter R (2011) Characterization of *Planctomyces limnophilus* and development of genetic tools for its manipulation establish it as a model species for the phylum *Planctomycetes*. *Appl Environ Microbiol* 77: 5826-5829.

Jogler C, Waldmann J, Huang X, Jogler M, Glöckner FO, Mascher T, Kolter R (2012) Identification of proteins likely to be involved in morphogenesis, cell division, and signal transduction in *Planctomycetes* by comparative genomics. *J Bacteriol* 197: 6419-6430.

Johnson LN, Phillips DC (1965) Structure of some crystalline lysozyme-inhibitor complexes determined by X-ray analysis at 6 Angstrom resolution. *Nature* 206**:** 761-763.

Jones DT (1999) Protein secondary structure prediction based on position-specific scoring matrices. *J Mol Biol* 292: 195-202.

Kamio Y, Nikaido H (1976) Outer membrane of *Salmonella typhimurium*: accessibility of phospholipid head groups to the phospholipase C and cyanogen bromide activated dextran in the external medium. *Biochemistry* 15: 2561-2570.

Kandler O, König H (1985) Cell envelopes of archaebacteria, p 413-457. *In* Woese CR, Wolfe RS (ed) The bacteria, vol. VIII. Archaebacteria. Academic Press, New York, USA. ISBN: 978-0323144742.

Kandler O, König H (1998) Cell wall polymers in Archaea (Archaebacteria). *Cell Mol Life Sci* 54: 305-308.

Kartal B, Rattray J, van Niftrik LA, van de Vossenberg J, Schmid MC, Webb RI, Schouten S, Fuerst JA, Sinninghe Damsté J, Jetten MSM, Strous M (2007) *Candidatus* "Anammoxoglobus propionicus" a new propionate oxidizing species of anaerobic ammonium oxidizing bacteria. *Syst Appl Microbiol* 30: 39-49.

Kartal B, van Niftrik L, Rattray J, van de Vossenburg JLCM, Schmid MC, Sinninghe Damsté J, Jetten MSM, Strous M (2008) *Candidatus* "Brocadia fulgida": an autofluorescent anaerobic ammonium oxidizing bacterium. *FEMS Microbiol Ecol* 63: 46-55.

Kartal B, Kuenen JG, van Loosdrecht MCM (2010) Sewage treatment with anammox. *Science* 328: 702-703.

Kartal B, Geerts W, Jetten MSM (2011a) Cultivation, detection, and ecophysiology of anaerobic ammonium-oxidizing bacteria, p 89-108. *In* Klotz MG (ed), Methods in enzymology, vol 486. Academic Press, San Diego, USA. ISBN: 978-0-12-381294-0.

Kartal B, Maalcke WJ, de Almeida NM, Cirpus I, Gloerich J, Geerts W, Op den Camp HJM, Harhangi H, Janssen-Megens EM, Francoijs K-J, Stunnenberg HG, Keltjens JT, Jetten MSM, Strous M (2011b) Molecular mechanism of anaerobic ammonium oxidation. *Nature* 479: 127-130.

Kartal B, de Almeida NM, Maalcke WJ, Op den Camp HJM, Jetten MSM, Keltjens, JT (2013) How to make a living from anaerobic ammonium oxidation. *FEMS Microbiol Rev* 37: 428-461.

Kawahara K, Seydel U, Matsuura M, Danbara H, Rietschel ET, Zähringer U (1991) Chemical structures of glycosphingolipids isolated from *Sphingomonas paucimobilis*. *FEBS Lett* 292: 107-110.

Kawahara K, Tsukano H, Watanabe H, Lidner B, Matsuura M (2002) Modification of the structure and activity of lipid A in *Yersinia pestis* lipopolysaccharide by growth temperature. *Infect Immun* 70: 4092-4098.

Kawasaki S, Moriguchi R, Sekiya K, Nakai T, Ono E, Kume K, Kawahara K (1994) The cell envelope structure of the lipopolysaccharide-lacking Gram-negative bacterium *Sphingomonas paucimobilis*. *J Bacteriol* 176: 284-290.

Kefala G, Ahn C, Krupa M, Esquivies L, Maslennikov I, Kwiatkowski W, Choe S (2010) Structures of the OmpF porin crystallized in the presence of fosfocholine-12. *Protein Sci* 19: 1117-1125.

Kelley LA, Mezulis S, Yates CM, Wass MN, Sternberg MJE (2015) The phyre2 web portal for protein modelling, prediction and analysis. *Nat Protoc* 10: 845-858.

Kellogg TA, Lazaron V, Wasiluk KR, Dunn DL (2001) Binding specificity of polymyxin B, BPI, LALF, and anti-deep core/lipid A monoclonal antibody to lipopolysaccharide partial structures. *Shock* 15: 124-129.

Kelly TM, Stachula SA, Raetz CRH, Anderson MS (1993) The *firA* gene of *Escherichia coli* encodes UDP-3-*O*-(*R*-3-hydroxymyristoyl)-glucosamine *N*-acyltransferase. The third step of endotoxin biosynthesis. *J Biol Chem* 268: 19866-19874.

Kelly G, Prasannan S, Daniell S, Fleming K, Frankel G, Dougan G, Connerton I, Matthews I (1999) Structure of the cell-adhesion fragment of intimin from enteropathogenic *Escherichia coli*. *Nat Struct Biol* 6: 313-318.

Kerger BD, Mancuso CA, Nichols PD, White DC, Langworthy T, Sittig M, Schlesner H, Hirsch P (1988) The budding bacteria, *Pirellula* and *Planctomyces*, with atypical 16S rRNA and absence of peptidoglycan, show eubacterial phospholipids and uniquely high proportions of long chain beta-hydroxy fatty acids in the lipopolysaccharide lipid A. *Arch Microbiol* 149: 255-260.

Killmann H, Benz R, Braun V (1996) Properties of the FhuA channel in the *Escherichia coli* outer membrane after deletion of FhuA portions within and outside the predicted gating loop. *J Bacteriol* 178: 6913-6920.

Kirkpatrick J, Oakley B, Fuchsman C, Srinivasan S, Staley JT, Murray JW (2006) Diversity and distribution of *Planctomycetes* and related bacteria in the suboxic zone of the black sea. *Appl Environ Microbiol* 72: 3079-3083.

Klingl A, Moissl-Eichinger C, Wanner G, Zweck J, Huber H, Thomm M, Rachel R (2011) Analysis of the surface proteins of *Acidithiobacillus ferrooxidans* strain SP5/1 and the new, pyrite-oxidizing *Acidithiobacillus* isolate HV2/2, and their possible involvement in pyrite oxidation. *Arch Microbiol* 193: 867- 882.

Klingl A, Flechsler J, Heimerl T, Rachel R (2013) Archaeal Cells. *eLS* DOI: 10.1002/9780470015902.a0000383.pub2

Köhler T, Stingl U, Meuser K, Brune A (2008) Novel lineages of *Planctomycetes*densily colonize the alkaline gut of soil-feeding termites (*Cubitermes*spp.). *Environ Microbiol* 10: 1260-1270.

König E, Schlesner H, Hirsch P (1984) Cell wall studies on budding bacteria of the *Planctomycetes-Pasteuria* group and on a *Prosthecomicrobium* sp. *Arch Microbiol* 138: 200-205.

Kostakioti M, Newman CL, Thanassi DG, Stathopoulos C (2005) Mechanisms of protein export across the bacterial outer membrane. *J Bacteriol* 187: 4306-4314.

Koval SF, Hynes SH (1991) Effect of paracrystalline protein surface layers on predation by *Bdellovibrio bacteriovorus*. *J Bacteriol* 173: 2244-2249.

Kovaleva OL, Merkel A, Novikov A, Baslerov R, Toschchakov S, Bonch-Osmolovskaya EA (2015) *Tepidisphaera mucosa* gen. nov., sp. nov., a new moderately thermophilic member of *Phycisphaerae* class in the *Planctomycetes*, and proposal of a new order *Tepidisphaerales*. *Int J Syst Evol Microbiol* 65: 549-555.

Kowarik M, Young NM, Numao S, Schulz BL, Hug I, Callewaert N, Mills DC, Watson DC, Hernandez M, Kelly JF, Wacker M, Aebi M (2006) Definition of the bacterial *N*-glycosylation site consensus sequence. *EMBO J* 25: 1957-1966.

Krogh A, Larsson B, von Heijne G, Sonnhammer ELL (2001) Predicting transmembrane protein topology with a hidden Markov model: Application to complete genomes. *J Mol Biol* 305: 567-580.

Krupovič M, Daugelavičius R, Bamford DH (2007) Polymyxin B induces lysis of marine pseudoalteromonads. *Antimicrob Agents Chemother* 51: 3908-3914.

Kulichevskaya IS, Baulina OI, Bodelier PLE, Rijpstra WIC, Sinninghe Damsté JS, Dedysh SN (2009) *Zavarzinella formosa* gen. nov., sp. nov., a novel stalked, *Gemmata*-like planctomycete from a Siberian peat bog. *Int J Syst Evol Microbiol* 59: 357-364.

Kuru E, Hughes HV, Brown PJ, Hall E, Tekkam S, Cava F, de Pedro MA, Brun YV, VanNieuwenhze MS (2012) *In situ* probing of newly synthesized peptidoglycan in live bacteria with fluorescent D-amino acids. *Angew Chem Int Ed Engl* 51**:** 12519-12523.

Kuypers MMM, Sliekers AO, Lavik G, Schmid M, Jørgensen BB, Kuenen JG, Sinninghe Damsté JS, Strous M, Jetten MSM (2003) Anaerobic ammonium oxidation by anammox bacteria in the Black Sea. *Nature* 422: 608-611.

Laemmli UK (1970) Cleavage of structural proteins during the assembly of the head of bacteriophage T4. *Nature* 15: 680-685.

Lage OM (2013) Characterization of a planctomycete associated with the marine dinoflagellate *Prorocentrum micans* Her. *Antonie van Leeuwenhoek* 104: 499-508.

Lage OM, Bondoso J (2011) *Planctomycetes* diversity associated with macroalgae. *FEMS Microbiol Ecol* 78: 366-375.

Lage OM, Bondoso J (2012) Bringing *Planctomycetes* into pure culture. *Front Microbiol* 3:405.

Lam H, Oh D-C, Cava F, Takacs CN, Clardy J, de Pedro MA, Waldor MK (2009) D-amino acids govern stationary phase cell wall remodeling in bacteria. *Science* 325: 1552-1555.

Lam P, Kuypers MMM (2011) Microbial nitrogen cycling processes in oxygen minimum zones. *Annu Rev Mar Sci* 3: 317/345.

Lazarevic V, Pooley HM, Mauël C, Karamata D (2005) Teichoic and teichuronic acids from Gram-positive bacteria. *Biopolymers Online* 5.

Lechner J, Wieland F (1989) Structure and biosynthesis of prokaryotic glycoproteins. *Annu Rev Biochem* 58: 173-194.

Lee K-C, Webb RI, Fuerst JA (2009) The cell cycle of the planctomycete *Gemmata obscuriglobus* with respect to cell compartmentalization. *BMC Cell Biol* 10: 4.

Leid JG, Willson CJ, Shirtliff ME, Hassett DJ, Parsek MR, Jeffers AK (2005) The exopolysaccharide alginate protects *Pseudomonas aeruginosa* biofilm bacteria from IFN-γ-mediated macrophage killing. *J Immunol* 175: 7512-7518.

Lieber A, Leis A, Kushmaro A, Minsky A, Medalia O (2009) Chromatin organization and radio resistance In the bacterium *Gemmata obscuriglobus*. *J Bacteriol* 191: 1439-1445.

Liechti G, Kuru E, Hall E, Kalinda A, Brun YV, VanNieuwenhze MS, Maurelli AT (2014) A new metabolic cell wall labeling method reveals peptidoglycan in *Chlamydia trachomatis*. *Nature* 506: 507-510.

Liesack W, König H, Schlesner H, Hirsch P (1986) Chemical composition of the peptidoglycan-free cell envelopes of budding bacteria of the *Pirella/Planctomyces* group. *Arch Microbiol* 145: 361-366.

Lindsay GK, Roslansky PF, Novitsky TJ (1989) Single step, chromogenic Limulus amebocyte lysate assay for endotoxin. *J Clin Microbiol* 27: 947-951.

Lindsay MR, Webb RI, Fuerst JA (1997) Pirellulosomes: a new type of membrane-bounded cell compartment in planctomycete bacteria of the genus *Pirellula*. *Microbiology* 143: 739-748.

Lindsay MR, Webb RI, Strous M, Jetten MSM, Butler MK, Forde RJ, Fuerst JA (2001) Cell compartmentalization in planctomycetes: novel types of structural organization for the bacterial cell. *Arch Microbiol* 175: 413-429.

Lombard V, Golaconda Ramula H, Drula E, Coutinho PM, Henrissat B (2014) The carbohydrate-active enzymes database (CAZy) in 2013. *Nucleic Acids Res* doi:10.1093/nar/gkt1178.

Lonhienne TGA, Sagulenko E, Webb RI, Lee K-C, Franke J, Devos DP, Nouwens A, Caroll BJ, Fuerst JA (2010) Endocytosis-like protein uptake in the bacterium *Gemmata obscuriglobus*. *Proc Natl Acad Sci USA* 107: 12883-12888.

Lotti T, Kleerebezem R, Abelleira-Pereira JM, Abbas B, van Loosdrecht MCM (2015) Faster through training: The anammox case. *Water Res* 81: 261-268.

Lovering AL, Safadi SS, Strynadka NCJ (2012) Structural perspective of peptidoglycan biosynthesis and assembly. *Annu Rev Biochem* 81: 451-478.

Lu C, Stricker J, Erickson HP (1998) FtsZ from *Escherichia coli*, *Azetobacter vinelandii*, and *Thermotoga maritima* – quantification, GTP hydrolysis, and assembly. *Cell Motil Cytoskeleton* 40: 71-86.

Lu C, Reedy M, Erickson HP (2000) Straight and curved conformations of FtsZ are regulated by GTP hydrolysis. *J Bacteriol* 182: 164-170.

Luchi M, Morrison DC (2000) Comparable endotoxic properties of lipopolysaccharides are manifest in diverse clinical isolates of Gram-negative bacteria. *Infect Immun* 68: 1899-1904.

Lupas A, Engelhardt H, Peters J, Santarius U, Volker S, Baumeister W (1994) Domain structure of the *Acetogenium kivui* surface layer revealed by electron crystallography and sequence analysis. *J Bacteriol* 176: 1224-1233.

Mainardi J-L, Villet R, Bugg TD, Mayer C, Arthur M (2008) Evolution of peptidoglycan biosynthesis under the selective pressure of antibiotics in Gram-positive bacteria. *FEMS Microbiol. Rev.* 32: 368-408.

Martin NI, Hu H, Moake MM, Churey JJ, Whittal R, Worobo RW, Vederas JC (2003) Isolation, structural characterization and properties of mattacin (polymyxin M), a cyclic peptide antibiotic produced by *Paenibacillus kobensis* M. *J Biol Chem* 278: 13124-13132.

Mayr J, Lupas A, Kellermann J, Eckerskorn C, Baumeister W, Peters J (1996) A hyperthermostable protease of the subtilisin family bound to the surface layer of the Archaeon *Staphylothermus marinus*. *Curr Biol* 6: 739-749.

McCoy AJ, Maurelli AT (2006) Building the invisible wall: updating the chlamydial peptidoglycan anomaly. *Trends Microbiol* 14: 70-77.

McDonald IJ, Adams GA (1971) Influence of cultural conditions on the lipopolysaccharide composition of *Neisseria sicca*. 65: 201-207.

McGinnis S, Madden TL (2004) BLAST: at the core of a powerful and diverse set of sequence analysis tools. *Nucleic Acids Res* 32: W20-W25.

Medema MH, Zhou M, van Hijum SAFT, Gloerich J, Wessels HJCT, Siezen RJ, Strous M (2010) A predicted physicochemically distinct sub-proteome associated with the intracellular organelle of the anammox bacterium *Kuenenia stuttgartiensis*. *BMC Genomics* 11:299.

Mempin R, Tran H, Chen C, Gong H, Kim Ho K, Lu S (2013) Release of extracellular ATP by bacteria during growth. *BMC Microbiol* 13: 301.

Meng G, Fronzes R, Chandran V, Remaut H, Waksman (2009) Protein oligomerization in the bacterial outer membrane (Review). *Mol Membr Biol* 26: 136-145.

Mesnage S, Fontaine T, Mignot T, Delepierre M, Mock M, Fouet A (2000) Bacterial SLH domain proteins are non-covalently anchored to the cell surface via a conserved mechanism involving wall polysaccharide pyruvylation. *EMBO J* 19: 4473-4484.

Messner P, Sleytr UB (1991) Bacterial surface layer glycoproteins. *Glycobiology* 1: 545-551.

Messner P, Sleytr UB (1992) Crystalline bacterial cell-surface layers. *Adv Microb Physiol* 33: 213-275.

Messner P, Schäffer C (2000) Surface layer glycoproteins of Bacteria and Archaea, p. 93-125. *In* R. J. Doyle RJ (ed), Glycomicrobiology. Kluwer Academic/PlenumPublishers, New York, USA. ISBN: 978-0306462399.

Messner P, Schäffer C (2003) Prokaryotic glycoproteins, p. 51-124. *In* Herz W, Falk H, Kirby GW (ed), Progress in the chemistry of organic natural products, vol. 85. Springer, Wien, Austria. ISBN: 3-211-83783-3.

Messner P, Steiner K, Zarschler K, Schäffer C (2008) S-layer nanoglycobiology of bacteria. *Carbohydr Res* 343: 1934-1951

Messner P, Egelseer EM, Sleytr UB, Schäffer C (2009) Surface layer glycoproteins and "non-classical" secondary cell wall polymers, p 109-128. *In* Moran AP, Brennan PJ, Holst O, von Itzstein M (ed) Microbial glycobiology: structures, relevance and applicat ions. Academic Press-Elsevier, San Diego, USA. ISBN: 978-0-12-374546-0.

Messner P, Schäffer C, Egelseer E-M, Sleytr UB (2010) Occurrence, structure, chemistry, genetics, morphogenesis, and functions of S-layers, p. 53-109. *In* König H, Claus H, Varma A (ed) Prokaryotic cell wall compounds – structure and biochemistry. Springer, Berlin, Germany. ISBN: 978-3-642-05062-6.

Messner P, Schäffer C, Kosma P (2013) Bacterial cell-envelope glycoconjugates. *Adv Carbohydr Chem Biochem* 69: 209-272.

Moore TA, Xing Y, Lazenby B, Lynch MDJ, Schiff S, Robertson WD, Timlin R, Lanza S, Ryan MC, Aravena R, Fortin D, Clark ID, Neufeld JD (2011) Prevalence of anaerobic ammonium-oxidizing bacteria in contaminated groundwater. *Environ Sci Technol Lett* 45: 7217-7225.

Moore EK, Hopmans EC, Rijpstra WIC, Villanueva L, Dedysh SN, Kulichevskaya IS, Wienk H, Schoutsen F, Sinninghe Damsté JS (2013) Novel Mono-, Di-, and Trimethylornithine membrane lipids in northern wetland Planctomycetes. *Appl Environ Microbiol* 79: 6874-6884.

Mukherjee A, Lutkenhaus J (1998) Dynamic assembly of FtsZ regulated by GTP hydrolysis. *EMBO J* 17: 462-469.

Mulloy B, Hart GW, Stanley P (2009) Chapter 47. Structural analysis of glycans. *In* Varki E, Cummings RD, Esko JD, Freeze HH, Stanley P, Bertozzi CR, Hart GW, Etzler ME (Eds.), Essentials of glycobiology, 2nd edition, Cold Spring Harbor Laboratory Press, Cold Spring Harbor, USA. ISBN: 9780879697709.

Needham BN, Trent MS (2013) Fortifying the barrier: the impact of lipid A remodelling on bacterial pathogenesis. *Nat Rev Microbiol* 11: 467-481.

Neef A, Amann RI, Schlesner H Schleifer K-H (1998) Monitoring a widespread bacterial group: in situ detection of planctomycetes with 16S rRNA-targeted probes. *Microbiology* 144: 3257-3266.

Netea MG, van Deuren M, Kullberg BJ, Cavaillon J-M, van der Meer JWM (2002) Does the shape of lipid A determine the interaction of LPS with Toll-like receptors. *Trends Microbiol* 23: 135-139.

Neumann S, van Teeseling MCF, van Niftrik L (2013) Cell biology of anaerobic ammonium-oxidizing bacteria: unique prokaryotes with an energy-conserving intracellular compartment, pp 89-123. *In* Fuerst JA (ed), Planctomycetes: cell structure, origins and biology, Humana Press/Springer, New York, USA. ISBN: 978-1-62703-502-6.

Neumann S, Wessels HJCT, Rijpstra WIC, Sinninghe Damsté JS, Kartal B, Jetten MSM, van Niftrik L (2014) Isolation and characterization of a prokaryotic cell organelle from the anammox bacterium *Kuenenia stuttgartiensis*. 94: 794-802.

Nguyen-Mau S-M, Oh S-Y, Kern VJ, Missiakas DM, Schneewind O (2012) Secretion genes as determinants of *Bacillus anthracis* chain length. *J Bacteriol* 194: 3841-3850.

Nielsen ML, Vermeulen M, Bonaldi T, Cox J, Moroder L, Man M (2008) Iodoacetamide-induced artifact mimics ubiquitination in mass spectrometry. *Nat Methods* 5: 459-460.

Nikaido H (1976) Outer membrane of *Salmonella typhimurium* transmembrane diffusion of some hydrophobic substances. *Biochim Biophys Act* 433: 118-132.

Nikaido H (2003) Molecular basis of bacterial outer membrane permeability revisited. *Microbiol Mol Biol Rev* 67: 593-656.

Noinaj N, Kuszak AJ, Gumbart JC, Lukacik P, Chang H, Easley NC, Lithgow T, Buchanan SK (2013) Structural insight into the biogenesis of β-barrel membrane proteins. *Nature* 501: 385-390.

Olaitan AO, Morand S, Rolain J-M (2014) Mechanisms of polymyxin resistance: acquired and intrinsic resistance in bacteria. *Front Microbiol* 5: 643.

Opal SM (2007) The host response to endotoxin, antilipopolysaccharide strategies, and the management of severe sepsis. *Int J Med Microbiol* 297: 365-377.

Osawa M, Anderson DE, Erickson HP (2008) Reconstitution of contractile FtsZ rings in liposomes. *Science* 320: 792-794.

Oshiki M, Shinyako-Hata K, Satoh H, Okabe S (2015) Draft genome sequence of an anaerobic ammonium-oxidizing bacterium, "*Candidatus* Brocadia sinica". *Genome Announc* 3: e00267-15.

Parker JH, Smith GA, Fredrickson HL, Vestal JR, White DC (1982) Sensitive assay, based on hydroxyl fatty acids from lipopolysavvharide lipid A, for Gram-Negative bacteria in sediments. *Appl Environ Microbiol* 44: 1170-1177.

Pantophlet R, Brade L, Brade H (1997) Detection of lipid A by monoclonal antibodies in S-form lipopolysaccharide after acidic treatment of immobilized LPS on Western blot. *J Endotoxin Res* 4: 89-95.

Petersen TN, Brunak S, von Heijne G, Nielsen H (2011) SignalP 4.0: discriminating signal peptides from transmembrane regions. *Nat Methods* 8: 785-786.

Pettersen EF, Goddard TD, Huang CC, Couch GS, Greenblatt DM, Meng EC, Ferrin TE (2004) UCSF Chimera—a visualization system for exploratory research and analysis. *J Comput Chem* 25: 1605-1612.

Pilhofer M, Aistleitner K, Biboy J, Gray J, Kuru E, Hall E, Brun YV, VanNieuwenhze MS, Vollmer W, Horn M, Jensen GJ (2013) Discovery of chlamydial peptidoglycan reveals bacteria with murein sacculi but without FtsZ. *Nat Commun* 4: 2856.

Polissi A, Georgopoulos C (1996) Mutational analysis and properties of the *msbA* gene of *Escherichia coli*, coding for an essential ABC family transporter. *Mol Microbiol* 20: 1221-1233.

Pollet T, Tadonléké RD, Humbert J-F (2010) Comparison of primer stes for the study of *Planctomycetes* communities in lentic freshwater ecosystems. *Environ Microbiol Rep* 3: 254-261.

Popescu A, Doyle RJ (1996) The Gram stain after more than a century. *Biotech Histochem* 71: 1415-1451.

Posch G, Andrukhov O, Vinogradov E, Lindner B, Messner P, Holst O, Schäffer C (2013) Structure and immunogenicity of the rough-type lipopolysaccharide from the periodontal pathogen *Tannerella forsythia*. *Clin Vaccine Immunol* 20: 945-953.

Pum D, Messner P, Sleytr UB (1991) Role of the S layer in morphogenesis and cell division of the archaebacterium *Methanocorpusculum sinense*. *J Bacteriol* 173: 6865-6873.

Pum D, Sára M, Sleytr UB (1989) Structure, surface charge, and self-assembly of the S-layer lattice from *Bacillus coagulans* E38-66. *J Bacteriol* 171: 5296-5303.

Qiu R, Regnier FE (2005) Use of multidimensional lectin affinity chromatography in differential glycoproteomics. *Anal Chem* 77: 2802-2809.

Quan Z-X, Rhee S-K, Zuo J-E, Yang Y, Bae J-W, Park JR, Lee S-T, Park Y-H (2008) Diversity of ammonium-oxidizing bacteria in a granular sludge anaerobic ammonium-oxidizing (anammox) reactor. *Environ Microbiol* 10: 3130–3139.

Rachel R, Meyer C, Klingl A, Gürster S, Heimerl T, Wasserburger N, Burghardt T, Küper U, Bellack A, Schopf S, Wirth R, Huber H, Wanner G (2010) Analysis of the Ultrastructure of Archaea by Electron Microscopy, p 47-69. *In* Müller-Reichert T (ed), Methods in Cell Biology vol 96. Elsevier, Philadelphia, USA. ISBN: 978-0-12-381007-6.

Raetz CRH, Whitfield C (2002) Lipopolysaccharide endotoxins. *Annu Rev Biochem* 71: 635-700.

Raetz CRH, Guan Z, Ingram BO, Six DA, Song F, Wang X, Zhao J (2009) Discovery of new biosynthetic pathways: the lipid A story. *J Lipid Res* 50: S103-S108.

Rattray JE, van de Vossenberg J, Hopmans EC, Kartal B, van Niftrik L, Rijpstra WIC, Strous M, Jetten MSM, Schouten S, Sinninghe Damsté JS (2008) Ladderane lipid distribution in four genera of anammox bacteria. *Arch Microbiol* 190: 51-66.

Rattray JE, van de Vossenberg J, Jaeschke A, Hopmans EC, Wakeham SG, Lavik G, Kuypers MMM, Strous M, Jetten MSM, Schouten S, Sinninghe Damsté JS (2010) Impact of temperature on ladderane lipid distribution in anammox bacteria. *Appl Environ Microbiol* 76: 1596-1603.

Ray BL, Raetz CRH (1987) The biosynthesis of Gram-negative endotoxin. *J Biol Chem* 262: 1122-1128.

Remmert M, Biegert A, Hauser A, Söding J (2012) HHblits: lightning-fast iterative protein sequence searching by HMM-HMM alignment. *Nat Methods* 9: 173-175.

Rezania S, Amirmozaffari N, Tabarraei B, Jeddi-Tehrani M, Zarei O, Alizadeh R, Masjedian F, Zarnani AH (2011) Extraction, purification and characterization of lipopolysaccharide from *Escherichia coli* and *Salmonella typhi*. *Avicenna J Med Biotechnol* 3: 3-9.

Ribeiro JP, Mahal LK (2013) Dot by dot: analyzing the glycome using lectin microarrays. *Curr Opin Chem Biol* 17: 827-831.

Richter W, Heinbockel L, Kaconis Y, Steiniger F, Gutsmann T, Bade L, Brandenburg K (2013) Cellular distribution of lipid A and LPS R595 after *in vitro* application to isolated human monocytes by freeze-fracture replica immunogold-labeling. *Innate Immun* 19: 588-595.

Rico AI, Krupka M, Vicente M (2013) In the beginning, *Escherichia coli* assembled the proto-ring: an initial phase of division. *J Biol Chem* 288: 20830-20836.

Ristl R, Steiner K, Zarschler K, Zayni S, Messner P, Schäffer C (2010) The S-layer glycome- adding to the sugar coat of bacteria. *Int J Microbiol* 2011: Article ID 127870.

Rund S, Lindner B, Brade H, Holst O (1999) Structural analysis of the lipopolysaccharide from *Chlamydia trachomatis* serotype L2. *J Biol Chem* 274: 16819-16824.

Rush D, Hopmans EC, Wakeham SG, Schouten S, Sinninghe Damsté JS (2012) Occurrence and distribution of ladderane oxidation products in different oceanic regimes. *Biogeosciences* 9: 2407-2418.

Rush D, Sinninghe Damsté JS, Poulton SW, Thamdrup B, Garside AL, González JA, Schouten S, Jetten MSM, Talbot HM (2014) Anaerobic ammonium-oxidising bacteria: A biological source of the bacteriohopanetetrol stereoisomer in marine sediments. *Geochim Cosmochim Ac* 140: 50-64.

Russ L (2015) Microbial nitrogen cycle interactions in laboratory-scale model systems. *PhD thesis*, Radboud Universiteit. Chapter 2, p 55-78. ISBN: 978-94-6259-642-9.

Saddler JN, Wardlaw AC (1980) Extraction, distribution and biodegradation of bacterial lipopolysaccharides in estuarine sediments. *Antonie van Leeuwenhoek* 46: 27-39.

Sagulenko E, Morgan GP, Webb RI, Yee B, Lee K-C, Fuerst JA (2014) Structural studies of planctomycete *Gemmata obscuriglobus* support cell compartmentalisation in a bacterium. *PLoS One* 9: e91344.

Sakakibara J, Nagano K, Murakami Y, Higuchi N, Nakamura H, Shimozato K, Yoshimura F (2007) Loss of adherence ability to human gingival epithelial cells in S-layer protein-deficient mutants of *Tannerella forsythensis*. *Microbiology* 153: 866-876.

Santarella-Mellwig R, Franke J, Jaedicke A, Gorjanacz M, Bauer U, Budd A, Mattaj IW, Devos DP (2010) The compartmentalized bacteria of the Planctomycetes-Verrucomicrobia-Chlamydiae superphylum have membrane coat-like proteins. *PLoS Biol* 8:e1000281.

Santarella-Mellwig R, Pruggnaller S, Roos N, Mattaj IW, Devos DP (2013) Three-dimensional reconstruction of bacteria with a complex endomembrane system. *PLoS Biol* 11:e1001565.

Sára M (2001) Conserved anchoring mechanisms between crystalline cell surface S-layer proteins and secondary cell wall polymers in Gram-positive bacteria. *Trends Microbiol* 9: 47-49.

Sára M, Sleytr UB (2000) S-layer proteins. *J Bacteriol* 182: 859-868.

Sargent F, Berks BC, Palmer T (2006) Pathfinders and trailblazers: a prokaryotic targeting system for transport of folded proteins. *FEMS Microbiol Lett* 254: 198-207.

Saxton WO (1996) Semper: Distortion compensation, selective averaging, 3-D reconstruction, and transfer function correction in a highly programmable system. *J Struct Biol* 116: 230-236.

Schäffer C, Graninger M, Messner P (2001) Prokaryotic glycosylation. *Proteomics* 1: 248-261.

Schäffer C, Wugeditsch T, Kählig H, Scheberl A, Zayni S, Messner P (2002) The surface layer (S-layer) glycoprotein of *Geobacillus stearothermophilus* NRS 2004/3a. Analysis of its glycosylation. *J Biol Chem* 277: 6230-6239.

Schäffer C, Messner P (2005) The structure of secondary cell wall polymers: how Gram-positive bacteria stick their cell walls together. *Microbiology* 151: 643-651.

Schelling M, Conti S (1986) Host receptor sites involved in the attachment of *Bdellovibrio bacteriovorus* and *Bdellovibrio stolpii*. *FEMS Microbiol Lett* 36: 319-323.

Scheuner C, Tindall BJ, Lu M, Nolan M, Lapidus A, Chong J-F, Goodwin L, Pitluck S, Huntemann M, Liolios K, Pagani I, Mavromatis K, Ivanova N, Pati A, Chen A, Palaniappan K, Jeffries CD, Hauser L, Land M, Mwirichia R, Rohde M, Abt B, Detter JC, Woyke T, Eisen JA, Markowitz V, Hugenholtz P, Göker M, Kyrpides NC, Klenk H-P (2014) Complete genome sequence of *Planctomyces brasiliensis* type strain (DSM 5305^T), phylogenomic analysis and reclassification of *Planctomycetes* including the descriptions of *Gimesia* gen.nov., *Planctopirus* gen.nov. and *Rubinisphaera* gen. nov. and emended descriptions of the order *Planctomycetales* and the family *Planctomycetaceae*. *Stand Genomic Sci* 9: 10.

Schlesner H (1994) The development of media suitable for the microorganisms morphologically resembling Planctomycetes spp., Pirellula spp., and other Planctomycetales from various aquatic habitats using dilute media. *Syst Appl Microbiol* 17: 135-145.

Schlesner H, Rensmann C, Tindall BJ, Gade D, Rabus R, Pfeiffer S, Hirsch P (2004) Taxonomic heterogeneity within the *Planctomycetales* as derived by DNA-DNA hybridization, description of *Rhodopirellula baltica* gen. nov., sp. nov., transfer of *Pirellula marina* to the genus *Blastopirellula* gen.nov. as *Blastopirellula marina* comb. nov. and emended description of the genus *Pirellula*. *Int J Syst Evol Microbiol* 54: 1567-1580.

Schmid K, Ebner R, Jahreis K, Lengeler JW, Titgemeyer F (1991) A sugar-specific porin, ScrY, is involved in sucrose uptake in enteric bacteria. *Mol Microbiol* 5: 941-950.

Schmid M, Twachtmann U, Klein M, Strous M, Juretschko S, Jetten M, Metzger JW, Schleifer K-H, Wagner M (2000) Molecular evidence for genus level diversity of bacteria capable of catalyzing anaerobic ammonium oxidation. *Syst Appl Microbiol* 23: 93-106.

Schmid M, Walsh K, Webb R, Rijpstra WIC, van de Pas-Schoonen K, Verbruggen MJ, Hill T, Moffett B, Fuerst J, Schouten S, Sinninghe Damsté JS, Harris J, Shaw P, Jetten M, Strous M (2003) *Candidatus* "Scalindua brodae", sp. nov., *Candidatus* "Scalindua wagneri", sp. nov., two new species of anaerobic ammonium oxidizing bacteria. *Syst Appl Microbiol* 26: 529–538.

Schmid MC, Risgaard-Petersen N, van de Vossenberg J, Kuypers MMM, Lavik G, Petersen J, Hulth S, Thamdrup B, Canfield D, Dalsgaard T, Rysgaard S, Sejr MK, Strous M, Op den Camp HJM, Jetten MSM (2007) Anaerobic ammonium-oxidizing bacteria in marine environments: widespread occurrence but low diversity. *Environ Microbiol* 9: 1476-1484.

Schneitz C, Nuotio L, Lounatma K (1993) Adhesion of *Lactobacillus acidophilus* to avaian intestinal epithelial cells mediated by the crystalline bacterial cell surface layer (S-layer). *J Appl Bacteriol* 74: 290-294.

Schouten S, Strous M, Kuypers MMM, Rijpstra WIC, Baas M, Schubert CJ, Jetten MSM, Sinninghe Damsté JS (2004) Stable carbon isotopic fractionations associated with inorganic carbon fixation by anaerobic ammonium-oxidizing bacteria. *Appl Environ Microbiol* 70: 3785-3788.

Schubert CJ, Durisch-Kaiser E, Wehrli B, Thamdrup B, Lam P, Kuypers MMM (2006) Anaerobic ammonium oxidation in a tropical freshwater system (Lake Tanganyika). *Environ Microbiol* 8: 1857-1863.

Schulz GE (2002) The structure of bacterial outer membrane proteins. *Biochim Biophys Acta* 1565: 308-317.

Scott NE, Parker BL, Connolly AM, Paulech J, Edwards AVG, Crossett B, Falconer L, Kolarich D, Djordjevic SP, Hojrup P, Packer NH, Larsen MR, Cordwell SJ (2010) Simultaneous glycan-peptide characterization using hydrophilic interaction chromatography and parallel fragmentation by CID, higher energy collisional dissociation, and electron transfer dissociation MS applied to the *N*-linked glycoproteome of *Campylobacter jejuni*. *Mol Cell Proteomics* 10: M000031-MCP201.

Segrest JP, Jackson RL (1972) Molecular weight determination of glycoproteins by polyacrylamide gel electrophoresis in sodium dodecyl sulfate, p 54-63. *In* Ginsburg V (ed), Methods in enzymology vol. 28. Academic Press, San Diego, USA. ISBN: 978-0-12-181891-3.

Siegrist MS, Whiteside S, Jewett JC, Aditham A, Cava F, Bertozzi CR (2013) D-amino acid chemical reporters reveal peptidoglycan dynamics of an intracellular pathogen. *ACS Chem Biol* 8: 500-505.

Silhavy TJ, Kahne D, Walker S (2010) The bacterial cell envelope. *Cold Spring Harb Perspect Biol* 2: a000414.

Sillanpää J, Martínez B, Antikainen J, Toba T, Kalkkinen N, Tankka S, Lounatmaa K, Keränen J, Höök M, Westerlund-Wikström B, Pouwels PH, Korhonen TK (2000) Characterization of the collagen-binding S-layer protein CbsA of *Lactobacillus crispatus*. *J Bacteriol* 182: 6440-6450.

Sinninghe Damsté JS, Strous M, Rijpstra WIC, Hopmans EC, Geenevasen JAJ, van Duin ACT, van Niftrik LA, Jetten MSM (2002) Linearly concatenated cyclobutane lipids form a dense bacterial membrane. *Nature* 419: 708-712.

Sinninghe Damsté JS, Rijpstra WIC, Geenevasen JAJ, Strous M, Jetten MSM (2005) Structural identification of ladderane and other membrane lipids of planctomycetes capable of anaerobic ammonium oxidation (anammox). *FEBS J* 272: 4270-4283.

Sittig M, Schlesner H (1993) Chemotaxonomic investigation of various prosthecate and/or budding bacteria. *Syst Appl Microbiol* 16: 92-103.

Škultéty L, Toman R, Pätoprstý V (1998) A comparative study of lipopolysaccharides from two *Coxiella burnetii* strains considered to be associated with acute and chronic Q fever. *Carbohydr Polym* 35: 189-194.

Sipkema D, Holmes B, Nichols SA, Blanch HW (2009) Biological characterization of *Haliclona* (?*gellius*) sp.: sponge and associated microorganisms. *Microb Ecol* 58: 903-920.

Sleytr UB (1978) Regular arrays of macromolecules on bacterial cell walls: structure, chemistry, assembly, and function. *Int Rev Cytol* 53: 1-64.

Sleytr UB (1997) Basic and applied S-layer research: an overview. *FEMS Microbiol Rev* 20: 5-12.

Sleytr UB, Messner P (1983) Crystalline surface layers on bacteria. *Annu Rev Microbiol* 37: 311-339.

Sleytr UB, Messner P (1989) Self-assemblies of crystalline bacterial cell surface layers, p 13-31. *In* Plattner H (ed), Electron microscopy of subcellular dynamics. CRC Press, Boca Raton, USA. ISBN: 9780849360794.

Sleytr UB, Sára M (1997) Bacterial and archaeal S-layer proteins: structure-function relationships and their biotechnological applications. *Trends Biotechnol* 15: 20-26.

Sleytr UB, Beveridge TJ (1999) Bacterial S-layers. *Trends Microbiol.* 7: 253-260.

Söding J (2005) Protein homology detection by HMM-HMM comparison. *Bioinformatics* 21: 951-960.

Söding J, Biegert A, Lupas AN (2005) The HHpred interactive server for protein homology detection and structure prediction. *Nucl Acids Res* 33: W244-W248.

Sonnhammer ELL, von Heijne G, Krogh A (1998) A hidden Markov model for predicting transmembrane helices in protein sequences, p 175-182. *In* Glasgow J, Littlejohn T, Major F, Lathrop R, Sankoff D, Sensen C (ed), Proceedings of the sixth international conference on intelligent systems for molecular biology. AAAI Press, Menlo Park, USA. ISBN: 1-57735-053-7.

Sonthiphand P, Hall MW, Neufeld JD (2014) Biogeography of anaerobic ammonia-oxidizing (anammox) bacteria. *Front Microbiol* 5: 399.

Speth DR, van Teeseling MCF, Jetten MSM (2012) Genomic analysis indicates the presence of an asymmetric bilayer outer membrane in Planctomycetes and Verrucomicrobia. *Front Microbiol* 3: 304.

Speth DR, Russ L, Kartal B, Op den Camp HJM, Dutilh BE, Jetten MSM (2015) Draft genome sequence of anammox bacterium "*Candidatus* Scalindua brodae," obtained using differential coverage binning of sequencing data from two reactor experiments. *Genome Announc* 3: e01415-14.

Srikumar R, Dahan D, Arhin FF, Tawa P, Diederichs K, Coulton JW (1997) Porins of *Haemophilus influenza* type b mutated in loop 3 and in loop 4. *J Biol Chem* 272: 13614-13621.

Stackebrandt E, Wehmeyer U, Liesack W (1986) 16S ribosomal RNA- and cell wall analysis of *Gemmata obscuriglobus*, a new member of the order Planctomycetales. *FEMS Microbiol Lett* 37: 289-292.

Steeghs L, den Hartog R, den Boer A, Zomer B, Roholl P, van der Ley P (1998) Meningitis bacterium is viable without endotoxin. *Nature* 392: 449.

Steeghs L, de Cock H, Evers E, Zomer B, Tommassen J, van der Ley P (2001) Outer membrane composition of a lipopolysaccharide-deficient *Neisseria meningitides* mutant. *EMBO J* 20: 6937-6945.

Steenbakkers PJM, Geerts WJ, Ayman-Oz NA, Keltjens JA (2006) Identification of pseudomurein cell wall binding domains. *Mol Microbiol* 62: 1618-1630.

Strecker G (1995) Chemical cleavage of O- and N-glycosidic linkages, p. 47-50, *In* Verbert A (ed), Methods on glycoconjugates. Harwood Academic Publishers, Chur, Switzerland. ISBN: 3-7186-5514-4.

Strous M, Heijnen JJ, Kuenen JG, Jetten MSM (1998) The sequencing batch reactor as a powerful tool for the study of slowly growing anaerobic ammonium-oxidizing microorganisms. *Appl Microbiol Biotechnol* 50: 589-596.

Strous M, Fuerst JA, Kramer EHM, Logemann S, Muyzer G, van de Pas-Schoonen KT, Webb R, Kuenen JG, Jetten MSM (1999) Missing lithotroph identified as new planctomycete. *Nature* 400: 446-449.

Strous M, Pelletier E, Mangenot S, Rattei T, Lehner A, Taylor MW, Horn M, Daims H, Bartol-Mavel D, Wincker P, Barbe V, Fonknechten N, Vallenet D, Segurens B, Schenowitz-Truong C, Médigue C, Collingro A, Snel B, Dutilh BE, Op den Camp HJM, van der Drift C, Cirpus I, van de Pas-Schoonen KT, Harhangi HR, van Niftrik L, Schmid M, Keltjens J, van de Vossenberg J, Kartal B, Meier H, Frishman D, Huynen MA, Mewes H-W, Weissenbach J, Jetten MSM, Wagner M, Le Paslier D (2006) Deciphering the evolution and metabolism of an anammox bacterium from a community genome. *Nature* 440: 790-794.

Struyvé M, Moons M, Tommassen J (1991) Carboxy-terminal phenylalanine is essential for the correct assembly of a bacterial outer membrane protein. *J Mol Biol* 218: 141-148.

Sud M, Fahy E, Cotter D, Brown A, Dennis E, Glass C, Murphy R, Raetz C, Russel D, Subramaniam S (2006) LIPID MAPS Structure Database (LMSD). *Nucl Acids Res* 35: D527-532.

Sumper M, Berg E, Mengele R, Strobel I (1990) Primary structure and glycosylation of the S-layer protein of *Haloferax volcanii*. *J Bacteriol* 172: 7111-7118.

Sumper M, Wieland FT (1995) Bacterial glycoproteins, p 455-473. *In* Montreuil J, Vliegenthart JFG, Schachter H (ed) Glycoproteins. Elsevier, Amsterdam, the Netherlands. ISBN: 9780444812605.

Sun Z, Kong J, Hu S, Kong W, Lu W, Liu W (2013) Characterization of a S-layer protein from *Lactobacillus crispatus* K313 and the domains responsible for binding to cell wall and adherence to collagen. *Appl Microbiol Biotechnol* 97: 1941-1952.

Sutcliffe IC (2010) A phylum level perspective on bacterial cell envelope architecture. *Trends Microbiol* 18: 464-470.

Sweet CR, Lin S, Cotter RJ, Raetz CRH (2001) A *Chlamydia trachomatis* UDP-*N*-acetylglucosamine acyltransferase selective for myristoyl-acyl carrier protein. Expression in *Escherichia coli* and formation of hybrid lipid A species. *J Biol Chem* 276: 19565-19574.

Tan J, Rouse SL, Li D, Pye VE, Vogeley L, Brinth AR, El Arnaout T, Whitney JC, Howell PL, Sansom MSP, Caffrey M (2014) A conformational landscape for alginate secretion across the outer membrane of *Pseudomonas aeruginosa*. *Acta Crystallogr D Biol Crystallogr* 70: 2054-2068.

Tarao M, Jezbera J, Hahn MW (2009) Involvement of cell surface structures in size-independent grazing resistance of freshwater *Actinobacteria*. *Appl Environ Microbiol* 75: 4720-4726.

Tobias PS, Soldau K, Iovine NM, Elsbach P, Weiss J (1997) Lipopolysaccharide (LPS)-binding proteins BPI and LBP form different types of complexes with LPS. *J Biol Chem* 272: 18682-18685.

Tomaras AP, McPherson CJ, Kuhn M, Carifa A, Mullins L, George D, Desbonnet C, Eidem TM, Montgomery JI, Brown MF, Reilly U, Miller AA, O'Donnel JP (2014) LpxC inhibitors as new antibacterial agents and tools for studying regulation of lipid A biosynthesis in Gram-negative pathogens. *mBio* 5: e01551-14.

Trent MS, Stead CM, Tran AX, Hankins JV (2006) Invited review: Diversity of endotoxin and its impact on pathogenesis. *J Endotoxin Res* 12: 205-223.

Trimmer M, Nicholls JC, Deflandre B (2003) Anaerobic ammonium oxidation measured in sediments along the Thames estuary, United Kingdom. *Appl Environ Microbiol* 69: 6447-6454.

Tsai C-M, Frasch CE (1982) A sensitive silver stain for detecting lipopolysaccharides in polyacrylamide gels. *Anal Biochem* 1: 115-119.

Tsirigos KD, Bagos PG, Hamodrakas SJ (2011) OMPdb: A database of ß-barrel outer membrane proteins from Gram negative bacteria. *Nucl Acids Res* 39: D324-D331.

Ulmke C, Kreth J, Lengeler JW, Welte W, Schmid K (1999) Site-directed mutagenesis of loop L3 of sucrose porin ScrY leads to changes in substrate specificity. *J Bacteriol* 181: 1920-1923.

Vantourout P, Radojkovic C, Lichtenstein L, Pons V, Champagne E, Martinez LO (2010) Ecto-F_1-ATPase: A moonlighting protein complex and an unexpected apoA-I receptor. *World J Gastroenterol* 16: 5925-5935.

van de Graaf AA, Mulder A, de Bruijn P, Jetten MSM, Robertson LA, Kuenen JG (1995) Anaerobic oxidation of ammonium is a biologically mediated process. *Appl Environ Microbiol* 61: 1246-1251.

van den Berg B, Bhamidimarri SP, Prajapati JD, Kleinekathöfer U, Winterhalter M (2015) Outer-membrane translocation of bulky small molecules by passive diffusion. *Proc Natl Acad Sci USA* 112: E2991-E2999.

van der Star WRL, Miclea AI, van Dongen UGJM, Muyzer G, Picioreanu C, van Loosdrecht MCM (2008) The membrane bioreactor: a novel tool to grow anammox bacteria as free cells. *Biotechnol Bioeng* 101: 286-294.

van der Star WRL, Dijkema C, de Waard P, Picioreanu C, Strous M, van Loosdrecht MCM (2010) An intracellular pH gradient in the anammox bacterium *Kuenenia stuttgartiensis* as evaluated by ^{31}P NMR. *Appl Microbiol Biotechnol* 86: 311-317.

van Donselaar E, Posthuma G, Zeuschner D, Humbel BM, Slot JW (2007) Immunogold labeling of cryosections from high-pressure frozen cells. *Traffic* 8: 471-485.

van Heijenoort J (2001) Formation of the glycan chains in the synthesis of bacterial peptidoglycan. *Glycobiology* 11: 25R-36R.

van Niftrik (2008) Cell biology of anaerobic ammonium-oxidizing bacteria. *PhD thesis*, Radboud Universiteit. Chapter 2, p 33-77. ISBN: 978-90-9022645-3.

van Niftrik L, Fuerst JA, Sinninghe Damsté JS, Kuenen JG, Jetten MSM, Strous M (2004) The anammoxosome: an intracytoplasmic compartment in anammox bacteria. *FEMS Microbiol Lett* 233: 7-13.

van Niftrik L, Geerts WJC, van Donselaar EG, Humbel BM, Webb RI, Fuerst JA, Verkleij AJ, Jetten MSM, Strous M (2008a) Linking ultrastructure and function in four genera of anaerobic ammonium-oxidizing bacteria: cell plan, glycogen storage, and localization of cytochrome *c* proteins. *J Bacteriol* 2008: 708-717.

van Niftrik L, Geerts WJC, van Donselaar EG, Humbel BM, Yakushevska A, Verkleij AJ, Jetten MSM, Strous M (2008b) Combined structural and chemical analysis of the anammoxosome: a membrane-bounded intracytoplasmic compartment in anammox bacteria. *J Struct Biol* 161: 401-410.

van Niftrik L, Geerts WJC, van Donselaar EG, Humbel BM, Webb RI, Harhangi HR, Op den Camp HJM, Fuerst JA, Verkleij AJ, Jetten MSM, Strous M (2009) Cell division ring, a new cell division protein and vertical inheritance of a bacterial organelle in anammox planctomycetes. *Mol Microbiol* 73: 1009-1019.

van Niftrik L, van Helden M, Kirchen S, van Donselaar EG, Harhangi HR, Webb RI, Fuerst JA, Op den Camp HJM, Jetten MSM, Strous M (2010) Intracellular localization of membrane-bound ATPases in the compartmentalized anammox bacterium '*Candidatus* Kuenenia stuttgartiensis'. *Mol Microbiol* 77: 701-715.

van Teeseling MCF, Neumann S, van Niftrik L (2013) The anammoxosome organelle is crucial for the energy metabolism of anaerobic ammonium oxidizing bacteria. *J Mol Microbiol Biotechnol* 23: 104-117.

van Teeseling MCF, de Almeida NM, Klingl A, Speth DR, Op den Camp HJM, Rachel R, Jetten MSM, van Niftrik L (2014) A new addition to the cell plan of anammox bacteria: "*Candidatus* Kuenenia stuttgartiensis" has a protein surface layer as the outermost layer of the cell. *J Bacteriol* 196: 80-89.

van Teeseling MCF, Mesman RJ, Kuru E, Espaillat A, Cava F, Brun YV, VanNieuwenhze MS, Kartal B, van Niftrik L (2015) Anammox plactomycetes have a peptidoglycan cell wall. *Nat Commun* 6: 6878.

Vollmer W, Blanot D, De Pedro M (2008) Peptidoglycan structure and architecture. *FEMS Microbiol Rev* 32: 149-167.

Vorachek-Warren MK, Ramirez S, Cotter RJ, Raetz CRH (2002) A triple mutant of *Escherichia coli* lacking secondary acyl chains on lipid A. *J Biol Chem* 277: 14194-14205.

Voulhoux R, Bos MP, Geurtsen J, Mols M, Tommassen J (2003) Role of a highly conserved bacterial protein in outer membrane protein assembly. *Science* 299: 262-265.

Wagner M, Horn M (2006) The *Planctomycetes*, *Verrucomicrobia*, *Chlamydiae* and sister phyla comprise a superphylum with biotechnological and medical relevance. *Curr Opin Biotechnol* 17: 241-249.

Ward JB (1981) Teichoic and teuchuronic acids: biosynthesis, assembly, and location. *Microbiol Rev* 45: 211-243.

Ward NL (2010) Order I. Planctomycetales Schlesner and Stackebrandt 1987, 179^{VP} (Effective publication: Schlesner and Stackebrandt 1986, 175) emend. Ward (this volume). *In* Krieg NR, Ludwig W, Whitman WB, Hedlund BP, Paster BJ, Staley JT, Ward N, Brown D (eds), Bergey's Manual of Systematic Bacteriology, 2^{nd} edition, volume 4. Springer, New York, USA. ISBN: 978-0-387-68572-4.

Warren L (1959) The thiobarbituric acid assay of sialic acids. *J Biol Chem* 234: 1971-1975.

Webster NS, Wilson KJ, Blackall LL, Hill RT (2001) Phylogenetic diversity of bacteria associated with the marine sponge *Rhopaloeides odorabile*. *Appl Environ Microbiol* 67: 434-444.

Weckesser J, Drews G, Fromme I, Mayer H (1973) Isolation and chemical composition of the lipopolysaccharides of *Rhodopseudomonas palustris* strains. *Arch Mikrobiol* 92: 123-138.

Weiner JH, Li L (2008) Proteome of the *Escherichia coli*envelope and technological challenges in membrane proteome analysis. *Biochim Biophys Acta* 1778: 1698-1713.

Weiss DS (2015) Last but not least: new insights into how FtsN triggers constriction during *Escherichia coli* cell division. *Mol Microbiol* 95: 903-909.

Wen-Li Z, Jian W, Yan-Fang T, Xing F, Yan-Hong L, Xue-Ming Z, Min Z, Jian N, Jian P (2012) Inhibition of the ecto-beta subunit of F1FO-ATPase inhibits proliferation and induces apoptosis in acute myeloid leukemia cell lines. *J Exp Clin Cancer Res* 31: 92.

Wessels HJCT, Vogel RO, van den Heuvel L, Smeitink JA, Rodenburg RJ, Nijtmans LG, Farhoud MF (2009) LC-MS/MS as an alternative for SDS-PAGE in blue native analysis of protein complexes. *Proteomics* 9: 4221-4228.

Wiegel J, Quandt L (1982) Determination of the Gram type using the reaction between polymyxin B and lipopolysaccharides of the outer cell wall of whole bacteria. *J Gen Microbiol* 128: 2261-2270.

Wilks JC, Slonczewski JL (2007) pH of the cytoplasm and periplasm of *Escherichia coli*: rapid measurement by green fluorescent protein fluorimetry. *J Bacteriol* 189: 5601-5607.

Wilmes B, Kock H, Glagla S, Albrecht D, Voigt B, Markert S, Gardebrecht A, Bode R, Danchin A, Feller G, Hecker M, Schweder T (2011) Cytoplasmic and periplasmic proteomic signatures of exponentially growing cells of the psychrophilic bacterium *Pseudoalteromonas haloplanktis* TAC125. *Appl Environ Microbiol* 77: 1276-1283.

Wimley WC (2003) The versatile ß-barrel membrane protein. *Curr Opin Struct Biol* 13: 404-411.

Woebken D, Teeling H, Wecker P, Dumitriu A, Kostadinov I, DeLong EF, Amann R, Glöckner FO (2007) Fosmids of novel marine *Planctomycetes* from the Namibian and Oregon coast upwelling systems and their cross-comparison with planctomycete genomes. *ISME J* 1: 419-435.

Wu ML, van Teeseling MCF, Willems MJR, van Donselaar EG, Klingl A, Rachel R, Geerts WJC, Jetten MSM, Strous M, van Niftrik L (2012) Ultrastructure of the denitrifying methanotroph "*Candidatus* Methylomirabilis oxyfera", a novel polygon-shaped bacterium. *J Bacteriol* 194: 284-291.

Wuhrer M, Koeleman CAM, Hokke CH, Deelder AM (2006) Mass spectrometry of proton adducts of fucosylated N-glycans: fucose transfer between antennae gives rise to misleading fragments. *Rapid Commun Mass Spectrom* 20: 1747-1754.

Yee B, Sagulenko E, Morgan GP, Webb RI, Fuerst JA (2012) Electron tomography of the nucleoid of *Gemmata obscuriglobus* reveals complex liquid crystalline cholesteric structure. *Front Microbiol* 3: 326.

Yoon J, Jang J-H, Kasai H (2014) *Algisphaera agarilytica* gen. nov., sp. nov., a novel representative of the class *Phycisphaera* within the phylum *Planctomycetes* isolated from a marine alga. *Antonie van Leeuwenhoek* 105: 317-324.

Young K, Silver LL, Bramhill D, Cameron P, Eveland SS, Raetz CRH, Hyland SA, Anderson MS (1995) The *envA* permeability/cell division gene or *Escherichia coli* encodes the second enzyme of lipid A biosynthesis. UDP-3-*O*-(*R*-3-hydroxymyristoyl)-*N*-acetylglucosamine deacetylase. *J Biol Chem* 270: 30384-30391.

Zachariae U, Klühspies T, De S, Engelhardt H, Zeth K (2006) High resolution crystal structures and molecular dynamics studies reveal substrate binding in the porin Omp32. *J Biol Chem* 281: 7413-7420.

Zhou Z, White KA, Polissi A, Georgopoulos C, Raetz CRH (1998) Function of *Escherichia coli* MsbA, an essential ABC family transporter, in lipid A and phospholipid biosynthesis. *J Biol Chem* 273: 12466-12475.

Zhu G, Wang S, Wang Y, Wang C, Risgaard-Petersen N, Jetten MSM, Yin C (2011) Anaerobic ammonia oxidation in a fertilized paddy soil. *ISME J* 5: 1905-1912.

Acknowledgements

Upon starting my PhD project I could have never imagined that I would learn so many new things, at so many places with the support and help of so many friendly, helpful and creative people. I feel quite touched and grateful that so many people helped me along the way of my PhD and now it's my pleasure to thank all of you.

Ten eerste, natuurlijk, Laura. Ik kan me nog goed herrinneren hoe leuk ik het practicum BvMO vond met jou als begeleidster. Ik was natuurlijk dolblij en trots om bij jou stage te mogen lopen en vind het heel bijzonder dat ik al die jaren met jou als begeleidster heb mogen werken. Ik heb heel veel van je geleerd en we hebben samen allerlei avonturen beleefd die ik nog lang met een lach op mijn gezicht zal herrinneren! Ik vind het heel knap en ben je erg dankbaar hoe je mij hebt begeleid met een combinatie van heel veel vertrouwen en aandacht, maar ook veel vrijheid om mijn eigen beslissingen te nemen en mijn eigen weg te kiezen. Het is heel waardevol om met jou iemand als begeleidster te hebben waarvan ik weet dat ze altijd achter me staat. Ik kijk er met veel plezier naar uit om van de zijlijn te volgen hoe jij met de celbio groep nog veel geheimen van annamox gaat ontrafelen, maar ook nieuwe spannende research lines gaat ontwikkelen.

Het is een eer en een erg leerzaam proces om te mogen promoveren bij de beroemde prof. Mike Jetten. Ik vind het bijzonder knap hoe je met zo'n grote groep in staat bent om overzicht te hebben en op de juiste momenten treffende aanwijzingen op maat te geven. Zoals die keer dat je me wees op een interessant congres in Duitsland- ik heb goed naar je geluisterd ;). Ik ben dankbaar voor de vrijgevigheid aan unieke kansen en mogelijkheden die je me hebt geboden om me op velerlei gebieden te kunnen ontwikkelen.

Huub, ik vond het leuk om ook deel uit te maken van het Verruco-team. Prachtig om te zien hoe het je gelukt is om de vulkanische microbiologie op de kaart te zetten: ik ga met plezier volgen wat voor mooie resultaten dat de komende tijd op gaat leveren.

Ik heb veel te danken aan Rob en je weet waarschijnlijk nog niet half hoe blij ik ben dat je het celbio team bent komen versterken! Ik ben er erg trots op hoe we samen 1001 ideeen hebben verzonnen die tot mooie resultaten hebben geleid en ga je niet aflatende stroom aan ideeen, tips, adviezen en lessen over EM technieken erg missen. Ik ben blij en trots dat je binnenkort als paranifm naast me staat!

Sarah, ik heb veel met je gelachen en je was de perfecte roommate op congressen! Ik had maar mooi mazzel dat ik van jou als senior PhD in de anammox celbio heb kunnen leren. Ik vind het superstoer dat je nu bij FEI zo'n goede baan hebt en hopelijk kan ik nog eens een kaartje bij je lospeuteren op een EM congres ;).

Ming, many thanks for sharing your advice and perspectives with me. And thanks for making it possible that Sietse has been your colleague as well; I am sad for the both of you it didn't last a bit longer.

Lavinia, it was lots of fun having you as a cell biology colleague and I enjoyed seeing you grow into a confident PhD student. I am sure you will fulfill your new role of Laura's most senior PhD student well.

Marjan, wat fijn om jou bij de celbio groep te hebben. Altijd enthousiast en relativerend: dankjewel daarvoor en voor het versturen van pakketjes en de immunoblot assays.

Arjan, het was goed en verhelderend om met je samengewerkt te hebben. Bedankt dat ik namen mocht verzinnen voor de Verruco's die je met gevaar voor eigen leven hebt gesampled, met toewijding op hebt gekweekt en waarvan je met karakteristieke gedegenheid allerlei (fysiologische) geheimen hebt losgepeuterd!

Ahmad, in het begin van mijn PhD en aan het eind van de jouwe hebben we goed samen kunnen werken op het SolV project en daar heb ik veel van geleerd. Bij het schrijven van mijn Verruco deel heb ik vaak jouw proefschrift als inspiratie gebruikt.

Daan, wat een geluk dat we 'tegelijk' als PhD's begonnen zijn en wat gaaf om te zien hoe we ons hebben ontwikkeld en elkaar vooruit hebben kunnen helpen. Niet alleen heb ik dankzij jou een beetje bioinformatica benul en allerlei inzicht in de wetenschap in t algemeen, ook hoop ik dat ik een klein beetje van je indrukwekkende helicoptervisie over de microbiologie heb kunnen oppakken. Ik ben zo benieuwd hoe je postdoc uitpakt en hoe het daarna zal lopen en ik hoop vooral dat we ondanks ons beider verhuizingen nog steeds kunnen blijven sparren over de microbiologie. Supermooi dat jij mijn paranifm bent en ik de jouwe!

Martine, het was echt een kadootje dat je bij ons in het kantoor kwam zitten. Jouw aanstekelijke positiviteit gecombineerd met nuchterheid zorgen er steeds weer voor dat ondanks als dingen tegen zitten, ik alles weer wat zonniger inzie. Heel erg bedankt daarvoor en voor alle gezelligheid en veel succes met je mosjes!

Naomi, I admire your spontaneity and attentiveness. Both your dinner parties and your proteome skills are legendary- thanks for letting me be part of both. I wish you all the best in Germany.

Cornelia, ik ben heel blij dat je naar Nijmegen bent gekomen; bedankt voor het luisterend oor, de adviezen en de gezelligheid.

Rob de G, leuk dat ik zo lang je buurvrouw in het kantoor heb kunnen zijn, het was altijd gezellig even bij te kletsen en het laatste nieuws uit de faculteit te bespreken.

Boran, I am really really happy that you got involved in my project as well. I am super proud of the scientific results of the "infamous PG team": it's not every day that one can "rewrite" Brock. Many thanks for cheering me up on multiple occasions, the good conversations and for all the laughter, jokes and great anecdotes.

Sebastian, you have helped me forward in multiple projects by introducing me to the right people. Many thanks for that!

Many thanks also to all the other colleagues and guests for your advice, enthusiasm, help, chats and for generating a good atmosphere in the department: Adam, Alvaro, Aniela, Annika, Arslan, Baoli, Bram, Claudia, Dimitra, Dorien, Eric, Francisca (wat superleuk dat je terug bent!), Frauke, Geert, Guylaine (in zo'n korte tijd al onmisbaar geworden), Harry, Jack, Jan, Jennifer, Jeroen, Joachim, Judith, Karin, Katharina, Katinka, Ke, Kim, Lina, Maartje, Mamoru, Mara, Marianne, Michela, Michiel, Mo, Nardy, Olivia, Sepehr, Simon, Suzanne, Theo, Tijs, Wouter M, Wouter V, Xristina (thanks for your pinterest foodie inspiration wall ☺) and Ziye. Without you, I would for sure not have had such a nice time at Microbiology!

Of course also many thanks to the numerous students that have contributed to the vibrant atmosphere in the department. Stijn, ik vond het een groot genoegen om jou te mogen helpen met je MreB project! Ik heb bewondering voor de manier waarop je grondigheid combineert met een soort van kalmte en optimisme die ervoor zorgt dat je je -ondanks de soms tegenvallende resultaten- niet uit het veld laat slaan. Ik wens je veel succes en veel goede resultaten toe in je verdere (onderzoeks)carrière! Goed om te weten dat jij en Dave de celbiologie nog een tijdje blijven versterken en van nieuwe impulsen blijven voorzien!

During my PhD, I was fortunate to visit several research groups. I have always felt very welcome and have enjoyed the visits which have broadened my view, introduced me to many new techniques and have been very valuable in several research lines.

Dear Reinhard, I feel really lucky that I could be part of your group in Regensburg and it has been a pleasure, an honor and a very valuable experience to learn so much in EM-related research from someone that has so much knowledge about this. Andreas, it was great fun working with you: many thanks for teaching me basic EM skills and introducing me to the Cressi and some nice aspects of life in Bavaria. I have had a lot of fun with my office mates Jenni, Thomas, Ben and Vroni and with Flo and Arnab with whom we shared the lab as well as many jokes. Jenni, I was so happy to have you around and even though we don't skype as often as we would like, we always have the butterfly connection! Liebe Beate, danke schön dass ich bei dir ein wirkliches Zuhause in Regensburg und eine ganze menge Spass hatte. Sibille und Laura, vielen Dank für die nette Zeit und die gemeinsame Ausflugen, wie zB. die legendäre Alpenausflug!

Paul and Tina, it has been great to be part of the glyco-group at the BOKU and I really enjoyed getting more insight into glycobiology. Visiting your group has been an impulse for several of my projects and I have always felt very welcome. Also many thanks to Paul Kosma for all the NMR analyses and meetings. Daniel, thanks for your MS analysis and your kind and elaborate interpretation and explanation of the results. Andrea S & Sonja, many thanks for helping me and teaching me several valuable glycobiology methods. Eva S

(we had so much fun when I stayed with you! And you helped me out at multiple occasions), Conny (many thanks for your help with both projects and all the chats), Valentin (your anecdotes are legendary!), Zoe, Heinz, Gary, Arturo, Eva L, Markus, Bettina, Julia, Andrea K, Behnam and Andrea L, I was so lucky to have you around, you were always happy to help me find something in the lab or give me advice on how to tackle the project or how to enjoy Vienna and I had a lot of fun with you :). Dass ich mir wirklich wohl gefühlt habe in Wien, war auch wegen meiner supernette WG-MitbewohnerInnen Ilka (und Hansi), Bini, Wilhelm und Or.

Christian and Mareike, it was a very nice experience to be part of your enthusiastic and ambitious group and to be surrounded by ideas focusing on the non-anammox *Planctomycetes*. I very much appreciate all your efforts to make me feel comfortable and welcome in your group and in Wolfenbüttel. Despite the singstar CD (thanks Anja ;)) the Christmas party is one of my favorite memories. I have grown very fond of my DSMZ colleagues that form a great, creative and supportive team: Olga, Christian B, Patrick, Timo and Anja. Olga, I very much enjoyed working as a team and I'm super proud of our keynote presentation!

Being at the famous lipid group of Jaap Sinninghe Damsté, even though only short, was a great experience. Ellen, met jou is het super samenwerken! Je kritische maar realistische blik op de protocollen, resultaten en mijn hoofdstuk vanuit het oogpunt van de chemie en je scherpe en humoristische uitleg van de MS hebben ervoor gezorgd dat ik echt verder kon komen dan een naieve bioloog. Eli, many thanks for helping me find my way in the lab.

My gratitude also goes out to Roland Benz and his group (Ivan, Eva, Satya, and the others) at the Jacobs University Bremen for the heartwarming hospitability and introducing me to the bilayer setups.

My projects would have been rather incomplete without the help of many collaborators. Many thanks for all the invested efforts and for making me a broader scientist.

Elly, ik prijs me erg gelukkig dat ik van jou (en Rob) de fijne kneepjes van het EM ambacht heb mogen leren en altijd bij jullie in Utrecht langs mocht komen voor hulp, adviezen en gezelligheid!

Geert-Jan & Liesbeth hartelijk dank voor jullie hulp bij de vele technieken en (de reparatie van) apparaten die het GI rijk is.

Hans, hartelijk dank voor je toewijding in de MS analyses en het doorspreken van de resultaten voor meerdere van mijn projecten, terwijl je al zo veel te doen had!

Thomas and coworkers in Heidelberg, great that you are looking at kustd1878; I am very curious how the crystal will look! I hope the protein behaves well.

The elegant method developed by the Bloomington team has quickly become the standard for detecting peptidoglycan in vivo and we were glad that we could collaborate with Erkin, Yves and Mike to show peptidoglycan in *Kuenenia stuttgartiensis*. It was a pleasure meeting the three of you at the GRC and always very nice to reflect on science and life with Erkin.

Felipe and Akbar, you are really great collaborators and I was very impressed by the speed with which you obtained the muropeptide results and provided the figures. Felipe, I am very much looking forward to join your lab and work with your amazing team!

Karin and Matthias, many thanks for sharing your experiences in the hunt for peptidoglycan in *Chlamydiae* with me during my visit to DOME and thereby putting us on track for finding peptidoglycan in anammox bacteria as well.

Met veel plezier heb ik deel uitgemaakt van de programmaraad RHA FNWI. Wat is het leuk om te zien hoe de studenten groeien terwijl zij met veel toewijding en creativiteit aan mooie projecten werken. Ik denk met een lach op mijn gezicht terug aan de vergaderingen in zowel de oude als de nieuwe samenstelling waar scherpe inzichten gecombineerd worden met veel humor. Wim, met je vragen zorgde jij er altijd voor dat de studenten met andere ogen naar hun eigen onderzoek gingen kijken. Als voorzitter gaf je altijd vrijheid en vertrouwen en was je er altijd op de momenten die erom gingen. Joop, zonder jou was het programma zeker niet zo robuust geweest als het nu is. Ik ben blij dat we de RHA-eer hoog hebben kunnen houden bij de IWWR quiz. Hay, jij bent de vaste waarde van de RHA, en degene die er steeds op een hele vriendelijke manier in slaagt de raad onder controle te houden en met veel interesse studenten volgt en de ouders bij de uitreikingen betrekt. Jan, terecht door de studenten op handen gedragen, bedankt voor de scherpe analyses en inzichten, waar ik veel van heb geleerd. Teun, het is maar goed dat je die dag toch naar het werkcollege bent gekomen, anders was je vast niet aangenomen (;)) en had ik nu niet met zoveel plezier met je samengewerkt en bijgepraat. Ik ben heel benieuwd in wat voor carriere je terecht gaat komen, maar ik ben er zeker van dat het iets gaafs en belangrijks gaat worden. Ook hartelijk dank aan Daniel, Elena, Ernst, Esra, Fleur, Frits, John, Klaas, Lejla, Leonie, Nicolette, Sjaak, Stephanie, Tim en Wilke, de mentoren, meesters en studenten voor de leuke tijd.

I've been fortunate to have a favorite pastime that brought me in contact with some of the most supportive and nicest people I know; it has always been a pleasure to play field hockey. Teamgenootjes van Union D5 (en Jouke), ik zal jullie vreselijk gaan missen; super bedankt voor alle gezelligheid en het altijd aanwezige begrip als ik weer eens een paar maanden weg was. Anneke, ik ben stiekem best blij dat je een hekel hebt aan zaalhockey, anders had ik niet jaarlijks in de winter mee kunnen doen met Apeliotes D1 onder leiding van het zaaltactiek-brein Willem. HC Wien Damen und Flo, es hat mir ganz viel spass gemacht euch kennen zu lernen und bei euch mit zu spielen. Auch ein Dankeschön an den Damen von Eintracht Braunschweig und Carsten, dass ich mit euch richtig Hallenhockey spielen durfte und mir ab jetzt immer eine Löwin nennen kann ;).

Als ik steun, relativering of advies nodig had kon ik ook altijd terecht bij een paar inspirerende mensen die ik hierboven nog niet genoemd heb. Dank jullie wel, Willemijn (je bent zo positief en lief en het was heel leuk om te zien hoe je gegroeid bent tot een hele goede dokter), Tim (eigenlijk kijk ik best wel tegen je op, en gelukkig kunnen we ook nog eens heel erg lachen samen), Lennert (wat waren we een illuster duo samen en wat ben ik blij dat we bevriend zijn geraakt), Koen (gesprekken met jou zijn altijd fijn en verhelderend), Ralph (wie had na onze eerste ontmoeting ooit gedacht dat we zulke goede vrienden zouden worden ;)) en Janric (jij doet altijd zulke indrukwekkende dingen en ik vind 't altijd super om te discussieren over van alles).

Ik heb altijd kunnen rekenen op steun en interesse van een uitgebreide (schoon)familie, bestaand uit o.a. meerdere neefjes, nichtjes, ooms, tantes, oudooms, oudtantes en opa's en oma's; heel erg bedankt en super dat ik zo veel van jullie op de 13e zal zien! Ik ben erg gesteld en heel trots op mijn broer Adriaan; het vervelendste aan het verhuizen naar Zweden vind ik waarschijnlijk dat ik jou minder zal zien. Als ik weer terug ben (of jij ook in Zweden woont) blazen we Muriaan nieuw leven in! Het is evident dat ik nooit op dit punt gekomen zou zijn zonder Erica, Wouter, Martin en Barbara: jullie hebben me zoveel bijgebracht en steunen me nog steeds op zo veel manieren. Ik ben heel trots dat ik duidelijke elementen van jullie alle vier in me heb.

Sietse, jouw geduld en je grenzeloze steun zijn voor mij eigenlijk niet te bevatten. Het is toch echt ook dankzij jou dat ik het vertrouwen had om allerhande projecten in binnen- en buitenland op te pakken en door te zetten, en je hebt daardoor niet alleen een duidelijke hand gehad in hoe het proefschrift is geworden, maar ook in wie ik nu ben. Ik kijk ernaar uit om samen nog veel avonturen te beleven. Ik hou van jou.

Curriculum Vitae

Muriël Caroline Frieda van Teeseling was born on 25 December 1986 in Naarden, the Netherlands. She graduated from the Gymnasium Apeldoorn in 2005. After finishing the first year of Classical Languages and Cultures at the Radboud University Nijmegen (RU) (cum laude) she switched to Biology in which she obtained her Bachelor in 2008 and her Master in 2011 (both degrees cum laude). During her studies she also participated in the Interdisciplinary Honours Programme and finished the first year program of Physics and Astronomy (cum laude), as well as taking place in many committees committed to improvement of educational programs at the RU. In the course of her biology education, she performed research projects at the Department of Molecular Materials (RU), the Department of Microbiology (RU) and at the Centre for Electron Microscopy (University of Regensburg, Germany). In 2011 she started her PhD project, of which the results are described in this thesis, at the Department of Microbiology under the supervision of dr. Laura van Niftrik, with prof. dr. Mike Jetten as her promotor. Parts of her project were performed during research visits to the Division of BioMolecular Imaging at the Utrecht University, the Centre for Electron Microscopy at the University of Regensburg, Germany (under supervision of prof. dr. Reinhard Rachel), the Department of Nanobiotechnology at the University of Natural Resources and Life Sciences, Vienna, Austria (under supervision of dr. Paul Messner and dr. Christina Schaeffer), the Microbial Cell Biology and Genetics research group at the DSMZ, Braunschweig, Germany (under supervision of dr. Christian Jogler), the department of Marine Organic Biogeochemistry at the NIOZ, Texel (supervised by dr. Ellen Hopmans) and the Department of Life Sciences and Chemistry at the Jacobs University, Bremen, Germany (under supervision of prof. dr. Roland Benz). In 2014 Muriel was awarded the Frye stipendium by the Radboud University as being one of ten most promising female PhD students of that year at the Radboud University. During her PhD she was a member of the seminar committee of the Institute for Water and Wetland Research and was part of the organizing committee of the Radboud Honours Acadamy for bachelor students at the Faculty of Science. Starting February 2016, Muriel will work as a post-doc at the Department of Molecular Biology under supervision of dr. Felipe Cava to study the molecular mechanisms and function of the curved morphology of *Vibrio* bacteria.

Publications

Publications relevant to this part of the thesis:

van Teeseling MCF, Mesman RJ, Kuru E, Espaillat A, Cava F, Brun YV, VanNieuwenhze MS, Kartal B, van Niftrik L (2015) Anammox Planctomycetes have a peptidoglycan cell wall. *Nat Commun* 6: 6878.

van Teeseling MCF, de Almeida NM, Klingl A, Speth DR, Op den Camp HJM, Rachel R, Jetten MSM, van Niftrik L (2014) A new addition to the cell plan of anammox bacteria: *"Candidatus* Kuenenia stuttgartiensis" has a protein surface layer as the outermost layer of the cell. *J Bacteriol* 196: 980-89.

van Teeseling MCF, Neumann S, van Niftrik L (2013) The anammoxosome organelle is crucial for the enrgy metabolism of anaerobic ammonium oxidizing bacteria. *J Mol Microbiol Biotechnol* 23: 104-117.

Neumann S, van Teeseling MCF, van Niftrik L (2013) Cell biology of anaerobic ammonium-oxidizing bacteria: unique prokaryotes with an energy-conserving intracellular compartment. *Planctomycetes: cell structure, origins and biology*, ed Fuerst JA (Humana Press/Springer, New York), pp 89-123.

Speth DR, van Teeseling MCF, Jetten MSM (2012) Genomic analysis indicates the presence of an asymmetric bilayer outer membrane in Planctomycetes and Verrucomicrobia. *Front Microbio* 3: 304.

Additional publications:

van Teeseling MCF, Pol A, Harhangi HR, van der Zwart S, Jetten MSM, Op den Camp HJM, van Niftrik L (2014) Expanding the verrucomicrobial methanotrophic world: description of three novel species of Methylacidimicrobium gen. nov.. *Appl Environ Microbio* 80: 6782-6791.

Khadem AF*, van Teeseling MCF*, van Niftrik L, Jetten MSM, Op den Camp HJM, Pol A (2012) Genomic and physiological analysis of carbon storage in the verrucomicrobial methanotroph "*Ca.* Methylacidiphilum fumariolicum" SolV. *Front Microbio* 3: 345.

*Both authors contributed equally.

Wu ML, van Teeseling MCF, Willems MJR, van Donselaar EG, Klingl A, Rachel R, Geerts WJC, Jetten MSM, Strous M, van Niftrik L (2012) Ultrastructure of the denitrifying methanotroph "*Candidatus* Methylomirabilis oxyfera," a novel polygon-shaped bacterium. *J Bacteriol* 194: 284-291.

Zisis T, Freddolino PL, Turunen P, van Teeseling MCF, Rowan AE, Blank KG. Interfacial activation of *Candida antarctica* lipase B: combined evidence from experiment and simulation. *Biochemistry* 54: 5969-5979.

Publications

Publications relevant to this part of the thesis:

van Teeseling MCF, Pol A, Harhangi HR, van der Zwart S, Jetten MSM, Op den Camp HJM, van Niftrik L (2014) Expanding the verrucomicrobial methanotrophic world: description of three novel species of Methylacidimicrobium gen. nov.. *Appl Environ Microbio* 80: 6782-6791.

Khadem AF*, van Teeseling MCF*, van Niftrik L, Jetten MSM, Op den Camp HJM, Pol A (2012) Genomic and physiological analysis of carbon storage in the verrucomicrobial methanotroph "*Ca.* Methylacidiphilum fumariolicum" SolV. *Front Microbio* 3: 345.

*Both authors contributed equally.

Additional publications:

van Teeseling MCF, Mesman RJ, Kuru E, Espaillat A, Cava F, Brun YV, VanNieuwenhze MS, Kartal B, van Niftrik L (2015) Anammox Planctomycetes have a peptidoglycan cell wall. *Nat Commun* 6: 6878.

van Teeseling MCF, de Almeida NM, Klingl A, Speth DR, Op den Camp HJM, Rachel R, Jetten MSM, van Niftrik L (2014) A new addition to the cell plan of anammox bacteria: *"Candidatus* Kuenenia stuttgartiensis" has a protein surface layer as the outermost layer of the cell. *J Bacteriol* 196: 980-89.

van Teeseling MCF, Neumann S, van Niftrik L (2013) The anammoxosome organelle is crucial for the enrgy metabolism of anaerobic ammonium oxidizing bacteria. *J Mol Microbiol Biotechnol* 23: 104-117.

Neumann S, van Teeseling MCF, van Niftrik L (2013) Cell biology of anaerobic ammonium-oxidizing bacteria: unique prokaryotes with an energy-conserving intracellular compartment. *Planctomycetes: cell structure, origins and biology*, ed Fuerst JA (Humana Press/Springer, New York), pp 89-123.

Speth DR, van Teeseling MCF, Jetten MSM (2012) Genomic analysis indicates the presence of an asymmetric bilayer outer membrane in Planctomycetes and Verrucomicrobia. *Front Microbio* 3: 304.

Wu ML, van Teeseling MCF, Willems MJR, van Donselaar EG, Klingl A, Rachel R, Geerts WJC, Jetten MSM, Strous M, van Niftrik L (2012) Ultrastructure of the denitrifying methanotroph "*Candidatus* Methylomirabilis oxyfera," a novel polygon-shaped bacterium. *J Bacteriol* 194: 284-291.

Zisis T, Freddolino PL, Turunen P, van Teeseling MCF, Rowan AE, Blank KG. Interfacial activation of *Candida antarctica* lipase B: combined evidence from experiment and simulation. *Biochemistry* 54: 5969-5979.

Curriculum Vitae

Muriël Caroline Frieda van Teeseling was born on 25 December 1986 in Naarden, the Netherlands. She graduated from the Gymnasium Apeldoorn in 2005. After finishing the first year of Classical Languages and Cultures at the Radboud University Nijmegen (RU) (cum laude) she switched to Biology in which she obtained her Bachelor in 2008 and her Master in 2011 (both degrees cum laude). During her studies she also participated in the Interdisciplinary Honours Programme and finished the first year program of Physics and Astronomy (cum laude), as well as taking place in many committees committed to improvement of educational programs at the RU. In the course of her biology education, she performed research projects at the Department of Molecular Materials (RU), the Department of Microbiology (RU) and at the Centre for Electron Microscopy (University of Regensburg, Germany). In 2011 she started her PhD project, of which the results are described in this thesis, at the Department of Microbiology under the supervision of dr. Laura van Niftrik, with prof. dr. Mike Jetten as her promotor. Parts of her project were performed during research visits to the Division of BioMolecular Imaging at the Utrecht University, the Centre for Electron Microscopy at the University of Regensburg, Germany (under supervision of prof. dr. Reinhard Rachel), the Department of Nanobiotechnology at the University of Natural Resources and Life Sciences, Vienna, Austria (under supervision of dr. Paul Messner and dr. Christina Schaeffer), the Microbial Cell Biology and Genetics research group at the DSMZ, Braunschweig, Germany (under supervision of dr. Christian Jogler), the department of Marine Organic Biogeochemistry at the NIOZ, Texel (supervised by dr. Ellen Hopmans) and the Department of Life Sciences and Chemistry at the Jacobs University, Bremen, Germany (under supervision of prof. dr. Roland Benz). In 2014 Muriel was awarded the Frye stipendium by the Radboud University as being one of ten most promising female PhD students of that year at the Radboud University. During her PhD she was a member of the seminar committee of the Institute for Water and Wetland Research and was part of the organizing committee of the Radboud Honours Acadamy for bachelor students at the Faculty of Science. Starting February 2016, Muriel will work as a post-doc at the Department of Molecular Biology under supervision of dr. Felipe Cava to study the molecular mechanisms and function of the curved morphology of *Vibrio* bacteria.

Als ik steun, relativering of advies nodig had kon ik ook altijd terecht bij een paar inspirerende mensen die ik hierboven nog niet genoemd heb. Dank jullie wel, Willemijn (je bent zo positief en lief en het was heel leuk om te zien hoe je gegroeid bent tot een hele goede dokter), Tim (eigenlijk kijk ik best wel tegen je op, en gelukkig kunnen we ook nog eens heel erg lachen samen), Lennert (wat waren we een illuster duo samen en wat ben ik blij dat we bevriend zijn geraakt), Koen (gesprekken met jou zijn altijd fijn en verhelderend), Ralph (wie had na onze eerste ontmoeting ooit gedacht dat we zulke goede vrienden zouden worden ;)) en Janric (jij doet altijd zulke indrukwekkende dingen en ik vind 't altijd super om te discussieren over van alles).

Ik heb altijd kunnen rekenen op steun en interesse van een uitgebreide (schoon)familie, bestaand uit o.a. meerdere neefjes, nichtjes, ooms, tantes, oudooms, oudtantes en opa's en oma's; heel erg bedankt en super dat ik zo veel van jullie op de 13e zal zien! Ik ben erg gesteld en heel trots op mijn broer Adriaan; het vervelendste aan het verhuizen naar Zweden vind ik waarschijnlijk dat ik jou minder zal zien. Als ik weer terug ben (of jij ook in Zweden woont) blazen we Muriaan nieuw leven in! Het is evident dat ik nooit op dit punt gekomen zou zijn zonder Erica, Wouter, Martin en Barbara: jullie hebben me zoveel bijgebracht en steunen me nog steeds op zo veel manieren. Ik ben heel trots dat ik duidelijke elementen van jullie alle vier in me heb.

Sietse, jouw geduld en je grenzeloze steun zijn voor mij eigenlijk niet te bevatten. Het is toch echt ook dankzij jou dat ik het vertrouwen had om allerhande projecten in binnen- en buitenland op te pakken en door te zetten, en je hebt daardoor niet alleen een duidelijke hand gehad in hoe het proefschrift is geworden, maar ook in wie ik nu ben. Ik kijk ernaar uit om samen nog veel avonturen te beleven. Ik hou van jou.

The elegant method developed by the Bloomington team has quickly become the standard for detecting peptidoglycan in vivo and we were glad that we could collaborate with Erkin, Yves and Mike to show peptidoglycan in *Kuenenia stuttgartiensis*. It was a pleasure meeting the three of you at the GRC and always very nice to reflect on science and life with Erkin.

Felipe and Akbar, you are really great collaborators and I was very impressed by the speed with which you obtained the muropeptide results and provided the figures. Felipe, I am very much looking forward to join your lab and work with your amazing team!

Karin and Matthias, many thanks for sharing your experiences in the hunt for peptidoglycan in *Chlamydiae* with me during my visit to DOME and thereby putting us on track for finding peptidoglycan in anammox bacteria as well.

Met veel plezier heb ik deel uitgemaakt van de programmaraad RHA FNWI. Wat is het leuk om te zien hoe de studenten groeien terwijl zij met veel toewijding en creativiteit aan mooie projecten werken. Ik denk met een lach op mijn gezicht terug aan de vergaderingen in zowel de oude als de nieuwe samenstelling waar scherpe inzichten gecombineerd worden met veel humor. Wim, met je vragen zorgde jij er altijd voor dat de studenten met andere ogen naar hun eigen onderzoek gingen kijken. Als voorzitter gaf je altijd vrijheid en vertrouwen en was je er altijd op de momenten die erom gingen. Joop, zonder jou was het programma zeker niet zo robuust geweest als het nu is. Ik ben blij dat we de RHA-eer hoog hebben kunnen houden bij de IWWR quiz. Hay, jij bent de vaste waarde van de RHA, en degene die er steeds op een hele vriendelijke manier in slaagt de raad onder controle te houden en met veel interesse studenten volgt en de ouders bij de uitreikingen betrekt. Jan, terecht door de studenten op handen gedragen, bedankt voor de scherpe analyses en inzichten, waar ik veel van heb geleerd. Teun, het is maar goed dat je die dag toch naar het werkcollege bent gekomen, anders was je vast niet aangenomen (;)) en had ik nu niet met zoveel plezier met je samengewerkt en bijgepraat. Ik ben heel benieuwd in wat voor carriere je terecht gaat komen, maar ik ben er zeker van dat het iets gaafs en belangrijks gaat worden. Ook hartelijk dank aan Daniel, Elena, Ernst, Esra, Fleur, Frits, John, Klaas, Lejla, Leonie, Nicolette, Sjaak, Stephanie, Tim en Wilke, de mentoren, meesters en studenten voor de leuke tijd.

I've been fortunate to have a favorite pastime that brought me in contact with some of the most supportive and nicest people I know; it has always been a pleasure to play field hockey. Teamgenootjes van Union D5 (en Jouke), ik zal jullie vreselijk gaan missen; super bedankt voor alle gezelligheid en het altijd aanwezige begrip als ik weer eens een paar maanden weg was. Anneke, ik ben stiekem best blij dat je een hekel hebt aan zaalhockey, anders had ik niet jaarlijks in de winter mee kunnen doen met Apeliotes D1 onder leiding van het zaaltactiek-brein Willem. HC Wien Damen und Flo, es hat mir ganz viel spass gemacht euch kennen zu lernen und bei euch mit zu spielen. Auch ein Dankeschön an den Damen von Eintracht Braunschweig und Carsten, dass ich mit euch richtig Hallenhockey spielen durfte und mir ab jetzt immer eine Löwin nennen kann ;).

(we had so much fun when I stayed with you! And you helped me out at multiple occasions), Conny (many thanks for your help with both projects and all the chats), Valentin (your anecdotes are legendary!), Zoe, Heinz, Gary, Arturo, Eva L, Markus, Bettina, Julia, Andrea K, Behnam and Andrea L, I was so lucky to have you around, you were always happy to help me find something in the lab or give me advice on how to tackle the project or how to enjoy Vienna and I had a lot of fun with you :). Dass ich mir wirklich wohl gefühlt habe in Wien, war auch wegen meiner supernette WG-MitbewohnerInnen Ilka (und Hansi), Bini, Wilhelm und Or.

Christian and Mareike, it was a very nice experience to be part of your enthusiastic and ambitious group and to be surrounded by ideas focusing on the non-anammox *Planctomycetes*. I very much appreciate all your efforts to make me feel comfortable and welcome in your group and in Wolfenbüttel. Despite the singstar CD (thanks Anja ;)) the Christmas party is one of my favorite memories. I have grown very fond of my DSMZ colleagues that form a great, creative and supportive team: Olga, Christian B, Patrick, Timo and Anja. Olga, I very much enjoyed working as a team and I'm super proud of our keynote presentation!

Being at the famous lipid group of Jaap Sinninghe Damsté, even though only short, was a great experience. Ellen, met jou is het super samenwerken! Je kritische maar realistische blik op de protocollen, resultaten en mijn hoofdstuk vanuit het oogpunt van de chemie en je scherpe en humoristische uitleg van de MS hebben ervoor gezorgd dat ik echt verder kon komen dan een naieve bioloog. Eli, many thanks for helping me find my way in the lab.

My gratitude also goes out to Roland Benz and his group (Ivan, Eva, Satya, and the others) at the Jacobs University Bremen for the heartwarming hospitability and introducing me to the bilayer setups.

My projects would have been rather incomplete without the help of many collaborators. Many thanks for all the invested efforts and for making me a broader scientist.

Elly, ik prijs me erg gelukkig dat ik van jou (en Rob) de fijne kneepjes van het EM ambacht heb mogen leren en altijd bij jullie in Utrecht langs mocht komen voor hulp, adviezen en gezelligheid!

Geert-Jan & Liesbeth hartelijk dank voor jullie hulp bij de vele technieken en (de reparatie van) apparaten die het GI rijk is.

Hans, hartelijk dank voor je toewijding in de MS analyses en het doorspreken van de resultaten voor meerdere van mijn projecten, terwijl je al zo veel te doen had!

Thomas and coworkers in Heidelberg, great that you are looking at kustd1878; I am very curious how the crystal will look! I hope the protein behaves well.

Sebastian, you have helped me forward in multiple projects by introducing me to the right people. Many thanks for that!

Many thanks also to all the other colleagues and guests for your advice, enthusiasm, help, chats and for generating a good atmosphere in the department: Adam, Alvaro, Aniela, Annika, Arslan, Baoli, Bram, Claudia, Dimitra, Dorien, Eric, Francisca (wat superleuk dat je terug bent!), Frauke, Geert, Guylaine (in zo'n korte tijd al onmisbaar geworden), Harry, Jack, Jan, Jennifer, Jeroen, Joachim, Judith, Karin, Katharina, Katinka, Ke, Kim, Lina, Maartje, Mamoru, Mara, Marianne, Michela, Michiel, Mo, Nardy, Olivia, Sepehr, Simon, Suzanne, Theo, Tijs, Wouter M, Wouter V, Xristina (thanks for your pinterest foodie inspiration wall ☺) and Ziye. Without you, I would for sure not have had such a nice time at Microbiology!

Of course also many thanks to the numerous students that have contributed to the vibrant atmosphere in the department. Stijn, ik vond het een groot genoegen om jou te mogen helpen met je MreB project! Ik heb bewondering voor de manier waarop je grondigheid combineert met een soort van kalmte en optimisme die ervoor zorgt dat je je -ondanks de soms tegenvallende resultaten- niet uit het veld laat slaan. Ik wens je veel succes en veel goede resultaten toe in je verdere (onderzoeks)carrière! Goed om te weten dat jij en Dave de celbiologie nog een tijdje blijven versterken en van nieuwe impulsen blijven voorzien!

During my PhD, I was fortunate to visit several research groups. I have always felt very welcome and have enjoyed the visits which have broadened my view, introduced me to many new techniques and have been very valuable in several research lines.

Dear Reinhard, I feel really lucky that I could be part of your group in Regensburg and it has been a pleasure, an honor and a very valuable experience to learn so much in EM-related research from someone that has so much knowledge about this. Andreas, it was great fun working with you: many thanks for teaching me basic EM skills and introducing me to the Cressi and some nice aspects of life in Bavaria. I have had a lot of fun with my office mates Jenni, Thomas, Ben and Vroni and with Flo and Arnab with whom we shared the lab as well as many jokes. Jenni, I was so happy to have you around and even though we don't skype as often as we would like, we always have the butterfly connection! Liebe Beate, danke schön dass ich bei dir ein wirkliches Zuhause in Regensburg und eine ganze menge Spass hatte. Sibille und Laura, vielen Dank für die nette Zeit und die gemeinsame Ausflugen, wie zB. die legendäre Alpenausflug!

Paul and Tina, it has been great to be part of the glyco-group at the BOKU and I really enjoyed getting more insight into glycobiology. Visiting your group has been an impulse for several of my projects and I have always felt very welcome. Also many thanks to Paul Kosma for all the NMR analyses and meetings. Daniel, thanks for your MS analysis and your kind and elaborate interpretation and explanation of the results. Andrea S & Sonja, many thanks for helping me and teaching me several valuable glycobiology methods. Eva S

Lavinia, it was lots of fun having you as a cell biology colleague and I enjoyed seeing you grow into a confident PhD student. I am sure you will fulfill your new role of Laura's most senior PhD student well.

Marjan, wat fijn om jou bij de celbio groep te hebben. Altijd enthousiast en relativerend: dankjewel daarvoor en voor het versturen van pakketjes en de immunoblot assays.

Arjan, het was goed en verhelderend om met je samengewerkt te hebben. Bedankt dat ik namen mocht verzinnen voor de Verruco's die je met gevaar voor eigen leven hebt gesampled, met toewijding op hebt gekweekt en waarvan je met karakteristieke gedegenheid allerlei (fysiologische) geheimen hebt losgepeuterd!

Ahmad, in het begin van mijn PhD en aan het eind van de jouwe hebben we goed samen kunnen werken op het SolV project en daar heb ik veel van geleerd. Bij het schrijven van mijn Verruco deel heb ik vaak jouw proefschrift als inspiratie gebruikt.

Daan, wat een geluk dat we 'tegelijk' als PhD's begonnen zijn en wat gaaf om te zien hoe we ons hebben ontwikkeld en elkaar vooruit hebben kunnen helpen. Niet alleen heb ik dankzij jou een beetje bioinformatica benul en allerlei inzicht in de wetenschap in t algemeen, ook hoop ik dat ik een klein beetje van je indrukwekkende helicoptervisie over de microbiologie heb kunnen oppakken. Ik ben zo benieuwd hoe je postdoc uitpakt en hoe het daarna zal lopen en ik hoop vooral dat we ondanks ons beider verhuizingen nog steeds kunnen blijven sparren over de microbiologie. Supermooi dat jij mijn paranifm bent en ik de jouwe!

Martine, het was echt een kadootje dat je bij ons in het kantoor kwam zitten. Jouw aanstekelijke positiviteit gecombineerd met nuchterheid zorgen er steeds weer voor dat ondanks als dingen tegen zitten, ik alles weer wat zonniger inzie. Heel erg bedankt daarvoor en voor alle gezelligheid en veel succes met je mosjes!

Naomi, I admire your spontaneity and attentiveness. Both your dinner parties and your proteome skills are legendary- thanks for letting me be part of both. I wish you all the best in Germany.

Cornelia, ik ben heel blij dat je naar Nijmegen bent gekomen; bedankt voor het luisterend oor, de adviezen en de gezelligheid.

Rob de G, leuk dat ik zo lang je buurvrouw in het kantoor heb kunnen zijn, het was altijd gezellig even bij te kletsen en het laatste nieuws uit de faculteit te bespreken.

Boran, I am really really happy that you got involved in my project as well. I am super proud of the scientific results of the "infamous PG team": it's not every day that one can "rewrite" Brock. Many thanks for cheering me up on multiple occasions, the good conversations and for all the laughter, jokes and great anecdotes.

Acknowledgements

Upon starting my PhD project I could have never imagined that I would learn so many new things, at so many places with the support and help of so many friendly, helpful and creative people. I feel quite touched and grateful that so many people helped me along the way of my PhD and now it's my pleasure to thank all of you.

Ten eerste, natuurlijk, Laura. Ik kan me nog goed herrinneren hoe leuk ik het practicum BvMO vond met jou als begeleidster. Ik was natuurlijk dolblij en trots om bij jou stage te mogen lopen en vind het heel bijzonder dat ik al die jaren met jou als begeleidster heb mogen werken. Ik heb heel veel van je geleerd en we hebben samen allerlei avonturen beleefd die ik nog lang met een lach op mijn gezicht zal herrinneren! Ik vind het heel knap en ben je erg dankbaar hoe je mij hebt begeleid met een combinatie van heel veel vertrouwen en aandacht, maar ook veel vrijheid om mijn eigen beslissingen te nemen en mijn eigen weg te kiezen. Het is heel waardevol om met jou iemand als begeleidster te hebben waarvan ik weet dat ze altijd achter me staat. Ik kijk er met veel plezier naar uit om van de zijlijn te volgen hoe jij met de celbio groep nog veel geheimen van annamox gaat ontrafelen, maar ook nieuwe spannende research lines gaat ontwikkelen.

Het is een eer en een erg leerzaam proces om te mogen promoveren bij de beroemde prof. Mike Jetten. Ik vind het bijzonder knap hoe je met zo'n grote groep in staat bent om overzicht te hebben en op de juiste momenten treffende aanwijzingen op maat te geven. Zoals die keer dat je me wees op een interessant congres in Duitsland- ik heb goed naar je geluisterd ;). Ik ben dankbaar voor de vrijgevigheid aan unieke kansen en mogelijkheden die je me hebt geboden om me op velerlei gebieden te kunnen ontwikkelen.

Huub, ik vond het leuk om ook deel uit te maken van het Verruco-team. Prachtig om te zien hoe het je gelukt is om de vulkanische microbiologie op de kaart te zetten: ik ga met plezier volgen wat voor mooie resultaten dat de komende tijd op gaat leveren.

Ik heb veel te danken aan Rob en je weet waarschijnlijk nog niet half hoe blij ik ben dat je het celbio team bent komen versterken! Ik ben er erg trots op hoe we samen 1001 ideeen hebben verzonnen die tot mooie resultaten hebben geleid en ga je niet aflatende stroom aan ideeen, tips, adviezen en lessen over EM technieken erg missen. Ik ben blij en trots dat je binnenkort als paranifm naast me staat!

Sarah, ik heb veel met je gelachen en je was de perfecte roommate op congressen! Ik had maar mooi mazzel dat ik van jou als senior PhD in de anammox celbio heb kunnen leren. Ik vind het superstoer dat je nu bij FEI zo'n goede baan hebt en hopelijk kan ik nog eens een kaartje bij je lospeuteren op een EM congres ;).

Ming, many thanks for sharing your advice and perspectives with me. And thanks for making it possible that Sietse has been your colleague as well; I am sad for the both of you it didn't last a bit longer.

Yu NY, Wagner JR, Laird MR, Melli G, Rey S, Lo R, Dao P, Sahinalp SC, Ester M, Foster LJ, Brinkman FSL (2010) pSORTb 3.0: Improved protein subcellular localization prediction with refined localization subcategories and predictive capabilities for all prokaryotes. *Bioinformatics* 26: 1608-1615.

van der Star WRL, Dijkema C, de Waard P, Picioreanu C, Strous M, van Loosdrecht MCM (2010) An intracellular pH gradient in the anammox bacterium *Kuenenia stuttgartiensis* as evaluated by ^{31}P NMR. *Appl Microbiol Biotechnol* 86: 311-317.

van Niftrik L, Geerts WJC, van Donselaar EG, Humbel BM, Webb RI, Fuerst JA, Verkleij AJ, Jetten MSM, Strous M (2008). Linking ultrastructure and function in four genera of anaerobic ammonium-oxidizing bacteria: cell plan, glycogen storage, and localization of cytochrome c proteins. *J Bacteriol* 190: 708-717.

van Teeseling MCF, Pol A, Harhangi H, van der Zwart S, Jetten MSM, Op den Camp HJM, van Niftrik L (2014) Expanding the verrucomicrobial methanotrophic world: description of three novel species of *Methylacidimicrobium* gen. nov.. *Appl Environ Microbiol* 80: 6782-6791.

Vorobev AV, Baani M, Doronina NV, Brady AL, Liesack W, Dunfield PF, Dedysh SN (2011) *Methyloferula stellate* gen.nov., sp.nov., an acidophilic, obligately methanotrophic bacterium that possesses only a soluble methane monooxygenase. *Int J Syst Evol Microbiol* 61: 2456-2463.

Wanner U, Egli T (1990) Dynamics of microbial-growth and cell composition in batch culture. *FEMS Microbiol Rev* 75: 19-44.

Ward N, Larsen Ø, Sakwa J, Bruseth L, Khouri H, Durkin AS, Dimitrov G, Jiang L, Scanlan D, Kang KH, Lewis M, Nelson KE, Methé B, Wu M, Heidelberg JF, Paulsen IT, Fouts D, Ravel J, Tettelin H, Ren Q, Read T, DeBoy RT, Seshadri R, Salzberg SL, Jensen HB, Birkeland NK, Nelson WC, Dodson RJ, Grindhaug SH, Holt I, Eidhammer I, Jonasen I, Vanaken S, Utterback T, Feldblyum TV, Fraser CM, Lillehaug JR, Eisen JA (2004) Genomic insights into methanotrophy: the complete genome sequence of *Methylococcus capsulatus* (Bath). *PLoS Biol* 2: e303.

Weijers JWH, Schouten S, Hopmans EC, Geenevasen JAJ, David ORP, Coleman JM, Pancost RD, Sinninghe Damsté JS (2006) Membrane lipids of mesophilic anaerobic bacteria thriving in peats have typical archaeal traits. *Environ Microbiol* 8: 648-657.

Weijers JWH, Schouten S, van den Donker JC, Hopmans EC, Sinninghe Damsté JS (2007) Environmental controls on bacterial tetraether membrane lipid distribution in soils. *Geochim Cosmochim Acta* 71: 703-713.

Wilson WA, Roach PJ, Montero M, Baroja-Fernandez E, Munoz FJ, Eydallin G, Viale AM, Pozueta-Romero J (2010) Regulation of glycogen metabolism in yeast and bacteria. *FEMS Microbiol Rev* 34: 952-985.

Wu ML, van Alen TA, van Donselaar EG, Strous M, Jetten MSM, van Niftrik L (2012a) Co-localization of particulate methane monooxygenase and cd_1 nitrite reductase in the denitrifying methanotroph ' *Candidatus* Methylomirabilis oxyfera'. *FEMS Microbiol Lett* 334: 49-56.

Wu ML, van Teeseling MCF, Willems MJR, van Donselaar EG, Klingl A, Rachel R, Geerts WJC, Jetten MSM, van Niftrik L (2012b) Ultrastructure of the Denitrifying Methanotroph "*Candidatus* Methylomirabilis oxyfera," a Novel Polygon-Shaped Bacterium. *J Bacteriol* 194: 284-291.

Wu ML, Wessels HJCT, Pol A, Op den Camp HJM, Jetten MSM, van Niftrik L, Keltjens J (2015) XoxF-type methanol dehydrogenase from the anaerobic methanotroph "*Candidatus* Methylomirabilis oxyfera". *Appl Environ Microbiol* 81: 1442-1451.

Rasigraf O, Kool DM, Jetten MSM, Sinninghe Damsté JS, Ettwig KF (2014) Autotrophic carbon dioxide fixation via the Calvin-Benson-Bassham cycle by the denitrifying methanotroph *Methylomirabilis oxyfera*. *Appl Environ Microbiol* 80: 2541-2460.

Reynolds ES (1963) The use of lead citrate at high pH as an electron-opaque stain in electron microscopy. *J Cell Biol* 17: 208-212.

Richter M, Rosselló-Móra R (2009) Shifting the genomic gold standard for the prokaryotic species definition. *Proc Natl Acad Sci USA* 106: 19126-19131.

Roth J (1982) The preparation of protein A-gold complexes with 3 nm and 15 nm gold particles and their use in labelling multiple antigens on ultra-thin sections. *Histochem J* 14: 791-801.

Schloss PD, Handelsman J (2004) Status of the Microbial Census. *Microbiol Mol Biol Rev* 68: 686-691.

Semrau JD, DiSpirito AA, Yoon S (2010) Methanotrophs and copper. *FEMS Microbiol Rev* 34: 496-531.

Seok YJ, Koo BM, Sondej M, Peterkofsky A (2001) Regulation of *E. coli* glycogen phosphorylase activity by HPr. *J Mol Microbiol Biotechnol* 3: 385-393.

Sharp CE, Stott MB, Dunfield PF (2012) Detection of autotrophic verrucomicrobial methanotrophs in a geothermal environment using stable isotope probing. *Front Microbiol* 3:303.

Sharp CE, Op den Camp HJM, Tamas I, Dunfield PF. 2013. Unusual members of the PVC Superphylum: The Methanotrophic Verrucomicrobia genus "Methylacidiphilum", p 211-227. *In* Fuerst JA (ed), Planctomycetes: Cell structure, origins and biology. Humana Press (Springer), New York, USA. ISBN: 978-1-62703-502-6.

Sharp CE, Smirnova AV, Graham JM, Stott MB, Khadka R, Moore TR, Grasby SE, Strack M, Dunfield PF (2014) Distribution and diversity of *Verrucomicrobia* methanotrophs in geothermal and acidic environments. *Environ Microbiol* 16: 1867-1878.

Stackebrandt E, Ebers J (2006) Taxonomic parameters revisited: tarnished gold standards. *Microbiol Today* 33: 152-155.

Stackebrandt E (2011) Molecular taxonomic parameters. *Microbiol Australia* 32: 59-61.

Tamura K, Peterson D, Peterson N, Stecher G, Nei M, Kumar S (2011) MEGA5: Molecular Evolutionary Genetics Analysis using Maximum Likelihood, Evolutionary Distance, and Maximum Parsimony methods. *Mol Biol Evol* 28: 2731-2739.

Taylor S, Ninjoor V, Dowd DM, Tappel AL (1974) Cathepsin b2 measurement by sensitive fluorometric ammonia analysis. *Anal Biochem* 60: 153-162.

Theisen AR, Ali MH, Radajewski S, Dumont MG, Dunfield PF, McDonald IR, Dedysh SN, Miguez CB, Murrel JC (2005) Regulation on methane oxidation in the facultative methanotroph *Methylocella silvestris* BL2. *Mol Microbiol* 58: 682-692.

Myronova N, Kitmitto A, Collins RF, Miyaji A, Dalton H (2006) Three-dimensional structure determination of a protein supercomplex that oxidizes methane to formaldehyde in *Methylococcus capsulatus* (Bath). *Biochemistry* 3: 11905-11914.

Naeem S, Li S (1997) Biodiversity enhances ecosystem reliability. *Nature* 390: 507-509.

Nakagawa T, Mitsui R, Tani A, Sasa K, Tashiro S, Iwama T, Hayakawa T, Kawai K (2012) A catalytic role of XoxF1 as La^{3+}-dependent methanol dehydrogenase in *Methylobacterium extorquens* Strain AM1. *PLoS One* 7: e50480.

Nguyen H-HT, Elliot SJ, Yip JH-K, Chan SI (1998) The particulate methane monooxygenase from *Methylococcus capsulatus* (Bath) is a novel copper-containing three-subunit enzyme. *J Biol Chem* 273: 7957-7966.

Op den Camp HJM, Islam T, Stott MB, Harhangi HR, Hynes A, Schouten S, Jetten MSM, Birkeland N-K, Pol A, Dunfield PF (2009) Environmental, genomic and taxonomic perspectives on methanotrophic *Verrucomicrobia*. *Environ Microbiol Rep* 1: 293-306.

Pagaling E, Yang K, Yan T (2014) Pyrosequencing reveals correlations between extremely acidophilic bacterial communities with hydrogen sulphide concentrations, pH and inert polymer coatings at concrete sewer crown surfaces. *J Appl Bacteriol* 117: 50-64.

Petersen TN, Brunak S, von Heijne G, Nielsen H (2011) SignalP 4.0: discriminating signal peptides from transmembrane regions. *Nat Methods* 8: 785-786.

Pieja AJ, Rostkowski KH, Criddle CS (2011a) Distribution and selection of poly-3-hydroxybutyrate production capacity in methanotrophic proteobacteria. *Microb Ecol* 62: 564-573.

Pieja AJ, Sundstrom ER, Criddle CS (2011b) Poly-3-hydroxybutyrate metabolism in the Type II methanotroph *Methylocystis parvus* OBBP. *Appl Environ Microbiol* 77: 6012-6019.

Pilhofer M, Rappl K, Eckl C, Bauer AP, Ludwig W, Schleifer K-H, Petroni G (2008) Characterization and Evolution of cell division and cell wall synthesis genes in the bacterial phyla *Verrucomicrobia*, *Lentisphaerae*, *Chlamydiae*, and *Planctomycetes* and phylogentic comparison with rRNA genes. *J bacterial* 190: 3192-3202.

Preiss J (1996) ADP-glucose pyrophosphorylase: basic science and applications in biotechnology. *Biotechnol Annu Rev* 2: 259-279.

Pol A, Heijmans K, Harhangi HR, Tedesco D, Jetten MSM, Op den Camp HJM (2007) Methanotrophy below pH1 by a new Verrucomicrobia species. *Nature* 450: 874-878.

Pol A, Barends TRM, Dietl A, Khadem AF, Eygensteyn J, Jetten MSM, Op den Camp HJM (2014) Rare earth metals are essential for methanotrophic life in volcanic mudpots. *Environ Microbiol* 16: 255-264.

Raghoebarsing AA, Pol A, van de Pas-Schoonen KT, Smolders AJP, Ettwig KF, Rijpstra WIC, Schouten S, Sinninghe Damsté JS, Op den Camp HJM, Jetten MSM, Strous M (2006) A microbial consortium couples anaerobic methane oxidation to denitrification. *Nature* 440: 918-921.

Knittel K, Boetius A (2009) Anaerobic oxidation of methane: Progress with an unknown process. *Ann Rev Microbiol* 63: 311-334.

Konstantinidis KT, Tiedje JM (2007) Prokaryotic taxonomy and phylogeny in the genomic era: advancements and challenges ahead. *Curr Opin Microbiol* 10: 504-509.

Krogh A, Larsson B, von Heijne G, Sonnhammer ELL (2001) Predicting transmembrane protein topology with a hidden markov model: application to complete genomes. *J Mol Biol* 306: 567-580.

Kvenvolden KA, Rogers BW (2005) Gaia's breath - global methane exhalations. *Marine Petrol Geol* 22: 579-590.

Laemmli UK (1970) Cleavage of structural proteins during the assembly of the head of bacteriophage T4. *Nature* 15: 680-685.

Lee K-C, Webb RI, Janssen PH, Sangwan P, Romeo T, Staley JT, Fuerst JA (2009) Phylum *Verrucomicrobia* representatives share a compartmentalized cell plan with members of bacterial phylum *Planctomycetes*. *BMC Microbiol* 9: 5.

Lieberman RL, Rosenzweig AC (2005) Crystal structure of a membrane-bound metalloenzyme that catalyses the biological oxidation of methane. *Nature* 434: 177-182.

Linton JD, Cripps RE (1978) Occurrence and identification of intracellular polyglucose storage granules in *Methylococcus* NCBI 11083 grown in chemostat culture on methane. *Arch Microbiol* 117: 41-48.

Macalady JL, Vestling MM, Baumler D, Boekelheide N, Kaspar CW, Banfield JF (2004) Tetraether-linked membrane monolayers in *Ferroplasma* spp: a key to survival in acid. *Extremophiles* 8: 411-419.

Malashenko YR, Pirog TP, Romanovskaya VA, Sokolov IG, Grinberg TA (2001). Search for methanotrophic producers of exopolysaccharides. *Appl Biochem Microbiol* 37: 599-602.

McDonald IR, Bodrossy L, Chen Y, Murrell JC (2007) Molecular ecology techniques for the study of aerobic methanotrophs. *Appl Environ Microbiol* 74: 1305-1315.

Mende DR, Sunagawa S, Zeller G, Bork P (2013) Accurate and universal delineation of prokaryotic species. *Nat Methods* 10: 881-884.

Merucci L, Bogliolo MP, Buongiorno MF, Teggi S (2006) Spectral emissivity and temperature maps of the Solfatara crater from DAIS hyperspectral images. *Annals Geophysics* 49: 235-244.

Milucka J, Ferdelman TG, Polerecky L, Franzke D, Wegener G, Schmid M, Lieberwirth I, Wagner M, Widdel F, Kuypers MMM (2012) Zero-valent sulphur is a key intermediate in marine methane oxidation. *Nature* 491: 541-546.

Mortazavi A, Williams BA, McCue K, Schaeffer L, Wold B (2008) Mapping and quantifying mammalian transcriptomes by RNA-Seq. *Nat Methods* 5: 621-628.

Hu B-L, Shen L-D, Lian X, Zhu Q, Liu S, Huang Q, He Z-F, Geng S, Cheng D-Q, Lou L-P, Xu X-Y, Zheng P, He Y-F (2014) Evidence for nitrite-dependent anaerobic methane oxidation as a previously overlooked microbial methane sink in wetlands. *Proc Natl Acad Sci USA* 111: 4495-4500.

Islam T, Jensen S, Reigstad LJ, Larsen Ø, Birkeland N-K (2008) Methane oxidation at 55 °C and pH 2 by a thermoacidiophilic bacterium belonging to the *Verrucomicrobia* phylum. *Proc Natl Acad Sci USA* 105: 300-304.

Jacob DJ (1999) Introduction to atmospheric chemistry. Princeton University Press, Princeton, USA. ISBN: 0-691-00185-5.

Jukes TH, Cantor CR. 1969. Evolution of protein molecules, p 21-132. *In* Munro HN (ed), Mammalian Protein Metabolism. Academic Press, New York.

Kalyuzhnaya MG, Hristova KR, Lidstrom ME, Chistoserdova L (2008) Characterization of a novel methanol dehydrogenase in representatives of *Burkholderiales*: implications for environmental detection of methylotrophy and evidence for convergent evolution. *J Bacteriol* 190: 3817-3823.

Kawase M, Motohashi N, Sakagami H, Kanamoto T, Nakashima H, Ferenczy L, Wolfard K, Miskolci C, Molnár J (2001) Antimicrobial activity of trifluoromethyl ketones and their synergism with promethazine. *Int J Antimicrob Agents* 18: 161-165.

Keltjens JT, Pol A, Reimann J, Op den Camp HJM (2014) PQQ-dependent methanol dehydrogenases: rare-earth elements make a difference. *Appl Microbiol Biotechnol* 98: 6163-6183.

Khadem AF, Pol A, Jetten MSM, Op den Camp HJM (2010) Nitrogen fixation by the verrucomicrobial methanotroph *Methylacidiphilum fumariolicum* SolV. *Microbiology SGM* 156: 1052-1059.

Khadem AF, Pol A, Wieczorek A, Mohammadi SS, Francoijs K-J, Stunnenberg HG, Jetten MSM, Op den Camp HJM (2011) Autotrophic methanotrophy in Verrucomicrobia: *Methylacidiphilum fumariolicum* SolV uses the Calvin-Benson-Bassham cycle for carbon dioxide fixation. *J Bacteriol* 193: 4438-4446.

Khadem AF, Wieczorek AS, Pol A, Vuilleumier S, Harhangi HR, Dunfield PF, Kalyuzhnaya MG, Murrel JC, Fracoijs K-J, Stunnenberg HG, Stein LY, DiSpirito AA, Semrau JD, Lajus A, Médigue C, Klotz MG, Jetten MSM, Op den Camp HJM (2012a) Draft genome sequence of the volcano-inhabiting thermoacidophilic methanotroph *Methylacidiphilum fumariolicum* strain SolV. *J Bacteriol* 194: 3729-3730.

Khadem AF, Pol A, Wieczorek AS, Jetten MSM, Op den Camp HJM (2012b) Metabolic regulation of "*Ca.* Methylacidiphilum fumariolicum" SolV cells grown under different nitrogen and oxygen limitations. *Front Microbiol* 3: 266.

Khadem AF, van Teeseling MCF, van Niftrik L, Jetten MSM, Op den Camp HJM, Pol A (2012c) Genomic and physiological analysis of carbon storage in the verrucomicrobial methanotroph "*Ca.* Methylacidiphilum fumariolicum" SolV. *Front Microbiol* 3: 345.

Khmelenina VN, Kalyuzhnaya MG, Sakharovsky VG, Suzina NE, Trotsenko YA, Gottschalk G (1999) Osmoadaptation in halophilic and alkaliphilic methanotrophs. *Arch Microbiol* 172: 321-329.

Eshinimaev BT, Khmelenina VN, Sakharovskii VG, Suzina NE, Trotsenko YA (2002) Physiological, biochemical, and cytological characteristics of a haloalkalitolerant methanotroph grown on methanol. *Microbiology* 71: 512-518.

Etiope G, Klusman RW (2002) Geologic emissions of methane to the atmosphere. *Chemosphere* 49: 777-7789.

Ettwig KF, Shima S, van de Pas-Schoonen KT, Kahnt J, Medema MH, op den Camp HJM, Jetten MSM, Strous M (2008) Denitrifying bacteria anaerobically oxidize methane in the absence of *Archaea*. *Environ Microbiol* 10: 3164-3173.

Ettwig KF, Butler MK, Le Paslier D, Pelletier E, Mangenot S, Kuypers MMM, Schreiber F, Dutilh BE, Zedelius J, de Beer D, Gloerich J, Wessels HJCT, van Alen T, Luesken F, Wu ML, van de Pas-Schoonen KT, Op den Camp HJM, Janssen-Megens EM, Francoijs K-J, Stunnenberg H, Weissenbach J, Jetten MSM, Strous M (2010) Nitrite-driven anaerobic methane oxidation by oxygenic bacteria. *Nature* 464: 543-548.

Ettwig KF, Speth DR, Reimann J, Wu ML, Jetten MSM, Keltjens JT (2012) Bacterial oxygen production in the dark. *Front Microbiol* 3: 273.

Fassel TA, Buchholz LA, Collins MLP, Remsen CC (1992) Localization of methanol dehydrogenase in two strains of methylotrophic bacteria detected by immunogold labeling. *Appl Environ Microbiol* 58: 2302-2307.

Forster P, Ramaswamy V, Artaxo P, Berntsen T, Betts R, Fahey DW, Haywood J, Lean J, Lowe DC, Myhre G, Nganga J, Prinn R, Raga G, Schulz M, Van Dorland R (2007) Changes in atmospheric constituents and in radiative forcing, p 129-234. *In* Solomon S, Qin D, Manning M, Chen Z, Marquis M, Averyt KB, Tignor M, Miller HL (eds), Climate Change 2007: the physical science basis. Contribution of Working Group I to the Fourth Assessment Report of the Intergovernmental Panel on Climate Change. Cambridge Univesity Press, Cambridge, UK. ISBN: 978-0521705967.

Goris J, Konstantinidis KT, Klappenbach JA, Coenye T, Vandamme P, Tiedje JM (2007) DNA-DNA hybridization values and their relationship to whole-genome sequence similarities. *Int J Syst Evol Microbiol* 57: 81-91.

Han J, Burgess K (2010) Fluorescent indicators for intracellular pH. *Chem Rev* 110: 2709-2728.

Hanson RS, Hanson TE (1996) Methanotrophic bacteria. *Microbiol Rev* 60: 439-471.

Haroon MF, Hu S, Shi Y, Imelfort M, Keller J, Hugenholtz P, Yuan Z, Tyson GW (2013) Anaerobic oxidation of methane coupled to nitrate reduction in a novel archaeal lineage. *Nature* 500: 567-570.

Hooper DU, Chapin III FS, Ewel JJ, Hector A, Inchausti P, Lavorel S, Lawton JH, Lodge DM, Loreau M, Naeem S, Schmid B, Setälä H, Symstad AJ, Vandermeer J, Wardle DA (2005) Effects of biodiversity on ecosystem functioning: a consensus of current knowledge. *Ecol Monograph* 75: 3-35.

Hou S, Makarova KS, Saw JHW, Senin P, Ly BV, Zhou Z, Ren Y, Wang J, Galperin MY, Omelchenko MV, Wolf YI, Yutin N, Koonin EV, Stott MB, Mountain BW, Crowe MA, Smirnova AV, Dunfield PF, Feng L, Wang L, Alam M (2008) Complete genome sequence of the extremely acidophilic methanotroph isolate V4, *Methylacidiphilum infernorum*, a representative of the bacterial phylum *Verrucomicrobia*. *Biol Direct* 3:26.

Chistoserdova L (2011) Modularity of methylotrophy, revisited. *Environ Microbiol* 13: 2603-2622.

Cid E, Geremia RA, Guinovarta JJ, Ferrer JC (2002) Glycogen synthase: towards a minimum catalytic unit? *FEBS Lett* 528: 5-11.

Conrad R (2009) The global methane cycle: recent advances in understanding the microbial processes involved. *Environ Microbiol Rep* 1: 285-292.

Culpepper MA, Rosenzweig AC (2012) Architecture and active site of particulate methane monooxygenase. *Crit Rev Biochem Mol Biol* 47: 483-492.

Daims H, Brühl A, Amann R, Schleifer K-H, Wagner M (1999) The domain-specific probe EUB338 is insufficient for the detection of all *Bacteria*: Development and evaluation of a more comprehensive probe set. *System Appl Microbiol* 22: 434-444.

De Boer W, Hazeu W (1972) Observations on the fine structure of a methane-oxidizing bacterium. *Antonie van Leeuwenhoek* 38: 33-47.

Dedysh SN, Liesack W, Khmelenina VN, Suzina NE, Trotsenko YA, Semrau JD, Bares AM, Panikov NS, Tiedje JM (2000) *Methylocella palustris* gen. nov., sp. nov., a new methane-oxidizing acidophilic bacterium from peat bogs, representing a novel subtype of serine-pathway methanotrophs. *Int J Syst Evol Microbiol* 50: 955-969.

Dedysh SN, Berestovskaya YY, Vasylieva LV, Belova SE, Khmelenina VN, Suzina NE, Trotsenko YA, Liesack W, Zavarzin GA (2004) *Methylocella tundra* sp.nov., a novel methanotrophic bacterium from acidic tundra peatlands. *Int J Syst Evol Microbiol* 54: 151-156.

Docampo R, Moreno SNJ (2001) The acidocalcisome. *Mol Biochem Parasit* 114: 151-159.

Domman DB, Steven BT, Ward NL (2010) Random transposon mutagenesis of *Verrucomicrobium spinosum* DSM 4136^T. *Arch Microbiol* 193: 666.

Dunfield PF, Khmelenina VN, Suzina NE, Trotsenko YA, Dedysh SN (2003) *Methylocella silvestris* sp. nov., a novel methanotroph isolated from an acidic forest cambisol. *Int J Syst Evol Microbiol* 53: 1231-1239.

Dunfield PF, Yuryev A, Senin P, Smirnova AV, Stott MB, Hou S, Ly B, Saw JH, Zhou Z, Ren Y, Wang J, Mountain BW, Crowe MA, Weatherby TM, Bodelier PLEm Liesack W, Feng L, Wang L, Alam M (2007) Methane oxidation by an extremely acidophilic bacterium of the phylum Verrucomicrobia. *Nature* 450: 879-882.

Erbilgin O, McDonald KL, Kerfeld CA (2014) Characterization of a planctomycetal organelle: a novel bacterial microcompartment for the aerobic degradation of plant saccharides. *Appl Environ Microbiol* 80: 2193-2205.

Erikstad H-A, Jensen S, Keen TJ, Birkeland N-K (2012) Differential expression of particulate methane monooxygenase genes in the verrucomicrobial methanotroph "*Methylacidiphilum kamchatkense*" Kam1. *Extremophiles* 16: 405-409.

References

Adékambi T, Shinnick TM, Raoult D, Drancourt M (2008) Complete *rpoB* gene sequencing as a suitable supplement to DNA-DNA hybridization for bacterial species and genus delineation. *Int J Syst Evol Microbiol* 58: 1807-1814.

Altschul SF, Gish W, Miller W, Myers EW, Lipman DJ (1990) Basic local alignment search tool. *J Mol Biol* 215: 403-410.

Anvar SY, Frank J, Pol A, Schmitz A, Kraaijeveld K, den Dunnen JT, Op den Camp HJM (2014) The genomic landscape of the verrucomicrobial methanotroph *Methylacidiphilum fumariolicum* SolV. *BMC Genomics* 5: 914.

Aziz RK, Bartels D, Best AA, DeJongh M, Disz T, Edwards RA, Formsma K, Gerdes S, Glass EM, Kubal M, Meyer F, Olsen GJ, Olson R, Osterman AL, Overbeek RA, McNeil LK, Paarmann D, Paczian T, Parrello B, Pusch GD, Reich C, Stevens R, Vassieva O, Vonstein V, Wilke A, Zagnitko O (2008) The RAST Server: rapid annotations using subsystems technology. *BMC Genomics* 9: 75.

Baker-Austin C, Dopson M (2007) Life in acid: pH homeostasis in acidophiles. *Trends Microbiol* 15: 165-171.

Balasubramanian R, Smith SM, Rawat S, Yatsunyk LA, Stemmler TL, Rosenzweig AC (2010) Oxidation of methane by a biological dicopper centre. *Nature* 465: 115-119.

Beal EJ, House CH, Orphan VJ (2009) Manganese- and iron-dependent marine methane oxidation. *Science* 325: 184-187.

Boetius A, Ravenschlag K, Schubert CJ, Rickert D, Widdel F, Gieseke A, Amann R, Jørgensen BB, Witte U, Pfannkuche O (2000) A marine microbial consortium apparently mediating anaerobic oxidation of methane. *Nature* 407: 623-626.

Boyd ES, Hamilton TL, Wang J, He L, Zhang CL (2013) The role of tetraether lipid composition in the adaptation of thermophilic archaea to acidity. *Front Microbiol* 4: 62.

Bradbury S, Stoward PJ (1967) The specific cytochemical demonstration in the electron microscope of periodate-reactive mucosubstances and polysaccharides containing vic-glycol groups. *Histochemie* 11: 71-80.

Brantner CA, Remsen CC, Owen HA, Buchholz LA, Collins MLP (2002) Intracellular localization of the particulate methane monooxygenase and methanol dehydrogenase in *Methylomicrobium album* BG8. *Arch Microbiol* 178: 59-64.

Castaldi S, Tedesco D (2005) Methane production and consumption in an active volcanic environment of Southern Italy. *Chemosphere* 58: 131-139.

Chan JZ-M, Halachev MR, Loman NJ, Constantinidou C, Pallen MJ (2012) Defining bacterial species in the genomic era: insights from the genus Acinetobacter. *BMC Microbiol* 12: 302.

Chistoserdova L, Kalyuzhnaya MG, Lidstrom ME (2009) The expanding world of methylotrophic metabolism. *Annu Rev Microbiol* 63: 477-499.

transferred subsequently to media with small pH differences. This suggests that adaptation plays an important role in the pH tolerance. An interesting approach to start such a research line would be to measure the pH in the different compartments of the cells, for instance using ^{31}P nuclear magnetic resonance (NMR) spectrometry (van der Star et al, 2010) or fluorescent pH indicators (Han & Burgess, 2010). The latter technique, however, might not provide sufficient resolution at the low pHs that are physiologically relevant for the methanotrophic *Verrucomicrobia*. If, as is common for acidophiles, the intracellular pH is higher than the pH in the environment (Baker-Austin & Dopson, 2007) the hunt for mechanisms responsible for this pH difference would be open.

One possible acid tolerance mechanism is a membrane composition that ensures protons to be effectively hindered to enter the cell. Indeed, some lipids are specifically associated with low proton permeability, such as the so-called GDGT (glycerol dialkyl glycerol tetraether) lipids that have been found in many (acidophilic) Archaea (Boyd et al, 2013), but also in some bacterial species (Weijers et al, 2006). These GDGTs tend to be more abundant and have a slightly different composition at a lower pH (Macalady et al, 2004; Weijers et al, 2007; Boyd et al, 2013). No investigations into the presence of GDGT lipids have been performed in methanotrophic *Verrucomicrobia*, but instead the phospholipid fatty acids (PLFAs) of the three *Methylacidiphilum* species were found to be highly saturated, which could also decrease the membrane permeability to protons (Op den Camp et al, 2009). Still it would be worthwhile to investigate if GDGTs are present and if the amount of saturated PLFAs changes when the methanotrophic *Verrucomicrobia* are grown at different pH values.

Another mechanism frequently used by acidophiles to keep the intracellular pH more or less neutral is the use of proton pumps to export protons out of the cell (Baker-Austin & Dopson, 2007). It would be a good start to search all available verrucomicrobial methanotroph genomes for putative proton efflux systems. The *Methylacidiphilum infernorum* genome indeed contains an additional operon encoding for the H^+-translocating F_1F_O-ATPase subunits, of which one operon might encode an enzyme that hydrolyzes ATP to pump protons out of the cell (Hou et al, 2008). A more in-depth study should be performed into this and potential other proton efflux systems in order to clarify if they pump out protons. A possible approach to study the role of proton efflux systems would be to use specific proton pump inhibitors such as trifluoromethyl ketones, although the concentration has to be well chosen since inhibition of proton pumps is lethal to many cells (Kawase et al, 2001).

All in all, many open questions remain about the cell biology of verrucomicrobial methanotrophs in specific, but also about this group of recently discovered organisms in general. Maybe additional research will show many more verrucomicrobial methanotrophs, which could have variations in the cell plan and might be able to live in a broader range of conditions. Future research will surely have many interesting findings in store concerning verrucomicrobial methanotrophs and will give a better insight in the importance of this group of micro-organisms on the atmospheric methane balance.

possible candidates involved in polyphosphate metabolism have been identified (polyphosphate kinase and exopolyphosphatase) and it might be a good start to localize these enzymes via immunogold localization. Another interesting approach would be to make knockout mutants (discussed below) of these genes and to assess for possible ED particle-associated phenotypes.

Electron light/glycogen particles. In comparison to the ED particles, more is known about the EL particles concerning the function and circumstances under which the particles are synthesized (chapter 2). However, it remains a question how the synthesis and degradation of these particles is regulated and which proteins are involved in synthesizing and degrading these particles. Again, it could be interesting to localize enzymes that are predicted to be involved in the synthesis and degradation of glycogen via immunogold localization. For a more thorough understanding of the role of the different proteins involved in glycogen metabolism, however, knock-out mutants might be necessary. In addition, it would be interesting to investigate if the particles have a protein shell or another structure that borders them and if the enzymes involved in their synthesis and degradation are in some way associated with this structure. For this purpose, it would be helpful to isolate the EL particles from the cell so that for instance mass spectrometry can be performed to identify proteins associated with these particles. An observation that poses additional questions is that the EL particles seem to have a preference to localize towards the poles of the cell. It remains an open question how the cells control the location (and size) of these particles and if this is arranged via the enzymes involved in synthesis or if other, structural, proteins are involved.

Genetic system. In order to study for instance the biosynthesis and degradation of the EL and ED particles as well as many other processes, it would be very valuable to have the ability to make targeted mutants of the methanotrophic *Verrucomicrobia*. Up to my knowledge, *Verrucomicrobium spinosum* is the only verrucomicrobial species that genetic tools have been applied to (Domman et al, 2010). In the case of *V. spinosum*, random transposon mutagenesis via electroporation was applied and this might also be an interesting approach for the methanotrophic *Verrucomicrobia*. This approach does, however, not make it possible to create targeted mutants of specific genes. Instead a mutant library could be created and screened for certain phenotypes, for instance the absence of ED or EL particles. This screening step of an entire library often takes a considerable time investment. It could, however, also lead to the identification of genes that were not expected to be involved in certain processes. An approach to generate targeted knockout mutants making use of homologous recombination has recently been applied to a species of *Planctomycetes*, another phylum where genetic tools are a very recent addition (Erbilgin et al, 2014). It seems worthwhile to apply this technique to (methanotrophic) *Verrucomicrobia* as well.

Ability to survive in extreme conditions. It is an intriguing question which mechanisms the verrucomicrobial methanotrophs have evolved to be able to survive the extremely low pH and elevated temperatures. Results from chapter 4 show that cells do not survive a large change in pH at once, but they can be adapted to quite a broad pH range if they are

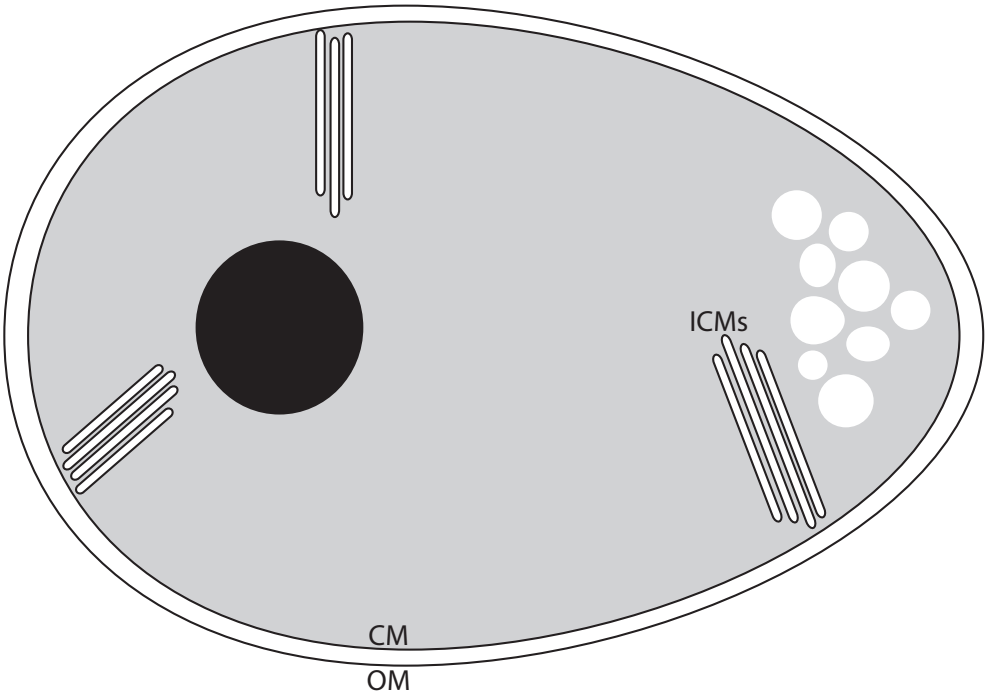

Figure 2. *Scheme of an average cell of a the verrucomicrobial methanotroph* M. fagopyrum 3C *showing the cell morphology, the cytoplasm (gray) with intracytoplasmic membrane systems (ICMs), an electron dense (ED) particle in black and multiple electron light (EL) particles in white and the Gram-negative cell envelope with the putative cytoplasmic (CM) and outer (OM) membranes.*

Possible topics for further research

This thesis provides the first comprehensive overview of the ultrastructure of the verrucomicrobial methanotrophs and as such provides a basis for future research. Apart from topics that were touched upon in the previous paragraphs, some additional potential future research lines are discussed below in more detail.

Electron dense particles. In chapter 4, the composition of the ED particles of the four species has been described and a function in storage of phosphate was suggested. Since the ED particles were observed in almost every cell and a second ED particle is seemingly generated during cell division in order to ensure that both daughter cells have such a particle, these particles apparently have an important function for the cells. It remains unknown which exact components are stored in these particles and for which purposes and in which circumstances the components stored in these particles are used. As the composition also differs between the species, the exact function might also be species-specific. In addition to the exact function, it would be interesting to elucidate how the synthesis, division and degradation of (the compounds stored in) these particles is regulated and which proteins are involved in these processes. From the genome, some

The image described above of the typical verrucomicrobial methanotrophic cell is based on investigations of the ultrastructure of the thermophilic *Methylacidiphilum fumariolicum* SolV (chapters 2, 3 and 4) as well as the mesophilic *Methylacidimicrobium* species *M. fagopyrum* 3C, *M. tartarophylax* 4AC and *M. cyclopophantes* 3B (chapter 4). Apart from the (putative) location of pMMO and MDH, which have been studied in *M. fumariolicum* SolV alone, all described features have been studied in all four species. Morphologically, three of these species (*M. fumariolicum* SolV, *M. tartarophylax* 4AC and *M. cyclopophantes* 3B) are very similar and fit well in the image of the typical cell described. Some small differences in dimensions between these species have been found and the composition of the ED particles was slightly different in *M. tartarophylax* 4AC, as not all particles contained phosphorus and sulfur was detected in the particles of this species only (chapter 4). Further research into the ED particles would be necessary to understand the significance of this difference in composition.

Cells of the mesophilic *M. fagopyrum* 3C did, however, deviate from the typical verrucomicrobial methanotrophic cell in several aspects (Fig. 2). First of all, the shape of these cells is more heterogeneous than that of the other cells and in most cases the broadest pole is broader rendering a cell shape that is more reminiscent of a buckwheat seed than an (elongated) egg. Occasionally, *M. fagopyrum* 3C cells were attached to each other via pilus-like structures that were not observed in the other species. It is unknown what these structures are made of and which functions they have. Concerning the ED particles, *M. fagopyrum* 3C cells were the only cells in which two electron dense particles per cell have been observed when these cells were not undergoing cell division. The biggest difference, however, is found inside the *M. fagopyrum* 3C cell: intracytoplasmic membrane systems (ICMs) are present in this species. Structural ICMs are characteristic for proteobacterial methanotrophs, but have not been found in other verrucomicrobial methanotrophs. In *Proteobacteria*, the pMMO enzyme involved in methane oxidation is located in the ICMs and it is an interesting and logical question for further research if the ICMs of *M. fagopyrum* 3C harbor the pMMO enzyme as well.

chapter 2), but carbon-containing compounds are present. Under these circumstances the cell stores carbon as glycogen inside these EL particles (see chapters 2 and 4) which can be consumed in the absence of methane.

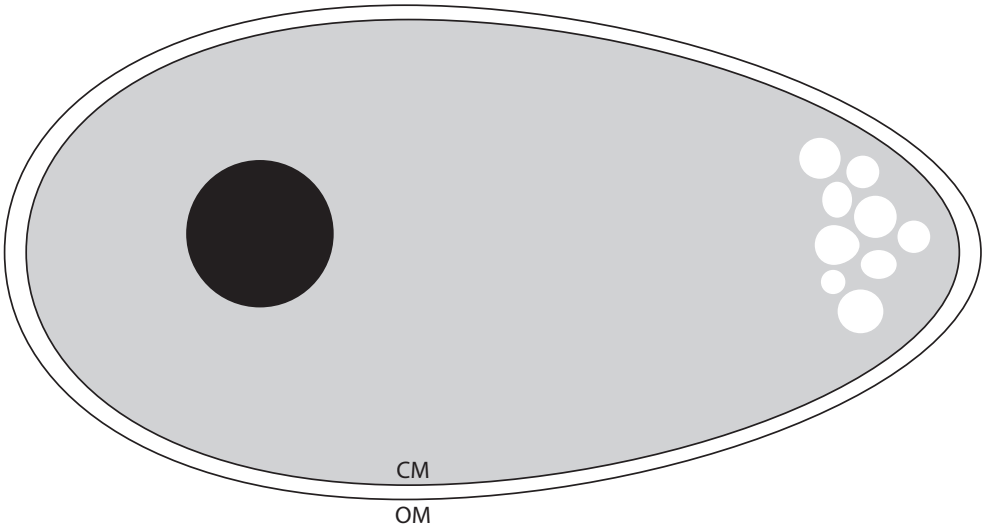

Figure 1. *Scheme of an average cell of a verrucomicrobial methanotroph showing the cell morphology, the cytoplasm (gray) with an electron dense (ED) particle in black and multiple electron light (EL) particles in white and the Gram-negative cell envelope with the putative cytoplasmic (CM) and outer (OM) membranes.*

Although the cell division of the verrucomicrobial methanotrophs was not studied in detail, it seems that the cells divide via binary fission. Before division, cells seem to elongate and the shape of the cell slightly changes so both poles are approximately equal in diameter. Although it should be investigated in more detail to make definite claims, it seems probable that the methanotrophic *Verrucomicrobia* divide via canonical (FtsZ-based) binary fission. This is alike other investigated *Verrucomicrobia*, but unlike the sister phyla *Planctomycetes* and *Chlamydiae* (Pilhofer et al, 2008), that both divide via FtsZ-less division.

When zooming in to the cell so to reach a molecular level, the location of two key enzymes involved in methane oxidation was investigated via immunogold localization (chapter 3). Using the present antibody against the first enzyme in the oxidation of methane, pMMO, on *M. fumariolicum* SolV, preliminary results seem to indicate a cytoplasmic location. This result was rather unexpected since all three pMMO subunits have predicted transmembrane regions and pMMO has been shown to be a membrane protein in other species of methanotrophs. Since the antibody used for the immunogold localization was not very specific, it would be a good idea to repeat the experiments with new antibodies that are generated against highly purified pMMO subunits. The second enzyme, methanol dehydrogenase (MDH), was shown to be present in the periplasm of *M. fumariolicum* SolV.

Following the initial investigations that led to the discovery of the characterized *Methylacidiphilum* species, multiple in-depth studies were performed focusing mostly on the genome and physiology of these organisms. This led to a better insight into their genomic organization (Hou et al, 2008; Khadem et al, 2012a; Anvar et al, 2014) and to a better understanding of the mechanisms of methane oxidation (Erikstad et al, 2012; Khadem et al, 2012b; Pol et al, 2014), carbon fixation (Khadem et al, 2011; Sharp et al, 2012) and nitrogen fixation (Khadem et al, 2010). These investigations showed that, unlike many other aerobic methanotrophs, verrucomicrobial methanotrophs use the Calvin cycle to fix carbon dioxide (Khadem et al, 2011; Sharp et al, 2012) and *M. fumariolicum* is able to fix dinitrogen gas via nitrogenase (Khadem et al, 2010). The methane oxidation pathway seems to go via the same enzymes as in other aerobic methanotrophs, although the MDH is different than previously described MDHs since it can oxidize methanol straight to formate with lanthanides instead of Ca^{2+} in its active site (Pol et al, 2014). The ultrastructure of these bacteria, however, has not been studied at all except for some basic observations made during the initial discovery. The main objective of the research presented in this thesis was to generate an overview of the ultrastructure of verrucomicrobial methanotrophs. This study thereby aimed to elucidate which intracellular structures are present and how these are associated with the metabolism of these micro-organisms.

An overview of the verrucomicrobial methanotroph cell

When combining all results obtained in this study, an image of a typical cell of a methanotrophic *Verrucomicrobium* emerges based on the four characterized species (Fig. 1). The typical cell has a rod shape in which one of the two poles is broader than the other, reminiscent of the shape of an (elongated) egg. A typical cell is 1.3 µm long and, at the broadest part of the cell, 0.6 µm wide. Inside the cytoplasm, ribosomes are present. The surface of the cells appears smooth, without a crystalline proteinaceous surface layer. The cell envelope has a typical Gram-negative architecture, consisting of two membranes (outer and cytoplasmic) with a thin space in between (periplasm). Although not clearly visible at all times, peptidoglycan seems to be present inside the periplasm.

Inside each cell typically one electron dense (ED) particle is present, appearing as black in electron microscopy images after negative staining and/or in thin sections of cryofixed and resin-embedded cells. The ED particle has a diameter of ca. 0.2 µm and is located near the center of the cell, sometimes shifted towards the broader pole. When the cell is dividing, a second ED particle appears, suggesting the formation of these particles is coordinated with the cell division. As is described in chapter 4, in most cases the ED particles seem to contain phosphate coupled to positive counter ions. A possible function in phosphate storage is likely.

Next to the ED particles another type of particle is present in the typical cell of a verrucomicrobial methanotroph. These particles are smaller and more numerous than the ED particles. The exact amount and size of these electron light (EL) particles depends on the availability of nutrients, as was shown in chapter 2. The cell starts accumulating EL bodies when depleted for nitrogen-containing compounds (ammonium in the case of

Methane is an important molecule in the earth's atmosphere and it contributes to the (enhanced) greenhouse effect. Via this effect the amount of methane influences the temperature on the surface of the earth. This gives an extra incentive to study the sources and sinks of methane on our planet. One sink of atmospheric methane is microbial methane oxidation, which reduces the amount of methane in the atmosphere. This oxidation can be coupled to the reduction of oxygen (Hanson & Hanson, 1996) (aerobic methane oxidation), sulfate (Boetius et al, 2000; Milucka et al, 2012), nitrate (Haroon et al, 2013) and manganese- or iron oxides (Beal et al, 2009) (anaerobic methane oxidation) and nitrite (Ettwig et al, 2008; 2010; 2012) (intra-aerobic methane oxidation). For many decades, *Proteobacteria* were thought to be the only micro-organisms capable of oxidizing methane aerobically (Hanson & Hanson, 1996). However, in 2007/2008 three independent studies showed that *Verrucomicrobia* can also perform aerobic methane oxidation (Dunfield et al, 2007; Pol et al, 2007; Islam et al, 2008). The three independently discovered verrucomicrobial methanotrophs were found to belong to the same genus, which was called *Methylacidiphilum* (Op den Camp et al, 2009). The *Methylacidiphilum* species were discovered in geothermal environments and were found to thrive at a very low pH (optima between 2 and 3.5) and a temperature around 40-60°C.

Already during the isolation of the thermophilic verucomicrobial methanotrophs, first hints appeared that the diversity of the verrucomicrobial methanotrophs might extend beyond the *Methylacidiphilum* species (Dunfield et al, 2007). This diversity had been missed by prior environmental studies focusing on *pmoA* (encoding one of the subunits of the particulate methane monooxygenase (pMMO) enzyme) as a marker for aerobic methanotrophs, since the *pmoA* sequence from the *Verrucomicrobia* is so divergent that the primers that were used did not detect the verrucomicrobial sequences (Op den Camp et al, 2009). When using a combination of *Verrucomicrobia*-specific *pmoA* primers and stable isotope probing (SIP) with ^{13}C-labeled carbon dioxide and either ^{13}C-labeled or unlabeled methane to recognize active autotrophic methanotrophs, multiple groups of *Verrucomicrobia* were identified (Sharp et al, 2012). An additional study also suggested a broader diversity of verrucomicrobial methanotrophs by showing the presence of three clusters of verrucomicrobial sequences from 165 geothermal sites (Sharp et al, 2014). In the same study an isolate from a colder, acidic geothermal site was described and thereby the total of characterized methanotrophic *Verrucomicrobia* is now four strains (Sharp et al, 2014).

For the understanding of the global importance of methane oxidation by *Verrucomicrobia*, it is of great interest to investigate the presence of additional verrucomicrobial methanotrophs and elucidate the environmental spectrum in which these organisms can occur. Although investigating this diversity was not the main goal of this thesis, the results in chapter 4 do provide new insights to this question by describing three novel species belonging to a novel genus of verrucomicrobial methanotrophs. These three *Methylacidimicrobium* species were found to be mesophilic, in contrast to the thermophilic *Methylacidiphylum* species. The temperature optima for growth for the three mesophilic species were slightly different, suggesting that methanotrophic *Verrucomicrobia* have adapted to different niches with respect to temperature.

Chapter 5

Integration & Outlook

Table S2. *Dimensions of the three mesophilic verrucomicrobial methanotrophs and* M. fumariolicum *SolV averaged over 100 cells. Standard deviations are given in brackets. The width is measured at the broadest part of the cell. The length/width (L/W) ratio gives an indication of the relative width of the cell; lower values mean relatively broader cells.*

	Strain 3B	**Strain 3C**	**Strain 4AC**	***M. fumariolicum***
Length (µm)	1.2 (±0.2)	1.4 (± 0.3)	1.2 (± 0.2)	1.5 (± 0.3)
Width (µm)	0.6 (± 0.1)	0.9 (± 0.1)	0.7 (± 0.1)	0.7 (± 0.1)
Ratio L/W	2.0	1.6	1.7	2.1

Table S3. *Properties of electron dense particles observed in the four veruccomicrobial methanotrophic strains. The average diameter (standard deviation in brackets) of 24 particles measured in negatively stained cells is quite similar in the four different strains. The amount of electron dense particles per cell (again 24 particles counted) slightly differs. For each strain, the dominant elements in the ED particle as measured by EDX analysis are listed with in brackets the percentage of the 10 analyzed cells that showed this enrichment.*

	Strain 3B	**Strain 3C**	**Strain 4AC**	***M. fumariolicum***
Amount of ED particles per cell	0.9	1.2	0.9	1.0
Average diameter of ED particles (µm)	0.12 (±0.04)	0.16 (±0.08)	0.15 (±0.03)	0.22 (±0.05)
ED particle is enriched in the following elements	-Phosphorus (100%) -Oxygen (80%)	-Phosporus (100%) -Oxygen (100%) -Magnesium (100%) -Nitrogen (90%)	-Sulfur (100%) -Oxygen (70%) -Phosphorus (20%)	-Oxygen (100%) -Phosphorus (70%) -Magnesium (70%) -Nitrogen (10%)

nirK	nitrite reductase, copper-containing	+	+	+	+	+	+
nirS	cytochrome cd1 nitrite reductase	ND	ND	ND	ND	ND	ND
cytL	cytochrome P460, nitric oxide: hydroxylamine dehydrogenase	ND	ND	ND	ND	ND	ND
cytS	putative nitric oxide reductase	ND	ND	ND	ND	ND	ND
norC	nitric oxide reductase subunit C	+**	+	+	+	+	+
norB	nitric oxide reductase subunit B	ND	+	+	+	+	+
Phosphate storage genes							
ppk1	polyphosphate kinase	+	+	+	+	+	+
ppx	Exopolyphosphatase	+ (2)	+ (2)	+ (2)	+ (2)	+ (2)	+ (2)
Glycogen genes							
glgA	glycogen synthase	+ (2)	+ (2)	+ (2)	+ (2)	+ (1)	+ (2)
gdb	glycogen debranching enzyme	+	+	+	+	+	+

	dehydrogenase subunit delta						
fdsA	NAD-dependent formate dehydrogenase subunit alpha	+	+	+	+	+	+
fdsB	NAD-dependent formate dehydrogenase subunit beta	+	+	+	+	+	+
fdsG	NAD-dependent formate dehydrogenase subunit gamma	+	+	+	+	+	+
hyfB	Formate hydrogenlyase subunit 3	+ (2)	+ (2)	+ (2)	+	+	+
hyfC	Formate hydrogenlyase subunit 4	+	+	+	+	+	+
hyfE	Formate hydrogenlyase membrane component	+	+	+	+	+	+
hycG	Formate hydrogenlyase subunit 7	+	+	+	+	+	+
fdhD	Formate dehydrogenase chain D	+	+	+	+	+	+
Serine cycle (key enzyme)							
Hpr	hydroxypyruvate reductase	ND	ND	ND	ND	ND	ND
Mcl	malyl-CoA lyase	ND	ND	ND	ND	ND	ND
Ribulose monophophate pathway (key enzyme)							
hxlA	3-hexulose-6-phosphate synthase	ND	ND	ND	ND	ND	ND
hslB	6-phospho-3-hexuloisomerase	ND	ND	ND	ND	ND	ND
Calvin-Benson-Bassham Cycle							
cbbS	Ribulose 1,5 biphosphate carboxylase, small subunit	+	+	+	+	+	+
cbbL	Ribulose 1,5 biphosphate carboxylase, large subunit	+	+ (2)	+	+	+	+
Pgk	3-phosphoglycerate kinase	+	+	+	+	+	+
cbbG/gapA	Glyceraldehyde-3-phosphate dehydrogenase	+	+	+	+	+	+
tpipA	Triosephosphate isomerase	+	+	+	+	+	+
fbaA	Fructose biphosphate aldolase Class II	+	+	+	+	+	+
fbaB	Fructose-1,6-phosphate aldolase Class I (archaeal type)	+	+	+	+	+	+
Fbp	Fructose-1,6-biphosphatase	+	+	+	+	+	+
cbbT	Transketolase	+	+	+	+	+	+
Rpe	Ribulose-5-phosphate-3-epimerase	+ (2)	+ (2)	+ (2)	+ (2)	+ (2)	+ (2)
xpkA	Phosphoketolase	+	+	+	+	+	+
rpiB	Ribose 5-phosphate isomerase	+	+	+	+	+	+
Udk	Phosphoribulokinase	+	+	+	+	+	+
Nitrogen metabolism							
haoAB	hydroxylamine oxidoreductase	ND	ND	ND	ND	+	+

Table S1. *Comparison based on presence/absence of key genes in methylotrophy, nitrogen metabolism and storage of polyphosphate and glycogen between the three newly described mesophilic* Verrucomicrobia*, strain LP2A and thermophilic species* Methylacidiphilum fumariolicum *SolV and* Methylacidiphilum infernorum *V4. Positive detection of genes was based on annotations by JGI (3C) and RAST (3B, 4AC) and on BLAST searches. In the case of strains LP2A and V4 the gene detection was noted as described previously (Sharp et al, 2014). For strain SolV, the analysis was based on the previously published genome (Khadem et al, 2012a). + = present; ND = not detected in genome. Numbers in parentheses indicate multiple copies of a gene. * = 2nd pmoC of strain 3C is partial; ** = the NorC gene in strain 3B is fragmented.*

Gene name	Product	3B	3C	4AC	LP2A	SolV	V4
Methane oxidation							
pmoC	particulate methane monooxygenase (pMMO), subunit gamma	+	+ (2) *	+	+ (3)	+ (3)	+ (4)
pmoA	particulate methane monooxygenase (pMMO), subunit beta	+ (2)	+	+ (2)	+ (2)	+ (3)	+ (3)
pmoB	particulate methane monooxygenase (pMMO), subunit alpha	+	+ (2)	+	+ (2)	+ (3)	+ (3)
mmoX	soluble methane monooxygenase (sMMO), subunit alpha	ND	ND	ND	ND	ND	ND
mmoY	soluble methane monooxygenase (sMMO), subunit beta	ND	ND	ND	ND	ND	ND
mmoZ	soluble methane monooxygenase (sMMO), subunit gamma	ND	ND	ND	ND	ND	ND
mmoB	soluble methane monooxygenase (sMMO), regulatory component	ND	ND	ND	ND	ND	ND
Methanol oxidation							
xoxF	PQQ-dependent methanol dehydrogenase	+ (2)	+ (2)	+ (2)	+ (3)	+	+
xoxJ	Periplasmic binding protein involved in methanol oxidation	+	+	+	+	+	+
xoxG	Cytochrome c family protein, electron acceptor for PQQ-methanol dehydrogenase	+	+	+	+	+	+
pqqA	coenzyme PQQ biosynthesis	+	+	ND	+	+	+
pqqB	coenzyme PQQ biosynthesis	+	+	+	+	+	+
pqqC	coenzyme PQQ biosynthesis	+	+	+	+	+	+
pqqD	coenzyme PQQ biosynthesis	+	+ (3)	+	+	+	+
pqqE	coenzyme PQQ biosynthesis	+	+	+	+	+	+
pqqF	coenzyme PQQ biosynthesis	ND	ND	ND	ND	+	ND
pqqG	coenzyme PQQ biosynthesis	ND	ND	ND	ND	ND	ND
Formate oxidation							
fdsD	NAD-dependent formate	+	+	+	+	+	+

Supplements

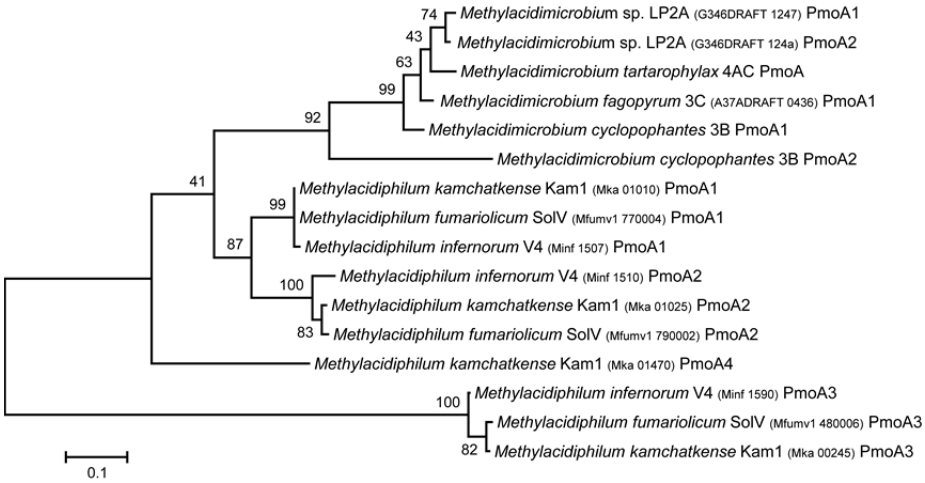

Figure S1. *PmoA gene-based phylogenetic tree of methanotrophic Verrucomicrobia shows that the mesophilic strains cluster together separately from the thermophilic species. The evolutionary history was inferred by using the Maximum Likelihood method based on the Dayhoff matrix based model. The tree with the highest log likelihood (-2842.1305) is shown. Initial tree(s) for the heuristic search were obtained automatically by applying Neighbor-Join and BioNJ algorithms to a matrix of pairwise distances estimated using a JTT model, and then selecting the topology with superior log likelihood value. The tree is drawn to scale, with branch lengths measured in the number of substitutions per site. The analysis involved 16 amino acid sequences. All positions with less than 95% site coverage were eliminated. There were a total of 243 positions in the final dataset. Evolutionary analyses were conducted in MEGA5.*

Acknowledgments

We thank Geert-Jan Janssen, Rob Mesman, Elly van Donselaar, Willie Geerts, Reinhard Rachel and Andreas Klingl for advice on and assistance with numerous aspects of the ultrastructural research. We thank Jelle Eygensteyn for performing the ^{13}C analysis. Daan Speth is acknowledged for help with the ANI(b) analysis. We thank Claudia Lüke for help with ARB. We thank Janric van Rookhuijzen for advice concerning the correct Ancient Greek and Latin grammatical construction of the names.
This research was supported by ERC 232937; ERC 339880, and Gravitation Grant SIAM OCW/NWO 024.002.002. LvN is supported by NWO VENI grant 863.09.009.

methanotrophic bacterial genus is the verrucomicrobial thermo- and acidophilic genus *Methylacidiphilum* (Op den Camp et al, 2009). Contains the type species *Methylacidimicrobium fagopyrum* 3C and *Methylacidimicrobium tartarophylax* 4AC, *Methylacidimicrobium cyclopophantes* 3B and *Methylacidimicrobium* strain LP2A (Sharp et al, 2014) as additional species. Habitat is acidic soil of elevated temperature, particularly in volcanic mudpots or near fumaroles.

Description of *Methylacidimicrobium fagopyrum* sp. nov.
Methylacidimicrobium fagopyrum (fa.go<<py.rum. N.L. neuter n. *fagopyrum* buckwheat; referring to the shape of the cell)

Description as for the genus plus the following traits. Cells are ca. 1.2 µm long and 0.7 µm wide. An intracytoplasmic membrane system was observed (Fig. 3) that consists of membrane stacks orthogonal to the cell wall. One or two particles (0.16 ±0.08 µm in diameter) containing phosphorus, oxygen, magnesium and nitrogen are present in most cells. The optimum temperature for growth is 35°C, no growth occurs above 39°C. Growth occurs at or above pH 0.6, with an optimum range of 1.5-3.0. The type strain is strain $3C^T$, which was isolated from soil of the Solfatara, at Pozzuoli, near Naples, Italy.

Description of *Methylacidimicrobium tartarophylax* sp. nov.
Methylacidimicrobium tartarophylax (tar.ta.ro<<phy.lax L. masc. n. *Tartarus* underworld; Gr. masc. n. *phylax* guardian; N.L. adj. *tartarophylax* guardian of the underworld; referring to the enrichment location which in Roman times was believed to be in the vicinity of an entrance to the underworld).

Description as for the genus plus the following traits. Cells are ca. 1.4 µm long and 0.9 µm wide. No intracytoplasmic membrane system was observed (Fig. 2). One particle (0.15 ±0.03 µm in diameter) containing sulfur, oxygen, and in some cases phosphorus is present in most cells. The optimum temperature for growth is 38°C, no growth occurs above 43°C. Growth occurs at and above pH 0.5, with pH 1-3 as optimum. Growth is inhibited by oxygen (growth at 5% oxygen is about two times faster than at ambient oxygen concentration). The type strain is strain $4AC^T$, which was isolated from soil of the Solfatara, at Pozzuoli, near Naples, Italy.

Description of *Methylacidimicrobium cyclopophantes* sp. nov.
Methylacidimicrobium cyclopophantes (cy.clo.po.phan<<tes L. masc. *cyclops* cyclops; Gr.adj. suffix *-phantes* resembling; N.L. n. adj. *cyclopophantes* resembling a Cyclops; referring to the large electron dense particle of which one is present in each cell).

Description as for the genus plus the following traits. Cells are ca. 1.2 µm long and 0.6 µm wide. No intracytoplasmic membrane system was observed (Fig. 1). One particle (0.12 ± 0.04 µm in diameter) containing phosphorus and oxygen is present in most cells. The optimum temperature for growth is 44°C, no growth occurs above 49°C. Growth occurs at or above pH 0.6, with an optimum range of 1.5-3.0. The type strain is strain $3B^T$, which was isolated from soil of the Solfatara, at Pozzuoli, near Naples, Italy.

possess Calvin cycle genes (Ward et al, 2004), although physiological evidence for an active Calvin cycle is lacking thus far.

The recent findings are just the beginning of understanding the diversity in verrucomicrobial methanotrophs. Much more research is needed to verify that an even larger methanotrophic diversity can exist as is suggested from operational taxonomic units (OTUs) that were retrieved from multiple geothermal sites (Sharp et al, 2014). For the organisms that these OTUs represented, it has to be investigated if they indeed perform methane oxidation and to find out which circumstances they need for their growth. Additional studies investigating the ecosystems are necessary to understand the interplay between the different genera and species of verrucomicrobial methanotrophs and the role they play in different environments.

Here we described three new species of a new genus of methanotrophic *Verrucomicrobia* isolated from a geothermal environment. The three species featured in this study indicate that a wide variety of methanotrophic *Verrucomicrobia* exists and that they are quite well adapted to different niches present in geothermal environments both with respect to temperature and acidity. The previously described strain LP2A (Sharp et al, 2014), which according to our analysis also belongs to the genus *Methylacidimicrobium*, has a lower temperature range than the three *Methylacidimicrobium* species described here. The *Methylacidiphilum* species described before have a higher temperature range than all *Methylacidimicrobium* species. Although the pH optimum range is essentially the same for all three *Methylacidimicrobium* species (1.5-3), these new mesophilic strains are more acid tolerant with strain 4AC even growing at pH 0.5. The pH range of the *Methylacidimicrobium* strain LP2A is similar, but slightly higher (1-5.2) (Sharp et al, 2014) and the same is true for the *Methylacidiphilum* species (0.8-6) (Op den Camp et al, 2009). It would be very interesting to study whether verrucomicrobial methanotrophs exist that live at higher pHs or if they are outcompeted by proteobacterial methanotrophs in these environments. It is therefore important to isolate and characterize additional verrucomicrobial methanotrophs.

Description of *Methylacidimicrobium* gen.nov.

Methylacidimicrobium (Me.thyl.a.ci.di.mi.cro<<bi.um N.L. n. *methyl* the methyl group; N.L. n. acidum acid from L. adj. *acidus* sour; N.L. n. *microbium* microbe; N.L. n. *Methylacidimicrobium* methyl-using microbe living in an acid environment)

Gram-negative, rod-shaped bacteria with a broadening at one of the two cell poles. Cells occur as single cells or as small groups; do not form rosettes. Reproduce by binary fission. Non-motile. Produce intracellular glycogen granules and additional intracellular (electron dense) particles. Except for the type species *M. fagopyrum* 3C, no intracellular membrane systems (ICMs) were observed. sMMO is not present in the genomes. Representatives are extremely acidophilic and mesophilic. . No growth occurs without lanthanides in the medium. Growth is also possible on methanol. Carbon is fixed via the Calvin cycle. The G-C content is 60.9 - 63.8 %. Belongs to the *Verrucomicrobia*; the closest described

The temperature and pH optima and ranges for the three *Methylacidimicrobium* species described in this study (Table 1) reflected the conditions in the acid geothermal soils from which they were isolated (pH ranging from 1.5 to below 1). The differences in pH and temperature optima between the three *Methylacidimicrobium* indicated that the three species might occupy different niches in their natural environment. The fact that these strains were enriched from the same soils indicates that local conditions are variable. This is evident for ecosystems like the Solfatara where heterogeneity in soil conditions occurs because of occasional rainfall and varying routes the volcanic gasses take through the soil. Further research will be needed to show how versatile verrucomicrobial methanotrophs can be in their growth conditions and if they could, for instance, grow at lower temperatures and even lower pH values.

When comparing the optimal growth conditions for the three newly described *Methylacidimicrobium* species to the previously described *Methylacidimicrobium* strain LP2A and *Methylacidiphilum* species, it appears that (at least verrucomicrobial) methanotrophic species are adapted to slightly different circumstances. Three *Methylacidimicrobium* species and one *Methylacidiphilum* species (*M. fumariolicum* SolV) were isolated from the same ecosystem, indicating that methanotrophic organisms with slightly different growth requirements can be present together in the same ecosystem. This could implicate that even when circumstances change, methanotrophy will occur in such an ecosystem. The diversification of methanotrophs in the ecosystem may thus lead to a more stable ecosystem. As has been shown before in other ecosystems with a high number of microbial species per functional group, the amount of biomass and the density were more stable (Naeem & Li, 1997). A high number of species that are adapted to slightly different conditions is also expected to stabilize ecosystem process rates in response to changes in environment (Hooper et al, 2005).

So far all studies in acidic, volcanic environments yield exclusively verrucomicrobial enrichments. From these environments no *Proteobacteria* have been isolated to date (e.g. (Sharp et al, 2014)). This suggests that *Verrucomicrobia* dominate these ecosystems, although additional (especially metagenomic) surveys would be needed to verify this hypothesis.

Not only the growth conditions, but also the mechanism used for carbon fixation of verrucomicrobial methanotrophs differs from most other aerobic methanotrophs. Most proteobacterial methanotrophs use methane both as energy and as carbon source. Carbon is assimilated at the formaldehyde oxidation level via the RuMP or Serine pathway (Chistoserdova et al, 2009). In contrast, *M. fumariolicum* SolV (Khadem et al, 2011) and *M. infernorum* V4 (Sharp et al, 2012), use carbon dioxide as carbon source using the Calvin cycle and therefore have an autotrophic lifestyle. In this study, the three mesophilic strains were found to grow autotrophically as well. Therefore, five out of five studied methanotrophic *Verrucomicrobia* are proven to be autotrophs. Furthermore, the genome of strain LP2A indicates that this organism too is an autotroph (Sharp et al, 2014). This suggests that all methanotrophic *Verrucomicrobia* have an autotrophic lifestyle. For the methanotrophic *Proteobacteria*, thus far only *Methylococcus capsulatus* was shown to

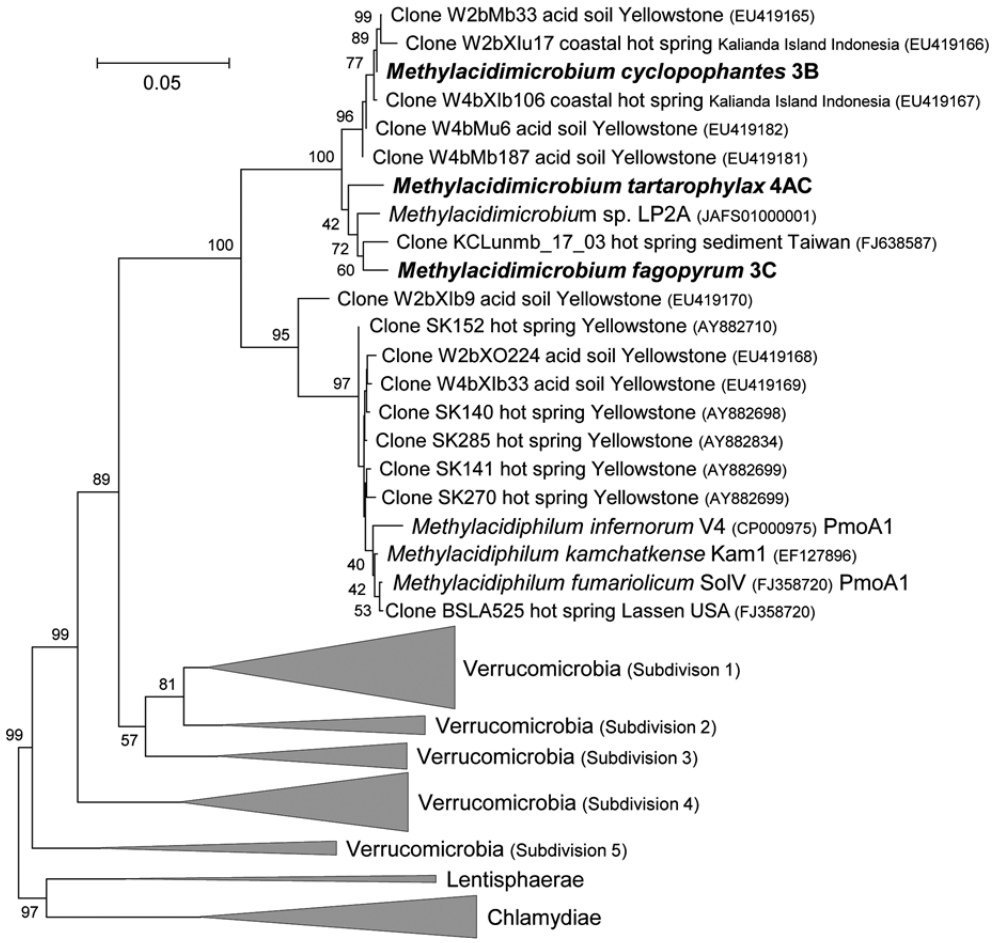

Figure 7. *16S rRNA gene-based phylogenetic tree of methanotrophic and other* Verrucomicrobia *shows that the methanotrophic mesophilic strains cluster together separately from the methanotrophic thermophilic species. The evolutionary history was inferred using the Neighbor-Joining method. The optimal tree with the sum of branch length = 4.46361805 is shown. The percentage of replicate trees (values above 40%) in which the associated taxa clustered together in the bootstrap test (10000 replicates) is shown next to the branches. The tree is drawn to scale, with branch lengths in the same units as those of the evolutionary distances used to infer the phylogenetic tree. The evolutionary distances were computed using the Jukes-Cantor method and are in the units of the number of base substitutions per site. The analysis involved 128 nucleotide sequences. All ambiguous positions were removed for each sequence pair. There were a total of 1647 positions in the final dataset. Evolutionary analyses were conducted in MEGA5.*

The three mesophilic strains described in this study share 89.1-98.1% 16S rRNA gene sequence identity (Table 2) and ANIb values are between 77.3-87.8% (Table 3). When using the strict species cut-offs for 16S rRNA gene sequence identity of 98.5% (Stackebrandt, 2011) or 98.7-99.1% (Mende et al, 2013; Stackebrandt & Ebers, 2006), the three strains should be characterized as three different species. Using the same species cut-offs, the mesophilic strain LP2A should be classified as a fourth species, since it shares 89.6-98.1% 16S rRNA gene sequence identity with the three mesophiles. However, multiple studies have shown that 16S rRNA gene analysis is often not fit for resolution on the species level and that ANI is better suitable for this purpose (Stackebrandt, 2011; Chan et al, 2012; Konstantinidis & Tiedje, 2007). Also based on the ANIb values (Table 3), the three mesophilic strains are proposed to belong to three different species using the standard species cut-off of 95% identity (Goris et al, 2007). It should therefore be concluded that each strain represents a different species. The proposed names for the three species described in this article are: *Methylacidimicrobium tartarophylax* 4AC, *Methylacidimicrobium fagopyrum* 3C and *Methylacidimicrobium cyclopophantes* 3B. We do not propose a species name for strain LP2A, but propose this strain is referred to as *Methylacidimicrobium* strain LP2A.

With the description of the three *Methylacidimicrobium* species, a broader base is present for describing the physiology and also the ultrastructure of the verrucomicrobial methanotrophs. Based on the four species described in this study, electron dense and electron light particles appear as components present in many verrucomicrobial methanotrophs. These are supposed to function in respectively glycogen and phosphate storage. The ultrastructure of *M. fagopyrum* 3C differs most notably from the other studied species, especially since it was shown to possess ICMs. Although in rare occurrences ICM have been observed in the verrucomicrobial methanotroph *Methylacidiphilum infernorum* (Dunfield et al, 2007), *M. fagopyrum* 3C is the first described verrucomicrobial methanotroph where membrane stacks are present in most cells.

In the proteobacterial methanotrophs, a complex ICM system consisting of membrane stacks is a wide-spread characteristic and the membranes are thought to harbor the enzyme pMMO. The appearance and orientation of ICMs differs between type I and type II methanotrophs (Hanson & Hanson, 1996). In type II methanotrophs the membranes occur as layers lining the periphery of the cell and in type I the membranes form stacks that are aligned more or less orthogonal to the cytoplasmic membrane. The membrane stacks of strain 3C resemble type I ICMs. It remains to be established if the pMMO enzymes are also localized in these membranes of *M. fagopyrum* 3C. The location of pMMO in the other verrucomicrobial methanotrophs, that seem to lack internal membranes, needs to be further investigated, since an initial investigation on *M. fumariolicum* (chapter 3) showed conflicting results.

and LP2A was included in the 16S rRNA gene sequence analysis. The 16S rRNA gene sequence identity between the four mesophilic species and *M. fumariolicum* SolV was 89.1-89.7% (Table 2). The three mesophilic strains (3B, 3C and 4AC) share 89.1-98.1% 16S rRNA gene sequence identity (Table 2). We have also analyzed the ANI(b) values for the three mesophilic strains and *M. fumariolicum* SolV to get more reliable results for resolution on the species level and this analysis showed ANIb values between 77.3-87.8% (Table 3).

Table 2. *Distance analysis (complete deletion) of 16S rRNA genes shows the similarities between the three mesophilic verrucomicrobial strains and previously described mesophilic strain LP2A and thermophilic* M. fumariolicum *SolV.*

		1	2	3	4	5
1	*Methylacidiphilum fumariolicum* SolV					
2	*Methylacidimicrobium fagopyrum* 3C	89.1%				
3	*Methylacidimicrobium tartarophylax* 4AC	89.6%	97.3%			
4	*Methylacidimicrobium cyclopophantes* 3B	89.7%	97.6%	97.1%		
5	Strain LP2A	89.6%	98.1%	97.3%	98.1%	

Table 3. *ANIb analysis shows the similarities between the draft genomes of the three mesophilic verrucomicrobial strains and thermophilic* M. fumariolicum *SolV.*

		1	2	3	4
1	*Methylacidiphilum fumariolicum* SolV		63.7%	63.2%	63.7%
2	*Methylacidimicrobium fagopyrum* 3C	63.8%		87.8%	77.3%
3	*Methylacidimicrobium tartarophylax* 4AC	62.9%	87.6%		77.6%
4	*Methylacidimicrobium cyclopophantes* 3B	63.4%	77.6%	77.7%	

Discussion

Recently the repertoire of known bacteria capable of aerobic methanotrophy was extended with the verrucomicrobial methanotrophs belonging to the genus *Methylacidiphilum* (Pol et al, 2007; Dunfield et al, 2007; Islam et al, 2008; Op den Camp et al, 2009). These species were isolated from geothermal environments and shared a thermophilic lifestyle. This study shows that methanotrophy can also be performed by *Verrucomicrobia* at mesophilic temperatures. The results from our phylogenetic analyses show that the three mesophiles described in this study and the previously described LP2A (Sharp et al, 2014) belong to a different genus than *M. fumariolicum* SolV. The 16S rRNA gene sequence identity of 89.1-89.7% between the four mesophilic species and *M. fumariolicum* SolV (Table 2) falls well below the minimum of 95% that is widely accepted to affiliate two strains to the same genus (Adékambi et al, 2008; Schloss & Handelsman, 2004). The four mesophilic species have 16S rRNA gene sequence identities between 97.3% and 98.1% and therefore belong to the same genus. For this genus we propose the name *Methylacidimicrobium*.

To investigate the composition of the cells and the ED particles in particular, EDX was performed on thin sections of cryo-sectioned, freeze-substituted cells. Qualitative maps show enrichments of specific elements throughout the cell and made clear that multiple elements were enriched in the ED particles. For *M. fumariolicum* SolV (Fig. 6) and strains 3C and 3B the ED particles were enriched in phosphorus and oxygen (Table S3). This suggests that (poly)phosphate is present in the ED particles. Genes encoding polyphosphate kinase and exopolyphosphatase were present in both mesophilic and thermophilic strains (Table S1). Polyphosphate encompassing vesicles have been found in other organisms, where they are known as acidocalcisomes (Docampo & Moreno, 2001). Because polyphosphate has a negative charge, positive counter ions are often found in the vicinity of these molecules. In the case of *M. fumariolicum* SolV and strain 3C magnesium ions seemed to have this role. In strain 4AC a minority of the ED particles showed a phosphorus signal. In addition, these particles showed sulfur enrichment. The role for sulfur however remains puzzling since thus far no genes for sulfur storage/utilization were detected in the draft genome (data not shown).

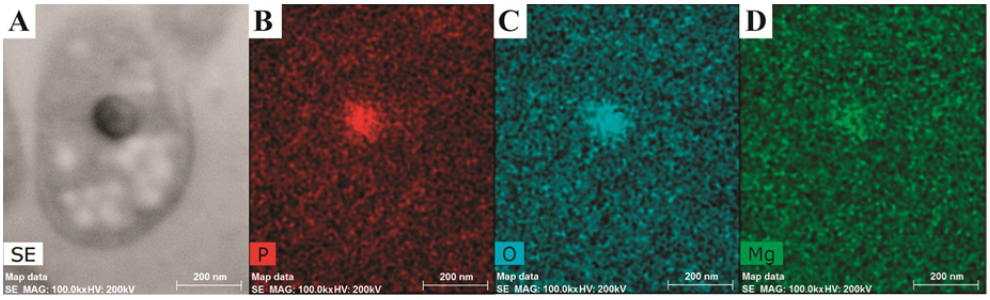

Figure 6. *Thin section of* M. fumariolicum *SolV analyzed by EDX shows the ED particle (dark particle in the sectioned cell in STEM mode (panel A)) to be enriched in phosphorus (panel B), oxygen (panel C) and magnesium (panel D).*

Phylogenetic and genomic analysis. Phylogenetic analysis of the 16S rRNA gene of the three mesophilic strains showed them to be affiliated to the previously described (Sharp et al, 2014) mesophilic strain LP2A (Table 2). The cluster of mesophiles separates clearly from the thermophilic cluster with which they share only just below 90% identity (Fig. 7). The *pmo*A-based phylogeny agreed well with the 16S rRNA-based phylogeny with strain LP2A as the closest cultivated neighbor (Table S1). The *pmo*A genes of new isolates showed about 92% identity at the amino acid level to strain LP2A and about 70-72% amino acid identity to the *pmo*A1 and *pmo*A2 genes of the thermophilic strains. The same clustering is obtained when using the *mxaF/xoxF* (Keltjens et al, 2014) gene. Analysis of the 16S rRNA genes also including the environmental OTUs described previously (Sharp et al, 2014) show that the newly described mesophilic isolates belong to one of the three described groups, more specifically to the same group as LP2A (data not shown).

To investigate if the three new strains represent three strains of the same or multiple species, 16S rRNA gene and average nucleotide identity based on Blast (ANIb) (on draft genomes) analysis were performed. *M. fumariolicum* SolV, was included in both analyses

The amount and the size of the ED particles were studied via negative staining. The amount of ED bodies was on average close to one per cell (Table S3). Only in some cells of strain 3C or in many dividing cells two ED bodies per cell were observed. The average diameter of ED particles was similar for all strains and is slightly lower than 200 nm (Table S3).

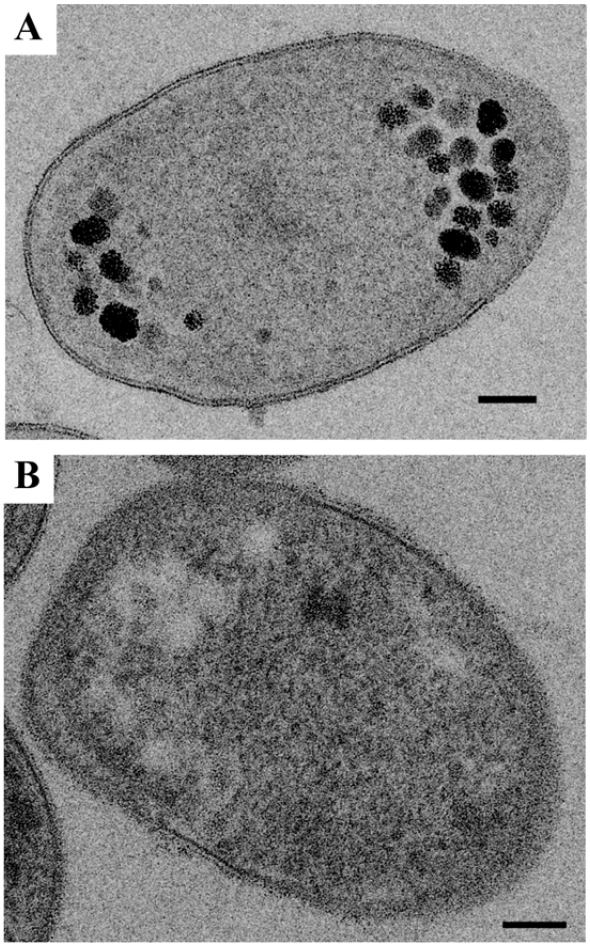

Figure 5. *A polysaccharide stain on thin sections of high-pressure frozen and freeze-substituted cells of the mesophilic verrucomicrobial methanotroph strain 4AC indicates that polysaccharides are present in the electron light particles. Electron light particles, appearing as white spots in the negative control (panel B), show clear staining in panel A (black silver aggregates) because of the polysaccharide content. Similar results were obtained for strains 3B and 3C (data not shown).*

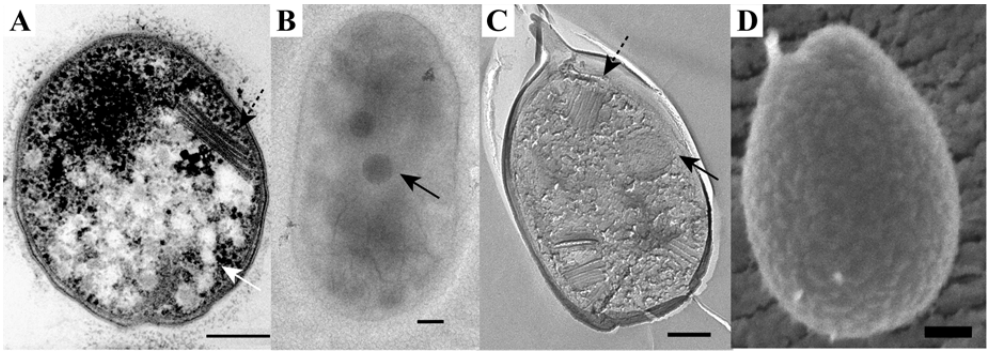

Figure 3. *Morphology of the mesophilic verrucomicrobial methanotroph strain 3C as visualized by thin-sections of high-pressure frozen and freeze-substituted cells (panel A), negative staining (panel B), FE (panel C) and cryoSEM (panel D).The cells are rod-shaped with one broader cell pole and contain membrane stacks (dashed arrow), electron dense (black arrows) and electron light (white arrow) particles. Scale bars 200 nm.*

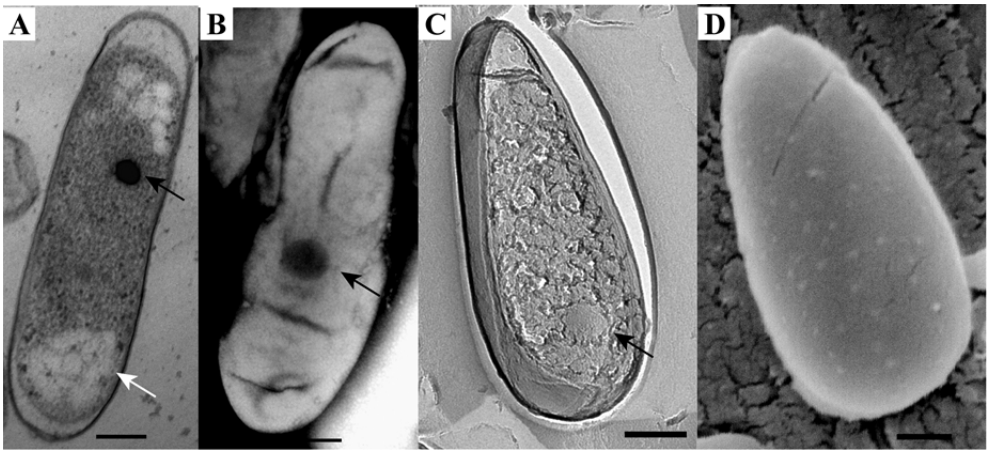

Figure 4. *Morphology of the thermophilic verrucomicrobial methanotroph M. fumariolicum SolV as visualized by thin-sections of high-pressure frozen and freeze-substituted cells (panel A), negative staining (panel B), FE (panel C) and cryoSEM (panel D). The cells are rod-shaped with one broader cell pole and contain electron dense (black arrows) and electron light (white arrow) particles. Scale bars 200 nm.*

In all strains, both electron dense (ED) and electron light (EL) particles were observed in the thin sections (Figs. 1A, 2A, 3A and 4A) and after FE. The EL particles were smaller and more numerous than the ED particles. The ED particles were typically located near the center of the cell and the EL particles seemed to localize preferentially to the cell poles. EL particles were observed in the majority of cells and they resembled the glycogen storage particles in *M. fumariolicum* SolV (Khadem et al, 2012c (chapter 2)). A polysaccharide stain verified that the EL particles indeed contained glycogen (Fig. 5). Accordingly, the genomes of all studied verrucomicrobial methanotrophs harbor the key genes for glycogen synthesis and glycogen degradation (Table S1).

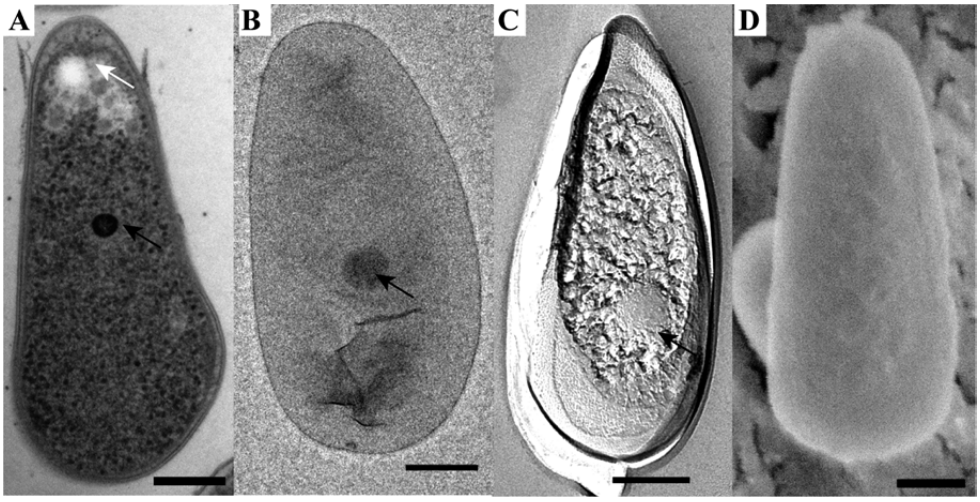

Figure 1. *Morphology of the mesophilic verrucomicrobial methanotroph strain 3B as visualized by thin-sections of high-pressure frozen and freeze-substituted cells (panel A), negative staining (panel B), FE (panel C) and cryoSEM (panel D). The cells are rod-shaped with one broader cell pole and contain electron dense (black arrows) and electron light (white arrow) particles. Scale bars 200 nm.*

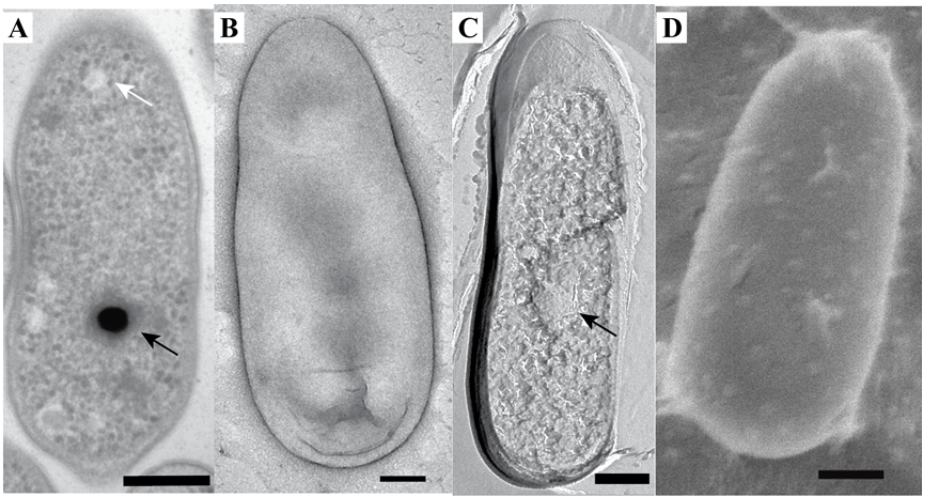

Figure 2. *Morphology of the mesophilic verrucomicrobial methanotroph strain 4AC as visualized by thin-sections of high-pressure frozen and freeze-substituted cells (panel A), negative staining (panel B), FE (panel C) and cryoSEM (panel D). The cells are rod-shaped with one broader cell pole and contain electron dense (black arrows) and electron light (white arrow) particles. Scale bars 200 nm.*

the ^{13}C label from methane was recovered as $^{13}CO_2$. The finding that the biomass produced was labeled for only 4-5% with ^{13}C, matching the average ^{13}C percentage of the CO_2 in the bottles during growth (that increased from 1.2 to 7-10%), confirmed that CO_2 was the actual carbon source. This showed that these strains do not use intermediates of methane oxidation for their carbon supply, as is the case for the Serine or RuMP pathway (which would lead to respectively 50 or 100% ^{13}C from methane incorporated into the biomass (Hanson & Hanson, 1996; Chistoserdova et al, 2009)). The key genes of the Serine and RuMP pathways were indeed absent from the draft genomes (Table S1).

Description of morphology. The morphology of the three mesophilic strains was studied in detail using multiple electron microscopy (EM) techniques. For comparison, the thermophilic verrucomicrobial methanotroph *M. fumariolicum* SolV was included in this study. The shape and dimensions of the cells were investigated using cryoSEM. This method showed the whole cells (in contrast to sections) in a near-native state (in contrast to negative staining were the cells can collapse during the procedure). The cell shape of all four studied microorganisms was rod-shaped with one of the cell poles being broader than the other pole (Figs. 1D, 2D, 3D and 4D). Using freeze-etching (FE), replicas of whole or fractured cells show overall morphology and especially the appearance of the cell surface. FE showed the same morphology of the cells as cryoSEM (Figs. 1-4). No S-layers were observed and instead the cell surface was smooth as demonstrated by both FE and cryoSEM. Cells of strain 3C exhibited a wider variety in shapes than those of the other strains, as was also observed by light microscopy. In cryoSEM, cells of strain 3C were occasionally attached to each other via a pilus-like structure. The dimensions of all strains were similar (approximately 1.3 µm by 0.6 µm) (Table S2). The width (measured at the broadest pole) was clearly higher for strain 3C, as was also obvious from the length/width (L/W) ratios (Table S2). This leads to the resemblance of these cells to buckwheat seeds.

Thin-sections of high-pressure frozen and freeze-substituted cells were studied to get an insight in the ultrastructure of the cells. Both *M. fumariolicum SolV* and the three mesophilic strains feature Gram-negative cell envelopes as two membranes can be visualized in thin sections (Figs. 1-4). There have been reports that multiple *Verrucomicrobia* (*Verrucomicrobium spinosum*, *Prosthecobacter dejongeii*, *Chthoniobacter flavus* and strain Ellin514) have a *Planctomycetes-Verrucomicrobia-Chlamydia* (PVC)-specific cell plan where the outermost membrane is in fact a cytoplasmic membrane (Lee et al, 2009). This is not apparent from our ultrastructural study of the four studied verrucomicrobial methanotrophs. In addition to the Gram-negative cell envelope, all four strains feature a typically looking cytoplasm containing ribosomes. No condensed DNA has been observed in the thin sections of the four strains. In strain 3C, intracytoplasmic membrane (ICM) stacks orthogonal to the membrane were observed in many sections (Fig. 3A), after FE (Fig. 3C) and during cryoSEM (data not shown).

three new isolates possessed only one complete *pmo*CAB operon, which is different from the thermophilic strains that have three complete operons (Khadem et al, 2012a; Hou et al, 2008). The sMMO encoding genes were absent in all strains. Other features of the draft genomes are included in the descriptions below.

Growth conditions. Acid tolerance of the isolated strains was tested by gradually changing the acid concentration in batch cultures (with OD between 0.1 and 0.4). For strains 3C and 3B, growth was optimal between pH 1.5 and 3 (Table 1). Strain 4AC was the most acid tolerant; its optimum extended down to pH 1 and it exhibited the lowest pH allowing growth, namely pH 0.5. Above pH 3 the growth rate of all strains dropped gradually. The maximum pH allowing growth was between pH 5 and 6. The temperature optima for growth were in the mesophilic range for all three strains: 35°C for strain 3C, 38°C for strain 4AC and 44°C for strain 3B (Table 1).

Table 1. *Conditions for optimal growth of the three mesophilic verrucomicrobial methanotroph strains as tested in batch cultures. Because of the oxygen sensitivity of strain 4AC, this organism was grown at 5% O_2 compared to 17% O_2 for the other two strains.*

Strain	**temp optimum °C (temp max)**	**μ_{max} (h^{-1}) (doubling time (h))**	**optimum pH range**	**lowest pH (% of μ_{max})**
3B	44 (49)	0.042 (16)	1.5 - 3	0.6 (30%)
4AC	38 (43)	0.035 (20)	1 - 3	0.5 (40%)
3C	35 (39)	0.013 (53)	1.5 - 3	0.6 (35%)

Like the thermophilic verrucomicrobial methanotrophs (Op den Camp et al, 2009), the three mesophilic strains were able to grow on methanol. All strains were strictly dependent on the addition of mudpot water to the growth medium. This water could be substituted by cerium (III) being one of lanthanides that can serve as a metal cofactor in methanol dehydrogenase of *M. fumariolicum* SolV (Pol et al, 2014). All mesophilic strains contain two different *xox*F genes encoding methanol dehydrogenases (Table S1). All genes possess the typical lanthanide (III) coordination specific aspartate located two amino acids downstream of the catalytic aspartate (Keltjens et al, 2014).

Since all of the three new strains contain the genes involved in the Calvin cycle (including the two subunits of the key enzyme RuBisCO) (Table S1), they were predicted to grow as autotrophs. The *cbb*L genes encoding the RuBisCO large subunit of the three strains were previously shown to form a phylogenetically distinct cluster closely related to *M. fumariolicum* SolV and *M. infernorum* V4 (Khadem et al, 2011). The ability to grow autotrophically was tested by culturing the strains on ^{13}C labeled methane (2-3% of the headspace) added to batch cultures that contained a high percentage (40%) of unlabeled $^{12}CO_2$ in the gas phase to serve as trap for the produced $^{13}CO_2$. After growth, 94-102% of

Sequence accession numbers. The genome data of strain 3C are deposited under BioProject PRJNA165235, those for strains 3B and 4AC under BioProject PRJNA255456. The *pmoA* and 16S rRNA sequences can be found in Genbank under the following numbers: KM210549 (3C_pmoA1), KM210550 (3B_pmoA1), KM210551 (3B_pmoA2), KM210552 (4AC_pmoA1), KM210553 (3C_16S), KM210554 (4AC_16S) and KM210555 (3B_16S).

Results

Enrichment and isolation. Samples from the bare soil area of the Solfatara were taken at spots at least 20 m away from hot fumaroles or the central mudpot. The temperature of these soils range from 25-40 ^{o}C (Merucci et al, 2006). Soil samples were extracted with water, serially diluted in medium and incubated with methane for over four months. Four out of eight soil sample enrichments showed methane consumption and growth up to 10^4 dilution. Lack of growth might be due to the sudden change in acidity that occurred when soils (pH 1) were extracted with water and diluted into medium (pH 2.5). Such pH shocks were found later to prevent the onset of growth of isolates from the enrichments. The positive enrichments contained almost exclusively *Verrucomicrobia*, as judged by FISH microscopy using verrucomicrobial specific probe EubIII (Daims et al, 1999) (data not shown). The 10^1 and 10^4 positive dilutions were chosen for further cultivation and isolation. After three transfers into new liquid medium, serial dilutions of the final cultures were transferred to floating membrane filters. After four weeks at 30 ^{o}C, the highest dilutions (10^7) showed isolated colonies that were either small, yellowish and shiny or larger and off-white. Different colony types were picked and purified by streaking on floating filters. Finally, this resulted in the isolation of strains 4AC (from 10^1 dilution), 3C and 3B (the latter two both from 10^4 dilution). We observed that strain 4AC was sensitive to oxygen and showed a twofold higher growth rate at an oxygen concentration of 5% compared to ambient oxygen concentration. Especially when shaken at ambient oxygen concentration, cultures of strain 4AC appeared to have a long lag phase, or even failed to grow. This may have prohibited the appearance of strain 4AC in higher serial dilutions. Strains 4AC and 3B consisted of rod-shaped bacteria as investigated with light microscopy. Cells of strain 3C were bigger and morphologically less homogenous than strain 4AC and 3B. Both long and short rod-shaped cells were observed as well as cells with a shape reminiscent of buckweed seeds of which some were connected to each other at distances of up to a few µm. For all three isolates only one rRNA operon was obtained upon genome sequencing (see below) and the isolates were considered to be a pure culture.

Genome properties. For further characterization, the draft genomes of the new strains were assembled and annotated (see Materials and Methods). The GC content was 60.9% for both strains 3C and 4AC and 63.8% for strain 3B. The draft genome sizes (and numbers of identified protein-encoding genes) were 2.77 Mb (2945 ORFs), 2.75 Mb (2804 ORFs) and 2.44 Mb (2511 ORFs) for strain 3C, 3B and 4AC, respectively. In general, the metabolic machinery was similar to the thermophilic strains SolV (Khadem et al, 2012a) and V4 (Hou et al, 2008) and the mesophilic strain LP2A (Sharp et al, 2014). The annotated genomes were used to compile a table with the key predicted methylotrophy genes (Table S1). The

Respectively, 66, 180, 88 and 173 images containing 1-50 typical cells were obtained by transmission EM for *M. fumariolicum* SolV, strains 3B, 3C and 4AC.

For freeze-etching, cryo-scanning electron microscopy (cryoSEM) and negative staining, cells were taken from batch cultures at two time points. Freeze-etching on the three mesophilic strains of verrucomicrobial methanotrophs and on *M. fumariolicum* SolV was performed as described previously (Wu et al, 2012b). Respectively, 73, 60, 79 and 66 typical images containing 1-4 freeze-etched cells per image were obtained using a CM12 transmission electron microscope (TEM) (FEI, Eindhoven, the Netherlands) for *M. fumariolicum* SolV, strains 3B, 3C and 4AC.

Negative staining was performed by applying a concentrated (centrifuged 4 min at 12000 g) cell suspension on a (formvar-)carbon coated copper grid. The grid was then immediately washed in two drops of MilliQ and subsequently incubated 15-20 sec on 2% uranyl acetate in MilliQ. The cells were then investigated by a 1010 TEM (Jeol, Tokyo, Japan). Per strain, 24 electron dense particles were examined, accounting for 27 cells for strains 3B and 4AC, 20 cells for strain 3C and 24 cells for *M. fumariolicum* SolV.

CryoSEM was performed on plunge-frozen cells from the four strains as described previously (Wu et al, 2012b) using a 6301F EDS FESEM (Jeol, Tokyo, Japan). Of each strain 100 typical non-dividing cells were analyzed. The length and width at the broadest part of the cell was measured for each cell.

A polysaccharide stain was performed to investigate if the electron light particles identified in the three mesophilic strains were polysaccharide inclusions, as described for *M. fumariolicum* SolV (Khadem et al, 2012c (chapter 2)). The stain and matching negative controls were performed as described previously (van Niftrik et al, 2008) on ultrathin sections of high-pressure frozen cells (freeze-substituted in acetone containing 2% osmium tetroxide, 0.2% uranyl acetate and 1% H_2O) of the mesophilic strains and visualized using a TEM 1010 (Jeol, Tokyo, Japan). In this method, electron dense silver albumin aggregates indicate the presence of polysaccharide molecules.

Energy dispersive X-ray (EDX) analysis was performed on all four strains to investigate the contents of the electron dense particles. For this purpose, cells were high-pressure frozen, freeze-substituted in 2% osmium tetroxide and sectioned as described previously (van Niftrik et al, 2008). The ultrathin sections (ca. 60 nm) were visualized (without poststaining) in STEM mode in a JEM 2100 (Jeol, Tokyo, Japan). Qualitative maps were made in which an enrichment of certain elements in specific locations of the cell could be investigated. Maps were acquired after 600 s of measurement time using the Bruker Quantax 200 esprit 1.9.4 software package. For each strain, 10 cells were analyzed in this fashion.

Deposition of cultures. Preservation of the strains in any other state than as living cultures proved difficult. Currently we are testing methods to generate viable frozen stocks. In the meantime, live cultures are available from the authors by request.

enrichments was investigated by light microscopy and fluorescence in-situ hybridization (FISH; EubIII probe). The purity of the strains was investigated via 16S rRNA gene sequence analysis.

Growth. Temperature and pH optima for the different strains were determined on the basis of growth rates in medium as described before (Khadem et al, 2010). The growth rate was determined by following the optical density (600 nm) of batch cultures under excess methane (> 2%) and fast shaking (350 rpm).

The pH range at which growth occurs was tested by gradually changing the pH when cultures were transferred (steps of one pH unit between pH 2 and pH 6, below pH 1 steps were only 0.1 pH unit). For pH 3 and below the medium pH was adjusted by sulfuric acid which also acted as a buffer. For pH 3 and above 50 mM MES was included as buffer (adjusted by NaOH), which did not influence the growth rates. After growth, only pH values above 3 were different from the starting value, but never more than 0.1 pH unit. The ability of the strains to grow on methanol was tested by adding 10 mM methanol to the growth media in the absence of methane.

The ability of the strains to grow autotrophically was tested by incubation with labeled methane. ^{13}C-labeled CH_4 experiments were done in batch cultures (in duplicate for each of the three strains) as described previously (Khadem et al, 2011), using 150 ml serum bottles containing 10 ml of culture medium and 40% of CO_2 in air. 3-5.5 ml ^{13}C-labeled CH_4 (99 atom % ^{13}C, Sigma-Aldrich) was added. Initial and final gas concentrations and amounts, as well as mass ratios for CO_2 were verified by Gas chromatography-mass spectrometry (GC-MS) analysis at the start and after growth (when at least 90% of the added CH_4 was consumed) in order to calculate the recovery of ^{13}C from CH_4 in CO_2. At the end of the experiment the $^{13}C/^{12}C$ ratio of the biomass was determined by isotope ratio mass spectrometry (IRMS) as described before (Khadem et al, 2011).

Phylogenetic and genomic analysis. The draft genomes of strains 3B and 4AC were assembled from Illumina sequencing runs using CLCBio software with standard settings. This resulted in 604 and 314 contigs for strain 3B and 4AC, respectively. The contigs were submitted to the RAST server for annotation (Aziz et al, 2008). The draft genome for strain 3C was assembled and annotated as part of a JGI Bioproject (PRJNA199166). The draft genomes of the three strains and the published genome of *M. fumariolicum* SolV (Pol et al, 2007; Khadem et al, 2012a) were used to obtain ANI(b) scores using JSpecies with standard settings (Richter & Rosselló-Móra, 2009). Phylogenetic and molecular evolutionary analyses were conducted using MEGA version 5 (Tamura et al, 2011). The 16S rRNA gene sequences used for the analysis were full length. The 16S rRNA gene similarity percentage analysis was performed via the Jukes-Cantor model (Jukes et al, 1969).

Morphological investigation by electron microscopy (EM) using different sample preparation techniques. High-pressure freezing, freeze-substitution, Epon-embedding and sectioning were performed as described previously (van Niftrik et al, 2008). For high-pressure freezing, cells were taken at one time point. Freeze-substitution was performed in acetone containing 2% osmium tetroxide, 0.2% uranyl acetate and 1% H_2O.

Methylacidiphilum share low pH optima (2-3.5) and high temperature optima (55-60°C) (Op den Camp et al, 2009). In addition, 16S rRNA gene sequences from different geothermal sites showed identities of only 95-99% to the 16S rRNA gene sequence of *M. fumariolicum* SolV (Pol et al, 2007; Sharp et al, 2012; Sharp et al, 2014). This indicated that a larger diversity in verrucomicrobial methanotrophs might exist in geothermal environments. Geothermal environments are often not only characterized by extreme conditions, but also by local and temporal fluctuations in pH, temperature and methane concentrations. The flux and composition of geothermal gasses, including methane and hydrogen sulfide, varies considerably over time (Etiope & Klusman, 2002). The hot gasses escape directly as fumaroles or seep through soil layers, via routes that may change continuously. Hydrogen sulfide is oxidized by microbes into sulfuric acid leading to very low pH values. It is likely that the pH is also influenced by rainfall.

During the isolation of the first (thermophilic) verrucomicrobial methanotrophs (Pol et al, 2007; Dunfield et al, 2007), mesophilic isolates were also encountered. A mesophilic verrucomicrobial enrichment culture was obtained during the isolation of *M. infernorum* V4 (Dunfield et al, 2007). Recently, strain LP2A was isolated in pure culture from this mesophilic enrichment culture (Sharp et al, 2014). Strain LP2A has a growth optimum at 30°C and its 16S rRNA gene sequence identity to the *Methylacidiphilum* genus is only 89.6%. In our search for more acid tolerant and mesophilic methane oxidizing species we started enrichment cultures from volcanic soil. Here we describe the isolation, physiology, phylogeny and morphology of three new highly acid tolerant, methanotrophic mesophilic *Verrucomicrobia*.

Materials & Methods

Enrichment and isolation. Soil samples were taken from various spots at the Solfatara crater, which is at the center of the Campi Flegrei caldera, near Naples (Italy). Spots were chosen at least 20 m away from the hot area which surrounds the central mudpot. Their temperatures as judged manually were well below 50 ^{o}C and pH values varied between 1 and 1.5. pH values were measured at the spots with indicator strips and confirmed by slurry measurements (about 0.3 ml g^{-1} soil). The rather dry top layer of about 0.5 -1 cm was first removed and samples of the humid layer just below were sampled into 50 ml sterile plastic tubes. Tubes were closed and within 10 h, 15 ml of samples were mixed with 15 ml store-bought mineral water. The mixtures were shaken by hand for 2 min in order to extract microorganisms from the soil. After settling for a few minutes, 1 ml from the liquid phase was transferred to a dilution series, each time 1 ml into 19 ml of medium in 60 ml bottles. The growth medium (Pol et al, 2007) was supplemented with 20% filtered (using a 0.22 µm filter) liquid from the central mudpot and adjusted to pH 2.5 (using H_2SO_4). Bottles had a gas phase of 5% carbon dioxide and 10% methane in air and were incubated at 29 ^{o}C with slow shaking (100 rpm) for four months. Bottles that showed growth were transferred three times and subsequently serially diluted to extinction (up to 10^{-8}). Serial dilutions were incubated for growth or immediately transferred on floating membrane filters and incubated at 30°C as described previously (Pol et al, 2007). Single colonies that appeared on the membranes were transferred to liquid medium. The composition of the

Abstract

Methanotrophic *Verrucomicrobia* were found in geothermal environments, characterized by high temperatures and low pH values. However, recently it has been hypothesized that methanotrophic *Verrucomicrobia* could be present at a broader range of environmental conditions. Here we describe the isolation and characterization of three new species of mesophilic acidophilic verrucomicrobial methanotrophs from a volcanic soil in Italy. The three new species showed 97-98% 16S rRNA gene identity to each other, but were only distantly related (89-90% on 16S rRNA level) to the thermophilic genus *Methylacidiphilum.* We propose the new genus *Methylacidimicrobium* including the novel species *M. fagopyrum*, *M. tartarophylax and M. cyclopophantes*. These mesophilic *Methylacidimicrobium* spp. were more acid tolerant than their thermophilic relatives, the most tolerant species *M. tartarophylax* still grew at pH 0.5. The variation in growth optima (35-44 ^{o}C) and maximum growth rates (0.013-0.040 h^{-1}) suggested that all species were adapted to a specific niche within the geothermal environment. All three species grew autotrophically using the Calvin cycle. The cells of all species contained glycogen particles and electron dense particles in their cytoplasm as visualized by electron microscopy. In addition, the cells of one of the species (*M. fagopyrum*) contained intracytoplasmic membrane stacks. The discovery of these three new species and their growth characteristics expands the diversity of verrucomicrobial methanotrophs and shows that they are present in much more ecosystems than previously assumed.

Introduction

Methane oxidation is a microbial process which limits the amount of methane released to the atmosphere (Conrad, 2009). Microbial methane oxidation can occur via different routes, either anaerobic (Knittel & Boetius, 2009; Ettwig et al, 2010; Haroon et al, 2013) or aerobic (Hanson & Hanson, 1996; Semrau et al, 2010; Op den Camp et al, 2009). The diversity of the biochemistry of methane oxidation is also reflected in the diversity of organisms performing these processes. For a long time, Alpha- and Gammaproteobacteria were considered to be the only organisms to perform aerobic methane oxidation. However, in 2007, methane-oxidizing *Verrucomicrobia* were discovered (genus *Methylacidiphilum* (Pol et al, 2007; Dunfield et al, 2007; Islam et al, 2008)) and also recently intra-aerobic bacteria belonging to the NC10 candidate phylum (Raghoebarsing et al, 2006; Ettwig et al, 2010) were described to oxidize methane using internally produced oxygen. Like most other aerobic methane oxidizers, the *Verrucomicrobia* use particulate methane monooxygenase (pMMO) to catalyze the first step of the methane oxidation. Unlike most proteobacterial methanotrophs (Op den Camp et al, 2009), but alike *Methylomirabilis oxyfera* (belonging to the NC10 phylum) (Rasigraf et al, 2014)), *M. fumariolicum* SolV (Khadem et al, 2011) and *M. infernorum* V4 (Sharp et al, 2012) grow as autotrophs, using only carbon dioxide as carbon source via the Calvin cycle.

All verrucomicrobial methanotrophs known to date have been enriched from geothermal environments (Op den Camp et al, 2009; Sharp et al, 2013; Sharp et al, 2014) and 16S rRNA gene surveys indicated their presence to be mainly limited to such environments (Sharp et al, 2014). The three thermophilic strains belonging to the genus

Chapter 4

Expanding the verrucomicrobial methanotrophic world: description of three novel species of *Methylacidimicrobium* gen. nov.

This chapter has been published as:

van Teeseling MCF[1], Pol A[1], Harhangi HR[1], van der Zwart S[1], Jetten MSM[1], Op den Camp HJM[1], van Niftrik L[1] (2014) Expanding the verrucomicrobial methanotrophic world: description of three novel species of *Methylacidimicrobium* gen. nov. *Appl Environ Microbiol* 80: 6782-6791.

[1]Department of Microbiology, Institute for Water and Wetland Research, Radboud University, Nijmegen, the Netherlands.

Acknowledgements

The employees of the General Instrumentation department are acknowledged for maintaining the Electron Microscopes. Muriel C. F. van Teeseling is supported by the European Research Council (ERC232937; granted to Mike S.M. Jetten).

that are recently synthesized in the cytoplasm and have not yet been transported to the periplasm.

Based on the pMMO secondary structure, this enzyme was predicted to be located in the cytoplasmic membrane. In the intra-aerobic methanotroph *Methylomirabilis oxyfera* (belonging to the NC10 phylum), the only other investigated methanotroph lacking ICMs, pMMO was present in the cytoplasmic membrane (Wu et al, 2012a). The immunogold localization performed in this study, however, pointed towards a cytoplasmic location of this enzyme in *M. fumariolicum* SolV. The statistical analysis showed with extreme significance that the pMMO antibody has a preference to bind in the cytoplasm rather than to the cytoplasmic membrane. In this respect it is important to note that all labels of which the center was located within a radius of 25 nm of the cytoplasmic membrane were counted as binding to this membrane, although they could have actually bound to an epitope in the cytoplasm. This means that the amount of labeling on the cytoplasmic membrane was probably even overestimated. These results are rather unexpected and this high amount of cytoplasmic labeling can probably not be explained by proteins that were synthesized in the cytoplasm and are in the process of transportation to the membrane. One possible explanation for this unexpected localization could be that the antibody against pMMO is not specific enough. Indeed, the immunoblot showed that the antibodies can also react to another protein, which might be located in the cytoplasm. Of course it could also be the case that the pMMO enzyme of *M. fumariolicum* SolV is actually located inside the cytoplasm, but this has never been observed before even though pMMO is a well-studied enzyme. All in all, it would be best to repeat the immunogold localization with a more specific antibody. This antibody should probably be generated against a highly purified pMMO enzyme rather than against a selected band from the membrane fraction, which might contain additional proteins.

Methylacidimicrobium fagopyrum 3C is as far as we know the only verrucomicrobial methanotroph with ICMs (van Teeseling et al, 2014 (chapter 4)). It would be interesting to investigate if pMMO is located in the ICMs of this organism – as in proteobacterial methanotrophs- or at another location. An additional question for further research is why some methanotrophs have ICMs to incorporate their pMMO in, while others seem to harbor the pMMO in their cytoplasmic membrane (*M. oxyfera*) or possibly in the cytoplasm itself (*M. fumariolicum* SolV). It would be of interest to study if the amount of pMMO per cell is higher in organisms with ICMs and if these organisms have a higher growth rate than organisms with pMMO located elsewhere.

In conclusion, this study is the first to show the location of a key enzyme of methane oxidation in *Verrucomicrobia*. The MDH of the verrucomicrobial methanotroph *M. fumariolicum* SolV was shown to be located at the same location as in other methanotrophs: the periplasm. In addition, this study suggests that pMMO might be located in the cytoplasm. However, repeating the immunogold labeling with a more specific antibody is necessary elucidate the location of pMMO in these *Verrucomicrobia*.

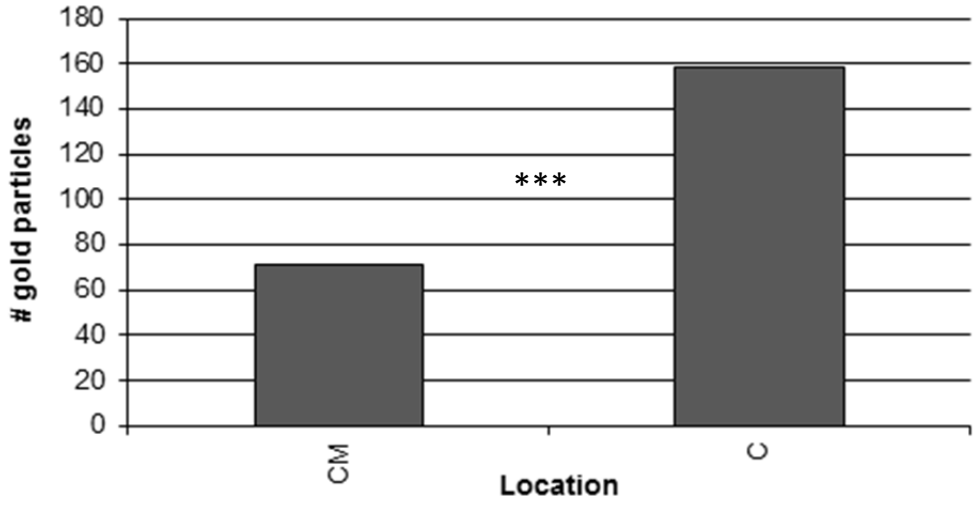

Figure 5. *Distribution of gold labels present in 62* M. fumariolicum *cells immunogold labeled with the pMMOb antibody over the categories cytoplasmic membrane (CM) and cytoplasm (C) shows with extreme significance (***) that the majority of labels was present in the cytoplasm. All labels of which the center was located within 25 nm of the cytoplasmic membrane were assigned to the CM category.*

Discussion

The recently discovered verrucomicrobial methanotrophs (Pol et al, 2007; Dunfield et al, 2007; Islam et al, 2008; Op den Camp et al, 2009) have an ultrastructure that differs from their proteobacterial counterparts. Where the latter often have intracytoplasmic membrane systems, these structures appear lacking from all but one species of the verrucomicrobial methanotrophs (van Teeseling et al, 2014 (chapter 4)). These ICMs have been shown to be the location of the pMMO enzyme in the proteobacterial methanotrophs (Brantner et al, 2002). MDH, the second enzyme in the methane oxidation pathway, is located in the (extended) periplasm of proteobacterial methanotrophs (Brantner et al, 2002). In the verrucomicrobial methanotrophs, pMMO and MDH also seem to play an important role in methane oxidation (Khadem et al, 2012b; Erikstad et al, 2012; Pol et al, 2014). The intracellular location of these two enzymes was investigated in the verrucomicrobial methanotroph *M. fumariolicum* SolV using antibodies and immunogold localization.

Immunogold localization using a highly specific antibody against the enzyme MDH, which catalyzes the oxidation of methanol to formate, showed this protein to be located in the periplasm. This localization was also supported by the periplasmic location predicted by pSORTb, the predicted signal peptide and the absence of transmembrane helices. Indeed a crystal structure of the MDH of *M. fumariolicum* SolV was shown to lack transmembrane helices (Pol et al, 2014). In some cases, gold particles were observed in the cytoplasm (Fig.3). In these cases, the antibody-protein A-gold complex might bind to MDH proteins

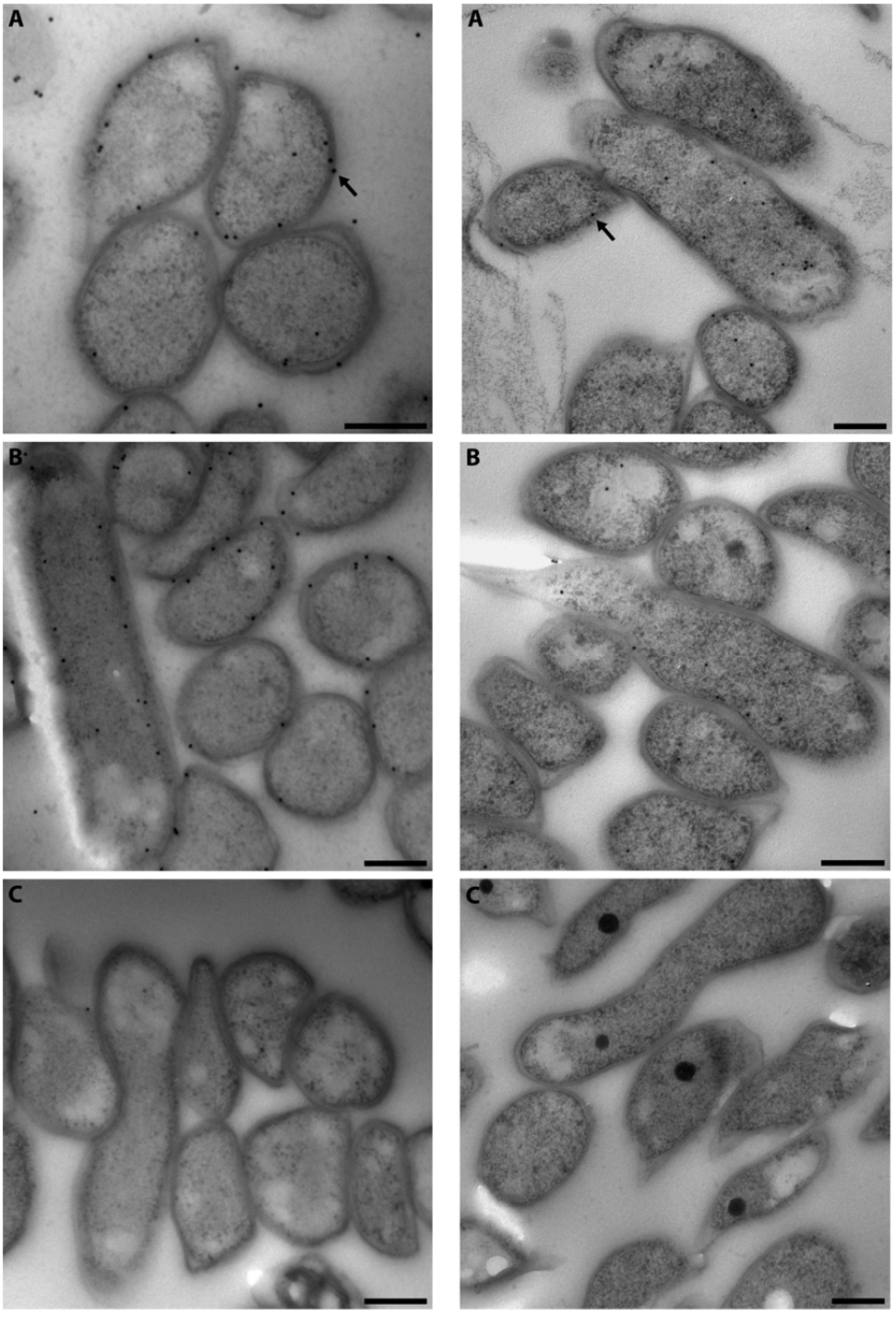
A
A
B
B
C
C

Immunolocalization of pMMOb in *M. fumariolicum* SolV. Ultrathin sections of lowicryl HM20 embedded *M. fumariolicum* cells were incubated with pMMOb antiserum to investigate the location of pMMOb in the cell. When the ultra-thin sections were incubated with the pre-immune serum, only one in about five cells harbored a gold label. In cells incubated with pMMOb antisera more labels, approximately four per cell, were observed. The labeling occurred mostly in the cytoplasm and some labeling occurred close to the cytoplasmic membrane (Fig. 4). Even when taking the 20 nm length of the antibody-protein A-gold complex in account, many labels should be interpreted as binding to an epitope in the cytoplasm. The statistical analysis performed on 62 cells showed an extremely significant difference between the labeling in the cytoplasm (the majority) and the labeling on the cytoplasmic membrane (the minority) (Fig. 5).

Figure 3 (right page, left image). *(A-B) Immunogold localization with the MDH antibody shows labeling almost exclusively in the periplasm of* M. fumariolicum *cells. The arrow indicates a gold label. (C) Incubation with the pre-immune serum shows almost no background labeling. Scale bar; 200 nm.*

Figure 4 (right page, right image). *(A-B) Immunogold localization with the pMMOb antibody shows labeling predominantly in the cytoplasm of* M. fumariolicum *cells. The arrow indicates a gold label. (C) Incubation with the pre-immune seuma shows no background labeling. Scale bar; 200 nm.*

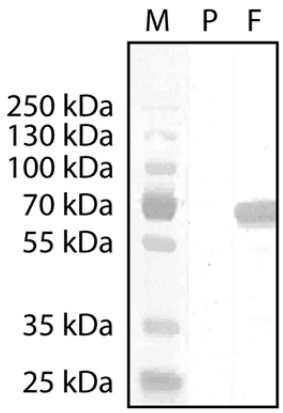

Figure 1. *Immunoblot analysis using pre-immune serum (P) and final bleed antiserum (F) against MDH on a blot with* M. fumariolicum *crude extract shows the specificity of the antibody against MDH (65 kDa). M = marker.*

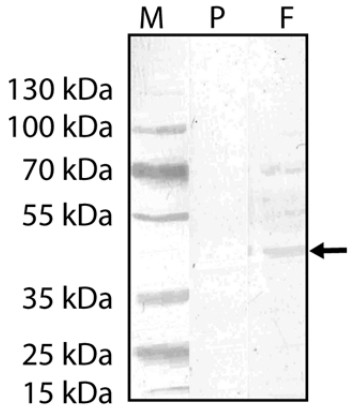

Figure 2. *Immunoblot analysis using pre-immune serum (P) and final bleed antiserum (F) against pMMOb on a blot with* M. fumariolicum *crude extract shows that the antibody is relatively specific against pMMOb (45 kDa; signal on the blot indicated by an arrow). M = marker.*

Immunolocalization of MDH in *M. fumariolicum* SolV. To study the intracellular location of the MDH protein in *M. fumariolicum*, ultrathin sections with cells embedded in lowicryl HM20 were incubated with MDH antiserum. When embedded in lowicryl HM20, the ultrastructure of the *M. fumariolicum* SolV cells was comparable to that seen in previous studies (Pol et al, 2007; Khadem et al, 2012c (chapter 2); van Teeseling et al, 2014 (chapter 4)). Only few labels (approximately 1 per 4 cells) were detected outside of the cells and the labeling present in the cells (ca. 5 labels per cell) was located in the periplasm itself or in its close vicinity (Fig. 3). Since the length of a full antibody-protein A-gold complex is approximately 20 nm (Roth, 1982), labels that are located up to 20 nm outside of the periplasm could target antigens that are present in the periplasm. Only few labels (approximately 1 per 4 cells) were present when the ultrathin sections were incubated with pre-immune serum (Fig. 3) and labels were practically absent when the sections were incubated with blocking buffer.

Statistical analysis. A statistical analysis was performed on the immunogold localization of the pMMO enzyme. The gold particles of which the center was located within 25 nm from the cytoplasmic membrane were interpreted as binding to this membrane and the gold particles in the cytoplasm that were further than 25 nm away from a membrane were counted in the cytoplasm category. No other categories were included. For statistical analysis, 62 cells, which were incubated with both antiserum and PAG-10 gold particles, were analyzed. For analysis, an unpaired *t*-test for normal distributed data with equal variances (GraphPad: http://www.graphpad.com/quickcalcs/) was performed. A *P*-value between 0.05 and 0.01 was considered significant, a *P*-value between 0.01 and 0.0001 very significant and a *P*-value of less than 0.0001 extremely significant.

Results

Bioinformatic analysis of MDH and pMMO. The MDH protein from *M. fumariolicum* SolV was predicted to be located in the periplasm by pSORTb (with a prediction value of 9.76 (cut-off 7.5)) and this was in accordance with the prediction of a signal peptide by SignalP and the absence of predicted transmembrane helices in the MDH sequence. The pMMOb protein was predicted to be present in the cytoplasmic membrane (prediction value of 10 by pSORTb). It is important to realize that pSORTb has no specific category for ICMs, which in this case does not seem to pose a problem since verrucomicrobial methanotrophs lack these structures. The prediction of the pMMOb subunit as a membrane protein is strengthened by the three predicted transmembrane helices in this subunit. Crystal structures of entire pMMO enzymes of three different methanotrophs also show transmembrane helices for the pMMOb subunit, although two instead of three (Culpepper & Rosenzweig, 2012). This fits with the fact that pMMO proteins are membrane proteins. The predicted absence of signal peptides also suggests the protein is not exported to the periplasm to be subsequently inserted into the outer membrane.

Specificity of antisera. Antisera were generated in rabbits against purified MDH and enriched pMMOb from *M. fumariolicum* SolV. To further purify these proteins, the samples were run on an SDS-PAGE gel and bands at the apparent molecular weight of the two proteins (MDH: ~ 60 kDa; pMMOb: ~ 48 kDa) were cut out. The affinity and specificity of the generated antisera (final bleed) was tested via immunoblotting against a whole cell extract of *M. fumariolicum* SolV.

Incubations with the antiserum targeting MDH showed a single band at an apparent molecular mass of approximately 60 kDa (Fig. 1), which was the predicted molecular mass for this protein. The antiserum thus seems to be very specific against MDH. No signals were seen when the blots were incubated with blocking buffer (data not shown) or pre-immune serum (Fig. 1) instead of antiserum. When blots were incubated with pMMOb antiserum, a band at approximately 48 kDa appeared and an additional, slightly weaker, band was present at 70 kDa (Fig. 2). This suggests that the antiserum against pMMOb is fairly specific, but might also recognize another protein with an apparent mass of ca. 70 kDa. No bands were present after incubation with blocking buffer (data not shown) or pre-immune serum (Fig.2) instead of antiserum.

100 mesh copper grids (Stork-Vesco, Eerbeek, Netherlands) containing a carbon-coated formvar film.

For labeling of pMMO subunit α, grids containing ultrathin sections of *M. fumariolicum* SolV cells were washed for 10 min on PHEM. Blocking was achieved by incubation on drops of PHEM containing 1% skim milk powder (Frema Reform, Lüneburg, Germany) for 15 min, after which the grids were incubated for 120 min with antiserum diluted 50-fold in PHEM containing 1% skim milk powder. Negative controls were incubated in PHEM containing 1% skim milk powder without antiserum for 120 min. In an additional negative control, grids were incubated with pre-immune serum instead of antiserum. After this incubation, the grids were washed for 10 min on drops of PHEM with 0.1% skim milk powder and incubated for 45 min with the secondary antibody, protein A coupled to 10 nm gold (PAG-10, CMC UMC Utrecht), diluted 60-fold in PHEM with 1% skim milk powder. The grids were then washed on 5 drops of PHEM with 0.1% skim milk powder and 5 min on drops of PHEM. The antibodies were fixed by incubating for 5 min on drops of 1% glutaraldehyde in PHEM and were consequently washed for 10 min on drops of MilliQ water. Post-staining was performed by incubating 20 min in 2% UAc in MilliQ water, after which the grids were washed for 5 min on drops of MilliQ water and air dried.

For labeling of MDH, grids containing ultrathin sections of *M. fumariolicum* SolV cells were washed for 10 min on PHEM. Blocking was achieved by incubation on drops of PHEM containing 1% BSA and 0.1% BSA-C for 15 min, after which the grids were incubated for 60 min with antiserum diluted 100-fold in PHEM containing 1% BSA and 0.1% BSA-C. Negative controls were incubated in PHEM containing 1% BSA and 0.1% BSA-C without antiserum for 60 min. In an additional negative control, grids were incubated with pre-immune serum instead of antiserum. After this incubation, the grids were washed for 10 min on drops of PHEM with 0.1% BSA and 0.01% BSA-C and incubated for 45 min with the secondary antibody, protein A coupled to 10 nm gold (PAG-10, CMC UMC Utrecht), diluted 60-fold in PHEM with 1% BSA and 0.1% BSA-C. The grids were then washed on 5 drops of PHEM with 0.1% BSA and 0.01% BSA-C and 5 min on drops of PHEM. The antibodies were fixed by incubating for 5 min on drops of 1% glutaraldehyde in PHEM and were consequently washed for 10 min on drops of MilliQ water. Post-staining was performed by incubating 20 min in 2% UAc in MilliQ water, after which the grids were washed for 5 min on drops of MilliQ water and air dried. All grids were investigated at 100 kV in a JEOL (Tokyo, Japan) JEM-1010 Transmission Electron Microscope (TEM). Images were recorded using the SIS Mega View III camera (Olympus, Münster, Germany).

Immunoblotting. Blots were made from 10% SDS-PAGE gels containing cell-free extract of *M. fumariolicum* SolV cells grown in batch. The cell-free extract was prepared as described above. This cell-free extract was boiled for 7 min in sample buffer (as described above) and an amount of ca. 20 µg protein per lane was loaded onto 10% SDS-PAGE gels. After the gel was run, proteins were transferred to a Protran nitrocellulose transfer membrane with pore size 0.45 µm (Whatman, Dassel, Germany) with the semi-dry transfer cell blotting system (Bio-Rad, Veenendaal, the Netherlands). Prior to blotting, the gel (for 5 min) and nitrocellulose membrane (for 30 min) were incubated in a blotting buffer consisting of 48 mM Tris and 39 mM glycine and 20% methanol. The blotting was performed at 50 mA for 60 min at room temperature and the dried blots were stored at 4°C.

Immunoblotting was performed on blots that were incubated in deionized water (dH_2O) for 30 min. Blocking was performed by incubating the blots for 30 min in blocking buffer consisting of 1% BSA in TBS pH7.4 (10 mM Tris-HCl, 137 mM NaCl and 2.7 mM KCl). Subsequently, the blots were incubated for 60 min in antiserum diluted 500-fold (in the case of the MDH antibody) or 250-fold (in the case of the pMMO antibody) in blocking buffer. Two negative controls were performed; instead of antiserum, one was incubated in blocking buffer and the other was incubated in pre-immune serum in the same dilution (in blocking buffer) as the antiserum. The blots were washed three times 10 min in TBS containing 0.05% Tween and incubated for 60 min in monoclonal mouse anti-rabbit IgG alkaline phosphatase conjugate (Sigma, Zwijndrecht, The Netherlands) diluted 150000-fold in blocking buffer. Subsequently, the blots were washed two times 10 min in TBS containing 0.05% Tween and two times 10 min in TBS. Finally, the blots were incubated in BCIP/NBT liquid substrate system (Sigma) for 2 min (in the case of the MDH antibody) or 3 min and 15 s (in the case of the pMMO antibody) and rinsed for 10 min in dH_2O. All lanes were imaged with the same settings.

Immunogold localization. For immunogold localization, 2 ml of cells grown in a continuous culture (OD_{600} ~1) were concentrated by centrifugation (800 g, 5 min) and resuspended in 30 µl of supernatant. After loading 1.5 µl of the cell suspension in a gold-plated platelet (2 mm inner diameter, 100 µm depth) (Leica Microsystems, Vienna, Austria), the sample was high-pressure frozen in a HPM-100 (Leica Microsystems). Freeze-substitution was performed in an AFS1 (Leica Microsystems) with 0.2% Uranyl Acetate (UAc) (Merck, Darmstadt, Germany) in Seccosolv anhydrous acetone (Merck Millipore, Darmstadt, Germany). The substitution started at -90°C for 86 h, followed by a 2°C/h slope to -70°C, where the sample remained for 12 h. Subsequently, the temperature was raised with 2°C/h to -50°C, where the sample remained for 12 h. Next, the sample was washed with anhydrous acetone (two changes) to remove UAc at -50°C and infiltrated with Lowicryl HM20 (Electron Microscopy Sciences, Hatfield PA, USA) in anhydrous acetone at -50°C. Infiltration was started with 12.5% HM20 for 2 h, than 2 h in 25% HM20, 2 h in 50% HM20, 2 h in 75% HM20, 1 x 2 h in 100% HM20, 12 h in 100% HM20 and 1x 3 h in 100% HM20. After the final change of 100% HM20, the lowicryl was polymerized by UV irradiation at -50°C for 96 h and 2 °C/h to 0°C, 10 h at 0°C. Ultrathin sections (ca. 65 nm) were cut using an UCT microtome (Leica Microsystems, Vienna, Austria) and applied to

Bioinformatic analysis of the *M. fumariolicum* SolV pMMO and MDH proteins. The subcellular location of the proteins MDH and pMMO was predicted using pSORTbv3.0.2 (Yu et al, 2010) with standard settings for Gram-negative bacteria. SignalP 4.1 (Petersen et al, 2011) was used to predict signal peptides in pMMO and MDH protein sequences using standard settings for Gram-negative bacteria. The amount of transmembrane helices was predicted using TMHMM v2.0 (Krogh et al, 2001) with standard settings. The accession code for the *xoxF* gene encoding for MDH of *M. fumariolicum* SolV is Mfumv2_1183. For pMMOb, the *pmoB2* gene (Mfumv2_1974) was selected, since this was shown to be the most abundant *pmoB* gene expressed (Khadem et al, 2012a) under the growth conditions used in this study.

SDS-polyacrylamide gel electrophoresis (PAGE). Protein samples that were analyzed by SDS-PAGE were first denatured by incubation for 7 min at 100°C with 158 mM Tris-HCl buffer pH 7 containing 5% β-mercaptoethanol, 2.6% sodium dodecyl sulfate (SDS) and 16% glycerol. SDS-PAGE was performed in the running buffer described previously (Laemmli, 1970) using 10% slab gels. After separation, the proteins were visualized by staining the gels with Coomassie Brilliant Blue (G250).

Preparation of cell-free extract and membrane fraction. Cell-free extract of *M. fumariolicum* SolV was prepared by harvesting cells by centrifugation (4000 g, 10 min), after which the cell pellet was resuspended in 25 mM PIPES buffer pH 7.5. The cells were passed through a French press at 20000 lb/in^2 and centrifuged at 12000 g for 20 min. The resulting turbid supernatant was the cell-free extract containing both *M. fumariolicum* SolV soluble proteins and membranes. From the cell-free extract a membrane fraction was obtained by centrifugation at 48000 g, 60 min. The resulting pellet is referred to as the *M. fumariolicum* SolV membrane fraction.

Antibody generation. Antibodies against MDH and pMMOb were generated by purifying or enriching the respective proteins, cutting their corresponding protein bands out of SDS-PAGE gels (10%) and using the protein from these bands to immunize rabbits (Eurogentec, Seraing, Belgium). Purified MDH was obtained from a culture grown in batch as described before (Pol et al, 2014) and loaded on an SDS-PAGE gel. Since pMMOb is one of the most abundant proteins in the *M. fumariolicum* SolV membrane fraction, a membrane fraction (prepared as described above) was loaded on a SDS-PAGE gel to cut out the pMMOb protein band. Gels with purified MDH or enriched pMMOb were stained and destained with solutions that included EtOH instead of MetOH. The bands corresponding to a protein of approximately 60 kDa (MDH) and 48 kDa (pMMOb) were cut out and sent in to Davids Biotechnology (Regensburg, Germany) for immunization of rabbits. To verify the contents of this protein band, one band from the same gel was analyzed by LC-MS/MS.

(Hanson & Hanson, 1996; Semrau et al, 2010). The ICMs are thought to be continuous with the cytoplasmic membrane (De Boer & Hazeu, 1972) and the periplasm is proposed to be extended into the space in between the ICMs (Brantner et al, 2002). Via immunogold localization the presence of pMMO in the ICMs has been verified for the methanotrophic Proteobacterium *Methylomicrobium album* BG8 and the MDH was found in the extended periplasm in between the ICMs (Brantner et al, 2002). In *M. oxyfera*, which lacks ICMs, immunogold localization targeting pMMOb showed this enzyme to be located at the cytoplasmic membrane (Wu et al, 2012a). No studies have yet been performed targeting the location of pMMO and MDH in the verrucomicrobial methanotrophs. Since all but one species of these methanotrophs apparently lack ICMs (van Teeseling et al, 2014 (chapter 4)) it is expected that the location of pMMO in these organism differs from the location in *Proteobacteria* and might rather resemble the location in the non-proteobacterial *M. oxyfera*.

This study aims to elucidate the intracellular location of the key enzymes pMMO and MDH in the methane oxidation pathway of the recently discovered *M*. fumariolicum, belonging to the methanotrophic *Verrucomicrobia*. Using antibodies specifically raised against these enzymes for immunogold localization it is shown that MDH is present in the periplasm. The location of pMMO remains ambiguous and needs further investigation but first results indicate a cytoplasmic location.

Materials & Methods

Growth of *Methylacidiphilum fumariolicum* SolV. The cells used for electron microscopy were grown in continuous culture and the cells used for protein purification or enrichment were grown in batch mode. The medium used for growth (until OD_{600}=1) in continuous culture consisted of 0.2 mM $MgCl_2 \cdot 6H_2O$, 0.2 mM $CaCl_2 \cdot 2H_2O$, 1 mM Na_2SO_4, 2 mM K_2SO_4, 5 mM KNO_3 and 1 mM $NaH_2PO_4 \cdot H_2O$. A trace element solution was added to the medium containing 1 µM each of Ni, Co, Mo, Zn and Ce, 5 µM of both Mn and Fe, 10 µM of Cu (all present in the form of salts) and 40-50 µM nitrilotriacetic acid. The pH of the medium was adjusted to 2.7 using 1 M H_2SO_4. To avoid precipitation, $CaCl_2.2H_2O$ was autoclaved separately from the rest of the medium and both were mixed after cooling. The medium used for batch mode growth was the same, with the exception that the 5 mM of KNO_3 was replaced with 8 mM $(NH_4)_2SO_4$.

The continuous culture was grown in a chemostat (volume: 500 ml) with CH_4 as an electron donor and NO_3^- as a nitrogen source. The chemostat was operated at 55°C with stirring at 900 rpm. The medium was supplied at a flow rate of 14.5 ml per h using a peristaltic pump and 10% CH_4 (v/v), 8% O_2 (v/v) and 68% CO_2 (v/v) were sparged into the medium.

In batch mode, a gas mixture of 10% CH_4 (v/v), 6% CO_2 (v/v), and 84% air (v/v) was supplied to the fermentor in a continuous flow. The initial pH of the medium was set to 2.7 and pH decreased to about 2.5 when growth stopped. The temperature and agitation speed were set to 55°C and 900 rpm, respectively.

2011; Sharp et al, 2012). The enzymes involved in the oxidation of methane are methane monooxygenase (either in a soluble form; sMMO or in a membrane-bound, particulate form: pMMO), methanol dehydrogenase (MDH), formaldehyde dehydrogenase (FADH) and formate dehydrogenase (FDH) (Hanson & Hanson, 1996; Chistoserdova, 2011). This study focuses on the first two enzymes in the aerobic oxidation of methane by verrucomicrobial methanotrophs: pMMO and MDH.

Of the two methane monooxygenases, pMMO is the most abundant and up to now only *Methylocella* and *Methyloferula* species have been observed to lack this enzyme and depend solely on sMMO (Dedysh et al, 2000; Dunfield et al, 2003; Dedysh et al, 2004; Theisen et al, 2005; Semrau et al, 2010; Vorobev et al, 2011). Because the pMMO enzyme is so unique to and widespread among aerobic methanotrophs, the *pmoA* gene encoding for one of its subunits is used as a marker to detect aerobic methanotrophs in the environment (McDonald et al, 2007). The pMMO is a copper containing enzyme and it consists of three copies of three subunits each: subunit α is encoded by *pmoB*, subunit β is encoded by *pmoA* and subunit γ is encoded by *pmoC* (Lieberman & Rosenzweig, 2005; Semrau et al, 2010). The active site is located in a soluble domain of the α subunit and is dependent on copper (Balasubramanian et al, 2010). All three *Methylacidiphilum* species contain at least three copies of the *pmoCAB* operon and the divergence of the copies within each species suggests a high selection pressure and potential differential expression in response to environmental parameters (Op den Camp et al, 2009). For both *Methylacidiphilum fumariolicum* SolV and *Methylacidiphilum kamchatkense* Kam1, a differential expression of the *pmo* genes was indeed observed and the expression was influenced by oxygen limitation (SolV) and methane availability (Kam1) (Erikstad et al, 2012; Khadem et al, 2012b).

Multiple different variants of the soluble enzyme MDH are found in nature. The classical MDH is encoded by *mxaFI*, forms a heterotetramer and has Ca^{2+} in its active center (Chistersodova, 2011). A new MDH variant, encoded by *mdh2*, was recently discovered and this enzyme is not yet studied in great detail (Kalyuzhnaya et al, 2008). A third group of MDHs is encoded by *xoxF* and these enzymes depend on lanthanides instead of Ca^{2+}, which probably allows them to be more specific for methanol than the *mxaFI* enzymes (Nakagawa et al, 2012; Pol et al, 2014; Keltjens et al, 2014; Wu et al, 2015). The verrucomicrobial methanotrophs have an MDH enzyme of the *xoxF* type, which was shown to oxidize methanol to formate (Hou et al, 2008; Pol et al, 2014).

Since the product of the reaction catalyzed by pMMO is the substrate used by MDH it would be a good strategy for the methanotrophic cell to have the membrane-bound pMMO and the soluble MDH enzymes located in close proximity in order to enhance the efficiency of the methane oxidation. Indeed such a close proximity was observed in the proteobacterial methanotroph *Methylococcus capsulatus* (Bath), in which pMMO and MDH form a supercomplex that was shown to facilitate a highly efficient oxidation of methane to formaldehyde (Myronova et al, 2006). Most methanotrophs incorporate their pMMOs in intracytoplasmic membrane systems (ICMs) and the amount of these ICMs is correlated with the amount of pMMO which both depend on the availability of copper

Abstract

Methane oxidation is a process that can be performed by various aerobic bacteria, including the recently discovered methanotrophic *Verrucomicrobia*. These thermoacidophilic methanotrophs use the canonical particulate methane monooxygenase (pMMO) and a lanthanide-containing methanol dehydrogenase (MDH) of the *xoxF*-type as the first two enzymes in the oxidation of methane. In proteobacterial methanotrophs, pMMO is located in intracytoplasmic membrane systems and MDH is located in the periplasmic space in between the intracytoplasmic membranes. However, intracytoplasmic membranes are absent in most verrucomicrobial methanotrophs. In this study, the intracellular location of the pMMO and MDH enzymes in the verrucomicrobium *Methylacidiphilum fumariolicum* SolV was investigated using antibodies specifically generated for both enzymes. The immunogold localization showed that MDH is located in the periplasm. The location of subunit α of pMMO could not be resolved. The location of the gold particles of the secondary antibody indicated a cytoplasmic location, although this pMMO subunit is predicted to have multiple transmembrane helices. Immunoblot analysis showed that the antibody against pMMO is not very specific, so the results obtained by immunogold localization might not reflect the actual intracellular location of this enzyme which needs further investigation. This study is the first to show the location of a key enzyme (MDH) of methane oxidation in a verrucomicrobial methanotroph.

Introduction

Microbial methane oxidation is a process that can take place both aerobically and anaerobically. For a long time it was thought that Proteobacteria were the only bacteria that could oxidize methane using oxygen (Hanson & Hanson, 1996). Recently, several non-proteobacterial aerobic methanotrophs were discovered; one species belonging to the NC-10 phylum (Raghoebarsing et al, 2006; Ettwig et al, 2008) and multiple species belonging to the *Verrucomicrobia* (Pol et al, 2007; Dunfield et al, 2007; Islam et al, 2008; Op den Camp et al, 2009). *Methylomirabilis oxyfera*, as the NC-10 member is called, was first thought to oxidize methane without oxygen, coupling partial denitrification to methane oxidation, since it lives in anaerobic environments. Later on it was discovered that this organism follows the route of aerobic methane oxidation, using internally produced oxygen. The oxygen is proposed to be derived from the dismutation of nitric oxide to dinitrogen gas and oxygen (Ettwig et al, 2010; Ettwig et al, 2012). The methanotrophic *Verrucomicrobia*, all belonging to the genus *Methylacidiphilum*, have been isolated from geothermal environments and grow at a low pH (growth is still possible below pH 1) and elevated temperatures (optima between 55 and 60°C) (Op den Camp et al, 2009).

All studied aerobic methanotrophs oxidize methane by first converting methane to methanol, then to formaldehyde, to formate and eventually to carbon dioxide (Hanson & Hanson 1996; Semrau et al, 2010; Chistoserdova, 2011). Most methanotrophic Proteobacteria can incorporate the formaldehyde into biomass by either the ribulose monophosphate or the serine pathway (Hanson & Hanson, 1996). However, the *Verrucomicrobia* use carbon dioxide for carbon fixation via the Calvin cycle (Khadem et al,

Chapter 3

Immunolocalization of the methane oxidation enzymes particulate methane monooxygenase and methanol dehydrogenase in the verrucomicrobial methanotroph *Methylacidiphilum fumariolicum* SolV

van Teeseling MCF[1], Mesman RJ[1],Pol A[1], Khadem AF[1],Mohammadi SS[1], Jetten MSM[1], Op den Camp HJM[1], van Niftrik L[1]

[1]Department of Microbiology, Institute for Water and Wetland Research, Radboud University, Nijmegen, the Netherlands.

Acknowledgments

We are grateful to Jelle Eygensteyn for help with the elemental analyses and Elly G. van Donselaar for help with the polysaccharide staining for electron microscopy. A.F.K. was supported by Mosaic grant 62000583 and L.v.N. by VENI grant 863.09.009, both from the Netherlands Organization for Scientific Research - NWO, M.S.M.J. & M.C.F.v.T. were supported by ERC grant no. 232937.

The benefit of accumulated glycogen for *M. fumariolicum* under energy-limiting conditions (no methane) was shown by the fact that cell numbers declined less and that the viability of remaining cells was maintained much better for glycogen loaded cells compared to cells with only small amounts of glycogen (exponentially grown). Glycogen loaded cells showed an initial lag phase which could be expected because the bacteria were in very different metabolic state as a result of the nitrogen depletion, with a much lower cytosolic protein content. This lag phase however became longer only after 40 days of starvation. During this period the glycogen was almost fully consumed, as was shown by ^{13}C-labeling experiments. These cells produced $^{13}CO_2$ in amounts that equal the initial glycogen content of the cells, while the headspace of exponential cells only showed a small increase in $^{13}CO_2$ during the first few days. Growth was only observed in the presence of methane and it could therefore be concluded that glycogen was not used for cell growth. Similar results were found for *Methylocystis parvus* OBBP, were no growth on PHB was observed (Pieja et al, 2011b). Therefore, we conclude that the glycogen storage enhances the viability of *M*. *fumariolicum* during methane starvation.

Regulation of glycogen synthesis/degradation seemed not to be at the transcriptional level since both pathways are simultaneously expressed (Table 2). Having a regulation on protein/enzyme level makes it possible for strain SolV to switch between biosynthesis or degradation of glycogen, depending on the conditions and prevents futile cycling. Bacterial (and plant) glycogen synthases use ADP-glucose as sugar donor and the ADP-glucose availability is the triggering factor for biosynthesis (Cid et al, 2022). Regulation of biosynthesis occurs at the synthesis of ADP-glucose. The enzyme producing this intermediate, glucose-1-phosphate adenylyltransferase (also named ADP-glucose pyrophosphorylase), is allosterically activated about 10- to over 40-fold by glycolytic intermediates and inhibited by AMP, ADP or Pi (Preiss, 1996). A conserved domain search of the SolV enzyme (Mfum_1020013) amino acid sequence showed all known ligand binding sites to be present. Knowledge on the regulation of the glycogen degradation pathways in bacteria is limiting, but for *Escherichia coli* allosteric regulation of the glycogen phosphorylase by a histidine phosphocarrier protein (HPr) has been described (Seok et al, 2011). The gene encoding this HPr is present in the genome of strain SolV and transcribed under different culture conditions (Khadem et al, 2012 a; b).

To conclude, we have showed that the thermoacidophilic verrucomicrobial methanotroph *M*. *fumariolicum* is able to store glycogen in the case of nitrogen depletion. This accumulated glycogen may be consumed in response to energy limitation. It is hypothesized that the bacteria use accumulated glycogen to enhance viability, since growth on accumulated glycogen was not observed. To the best of our knowledge this is the first experimental validation of glycogen storage in the phylum *Verrucomicrobia*.

little bit of glycogen produced during exponential phase. Electron microscopy showed that at the end of the transition phase I (1.5 days after ammonium depletion), cells were packed with glycogen bodies. In addition, the strong increase in total amount of carbon in the pellet fraction per cell, pointed to glycogen storage in phase I.

The increase in dry weight and total carbon (mg per ml cell culture) in transition phase I was not only due to glycogen storage (26% of the dry weight), but also to cell growth, since cell numbers doubled. This growth was not due to other nitrogen sources present in the medium or nitrogen fixation. Nitrogen fixation would also be impossible since dissolved oxygen concentrations in the cultures were too high to support nitrogen fixation by *M. fumariolicum* (Khadem et al, 2010). Moreover, the total protein and nitrogen content (mg per ml cell culture) stabilized immediately after ammonium depletion. The observation that the amount of protein and total nitrogen (mg per ml cell culture) in the pellet fraction of the crude extracts doubled, was in accordance with the doubling of cell numbers.

Completion of cell division once DNA replication has started, seems to be of utmost importance when growth substrates are limiting as has been documented before (Wanner & Egli, 1990 and references therein). While some bacteria become smaller under such conditions (reductive cell division), strain SolV maintained its normal shape and size.

On basis of the carbon percentages, the changes in carbon to nitrogen ratio and assuming a constant amount of nitrogen at the start and end of transition phase II we calculated that dry weight in this phase should have increased about 20%. The measured increase (based on weighing) was about 30%. The increase of the glycogen percentage from 26 to 36% can account for only 15% of the dry weight increase. The observed biomass increase may have resulted from some ongoing growth in this phase, but the increase in cell numbers was too small to result in a significant difference.

Under the circumstances tested (nitrogen depletion), the maximum amount of glycogen measured in the cells of strain SolV was 36% of the dry weight. Under nitrogen limitation, a similar percentage of glycogen was found in the halotolerant methanotroph *Methylobacter alcaliphilus* 20Z using ^{1}H-NMR (Khmelenina et al, 1999). Under other growth conditions, percentages of 16% (calcium limitation) and 35% (growth on methanol) are reported for methanotrophs (Linton et al, 1978; Eshinimaev et al, 2002). However, under nitrogen depletion PHB can account for up to 50% of the dry weight in *Methylocystis parvus* OBBP (Pieja et al, 2011b).

Glyceraldehyde-3-phosphate produced from CO_2 via the Calvin-Benson-Bassham cycle (Khadem et al, 2011), is the most likely precursor of glucose-6-phosphate in strain SolV. The consecutive action of triose-P-isomerase, fructose 1,6-bisphosphate aldolase, fructose 1,6-bisphosphate phosphatase and glucose-6-P isomerase results in glucose-6-phosphate. The presence of a gene encoding for phosphoglucomutase (*pgm*), suggests that the latter enzyme in turn can convert glucose-6-phosphate and its product glucose-1-phosphate can be used for glycogen synthesis (Wayne et al, 2010). The same route (in reverse) can be used for the degradation of glycogen.

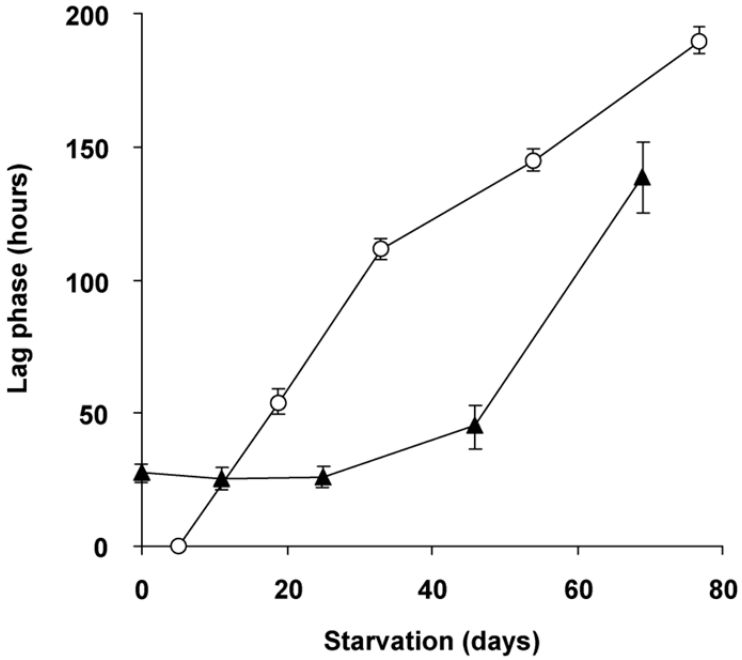

Figure 8. *Viability and recovery of glycogen containing* M. fumariolicum *SolV cells (closed triangles) and exponentially growing cells (open circles) after methane and ammonium starvation for different periods of time. At time 0, cells were inoculated into optimal medium (4 mM ammonium and methane in the headspace) and lag phases were recorded. Error bars represent S.E.M. (n = 3-4).*

Discussion

Many bacteria store carbon when nitrogen becomes growth limiting (Wanner & Egli, 1990 and references therein). Methanotrophs are also known for their ability to store carbon, either in the form of polyhydroxybutyrate (PHB), glycogen or by exopolysaccharide (EPS) production. Many studies have focused on PHB storage and its role in methanotrophs, and the genes involved in its synthesis (Pieja et al, 2011b). In addition, EPS production in multiple methanotrophs has been studied in some detail (Malashenko et al, 2001). However, detailed studies about glycogen production and its role in methanotrophs are scarce (Linton et al, 1978; Khmelenina et al, 1999; Eshinimaev et al, 2002).

Although the electron microscopic polysaccharide stain used in our study is not specific for glycogen (Bradbury & Stoward, 1967), our results in combination with the biochemical assay clearly show the presence of glucose polymers in strain SolV. As all the genes for glycogen production and consumption were shown to be present and transcribed, this glucose polymer is most likely glycogen. For more definite proof a biochemical analysis of chain length and type of branching will be necessary.

Based on the growth experiments, it can be assumed that glycogen storage starts soon after ammonium depletion in the medium. However, the glycogen measurements, electron microscopic observations and the transcriptome data suggest that there was a

exponentially grown cultures and by a factor 2.4 in the case of cells obtained at the end of transition phase II. The lag phase observed upon recultivation in optimal growth conditions was taken as a measure of viability of the remaining cultures of both types. Exponentially grown cultures were losing viability rapidly after four days of methane starvation (Fig. 8). Recultivation starting from glycogen loaded cultures showed a lag phase (28 h) from the start. This lag phase remained unchanged for about 40 days of methane starvation (Fig. 8). Only after 45 days the lag phase of glycogen loaded cells increased, pointing to a depletion of the stored glycogen (Fig. 8). This is well in accordance with the results of the ^{13}C-labeled glycogen consumption experiment, which showed that in about 47 days all glycogen in the cells was consumed.

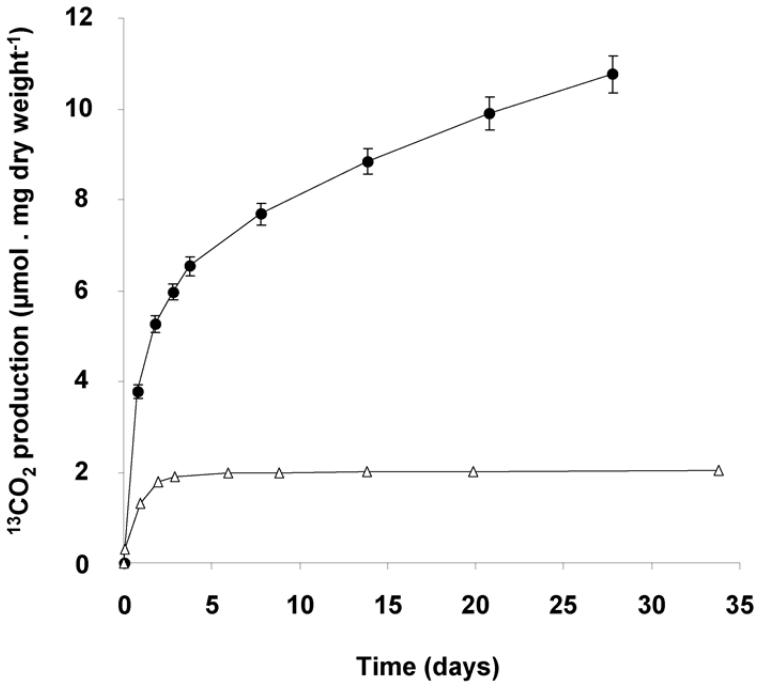

Figure 7. *$^{13}CO_2$ production originating from ^{13}C-glycogen loaded cells (4.4 mg dry weight), obtained at the end of the transition phase II (closed circles). Exponentially growing cells (2.1 mg dry weight; open triangles) served as a control. $^{13}CO_2$ measured after 1 hour of incubation at 55°C, was subtracted from all measured values during the experiment. Error bars represent S.E.M. (n = 4).*

Glycogen consumption and function. The consumption of glycogen was detected by the release of ^{13}C-labeled CO_2 from cells that had accumulated ^{13}C-labeled glycogen. Accumulation of ^{13}C containing glycogen was achieved by growing cultures till late transition phase II in the presence of both ^{13}C-labeled methane and carbon dioxide. When such cells are transferred to a medium without methane, stored glycogen is likely to be consumed to meet the energy requirement of the starving cells, and thus ^{13}C-labeled CO_2 is produced. The ratio of $^{12}C/^{13}C$ was determined accurately by GC-MS analysis, against a background of 10% unlabeled CO_2 in the culture bottles. During the first day a rapid $^{13}CO_2$ production was observed (initial rate of 5 µmol $^{13}CO_2$ produced per mg dry weight of cells per day; Fig. 7). This rate dropped gradually to a linear rate of 0.2 µmol $^{13}CO_2$ produced per mg dw cells per day, which did not change at least till day 28. The total amount of $^{13}CO_2$ produced over this period was calculated to be 51.4 ± 1.9 µmol of $^{13}CO_2$ (n=4). On basis of the glycogen content of the cells (36% of 4.4 mg dry weight of cells), 9.8 µmol of glycogen was introduced in the incubation. This could result in a maximum of 58.6 µmol of CO_2 to be produced. This means that about 88% of the ^{13}C-labeled glycogen was recovered as $^{13}CO_2$. In a parallel experiment it was shown that $^{13}CO_2$ production ceased after about 47 days of starvation and during this extended period an additional 9% of the glycogen was converted to $^{13}CO_2$ (data not shown). The control incubations with ^{13}C-labeled cells from the exponential phase produced only small amounts of $^{13}CO_2$, and at lower initial rate (1 µmol $^{13}CO_2$ produced per mg dry weight of cells per day), and this production ceased after three days. This corresponded with the observation that cells from cultures growing exponentially contained little glycogen (based on both electron microscopy and biochemical analysis).

The possibility of growth on stored glycogen was investigated in a similar experiment as described above without ^{13}C-labeling. For this study, cultures that had accumulated glycogen (obtained at the end of transition phase II; Fig. 1) were diluted and transferred to a medium without methane but with 2 mM of ammonium in order to allow growth. During 10 days of starvation, in which the ^{13}C-labeling experiments suggested that most of the glycogen was already consumed, no growth was observed as cell numbers remained the same (Fig. 1A). The optical density decreased rapidly during this incubation (Fig. 1B), probably as a result of glycogen consumption. In a parallel experiment in the presence of methane (and no ammonium), the optical density was stable in this period (data not shown). Apparently glycogen in the cell caused some more light scattering; this effect was also observed during the transition phase II, were only glycogen was produced, the optical density increased while cell numbers remained constant (size differences of the bacteria at the different growth phases were only marginal).

To study the role of glycogen in viability of the cells, a long-term (70 days) starvation experiment for methane was performed with cultures undergoing exponential growth and cultures that were in transition phase II for 20 days. Exponentially growing cultures were grown till the moment that all ammonium was consumed and the starvation for both cell types was initiated by removing methane from the headspace of the bottles. During the starvation period, cell numbers of both cell types gradually decreased during methane starvation. The cell numbers decreased by a factor of 4.5 in the case of cells obtained from

Table 2. *Genes involved in glycogen synthesis and degradation in* M. fumariolicum *SolV and their expression levels.*

Enzyme	*Gene name*	*E.C. number*	*Accession nr.*	*Identity to V4 ortholog (%)*[a]	*Expression (RPKM value)*[b]
Glycogen synthase	*glgA*	*2.4.1.21*	*Mfumv1_1010040*	*74*	*306*
1,4-alpha-glucan-branching enzyme	*glgB*	*2.4.1.18*	*Mfumv1_170041*	*70*	*154*
Glucose-1-phosphate adenylyltransferase	*glgC*	*2.7.7.27*	*Mfumv1_1020013*	*89*	*391*
Glycogen phosphorylase	*glgP*	*2.4.1.1*	*Mfumv1_1020098*	*81*	*656*
			Mfumv1_220010	*86*	*113*
			Mfumv1_880004	*88*	*447*
Glycogen debranching enzyme	*glgX*	*3.2.1.-*	*Mfumv1_40003*	*70*	*381*
Amylo-alpha 1,6 glucosidase	*gdb*	*3.2.1.33*	*Mfumv1_200059*	*84*	*256*
Glycosyl transferase (group 1)	*rfaG*	*2.4.1.-*	*Mfumv1_200060*	*81*	*43*
Phosphoglucomutase	*pgm*	*5.4.4.2*	*Mfumv1_550015*	*73*	*398*

[a] *Comparison with proteins encoded in the genome of* Methylacidiphilum infernorum *V4.*
[b] *mRNA expression in exponentially growing cells as determined by RNA-seq is expressed as RPKM (Mortazavi et al, 2008).*

Table 1. *Amount and diameter of electron light bodies per cell in different growth phases as observed with transmission electron microscopy of chemically fixed in* M. fumariolicum *SolV cells.*

Growth phase	*Amount of electron light bodies per cell area (1/µm²)*[a]	*Diameter of electron light bodies (nm)*[b]
Exponential	*8 ± 8*	*48 ± 15*
End transition phase 1	*51 ± 19*	*84 ± 27*
End transition phase 2	*44 ± 13*	*96 ± 35*

[a] *Analysis performed on 50 cells.*
[b] *Analysis performed on 50 electron light bodies.*

Glycogen metabolism genes. In the draft genome of strain SolV (Khadem et al, 2012a) genes encoding for glycogen synthesis (*glgA*, *glgB* and *glgC*) and degradation (*glgP*, *glgX*, *gdb* and *pgm*) were present (Table 2). All genes were present in a single copy except for *glgP* encoding the glycogen phosphorylase for which strain SolV possesses three copies. All genes showed orthologs in "*Ca. M. infernorum*" V4 (Hou et al, 2008) with amino acid identities ranging from 70-89%. Compared to this, identities to other more distantly related species were always below 47-61%. Phylogenetic analysis of the glycogen synthase (encoded by *glgA*) showed that the verrucomicrobial methanotrophs form a separate cluster. mRNA analysis of cells from an exponentially growing culture by RNA-seq showed transcription of the aforementioned genes comparable to house keeping genes (Table 2 and Khadem et al, 2012b). RNA-seq analysis of nitrogen fixing cells and cells under low oxygen concentration showed comparable transcription levels of glycogen synthesis/degradation genes (Khadem et al, 2012b). Key genes involved in poly-3-hydroxybutyrate (PHB) synthesis (*phaC*, *phaA*, *phaB*) were absent.

Glycogen assay. To confirm the presence of glycogen as a carbon storage compound in *M. fumariolicum*, a glycogen assay was performed on crude cell extracts prepared from bacteria from an exponentially growing culture and from a culture obtained at the end of transition phase I and II. The glycogen amount as a percentage of dry weight in the crude extracts was 2% for the exponentialy growing culture, and 26% and 36% for the culture obtained at the end of transition phase I and II, respectively.

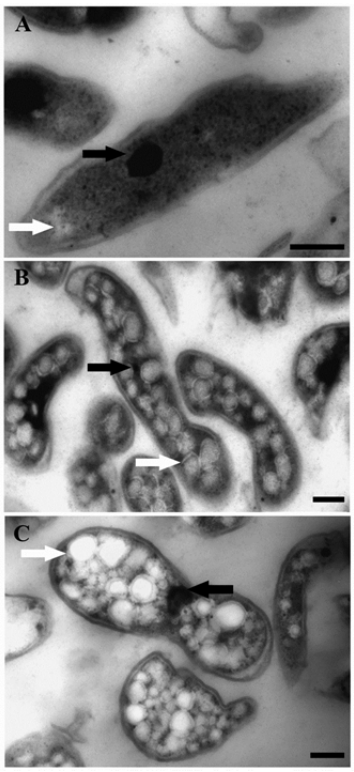

sections of M. fumariolicum *SolV cells in different growth phases. (A) Cell from the exponential phase. (B) Cells taken at the end of transition phase I. (C) Cells taken at the end of transition phase II. Electron light (white arrows) particles are seen in all growth phases, but are especially abundant in cells of transition phase I and II. Electron dense particles (black arrows) are present in all growth phases. Scale bars, 200 nm.*

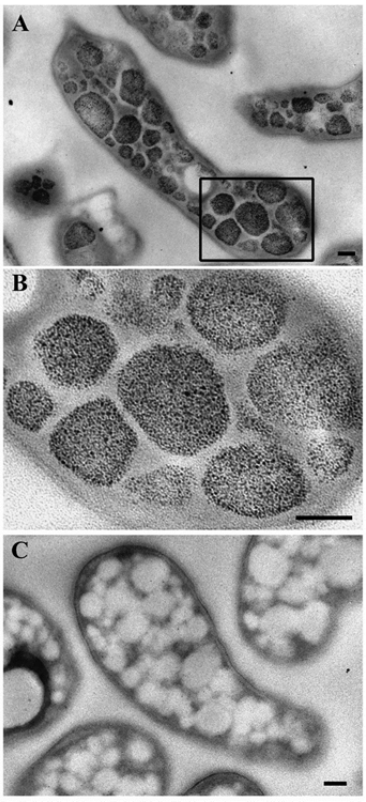

Figure 6*. Transmission electron micrographs showing glycogen staining of chemically fixed, Epon-embedded thin sections of* M. fumariolicum *SolV cells in transition phase II. (A) Glycogen staining is seen in the otherwise electron light particles abundantly present in the cytoplasm. (B) Zoom-in of the box drawn in (A). (C) Negative control incubated with water instead of periodic acid. Scale bars, 100 nm.*

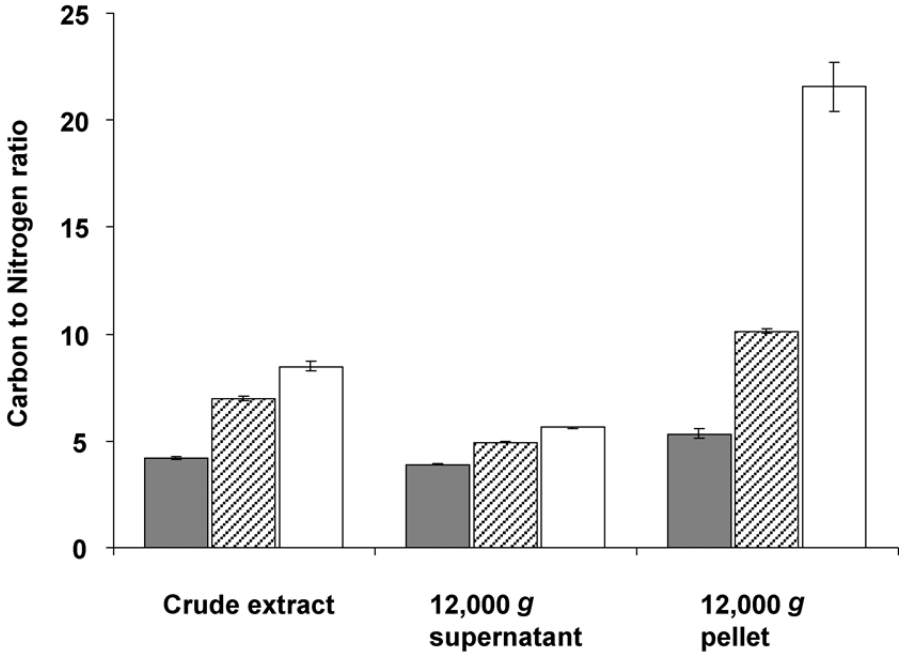

Figure 4*. Carbon to nitrogen ratio (mg/mg) in the crude extract, 12,000 x g supernatant and 12,000 x g pellet prepared from cells harvested in the exponential phase (grey bars), at the end of transition phase I (dashed bars) and II (white bars). Error bars represent S.E.M. (n = 3).*

Transmission electron microscopic investigation of the cells. The ultrastructure of *M. fumariolicum* cells from three different growth phases (exponential, end transition phase I and II) was studied by transmission electron microscopy. Circular or ellipsoid (electron light) bodies were observed in high amounts in cells at the end of transition phase I and II (Fig. 5 (white arrows) and Table 1). This resulted in a dense occupation of the whole cell area (as seen in the thin sections) by these bodies. A silver albumin staining performed on cells from transition phase II confirmed that these bodies consist of polysaccharide (Fig. 6). In exponentially growing cells these bodies could be discriminated but only in low numbers and smaller in size.

In addition, some *M. fumariolicum* cells featured an elliptical to circular body (100-200 nm in diameter) of high electron density (appeared black in images; Fig. 5 (black arrows)). In most cases only one of these electron dense bodies seemed to be present per *M. fumariolicum* cell, although dividing cells occasionally showed two electron dense bodies.

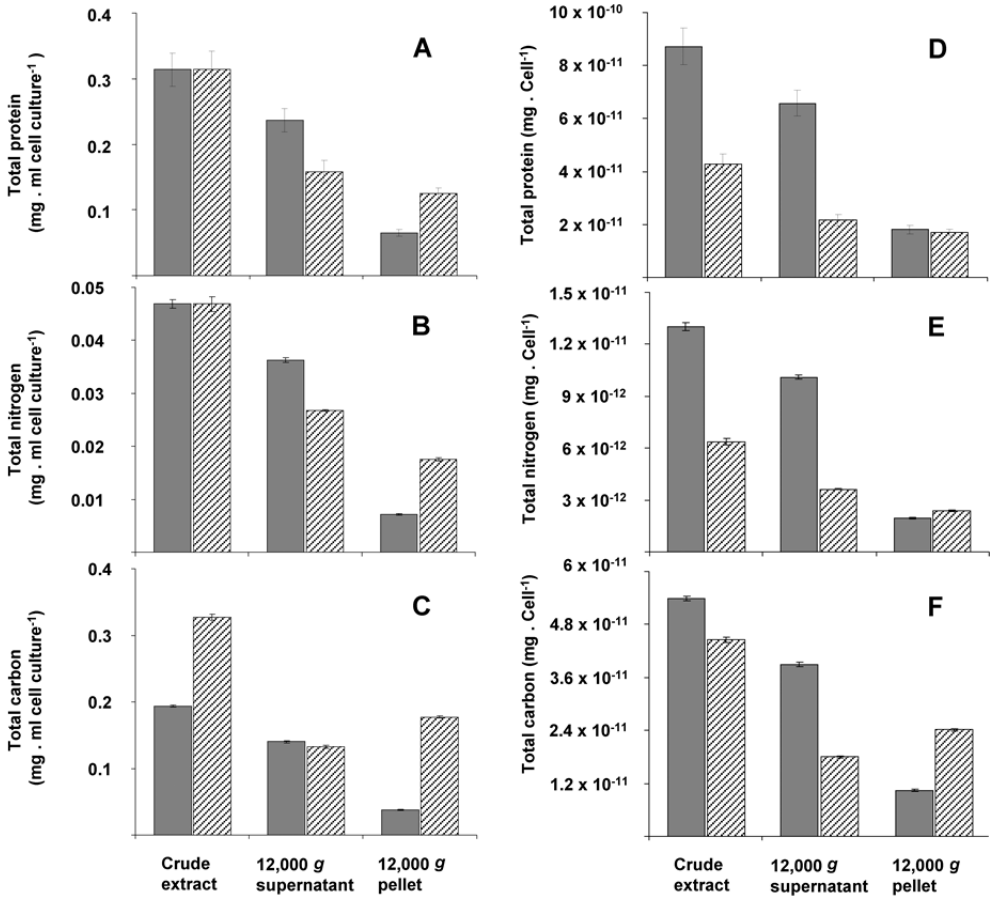

Figure 3. *The distribution calculated per ml of cell culture (A, B, C) or per cell of total protein (D, E, F) of total protein (A, D), nitrogen (B, E) and carbon (C, F) over pellet and cytosol fractions at the beginning (grey bars) and end (dashed bars) of transition phase I in the crude extract, 12,000 x g supernatant and 12,000 x g pellet. This experiment was performed with exponentially growing cells that had reached an optical density of 0.5 (see Fig. 2A).The amount of total protein and total nitrogen in this exponentially growing cells were normalized to values from cells obtained at the start of transition phase I, since total protein (see Fig. 1C) and total nitrogen (see Fig. 2B) stabilized after ammonium depletion. The total carbon of the exponentially growing cells was normalized to values from cells obtained at the end of the exponential growth phase (at optical density of 1.12). Error bars represent S.E.M. (n = 4).*

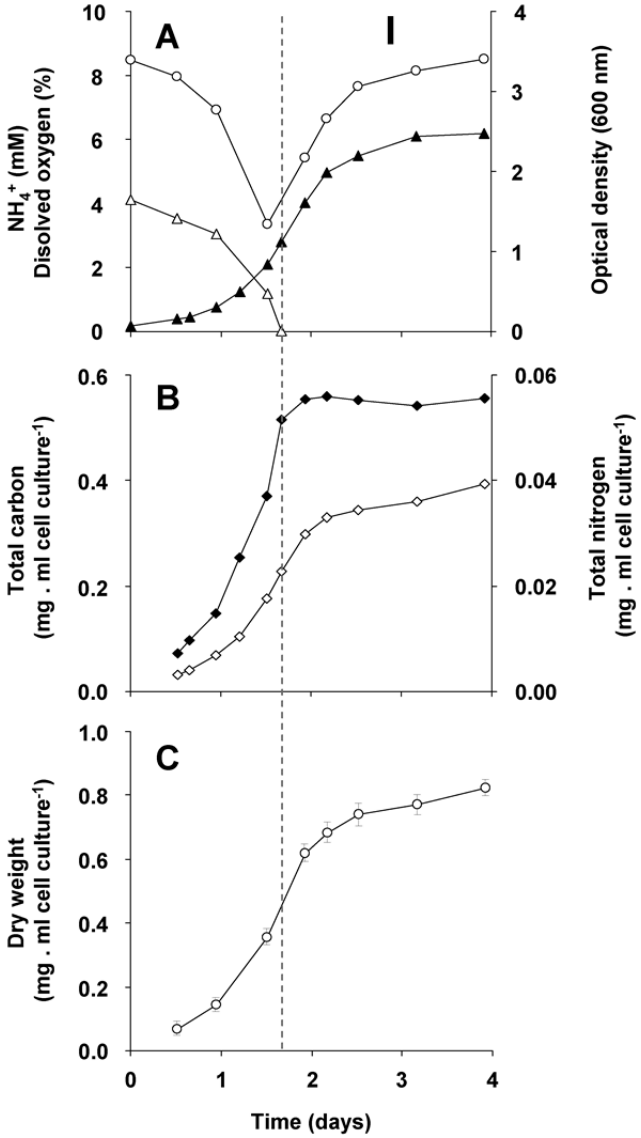

Figure 2. *Growth response of* M. fumariolicum *SolV upon ammonium depletion during transition phase I (the start is indicated by the dashed line). (A) The optical density (closed triangles), ammonium (open triangles) and dissolved oxygen in culture medium (open circles). (B) total nitrogen (closed squares) and total carbon (open squares). (C) Dry weight (open circles). Error bars represent S.E.M. (n = 5).*

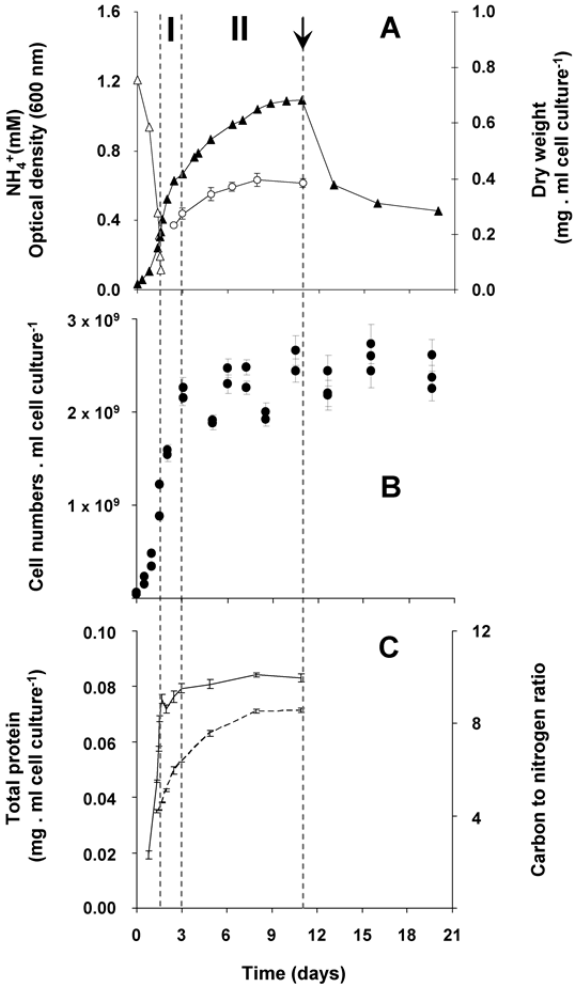

Figure 1. *Growth response of* M. fumariolicum *SolV upon ammonium depletion. (A) Growth was monitored by measuring increase in optical density (closed triangles) and dry weight (open circles). Error bars represent S.E.M. (n = 4). Concentration of ammonium is represented by open triangles. After 1.5 days of exponential growth (μmax = 0.07 h-1) ammonium was depleted and two phases were observed, indicated by dashed lines and the symbols I and II. At day 11 (arrow), cell cultures were diluted into ammonium containing medium, but without methane added. To compare with the original optical density and cell numbers, values were multiplied by the dilution factor. (B) Cell numbers per ml cell culture of* M. fumariolicum *SolV (solid circles). Error bars represent S.E.M. (n = 30). (C) Total protein (solid line), determined in the crude extracts prepared from harvested cells and carbon to nitrogen ratio of the harvested cells (dashed line). Error bars represent S.E.M. (n = 4-5).*

optical density curve was observed. This seemed to be caused by the fact that growth of the culture stopped, because cell numbers remained more or less constant (Figs. 1A and 1B). However, the optical density still increased for 7 more days (transition phase II).

To exclude any possibility of nitrogen fixation following ammonium depletion, the nitrogen in the headspace of the batch incubations was replaced by argon. Before starting the batch incubation, the cultures undergoing exponential growth were washed and put in an ammonium-free medium (methane was present). In these bottles, the same growth pattern was observed as in bottles with nitrogen in the headspace. In addition, growth by uptake of exogenous sources of nitrogen (produced during the exponential phase by *M. fumariolicum*) was excluded. This was done by incubating washed cultures from the exponential phase in medium obtained from a culture at the end of transition phase II. Since no increase in growth parameters was observed in these transition phase II cultures, it could be concluded that all nitrogen in the medium was depleted by the cultures. Again, the same growth pattern was observed as for transition phase I. Moreover, the protein content of the culture remained constant after ammonium depletion (Fig. 1C).

The changes during transition phase I were studied in more detail in separate cultures with higher cell concentrations (higher initial ammonium concentration). These yielded more accurate dry weight values and allowed preparing adequate quantities of crude cell extracts. Cultures grew exponentially till ammonium was depleted, after which the metabolic rate changed abruptly as indicated by a sharp increase in the dissolved oxygen concentration and the growth rate dropped gradually (Fig. 2A). The total nitrogen content of the culture remained constant as inferred from analysis of crude extract of harvested cells (Fig. 2B). As cell numbers (Fig. 1A), total carbon and dry weight were all almost doubled during this phase (Figs. 2B and 2C) and cells maintained their normal size, the protein content per cell must have been reduced by half. The consequence of this change of protein content of the cell wall and cytosol was investigated by analyzing the pellet and supernatant fractions of crude extracts of cells at the start (exponentially grown) and the end of transition phase I. When expressed per ml culture, a clear shift of proteins and total nitrogen was observed from the supernatant to the pellet fraction, for which the protein content almost doubled (Figs. 3A and 3B). As the cell numbers in the culture doubled, it means that when results are expressed per cell, the protein and total nitrogen content of the pelleted fraction remained constant at the expense of the supernatant fraction of which the proteins content dropped by a factor of three (Figs. 3D and 3E). In contrast to total nitrogen, total carbon in the pellet fraction increased more than four times for the total culture and more than two times when expressed per cell (Figs. 3C and 3F). This high content of carbon pointed to intracellular particulate storage material.

This storage seems to continue in transition phase II, where the carbon to nitrogen ratio and dry weight increased at stabilizing cell numbers (Fig. 1). Storage of an insoluble form of carbon was most evident from the strong increase in the carbon to nitrogen ratio of the pellet fraction of crude cell extract in both phases (Fig. 4).

were then resuspended in 0.1 M sodiumcacodylate buffer (pH 7.4) for 15 min, followed by a post-fixation for 2 h in 1% OsO_4 and 1.5% K_4FeCN_6 in 0.08 M sodiumcacodylate buffer (pH 7.4) on ice in the dark. After washing with MilliQ water, the cells were dehydrated in a graded ethanol series (70-100%). Samples were gradually infiltrated with Epon resin. Polymerization of Epon took place at 60°C for 72 hours. Ultrathin sections (60-70 nm) of the Epon-embedded cells were cut with the use of a glass knife in a Leica Ultracut UCT microtome.

Before investigation, the sections were post-stained by incubating the grids on drops of 4% uranyl acetate in MilliQ water (30 min in the dark) and 2 min in Reynolds lead citrate stain (Reynolds, 1963), with MilliQ washing in between and afterwards. The sections were then investigated in a TEM 1010, JEOL transmission electron microscope. 50 cells were used for each analysis.

Polysaccharide (glycogen) stain. Ultrathin sections of chemically fixed *M. fumariolicum* cells (as described above) were treated with the polysaccharide stain as described previously (van Niftrik et al, 2008). In this method, electron dense silver albumin aggregates indicate the presence of polysaccharide molecules.

Glycogen metabolism genes. Genes encoding proteins involved in glycogen metabolism were identified in the available draft genome of strain SolV by Blast searches (Khadem et al, 2012a), which also showed amino acid identities to homologous proteins. Representative reference *glgA* sequences, encoding the glycogen synthase, were obtained from GenBank and aligned using the MUSCLE aligner in MEGA 5.0 (Tamura et al, 2011). Phylogenetic trees were calculated using the neighbor-joining method with 1000 bootstraps to infer the evolutionary relationship. Positions containing alignment gaps and missing data were eliminated only in pairwise sequence comparisons (Pairwise deletion option). The Dayhoff-matrix based method was used to compute the evolutionary distances. For transcriptome analysis RNA was extracted from exponentially growing cells as described before (Khadem et al, 2011). After synthesis of cDNA, single-end Illumina sequencing was performed and transcription analysis was performed using the RNA-Seq Analysis tool from the CLC Genomic Workbench software (version 5.0, CLC-Bio, Aarhus, Danmark) and values are expressed as RPKM (Reads Per Kilobase of exon model per Million mapped reads; Mortazavi et al, 2008). Raw RNA-seq sequence data are available from the GEO depository under accession number GSE40528.

Results

Growth response of *M. fumariolicum* upon nitrogen depletion. In order to study the growth response of *M. fumariolicum* upon nitrogen depletion, the bacteria were cultivated in a fermentor with methane in excess and ammonium as nitrogen source. The dissolved oxygen concentration in the culture was always maintained above 2% O_2 which prohibits nitrogen fixation to occur (Khadem et al, 2010). After ammonium was depleted, an unexpectedly large increase in optical density was observed that occurred in two phases (Fig. 1A). During the first phase (transition phase I) that lasted 1.5 days, both the cell numbers and optical density doubled. At the end of this phase a shoulder in the

In the experiments where methane was removed from the bottles, the cell suspension was sparged with air for about 5 min and 5% (v/v) CO_2 was added after sealing.

Preparation of cell extracts. Cells were collected by centrifugation (4000 $\times$ *g*, 4°C, 10 min). The cell pellet was washed twice in phosphate-buffer (20 mM, pH 7.1) and resuspended in the same buffer. The suspension, which had a final pH of 6, was passed 4 times through a French press at 20,000 psi and cell lysis (at least 90%) was confirmed by counting DAPI stained cells with light microscopy. Unbroken cells and cell debris were removed from the resulting crude extract by centrifugation at 12,000 $\times$ *g* for 30 min (4°C, Sorvall SS-34 rotor).

Gas analysis. Methane (CH_4) was analyzed on a HP 5890 gas chromatograph (Agilent, USA) equipped with a Porapak Q column (1.8 m $\times$ 2 mm) and a flame ionization detector. ^{12}C and ^{13}C-labeled carbon dioxide (CO_2) were analyzed on an Agilent series 6890 gas chromatograph (Agilent, USA) equipped with a Porapak Q and a Molecular sieve column, coupled to a thermal conductivity detector and mass spectrometer (MS) (Agilent 5975C inert MSD; Agilent, USA) as described before (Ettwig et al, 2008). For all gas analyses, 100 µl sample of gas was injected into the gas chromatograph.

Light microscopy. Cell numbers were determined by counting cells in 30 fields (volume per field 2.5 $\times$ 10^{-8} cm^3) of a hemocytometer slide, using an Axioplan 2 imaging phase contrast microscope (Carl Zeiss B.V.).

Ammonium and protein analysis. Ammonium concentrations were measured using the orthophthaldialdehyde (OPA) method (Taylor et al, 1974). Protein concentrations were measured using the bicinchoninic acid (BCA) assay as described before (Ettwig et al, 2008).

Elemental analysis. The cells were harvested by centrifugation, after which the pellet was washed with demineralized water and dried overnight in a vacuum oven at 70°C. The dried material (about 0.4 mg) was analyzed on a Thermo Fisher Scientific EA 1110 CHN element analyzer coupled to a Finnigan DeltaPlus mass spectrometer.

Glycogen assay. The concentration of glycogen in the crude extracts was determined by a two-step enzymatic assay. To enhance the enzyme accessibility of the glycogen granules, crude extracts were first shaken for 10 minutes at 30 s^{-1} with glass beads (80-110 µm in diameter) in a Retsch MM 301 ball mill. The bead-beaten crude extracts (in triplicate) were then incubated with amyloglucosidase (35 units per ml crude extract in the case of transition phase I and II cells and 17.5 units per ml crude extract for the exponential phase cells) from *Aspergillus niger* (Sigma Aldrich) in 0.05 M acetate buffer (pH 4.8) for 4 h at 45°C to convert glycogen into glucose. In the second step, the resulting glucose was quantified by the glucose oxidase kit (Sigma Aldrich). To correct for the amount of glucose already present in the crude extracts, controls of bead-beaten crude extracts that did not undergo amyloglucosidase incubation were also analyzed.

Chemical fixation and Epon-embedding. *M. fumariolicum* cells were fixed in Karnovsky fixative (2% paraformaldehyde, 2.5% glutaraldehyde, 0.025 mM $CaCl_2$ and 0.05 mM $MgCl_2$ in 0.08 M sodiumcacodylate buffer pH 7.4) at 4°C for a maximum of 17 days. The cells

This study focuses on the growth response of *M. fumariolicum* during nitrogen depletion. When nitrogen is limited and carbon compounds are in excess, methanotrophs, as many other bacteria (Wanner & Egli, 1990 and reference therein), start to accumulate carbon-rich reserve polymers, such as poly-3-hydroxybutyrate (PHB) or glycogen (Linton et al, 1978; Eshinimaev et al, 2002; Pieja et al, 2011a and reference therein). The cells of *M. fumariolicum* are rod-shaped and have a length of 0.8-2.0 µm and a width of 0.4-0.6 µm (Op den Camp et al, 2009). Electron microscopy demonstrated the presence of intracellular inclusions in all three "*Methylacidiphilum*" strains (Pol et al, 2007; Islam et al, 2008; Op den Camp et al, 2009), which might represent storage material. Genes encoding for PHB synthesis are absent from the genomes of the "*Methylacidiphilum*" strains, as is also the case for type I proteobacterial methanotrophs (Hou et al, 2008; Pieja et al, 2011a; Khadem et al, 2012a). However, based on the draft genome of *M. fumariolicum*, genes encoding for glycogen metabolism are predicted (Khadem et al, 2012a). This study combines growth experiments, transcriptome analysis, electron microscopy and biochemical analysis to elucidate the ability of glycogen storage in *M. fumariolicum*.

Materials and methods

Organism and medium composition for growth. *Methylacidiphilum fumariolicum* SolV used in this study was originally isolated from the Solfatara volcano, near Naples, Italy (Pol et al, 2007). *M. fumariolicum* was grown in the standard medium (pH 2) as described before (Khadem et al, 2010), with 10% (v/v) liquid mud pool extract and 2 mM of ammonium.

Materials. ^{13}C-labeled CO_2 was prepared by injecting a 0.6 M $NaH^{13}CO_3$ (99% ^{13}C) solution into a solution of 1.2 M HCl in a closed 60 ml serum bottle. The headspace was then used as source of ^{13}C-labeled CO_2. ^{13}C-labeled CH_4 (99% atom % ^{13}C) was obtained from Sigma-Aldrich.

Fed-batch cultivation. Cultivation of *M. fumariolicum* was performed in a 10 L fermentor (Applikon, Schiedam, the Netherlands). The medium (5 liter) contained 1.2 mM ammonium. A gas mixture of (all in v/v); 9.5% methane (CH_4), 23.9% carbon dioxide (CO_2) and 66.6% air, was supplied to the fermentor in a continuous flow. The oxygen sensor showed a dissolved oxygen level of 8.8% at the onset of cultivation. The pH of the medium was set with sulfuric acid at pH 2 and remained close to pH 2 during growth. The temperature and agitation speed were set to 55°C and 1000 rpm, respectively.

To determine the dry weight, samples of 10 ml from the culture suspension were filtered through pre-weighed 0.45 µm filters and dried to constant weight in a vacuum oven at 70°C.

Batch cultivation. Batch incubations were performed in serum bottles containing 5% (v/v) medium. The bottles were sealed with red butyl rubber stoppers (Rubber BV, Hilversum, The Netherlands). The headspace contained air as the source of oxygen and CH_4 and CO_2 concentrations of 10% and 5% (v/v), respectively. The incubations were performed in duplicate at 55°C with shaking at 180 rpm.

Abstract

Methylacidiphilum fumariolicum SolV is a verrucomicrobial methanotroph that can grow in extremely acidic environments at high temperature. Strain SolV fixes carbon dioxide (CO_2) via the Calvin-Benson-Bassham cycle with methane as energy source, a trait so far very unusual in methanotrophs. In this study, the ability of *M. fumariolicum* to store carbon was explored by genome analysis, physiological studies and electron microscopy. When cell cultures were depleted for nitrogen, glycogen storage was clearly observed in cytoplasmic storage vesicles by electron microscopy. After cessation of growth, the dry weight kept increasing and the bacteria were filled up almost entirely by glycogen. This was confirmed by biochemical analysis, which showed that glycogen accumulated to 36% of the total dry weight of the cells. When methane was removed from the culture, this glycogen was consumed within 47 days. During the period of glycogen consumption, the bacteria kept their viability high when compared to bacteria without glycogen (from cultures growing exponentially). The latter bacteria lost viability already after a few days when starved for methane. Analysis of the draft genome of *M. fumariolicum* demonstrated that all known genes for glycogen storage and degradation were present and also transcribed. Phylogenetic analysis of these genes showed that they form a separate cluster with *M. infernorum* V4, and the most closely related other sequences only have an identity of 40%. This study presents the first physiological evidence of glycogen storage in the phylum *Verrucomicrobia* and indicates that carbon storage is important for survival at times of methane starvation.

Introduction

The use of methane (CH_4) as carbon and energy source distinguishes the aerobic methanotrophs as a unique group within the methylotrophs. Aerobic methanotrophs are found within the *Proteobacteria*, *Verrucomicrobia* and the NC10 phylum (Hanson & Hanson, 1996; Op den Camp et al, 2009; Semrau et al, 2010; Ettwig et al, 2010). The verrucomicrobial methanotrophs, for which the genus name "*Methylacidiphilum*" was proposed (Op den Camp et al, 2009), were recently discovered. They were isolated in pure cultures from volcanic regions (Pol et al, 2007; Dunfield et al, 2007; Islam et al, 2008), which may be important natural sources of methane (Castaldi & Tedesco, 2005; Kvenvolden & Rogers, 2005). The verrucomicrobial methanotrophic bacteria are able to grow in these highly acidic and hot conditions and might have an essential role in reducing global methane emissions into the atmosphere.

Methylacidiphilum fumariolicum strain SolV is one of the thermoacidophilic verrucomicrobial methanotrophs and its physiology has been studied in some detail. This microorganism can use ammonium, nitrate or atmospheric nitrogen as nitrogen source (Pol et al, 2007; Khadem et al, 2010), and fixes carbon dioxide (CO_2) into biomass via the Calvin-Benson-Bassham cycle, using methane as its energy source (Khadem et al, 2011). The latter is in contrast to proteobacterial methanotrophs that use formaldehyde in the ribulose monophosphate pathway (type I) or the serine pathway (type II) for carbon assimilation (Chistoserdova, 2009; Semrau et al, 2010).

Chapter 2

Genomic and physiological analysis of carbon storage in the verrucomicrobial methanotroph *Methylacidiphilum fumariolicum* SolV

This chapter has been published as:

Khadem AF[1+], van Teeseling MCF[1+], van Niftrik L[1], Jetten MSM[1], Op den Camp HJM[1], Pol A[1] (2012) Genomic and physiological analysis of carbon storage in the verrucomicrobial methanotroph "*Ca.* Methylacidiphilum fumariolicum" SolV. *Front Microbiol* 3: 345.

[+] Both authors contributed equally.

[1]Department of Microbiology, Institute for Water and Wetland Research, Radboud University, Nijmegen, the Netherlands.

16 (ii)

four verrucomicrobial methanotrophs was investigated via energy dispersive X-ray analysis.

The results of the previous chapters are reviewed and discussed in **chapter 5**, which gives an overview of a typical cell of a verrucomicrobial methanotroph and sketches possible future research lines.

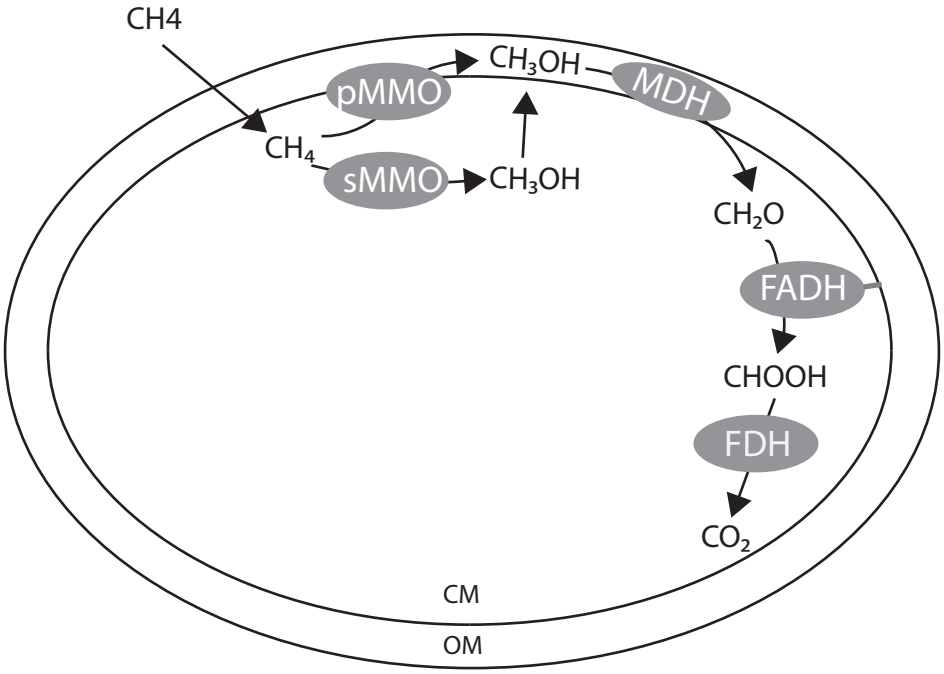

Figure 2. *Schematic representation of the enzymes (in grey) and intermediates (in black) involved in aerobic methane oxidation, depicted inside a methanotrophic cell. pMMO, particulate methane monooxygenase; sMMO, soluble methane monooxygenase; MDH, methanol dehydrogenase; FADH, formaldehyde dehydrogenase; FDH, formate dehydrogenase; CM, cytoplasmic membrane; OM, outer membrane.*

The last two enzymes of the aerobic methane oxidation are formaldehyde dehydrogenase (FADH), converting formaldehyde to formate, and formate dehydrogenase (FDH), which forms carbon dioxide from formate (Hanson & Hanson, 1996). Since the MDH of *M. fumariolicum* SolV can convert methanol to formate directly, the enzyme FADH might not be necessary for methane oxidation in verrucomicrobial methanotrophs. The aerobic oxidation of methane is coupled to energy conservation through a membrane-bound respiratory chain, which ultimately results in the phosphorylation of ADP to ATP. In addition to methane oxidation, *M. fumariolicum* SolV was shown to fix N_2 at low oxygen levels using a highly oxygen sensitive nitrogenase (Khadem et al, 2010).

The ultrastructure of verrucomicrobial methanotrophs has not been studied in much detail. Electron microscopy on chemically fixed cells showed that all three discovered species are Gram-negative, rod shaped cells with cytoplasmic particles (Op den Camp et al, 2009). The identity of these particles has not yet been elucidated, partly because of the lacking resolution due to room temperature chemical fixation. These particles were speculated to resemble carboxysomes (Islam et al, 2008) although it later became apparent that no genes for carboxysome formation are present in the genome (Khadem et al, 2011). Therefore further research is needed to unravel the identity and function of these structures. In addition, structures that were described to resemble tubular membranes have been observed in rare occasions in *M. infernorum* V4 (Dunfield et al, 2007). The precise identity and function of these putative membranes, which have been speculated to be the location of pMMO (Dunfield et al, 2007), has not been studied. It also remains a mystery under which conditions the cells form these membranes and if this represents a viable and active state of the cells.

Outline and aim of the study

The aim of this study is to elucidate the ultrastructure of the recently discovered verrucomicrobial methanotrophs in order to increase our understanding of how their cells are best adapted to make a living.

Chapter 2 focused on the thermophile *M. fumariolicum* SolV and aimed to characterize the electron light particles present inside these cells. The accumulation of these particles during growth was followed via electron microscopy. A specific stain and physiological and enzymatic assays were used to elucidate the composition and function of these particles.

In **chapter 3** antibodies were generated against MDH and pMMO, two enzymes involved in methane oxidation, of *M. fumariolicum* SolV. These antibodies were used for immunogold localization to show the intracellular location of MDH and pMMO in *M. fumariolicum* SolV cells.

Chapter 4 describes three novel isolates of methanotrophic *Verrucomicrobia*. The ultrastructure of these three isolates was compared to that of the thermophilic *M. fumariolicum* SolV. In addition, the identity of electron dense bodies observed in all

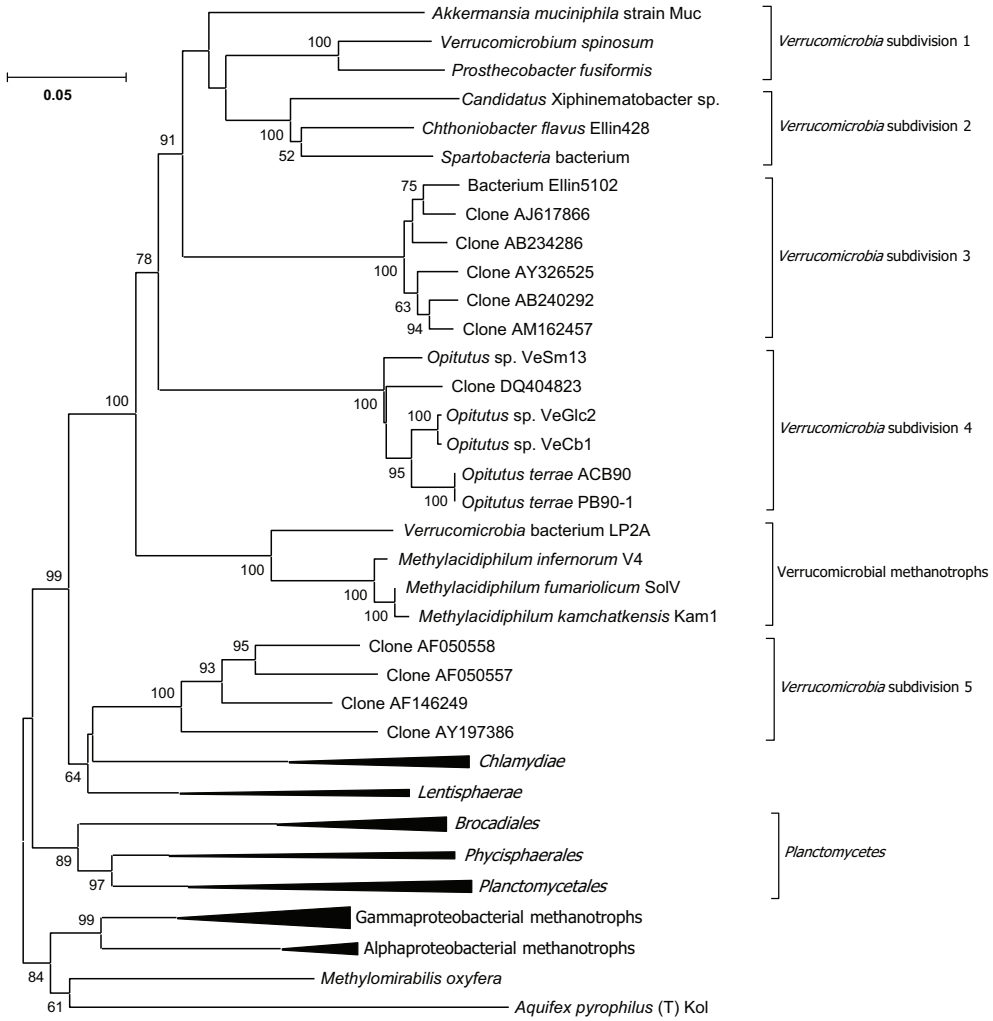

Figure 1. *Phylogenetic neighbour-joining tree of 16S rRNA gene sequences showing the evolutionary relationships of the verrucomicrobial methanotrophs (*Methylacidiphilum*) to other members of the phylum* Verrucomicrobia *and other selected phyla, including proteobacterial methanotrophs. The optimal tree with the sum of branch length = 4.05005666 is shown. The percentage of replicate trees in which the associated taxa clustered together in the bootstrap test (500 replicates) are shown next to the branches for values >60. The tree is drawn to scale, with branch lengths in the same units as those of the evolutionary distances used to infer the phylogenetic tree. The evolutionary distances were computed using the Jukes-Cantor method and are in the units of the number of base substitutions per site. The analysis involved 64 nucleotide sequences. All ambiguous positions were removed for each sequence pair. There were a total of 1656 positions in the final dataset. Evolutionary analyses were conducted in MEGA6.*

organisms can also be present outside geothermal environments (Pagaling et al, 2014). It has become clear that the verrucomicrobial methanotrophs not only differ in taxonomy and preferential environment, but also in the mechanism for carbon fixation. Proteobacterial methanotrophs typically fix carbon either via the serine cycle or the ribulose monophosphate (RuMP) pathway using formaldehyde, which is an intermediate in the oxidation of methane (Hanson & Hanson, 1996; Op den Camp et al, 2009). The verrucomicrobial methanotrophs are autotrophs, fixing carbon from CO_2 using the Calvin-Benson-Bassham cycle (Khadem et al, 2011; Sharp et al, 2012).

During aerobic methane oxidation, methane is oxidized to carbon dioxide via the intermediates methanol, formaldehyde and formate (Fig. 2) (Hanson & Hanson, 1996). The first enzyme, catalyzing the oxidation of methane to methanol, is methane monooxygenase (MMO). This enzyme occurs both in a particulate (pMMO) and soluble (sMMO) form. Typically, sMMO is located in the cytoplasm and pMMO is located in the intracytoplasmic membranes (ICMs) present in many proteobacterial methanotrophs (Nguyen et al, 1998; Brantner et al, 2002). In *Verrucomicrobia*, however, no structural ICMs have been observed so far (Op den Camp et al, 2009) and the location of pMMO is unknown. In the verrucomicrobial methanotrophs *M. fumariolicum* SolV and *M. infernorum* V4, three complete copies of the *pmoCAB* operon encoding for pMMO are present (Hou et al, 2008; Khadem et al, 2021a). Two of these three copies have been found in transcriptomes of *M. fumariolicum* SolV, one being preferentially expressed under oxygen limitation and the other when oxygen was present in excess (Khadem et al, 2012b). In *M. kamchatkense* Kam1, three complete *pmoCAB* operons and a fourth operon lacking *pmoB* are present and expressed (Erikstad et al, 2012). In this study it was found that growth on methanol instead of methane led to a down-regulation of all *pmoA* genes. No copies of sMMO were identified in any of the *Methylacidiphilum* genomes, nor was any sMMO activity detected in these species (Pol et al, 2007; Hou et al, 2008; Khadem et al, 2012a).

The second enzyme in the aerobic oxidation of methane is the PQQ-dependent methanol dehydrogenase (MDH), which catalyzes the oxidation of methanol to formaldehyde. It has been recently discovered that the MDH of *M. fumariolicum* SolV contains lanthanides, whereas previously studied MDHs have calcium as metal in the active site (Pol et al, 2014; Keltjens et al, 2014). In addition, the MDH from *M.* fumariolicum differs from other MDHs because it oxidizes methanol in one step to formate instead of formaldehyde (Pol et al, 2014). This might be one of the reasons why verrucomicrobial methanotrophs do not use the RuMP pathway or the serine cycle for carbon fixation, since these would require formaldehyde to be present. The canonical MDH is often referred to as a periplasmic enzyme and it was shown to be associated with the space in between the ICMs, which can be seen as an enlargement of the periplasm, in multiple methanotrophs (Fassel et al, 1992; Brantner et al, 2002). The intracellular location of MDH in verrucomicrobial methanotrophs awaits clarification.

Methane is the 8th most abundant component of earth's atmosphere (Jacob, 1999) at a concentration of about 1800 ppb and a significant contributor to the (enhanced) greenhouse effect. Via this effect the increasing concentration of methane in the atmosphere contributes to the rising temperature on the surface of the earth. An approximate 5-6 x 10^{14} ton of methane enters the atmosphere each year (Conrad, 2009). The most important sources of this methane are microbial biogenesis, mining and combustion of fossil fuels and burning of biomass. An average methane molecule is present in the atmosphere for about eight years. Methane can leave the atmosphere by reacting with the oxygen radical OH• or free chlorine present in the atmosphere or by diffusing into the soil, where it is oxidized by prokaryotes (Forster et al, 2007; Conrad, 2009). The latter process is called methanotrophy and plays an important role in the methane cycle. Not only does this process act on methane that is already present in the atmosphere and diffuses into the soil or sediment, it also acts on methane molecules generated in soil or water ecosystems by methanogenesis. Methanotrophy thus controls the amount of methane emitted to the atmosphere, since some of the methane is already oxidized in the soil or sediment water layer before it can actually escape to the atmosphere (Conrad, 2009).

The microbial oxidation of methane can take place either aerobically or anaerobically. Anaerobic methane oxidation (AOM) can be coupled to reduction of sulfate (Boetius et al, 2000, Milucka et al, 2012), nitrate (Haroon et al, 2013), manganese- and iron oxides (Beal et al, 2009) or nitrite (Ettwig et al, 2008). AOM can be performed by either a consortium of bacteria and archaea (often referred to as ANME; anaerobic methanotrophic), by the ANME archaea themselves, or by *Methylomirabilis oxyfera*-like bacteria, belonging to the NC10 phylum (Ettwig et al, 2010). Strikingly, the anaerobic *M. oxyfera* performs "aerobic" methane oxidation, for which it probably uses internally produced oxygen derived from nitric oxide dismutation (Ettwig et al, 2010; 2012). Since AOM is a rapidly evolving field of research, it is expected that additional organisms will be identified in the coming years.

For a long time it was believed that aerobic methanotrophy was a trait only present in the phylum *Proteobacteria*, especially in the subphyla Alpha- and Gammaproteobacteria (Op den Camp et al, 2009) (Fig. 1). Methanotrophic *Proteobacteria* have been isolated from many different environments (Hanson & Hanson, 1996), but they were never found at environments combining low pH values with high temperatures (Op den Camp et al, 2009). Recently, two additional phyla were found to harbor aerobic methanotrophs: the intra-aerobic NC10 phylum already introduced above (Raghoebarsing et al, 2006; Ettwig et al, 2010; Hu et al, 2014) and the *Verrucomicrobia* (Pol et al, 2007; Dunfield et al, 2007; Islam et al, 2008) (Fig. 1). The verrucomicrobial methanotrophs of the genus *Methylacidiphilum* have been discovered in geothermal environments: they are able to grow at a pH below 1 and temperatures up to 65°C (Pol et al, 2007; Dunfield et al, 2007; Islam et al, 2008; Op den Camp et al, 2009). In addition to low pH values and elevated temperatures, many geothermal environments are characterized by emission of variable amounts of methane, making it an interesting environment for methanotrophs (Etiope & Klusman, 2002). In the meantime, molecular evidence for the presence of *Methylacidiphilum* species in man-made sewage systems with low pH suggests that these

Chapter 1

General introduction

8 (ii)

fagopyrum 3C, *M. tartarophylax* 4AC en *M. cyclopophantes* 3B. Er werd ontdekt dat deze soorten autotroof groeien bij gematigde temperatuur en lage pH-waardes. De ultrastuctuur van deze drie *Methylacidimicrobium* soorten werd vergeleken met die van *M. fumariolicum* SolV. Het meest opvallende verschil tussen deze vier soorten was dat *M. fagopyrum* 3C intracytoplasmatische membraanstructuren (ICMs) had, terwijl de andere drie soorten deze niet hadden. Gedurende het onderzoek werd de chemische samenstelling opgehelderd van de donkere bollen, die in alle vier de soorten gevonden werden. Op basis van deze resultaten lijken deze bollen een rol te spelen bij opslag van fosfaat.

De in dit deel van het proefschrift gepresenteerde resultaten worden samengebracht en besproken in **hoofdstuk 5**, waarin een overzicht wordt gegeven van de ultrastructuur van de bestudeerde verrucomicrobiële methanotrofen. Daarnaast wordt de koers voor vervolgonderzoek uitgestippeld.

Samenvatting

Methaan is een belangrijk molecuul in de atmosfeer van de aarde, waar het bijdraagt aan het (versterkte) broeikaseffect. Methaan kan worden gebruikt door een groep micro-organismen die methanotrofen heet. Methanotrofen kunnen methaanoxidatie ofwel met zuurstof (aëroob) ofwel zonder zuurstof (anaëroob) uitvoeren. Recentelijk is er een nieuwe groep aërobe methanotrofen ontdekt in verschillende zure vulkanische milieus. Deze zuurminnende methanotrofen behoren tot het phylum van de *Verrucomicrobia*, terwijl alle andere aërobe methanotrofen die destijds bekend waren deel uitmaken van de *Proteobacteria*. De afgelopen jaren heeft het onderzoek naar verrucomicrobiële methanotrofen zich vooral gericht op hun fysiologie, met name om te achterhalen welke mechanismen de bacteriën gebruiken om koolstofdioxide en stikstofgas te fixeren en om energie te winnen uit methaanoxidatie. Met uitzondering van enkele basale observaties is de manier waarop deze micro-organismen hun cellen inrichten om hun levensstijl te faciliteren onbekend gebleven. Het doel van het onderzoek dat in dit deel van het proefschrift wordt gepresenteerd, was om de ultrastructuur van de verrucomicrobiële methanotrofen op te helderen. Hiervoor is hoofdzakelijk elektronenmicroscopie gebruikt, waarbij gebruikt werd gemaakt van verschillende technieken om de monsters voor te behandelen en te visualiseren.

Na een inleiding over verrucomicrobiële methanotrofen in **hoofdstuk 1**, richt **hoofdstuk 2** zich op de soort *Methylacidiphilum fumariolicum* SolV die groeit bij een lage pH en een hoge temperatuur (thermofiel). In deze verrucomicrobiële methanotroof werden twee types intracellulaire bollen gevonden, die verschilden in de hoeveelheid contrast die zij geven onder de elektronenmicroscoop: donkere bollen (**hoofdstuk 4**) en lichte bollen. De compositie van de lichte bollen werd onderzocht met een methode die polysacchariden specifiek aankleurt. In combinatie met enzymatische en fysiologische testen en elektronenmicroscopisch onderzoek, toonde deze kleuring aan dat de licht gekleurde bollen glycogeen opslagblaasjes zijn. Cellen hoopten glycogeen op in deze opslagblaasjes als stikstof slechts in zeer beperkte mate en koolstof in overmaat aanwezig was. Het opgeslagen glycogeen werd door de cellen gebruikt wanneer koolstof in de vorm van methaan afwezig was.

Hoofdstuk 3 bekijkt de *M. fumariolicum* SolV cel in meer detail met het doel om de locatie van twee belangrijke enzymen betrokken bij de methaanoxidatie op te helderen. Deze twee eiwitten, “particulate methaan monooxygenase” (pMMO) en “methanol dehydrogenase” (MDH) , werden (deels) opgezuiverd uit de *M. fumariolicum* SolV kweek en gebruikt om antilichamen tegen te genereren. Immunogoudlokalisatie met deze antilichamen toonde aan dat MDH zich in het periplasma bevindt. De locatie van pMMO is controversieel vanwege de suboptimale kwaliteit van het antilichaam.

In **hoofdstuk 4** wordt het blikveld verruimd en worden meerdere soorten verrucomicrobiële methanotrofen behandeld. Drie nieuw geïsoleerde soorten behorend tot het nieuw gedefiniëerde geslacht *Methylacidimicrobium* werden beschreven en gekarakteriseerd. Deze nieuw ontdekte soorten hebben de volgende namen gekregen: *M.*

Methylacidimicrobium species was compared to that of *M. fumariolicum* SolV. The most striking difference between the four species was that *M. fagopyrum* 3C possessed intracytoplasmic membrane structures (ICMs), whereas the three other species lacked these. In the course of this investigation, the composition of the electron dense particles that occurred in all four species was elucidated and based on this composition a possible function in phosphate storage was suggested.

The results presented in this part of the thesis are integrated and discussed in **chapter 5**, which provides an overview of the ultrastructure of the verrucomicrobial methanotrophic species studied. In addition, multiple directions for future research are discussed.

Summary

Methane is an important molecule in the atmosphere of the earth, where it contributes to the (enhanced) greenhouse effect. Methane can be consumed by a group of micro-organisms called methanotrophs. The oxidation of methane by methanotrophs can take place with oxygen (aerobic) or without oxygen (anaerobic). Recently, an entirely new group of aerobic methanotrophs was discovered in various acidic volcanic environments. These acid-loving methanotrophs belong to the *Verrucomicrobia* phylum, whereas all other aerobic methanotrophs known at that time are members of the *Proteobacteria*. For the past few years, research on verrucomicrobial methanotrophs focused mostly on various aspects of their physiology, studying the mechanisms they use to obtain energy from methane oxidation and via which they fix carbon and nitrogen. Apart from very basic observations, the way these micro-organisms organize their cells in order to facilitate their lifestyle remained unknown. The aim of the research presented in this part of the thesis was to elucidate the ultrastructure of the verrucomicrobial methanotrophs. The main method used for this purpose was electron microscopy, employing multiple different techniques for sample preparation and visualization.

After an introduction of verrucomicrobial methanotrophs in **chapter 1**, **chapter 2** focuses on the species *Methylacidiphilum fumariolicum* SolV that grows at low pH and high temperatures (thermophilic). In this verrucomicrobial methanotroph, two types of intracellular particles were observed that differ in the amount of contrast seen in electron microscopy images: electron dense (see **chapter 4**) and electron light particles. The composition of the electron light particles was investigated using a method to specifically stain polysaccharides. This stain, together with enzymatic and physiological assays and electron microscopic investigations, showed the electron light particles to be glycogen storage vesicles. Cells accumulated glycogen in these storage vesicles only when very limited amounts of nitrogen were present, but carbon was present in ample supply. The stored glycogen was used by the cells when they were starved for carbon compounds (methane).

Chapter 3 zooms in on the *M. fumariolicum* SolV cell with the aim to clarify the location of the two primary enzymes involved in the oxidation of methane. These two proteins, particulate methane monoxygenase (pMMO) and methanol dehydrogenase (MDH), were (partially) purified from the *M. fumariolicum* SolV culture and used to generate antibodies. Immunogold localization using these antibodies showed that MDH resides in the periplasm. The location of pMMO remained controversial due to the suboptimal quality of the antibody.

In **chapter 4**, the scope is broadened to mesophilic verrucomicrobial methanotrophs and three new species belonging to the new genus *Methylacidimicrobium* are described and characterized. The newly discovered species that were cultured into pure culture have been named *M. fagopyrum* 3C, *M. tartarophylax* 4AC and *M. cyclopophantes* 3B. These species were found to grow at moderate temperatures (mesophilic) and low pH values and were shown to grow autotrophically. The ultrastructure of these three

2 (ii)

Contents

Promotor
Prof. dr. ir. M.S.M. Jetten

Copromotor
dr. L. van Niftrik

Manuscriptcommissie
Prof. dr. C. Mariani
Prof. dr. W. Bitter (Vrije Universiteit Amsterdam)
Prof. dr. S-V. Albers (Albert-Ludwigs-Universität Freiburg, Duitsland)

Cell biology of anammox *Planctomycetes* and methanotrophic *Verrucomicrobia*

Proefschrift
ter verkrijging van de graad van doctor
aan de Radboud Universiteit Nijmegen
op gezag van de rector magnificus,
volgens besluit van het college van decanen
in het openbaar te verdedigen op
woensdag 13 januari 2016 om 14.30 uur precies

door
Muriël Caroline Frieda van Teeseling
geboren op 25 december 1986
te Naarden

Muriel van Teeseling (2015)
Cell biology of anammox *Planctomycetes* and methanotrophic *Verrucomicrobia*.
PhD thesis, Radboud University Nijmegen.

This PhD project was financially supported by ERC AG 232937.
Printing of this thesis was financially supported by SIAM gravitation grant 024002002 and by the Netherlands Society of Medical Microbiology (NVMM) and the Royal Netherlands Society for Microbiology (KNVM).

Cover: Freeze-fractured *Methylacidimicrobium fagopyrum* cell by Muriel van Teeseling.
Print: Gildeprint Drukkerijen, Enschede, the Netherlands.
ISBN: 978-94-6233-163-1.

Cell biology of anammox *Planctomycetes* and methanotrophic *Verrucomicrobia*

Part ii

Cell biology of verrucomicrobial methanotrophs

Muriel van Teeseling

Cell biology of anammox *Planctomycetes* and methanotrophic *Verrucomicrobia*

The cell biology of verrucomicrobial methanotrophs

Muriel van Teeseling